Characterization of Envelope-Specific Antibody Response Elicited by HIV-1 Vaccines: A Dissertation

Yuxin Chen
University of Massachusetts Medical School Worcester

Let us know how access to this document benefits you.

Repository Citation

CHARACTERIZATION OF ENVELOPE-SPECIFIC ANTIBODY RESPONSE
ELICITED BY HIV-1 VACCINES

A Dissertation Presented

By

Yuxin Chen

Submitted to the Faculty of the University of Massachusetts Graduate School of
Biomedical Sciences, Worcester in partial fulfillment of the requirement for the degree of

DOCTOR OF PHILOSOPHY

Jan 6, 2015

Immunology and Microbiology Program

CHARACTERIZATION OF ENVELOPE-SPECIFIC ANTIBODY RESPONSE
ELICITED BY HIV-1 VACCINES

A Dissertation Presented

By

Yuxin Chen

The signatures of the Dissertation Defense Committee signifies completion and approval
as to style and content of the Dissertation

_____

Shan Lu, Thesis Advisor

_____

Paul Clapham, Member of Committee

_____

Eva Szomolanyi-Tsuda, Member of Committee

_____

Gary Ostroff, Member of Committee

_____

George Lewis, Member of Committee

The signature of the Chair of the Committee signifies that the written dissertation meets
the requirements of the Dissertation Committee

_____

Trudy Morrison, Chair of Committee

The signature of the Dean of the Graduate School of Biomedical Sciences signifies that
the student has met all graduation requirement of the school.

_____

Anthony Carruthers, Ph.D.
Dean of the Graduate School of Biomedical Sciences

Immunology and Microbiology Program

Jan 6, 2015

Copyright Information

Parts of this dissertation have appeared in separate publications:

Acknowledgements

First, I want to thank my mentor, Dr. Shan Lu, for his constant support and guidance throughout my graduate school. He offered me the opportunities to join the lab and work on several interesting lines of research and collaboration, which greatly expand my intellect and scientific development. Most importantly, he always encouraged me to develop my potential to explore the new challenges in both science and life. I would like to thank Dr. Shixia Wang for her insightful advice on experimental design and technique questions in my daily work. Also, I thank Dr. Jill Serrano for her assistance with editing.

I would like to thank Dr. Xiang-Peng Kong for his guidance and collaboration on the rabbit monoclonal antibody structure project. His productive work advanced our knowledge of vaccine-elicited rabbit monoclonal antibodies. I also would like to thank Dr. Shiu-lok Hu for his gp160 Env immunogen. His generosity and intellectual guidance made this project possible. I would like to thank the members of my thesis advisory committee Dr. Trudy Morrison, Dr. Paul Clapham, and Dr. Eva Szomolanyi-Tsuda for their advice and contribution over the past few years. I would like to thank Dr. George Lewis and Dr. Gary Ostroff for taking the time to serve on my defense committee.

I would like to thank all the members, past and present, of the Lu lab. In particular, I work closely with Dr. Huaiqing Chen, Dr. Dong Han, Dr. Aaron Wallance, and Shengqin Wan. The work described herein would not have been possible without your valuable help and support. All other lab members were also extremely helpful and friendly.

Finally, I could not have made it to the point I am at today, personally and professionally, without the invaluable support of my family and friends.

ABSTRACT

Despite 30 years of intensive research，an effective human immunodeficiency virus (HIV) vaccine still remains elusive. The desirable immune response capable of providing protection against HIV acquisition is still not clear. The accumulating evidence learned from a recent vaccine efficacy correlate study not only confirmed the importance of antibody responses, but also highlighted potential protective functions of antibodies with a broad repertoire of HIV-1 epitope specificities and a wide range of different antiviral mechanisms. This necessitates a deep understanding of the complexity and diversity of antibody responses elicited by HIV-1 vaccines. My dissertation characterizes antibody response profiles of HIV-1 Env antibodies elicited by several novel immunogens or different immunization regimens, in terms of magnitude, persistence, epitope specificity, binding affinity, and biological function.

First, to overcome the challenge of studying polyclonal sera without established assays, we expanded a novel platform to isolate Env-specific Rabbit mAbs (RmAb) elicited by DNA prime-protein boost immunization. These RmAbs revealed diverse epitope specificity and cross-reactivity against multiple gp120 antigens from more than one subtype, and several had potent and broad neutralizing activities against sensitive Tier 1 viruses. Further, structural analysis of two V3 mAbs demonstrated that a slight shift of the V3 epitope might have a dramatic impact on their neutralization activity. All of these observations provide a useful tool to study the induction of a desired type of antibody by different immunogens or different immunization regimens.

Since heavily glycosylated HIV Env protein is a critical component of an HIV vaccine, we wanted to determine the impact of the HIV Env-associated glycan shield on

antibody responses. We were able to produce Env proteins with a selective and homogeneous pattern of N-glycosylation using a glycoengineered yeast cell line. Antigenicity of these novel Env proteins was examined by well-characterized human mAbs. Immunogenicity studies showed that they were immunogenic and elicited gp120-specific antibody responses. More significantly, sera elicited by glycan-modified gp120 protein immunogens revealed better neutralizing activities and increased diversity of epitopes compared to sera elicited by traditional gp120 produced in Chinese Hamster Ovary (CHO) cells.

Further, we examined the impact of the delivery order of DNA and protein immunization on antibody responses. We found that DNA prime-protein boost induced a comparable level of Env-specific binding Abs at the peak immunogenicity point to co-delivery of DNA. However, antibody responses from DNA prime-protein boost had high avidity and diverse specificities, which improved potency and breadth of neutralizing Abs against Tier 1 viruses. Our data indicate that DNA vaccine priming of the immune system is essential for generation of high-quality antibodies.

Additionally, we determined the relative immunogenicity of gp120 and gp160 Env in the context of DNA prime-protein boost vaccination to induce high-quality antibody responses. Immunized sera from gp120 DNA primed animals, but not those primed with gp160 DNA, presented with distinct antibody repertoire specificities, a high magnitude of CD4 binding site-directed binding capabilities as well as neutralizing activities. We confirmed the importance of using the gp120 Env form at the DNA priming phase, which directly determined the quality of antibody response.

Table of Contents

Chapter II:

Section I: A novel rabbit monoclonal antibody platform to dissect the diverse

repertoire of antibody epitopes for HIV Env immunogen design

Section II: Rabbit anti-Env monoclonal antibodies raised by immunization can

mimic the antigen-binding modes of antibodies derived from HIV-1-infected

humans

Section III: Masking of an immunogenic epitope region in HIV-1 gp120 C4 critical

for receptor and co-receptor binding

Section IV: Structure basis to differentiate a broadly cross-neutralizing V3 mAb

and other V3 mAbs targeting at overlapping epitopes

Section V: Diverse repertoire of rabbit monoclonal antibodies elicited by a Clade

AE gp120 immunogen

Chapter III: Immunogenicity of HIV-1 Envelope proteins with unique N-glycan patterns

Chapter IV: Sequential versus concomitant delivery of DNA and protein vaccines

Chapter V: Antigenicity and immunogenicity of gp120 and gp160 in the context of

heterologous DNA prime protein boost

List of Tables

List of Figures

List of Abbreviations

ADCC   Antibody Dependent Cell mediated Cytotoxicity

AIDS   Acquired Immunodeficiency Syndrome

Ab   Antibody

Ad5   Adenovirus 5

bNAb   Broadly neutralizing antibody

CAVD   Collaboration for AIDS Vaccine Discovery

CD4bs   CD4 binding site

CDR   Complementarity determining regions

CD4i   CD4 inducible

CMV   Cytomegalovirus

CTL   Cytotoxic T Lymphocyte

CRFs   Circulating recombinant forms

ELISA   Enzyme Linked ImmunoSorbent Assay

EWB   ELISA Wash Buffer

Env   Envelope

GC   Germinal center

GALT   Gut-associated lymphoid tissue

HBV   Hepatitis B vaccines

HCMV   Human cytomegalovirus

HIV-1   Human Immunodeficiency Virus type I

Kif   kifunensine

IFA   Incomplete Freund's Adjuvant

mAb	Monoclonal Antibody
MHC	Major histocompatibility
MLV	Murine Leukemia Virus
MPER	Membrane Proximal External Region
MVA	Vaccinia virus Ankara
NAb	Neutralizing Antibody
NaSCN	Sodium Thiocynate
NZW	New Zealand White
PNGS	Potential N-Linked Glycosylation Site
PBMC	Peripheral blood mononuclear cells
RhCMV	Rhesus CMV
RmAb	Rabbit monoclonal antibody
SIV	Simian Immunodeficiency Virus
SFV	Semliki Forest virus
sCD4	Soluble CD4
WHO	World Health Organization
PrEP	Pre-exposure antiretroviral prophylaxis
VSV	Vesicular stomatitis virus
URFs	Unique recombinant forms

Preface

The structural analysis of Rabbit monoclonal antibodies from Chapter II in this dissertation (Fig.2.10, Fig. 2.11 and Fig.2.12) was performed in the laboratory of Dr. Xiang-Peng Kong.

The glycan composition analysis for Env proteins (Fig.3.2) was performed in the laboratory of Dr. Lance Well and Dr. Mike Tiemeyer.

Chapter in this dissertation was taken from the following publication currently in preparation for submission:

Chapter II section II: Ruimin Pan, Yuxin Chen, Michael Vaine, Shixia Wang, Shan Lu and Xiang-Peng Kong. Conformational masking of an immunogenic epitope region critical for CCR5/CXCR4 binding and tropism. *In preparation for submission.*

CHAPTER I

Introduction

1. HIV pandemic and HIV virus

1.1 HIV pandemic

Entering the fourth decade of the AIDS epidemic, death caused by HIV-1 remains a leading cause of mortality worldwide. By the end of 2013, reports from the World Health Organization (WHO) show about 35 million people are living with HIV. In the year 2013, 2.1 million people are newly infected with HIV globally, and 1.5 million people die of HIV caused illness (1), with sub-Saharan Africa being the most affected region, followed by eastern Europe and the Caribbean. HIV-related deaths have steadily declined since 2010 and new HIV infections have declined by 38% since 2001, mostly due to widely available free drug treatment in sub-Saharan Africa.

Several interventions have contributed to this unprecedented progress in HIV prevention, especially in South Africa. First, combination antiretroviral treatment not only helps reduce the viral load in HIV infected patients but also greatly reduces the risk of transmission to their HIV-negative partners. Second, behavioral interventions, including the introduction of condoms, regular HIV testing, needle syringe exchange programs for injecting drug users, and male circumcision, have also, at least partially, reduced the risk of infection (2-4). Third, pre-exposure antiretroviral prophylaxis (PrEP) with 1% tenofovir gel also reduces the risk of HIV acquisition by 39% in HIV-negative women (5), and daily use of oral combination prophylaxis with tenofovir and emtricitabine reduced HIV acquisition by 44% among homosexual men and transgender women (6-8), although one trial did not show any reduction of HIV infection rate using antiviral prophylaxis treatment (9). Nonetheless, PrEP intervention is expensive and requires persistent adherence to topical or

oral antiretrovirals. Moreover, mathematical modeling analysis has predicted that, on a large scale, a combination of these various interventions may be able to dramatically reduce HIV incidence, but may not diminish HIV infection (9, 10). Therefore, developing an effective vaccine for HIV infection is a still global priority.

1.2 HIV subtypes and genome

HIV is a member of lentivirus genus, a part of the Retroviridae family. Its life cycle involves reverse transcription of the viral RNA genome to DNA and subsequent insertion into the host genome. Due to error prone replication and retroviral recombination events, the HIV-1 viral sequence has daunting genetic diversity. HIV is divided into two types, HIV-1 and HIV-2 and both of them cause AIDS; however, HIV-1 causes the majority of HIV infection throughout the world. HIV-1 can be further categorized into four viral groups: the "major" group M, the "outliner" group O, and two new groups, N and P. Group M is the predominant circulating HIV-1 group，which is further divided into nine subtypes, A-D, F-H, J and K. Intersubtype combinations are very common and at least 55 circulating recombinant forms (CRFs), such as AE, and unique recombinant forms (URFs) have been identified.

Three major genes in the HIV-1 genome, *gag*, *pol* and *env*, encode polyproteins that are subsequently cleaved into multiple short functional proteins. The *gag* gene encodes the Gag protein, which is sufficient to drive the assembly and release of virus-like particles from the host cell. The *pol* gene encodes reverse transcriptase and does not have proofreading activity, therefore, the replication process is error-prone and point mutations are introduced into each new copy of the viral genome. The Env gp160 protein expressed by the *env* gene forms a trimer and is then cleaved by a furin protease into

gp120 and gp41, which are involved in receptor binding and membrane fusion, respectively. In addition, the HIV genome contains genes encoding regulatory factors including *tat* and *rev* and accessory genes *nef, vpr, vpu*, and *vif*. Genetic variation between subtypes within group M can be as high as 35%, with the *env* gene having the most significant genetic diversity.

Since HIV exhibits such daunting global genetic diversity and has the mutation capacity to escape adaptive immune responses and the early establishment of latent viral reservoirs, development of a prophylactic HIV-1 vaccine is urgently needed but it is clear that such development is not without major challenges and obstacles.

1.3 Env structure

A critical HIV-1 vaccine target protein is the Env spike. It is the only protein on the HIV virus particle and mediates virus entry. The mature HIV-1 envelope spike is composed of three copies of non-covalently associated gp120 and gp41. Once gp120 protein binds to the primary receptor, CD4, conformational changes expose the binding site for chemokine co-receptors (CCR5 and CXCR4). CD4 binding induces conformational changes within the Env trimer that result in the transition of the gp41 ectodomain into prehairpin intermediates. Upon chemokine receptor binding, heptad repeat regions, HR1 and HR2, form a six-helical bundle, promoting the fusion of viral and target cell membranes(11, 12).

The gp120 subunit protein is composed of five conserved regions (C1-C5) that are interspersed with five variable regions (V1-V5). Due to intrinsic heterogeneity, the presence of a complex glycan shield, and the conformational flexibility of Env, gp120 structure characterization has been a great challenge. To visualize HIV-1 gp120 Env at an

atomic level, early crystallization studies stabilized Envs in their CD4-bound conformation with V1/V2/V3 truncated and N-glycans removed (13, 14). These structural studies revealed that gp120 core protein consists of an inner domain and an outer domain, referring to parts of gp120 that are close to inner and outer regions of the trimer spike, respectively. Through these studies, it was determined that the outer domain is structurally constant, whereas the inner domain displays extraordinary structural diversity(15). CD4 makes initial contact with the outer domain of gp120, a surface constitutively exposed on the envelope spike. Soon after this interaction between CD4 and the outer domain of gp120, the inner domain rearranges in a highly coordinated manner to form a four-stranded bridging sheet mini-domain, which holds the CD4 molecule in place. The initial CD4 attachment site is identified as a critical site of vulnerability and is a most desirable neutralizing epitope for vaccine targets (16).

In addition to conserved regions, the five variable regions are also highly glycosylated and project surface-exposed loops, protecting the core from potentially neutralizing antibodies. Electron tomography and cryo-electron microscope studies showed V1/V2 of the viral spike is a membrane distal 'cap', suggesting that the V1/V2 region is accessible in the context of trimer (17-20). Although V1/V2 is not necessary for viral entry, deletion of this region makes viruses sensitive to antibody neutralization. α4β7 integrin receptor, which is highly expressed in gut-associated lymphoid tissue (GLAT), was suggested to bind to the Env spike via a conserved integrin binding motif, LDI/V, within the V2 region (21, 22). This accumulating evidence is compatible with a critical role of V2-specific antibody responses in inhibiting HIV infection as observed in immune-correlate analysis of samples from the RV144 trial (23). The V3 loop forms an

extended structure whose tip protrudes ~30Å from the main portion of the gp120 core (24, 25). It is localized directly beneath the V1/V2 hairpin with the tip pointing toward the trimer axis and interacts with the V2 base from the adjacent promoter. The V3 region mediates direct binding with entry co-receptor and determines whether CCR5 or CXCR4 will be used for HIV-1 entry. Its protruding loop-like structure makes the V3 region highly immunogenic and accordingly has been named the 'principle neutralizing determinant' of HIV-1. At a sequence level, V3 is the most conserved region in comparison with the other variable regions, as it is almost always 35 residues long and its tip harbors a highly conserved motif, Gly-Prop-Gly-Arg/Gln (GPGR/Q), a key neutralizing epitope (26). The V4-V5 regions are highly disordered in most crystal structures (27), as to be expected based on both their location and the variability in sequence within these regions. Overall, V1-V5 loop residues have adopted multiple conformations, depending on which antibody is bound with Envs.

While gp120 on Env mediates virus attachment to target cells, the transmembrane region gp41 subunit is responsible for membrane fusion between virus and target cells. It consists of two long prominent helices; heptad repeat 1 forms a three-helix bundle with neighboring protomers in the trimer core and heptad repeat 2 wraps around the outer periphery of the trimer base, angling downward with its C terminal proximal to viral membrane. Once CD4 and co-receptor are bound to Env, the gp120 promoters is rotated outwards and gp41 is exposed, which undergoes a structural rearrangement and finally forms a six-helix bundle structure, perpendicular to the viral membrane, as a post-fusion conformation.

The high resolution architecture of the Env trimer has remained elusive until a

recent major breakthrough. Results from a recent study identified a trimer from a clade A HIV-1 isolate (BG505) as a naturally stable trimer, which was further engineered to remove the hydrophobic transmembrane anchor and the MPER region (19, 20). In addition, a disulfide bond was introduced to increase trimer stability, and cleavage efficiency of the precursor into a mature trimer was further optimized. Crystal structure and cryo-electron microscopy of this so-called SOSIP.664 trimer provided unprecedented insight regarding spatial arrangements for HIV-1 Env. It has a tightly packed mushroom shape with the gp120 trimer as its cap and the transmembrane gp41 trimer as its stem. There is a small opening between the Env apex and the top of the central gp41 helices. gp120 subunits are held together, partially associated with V1/V2/V3 regions at the top of trimer. For the CD4 binding site, only a narrow range of approach angles are available for this area to engage with trimer. This comprehensive quaternary nature of CD4bs epitopes on trimer might not be identical with that from monomer. Indeed, thorough antigenicity analysis of this trimer showed high reactivity with all Env-specific broadly neutralizing antibodies (bNAb) but no detectable binding with non-NAb against CD4bs, CD4i, or the gp41 region (28). V3-specific non-NAb only recognizes trimer by enzyme-linked immunosorbent assay but not at all by surface plasmon resonance and only a limited extent by electron microscopy.

The structural characterization of the SOSIP trimer revealed a fundamental antigenic difference between the SOSIP trimer and traditional gp120 protein (19, 20). Only broadly neutralizing epitopes are accessible on the SOSIP trimer. However, immunogenicity data from both rabbits and macaques (29) showed that the SOSIP trimer does not improve neutralization activities; the trimers induced strong but transient NAb

response against autologous, neutralization-resistant (Tier 2) BG505. For heterologous viruses, the immune sera also can neutralize Tier 1 viruses, but not Tier 2 viruses. Epitope mapping analysis showed antibody responses targeted at the conformational epitope on gp120 and linear V3 region, but this activity was without linear V1/V2-specific or CD4bs antibody-specific responses. This suggests that a trimer-based immunogen alone might not be the most useful tool for development of an effective vaccine.

One important feature of the Env protein is that it is heavily coated with potential N-glycosylation sites (PNGS); nearly 50% of its molecular weight is made up of a heterogeneous population of N-glycans. There are three different types, including high mannose, hybrid, and complex. Different Env strains have different numbers of PNGS; different glycoforms could present at the same glycosylation site and not all glycosylation sites are utilized (30, 31). Furthermore, glycosylation patterns from different cell types or even the same cell type under different metabolic conditions are distinct (32). For example, the recombinant gp120 protein produced from traditional mammalian CHO cells has more than 70% complex-type glycans, whereas the native Env amplified from peripheral blood mononuclear cells (PBMC) shows mostly a high mannose population ($Man_5GlcNAc_2$) (33), adding an additional layer of microheterogenity on the glycan shield on Env proteins.

The contribution of these Env protein glycan shields to immune evasion and recognition were still only partially understood. It was shown that a lack of complex N-glycans on HIV-1 Env preserves protein conformation and virus entry function (34). Even a partial enzymatic deglycosylation can preserve the structure of cleaved Env

trimers (35). However, the antennae of complex N-glycan serves to protect the V3 loop and CD4 binding site, while N-glycan stems regulate the native trimer conformation. Removal of these N-glycans causes neutralization sensitivity change and failure to complete the conformational rearrangement necessary for infection (36). Although carbohydrates were considered the "glycan shield" used to protect Env, it recently was found that both high mannoses and complex carbohydrates are targeted by the humoral immune system at an early stage of infection, thus glycan-dependent broadly neutralization activities were commonly observed among infected animals and human (37, 38).

2. Immunization approaches for HIV vaccine

2.1 Protein-based HIV vaccine

Despite the triumph of recombinant protein-based hepatitis B vaccines (HBV) in the 1980s, the first two large-scale HIV vaccine trials using a similar strategy did not have such fortune. Between 1998 and 2003, two phase III HIV vaccine efficacy trials were performed by VaxGen among HIV-1 seronegative volunteers (39-41). The VAX004 trial was held in North America and the Netherlands, using AIDSVAX B/B vaccine, consisting of bivalent recombinant HIV Env gp120 proteins (MN and GNE8) from Clade B. VAX003 was conducted in Thailand, evaluating the immunogenicity of AIDSVAX B/E, incorporating Env gp120 antigens from the predominant circulating viruses in Thailand. Neither trial prevented virus acquisition or reduced viremia in those later infected with HIV. The immunized sera showed Env-specific binding antibody and NAb responses against vaccine strains; however, there was no strong heterologous NAb

response against primary isolates. It was determined that the protein-based immunization alone was ineffective to generate a comprehensive immune response against HIV.

2.2 Viral vector-based vaccine

In early HIV research, vaccines consisting of live attenuated SIV viruses with deletion of *nef* genes demonstrated nearly full protection from either homologous or heterologous SIV challenge (42-45). However, the attenuated SIV strain was able to revert to virulence by repairing the engineered deleted genes via their error-prone reverse transcriptase, which poses a serious safety risk for administration of such attenuated virus in humans. However, these studies reassured the field that it may be feasible for a vaccine to elicit specific enough immune responses to fight against the HIV virus.

Following the failure of the VaxGen trial to elicit protective antibodies, Merck Research Laboratories specifically designed an adenovirus 5 (Ad5) vector-based strategy to induce only T cell-mediated immunity. The Ad5 vector is a non-replicating vector resulting from deletion of the early region 1 (E1) gene, which is necessary for virus replication. Two phase IIb vaccine trials, STEP and Phambili in the United States and South Africa, respectively, studied the efficacy of the rAd5 vector vaccine expressing HIV gene, *gag*, *pol*, and *nef* to prevent HIV infection (46). The vaccine proved to be safe and strongly immunogenic, demonstrated by antigen-specific IFN-γ responses in 77% of immunized subjects, poly-functional CD4+ T cell response among 41% of vaccinees, and antigen-specific CD8+ T cell responses from 73% of immunized volunteers (47). Unfortunately, such strong T cell immunity did not confer prevention against virus acquisition or reduce the viremia in those who later became infected with HIV. Both trials were halted since this vaccine appeared to increase the risk of HIV-1 infection

among those vaccinees previously exposed to Ad5 adenovirus (48). It was hypothesized that activation of pre-existing Ad5 vector-specific CD4 T cells at mucosal surfaces following Ad5 vaccination might have resulted in an elevated number of target cells for HIV infection (49). However, this hypothesis was later challenged by a new observation that Ad5-seropositive volunteers in the STEP trial did not develop higher vector-specific cellular immune responses when compared to Ad5-seronegative subjects (50). The mechanism of higher HIV susceptibility for the vaccine group in the STEP trial remains to be resolved.

Given the safety concerns of the rAd5 viral vector, there have been ongoing efforts to develop alternative rAd vector serotypes for HIV-1 vaccines, to overcome this problem of pre-existing anti-Ad5 immunity and facilitate the development of adenovirus vector-based regimens. In preclinical studies, some of these serotypes have demonstrated an ability to induce strong cellular responses despite of pre-existing Ad5 immunity (51-53). Some promising vectors, including rAd26, rAd35, and rAd5HVR48, which are biologically different from Ad5, are being evaluated in phase 1 clinical trials. An initial analysis showed that Ad26-Env immunization induced HIV-specific mucosal humoral and cellular immune response without a detectable vector-specific response (54).

Furthermore, pox viral vectors also have been widely used for vaccine development since the success of the vaccinia virus-vectored vaccine for the eradication of smallpox. Poxvirus has large genome, which is able to accommodate more than 10 kb of foreign DNA. Furthermore, inserted transgene products can be expressed at high levels, resulting in potent cellular responses. Based on efficiency of expression and safety record, the three most promising non-replicating poxviral vectors are ALVAC, attenuated

modified vaccinia virus Ankara (MVA), and the modified Copenhagen vaccinia strain (NYVAC); other pox vectors in development include Tiantan pox vector (55) and fowlpox vector (56, 57).

ALVAC is a naturally-attenuated canarypox construct that effectively induces an HIV-specific CD8+ cytotoxic T lymphocyte (CTL) response, as it can process expressed antigen through the major histocompatibility (MHC) class I pathway. A phase II clinical trial showed poor immunogenicity of ALVAC expressing gp120 antigen (58). Low titer neutralizing antibodies were detected in 56% of recipients, 30% of vaccine subjects showed a CD8+ CTL response, and 28% of volunteers showed lymphocyte proliferation. This suggested that ALVAC alone vaccination could not elicit optimal T cell or antibody responses.

Both MVA and NYVAC vectors had a highly attenuated phenotype and high expression of heterologous antigens and in previous studies they both showed good safety profiles and triggered broad and durable immune response to HIV antigens. MVA has been shown to preferentially drive CD4+ T cell response, while NYVAC focuses on activation of CD8+ T cell response (59). However, similar to the ALVAC vector, administration of MVA or NYVAC vector expressing HIV antigen alone showed only modest immune responses. In the MVA study, MVA immunization lead to a IFN-γ response among 25% of the low dose group and 62% of the high dose group (59) whereas in the NYVAC study, two doses of NYVAC resulted in induction of T cell immune responses in 40% of volunteers but this response disappeared by 48 weeks after immunization (60).

An attenuated cytomegalovirus (CMV) vector has also drawn substantial attention

as a T cell vaccine delivery vector. It can induce persistent, systemic, high frequency, circulating and tissue-resident effector memory T cells, which have unprecedented breadth and can recognize promiscuous epitopes that are restricted both by MHC class I and II molecules (61). A challenge study in rhesus monkey has shown that these virus-specific, effector memory T cells could be maintained by a persistent rhesus CMV (RhCMV) vector. Although they could not protect the host against acquisition of infection, they can shut down productive SIV infection, maintain immune surveillance over time, or functionally cure and possibly eradicate SIV infection (62). To use this promising CMV platform for HIV vaccine development, several concerns must be addressed. First, it will need to be determined whether the human CMV vector has similar properties to RhCMV and if such substantial efficacy of protection observed in an animal model can be translated into humans. Second, although CMV infection is nonpathogenic in the majority of individuals, it is still considered a potential risk for pregnant women and immunocompromised individuals. Nevertheless, the substantial efficacy of CMV vectors in an animal model, combined with identification of human homologs to RhCMV genes, make a promising CMV vector platform for HIV vaccine development. Clinical trials are currently planned for CMV vectors.

In addition, live-attenuated vesicular stomatitis virus (VSV) (63), alphavirus vector (64, 65), and Semliki Forest virus (SFV) have also been adopted for HIV pre-clinical vaccine studies.

2.3 DNA vaccines

The introduction of DNA vaccine in HIV field started at early nineties when a DNA plasmid encoding HIV-1 Env was able to raise both humoral and cellular response

in small animals. The first human DNA vaccine study was done in HIV-1 infected patients as a Phase I clinical trial for safety analysis, followed by studies in healthy, HIV-1 negative volunteers (66, 67). These studies confirmed the overall safety profile for DNA vaccines but the immunogenicity results were disappointing. The magnitude and frequency of T cell immune responses were low and HIV-1 antigen-specific antibody responses were generally low or below detection.

In an attempt to improve the immunogenicity of DNA vaccine, several technical improvements to the design of DNA vaccine vectors have contributed to improved antigen expression and immunogenicity of HIV-1 DNA vaccines in both animal and human. First, codon-optimization of immunogen genes was found highly effective in elevating immunogen protein expression *in vitro* and enhancing T cell and antibody response *in vivo* (68-71). Second, replacement of HIV-1 Env leader sequence with signal peptides from other mammalian proteins, such as human tissue plasminogen activator (tPA), was able to greatly improve the protein expression of Env-based HIV-1 DNA vaccine (72, 73). Third, the viral promoter efficiency improved greatly gene transcription of HIV DNA vaccine. Intermediate-early gene 1 promoter adopted from human cytomegalovirus (HCMV), a non-carcinogenic virus, has been widely used with high efficiency in most DNA vaccine design (74). Furthermore, adding an intron A sequence from HCMV to an immediate downstream region of the HCMV promoter was able to further enhance the immunogenicity of HIV-1 DNA vaccines (72). With such modification, HIV DNA vaccine was able to effectively elicit both T cell response and antibody response in small animal and non-human primate models; however, the immunogenicity of DNA vaccines was still poor when used alone in humans.

2.4 Heterologous prime boost immunization

Each novel immunization approach mentioned above has been tested in clinical trials; however, each appears to have their shortcomings. The VaxGen trial showed that the traditional recombinant subunit protein was immunogenic but failed to generate high quality antibody against HIV-1 virus and limited T cell immune responses; whereas viral vector vaccines and DNA vaccines alone were not immunogenic enough to elicit robust T cell and antibody response in humans. A landmark study adopted a heterologous prime-boost strategy that used vaccinia vector encoding SIV Env glycoprotein, boosted with recombinant gp160 protein (75, 76). Animals primed with vaccinia vector vaccines showed robust Env-specific T cell responses, with weak antibody responses. Remarkably, soon after the boost immunization, the animals showed a substantial increase in Env-specific antibody titers as well as broad neutralizing activities against homologous and heterologous viral antigens. Further, these immunized animals showed complete protection against intravenous challenge of homologous viral challenge. Since then, the heterologous prime-boost strategy has been widely investigated and optimized to combine different immunization modalities to reach the optimal immune response.

2.4.1 DNA prime viral vector boost

The idea of DNA prime Ad5 vector boost to elicit HIV-specific T cell response was most recently tested in a phase IIb clinical trial, HVTN505 (77). Study participants were primed with DNA vaccines and boosted with Ad5 vectors expressing Env, Gag, and Pol. During this HVTN505 trial conducted in the United States, the volunteers were fully circumcised and did not have pre-existing anti-Ad5 neutralizing antibodies. However, the use of the Ad5 vector is being challenged following this clinical trial. This trial was

discontinued since it showed a lack of protection in terms of reduction of the rate of virus acquisition or viral load set point among vaccinees. Both humoral and cellular immune responses were observed in the majority of recipients. While 61.5% of CD4+ T cells and 64.1% of CD8+ T cells showed HIV-1 specific response demonstrated by intracellular cytokine staining, antibody response including neutralizing antibody, non-neutralizing antibody, and V2-sepecific antibody levels were low. More detailed analysis is currently under investigation.

To generate robust T cell responses, several combined immunization approaches using DNA prime followed by MVA or NYVAC boost has been demonstrated to synergistically improve vaccines-specific cell mediated immunity. Researchers from Oxford University (Oxford, UK) used a DNA vaccine, composed of several T cell epitopes for HIV-1 including a fragment encoding the gag antigen as a prime followed by a MVA vaccine boost expressing the matched antigen. However, only low level T cell responses were generated, which may be due to limitations of epitope vaccines delivered by DNA vaccines (78-82). The HVTN065 trial later tested a DNA vaccine containing several HIV-1 antigens as the priming immunization, followed by boost with a recombinant MVA expressing HIV-1 antigens. This DNA prime-MVA boost vaccine was well tolerated and produced detectable and reproducible HIV-1-specific cellular immunity in humans (83, 84). In this regimen, DNA priming was responsible for the induction of HIV-1-specific T cell immune responses following the boost of MVA. The T cell responses were poly-functional; about 50% of the HIV-specific CD4 and CD8 T cells induced in vaccinated subjects produced more than three cytokines. Furthermore, strong T cell proliferation, as well as robust production of the T cell growth factor IL-2 by HIV-

1-specific CD4 and CD8 cells, was observed. A phase II clinical trial (HVTN205) using a similar DNA prime-MVA boost regimen has been completed and the immune responses are currently under analysis.

Data from the EuroVacc 02 trial using DNA prime-NYVAC boost demonstrated the safety and high immunogenicity of this platform (60). Both the DNA and NYVAC expressed fused Gag-Pol-Nef and Clade C isolate CN54 gp120 Env. T cell responses were detected in 90% of DNA prime-NYVAC boost vaccinees, which was superior to responses induced by NYVAC alone (33% of responders). However, T cell responses were predominantly mediated by $CD4^+$ T cells, while only a modest level of $CD8^+$ T cells specific for HIV-1 antigens Gag, Pol, and Nef were detected.

2.4.2 Viral vector prime protein boost

In an attempt to elicit balanced T cell and antibody-mediated immune responses, the phase III RV144 trial combined two HIV vaccine components that focused on a distinct mechanism. The prime, a canarypox vector (ALVAC-HIV), encodes HIV-1 gp120, gag and pol protein, and several CTL epitopes from *nef* and *pol*, which focus on T cell responses; whereas two vaccinations with recombinant gp120 protein from isolate A244 (Clade AE) and MN (Clade B) (AIDSVAX B/E) was used as the boost, which is responsible for high antibody responses. Although these two vaccine components failed to show any efficacy, this combined regimen, for the first time in history, showed 31% of vaccine efficacy at preventing HIV infection.

The immunogenicity of this vaccination was analyzed; a modest T cell-mediated immune response was observed. Among 19.7% of vaccines at 6 months post-vaccination, Env- or gag-specific T cell immune response were observed as determined by IFN-γ

ELISPOT assay. Furthermore, CD4+ Env-specific intracellular cytokine staining was observed more in the vaccine group compared to the control group. One interesting finding was that T cells preferentially targeted the V2 region (85). Almost all volunteers (99%) developed Env-specific binding antibody response, however, these responses waned considerably after 6 months (86). In terms of epitope specificity, strong antibody responses against C1, V2, V3, and C5 regions of gp120 were observed by overlapping peptide microarray (23). There was a low level of neutralizing antibodies against Tier 1 viruses, but not Tier 2 viruses demonstrated by TZM-bl assay. Interestingly, overall NAb responses from RV144 were even lower compared to those elicited by VAX003 (87).

To determine a potential immune correlate of decreased infection risk by vaccination, six primary variables were included into a statistical analysis, including 1) IgA Abs binding to Env, 2) avidity of IgG antibodies for Env, 3) antibody-dependent cell mediated cytotoxicity (ADCC), 4) neutralizing antibodies, 5) gp70-V1V2 binding, 6) CD4+ T cells (88). It turns out that gp70-V1V2 binding antibody inversely correlates with infection, while plasma IgA directly correlates with infection. To further confirm this finding, sieve analysis was performed to identify if vaccine efficacy would vary with different genotypic HIV viruses. Indeed, the estimated vaccine efficacy against viruses matching the vaccine at the position 169 (K169) was 48%, whereas vaccine efficacy versus position-181-mismatched (I181) viruses was 78%, and vaccine protection against viruses both matched with K169 and mismatched with I181 was 80%, suggesting a V2 antibody response specifically targets the K169 position (89). Furthermore, four mAbs isolated from RV144 vaccinees mediated ADCC activity, which was dependent upon position 169 in breakthrough Envs (90). All of this evidence suggests that the V2-specific

antibody response is critical to prevent infection with viruses matching the vaccine at the V2 K169 residue. An independent analysis of plasma IgG responses against linear epitopes as potential correlates of risk of infection also confirmed the importance of V2 antibody (23). Overlapping linear peptide microarray showed dominant responses against the C1, V2, V3, and C5 regions of gp120 in the RV144 trial. Statistical analysis further confirmed that V2-specific IgG significantly inversely correlated with infection risk; meanwhile, V3-specific IgG showed a similar trend but only in vaccine recipients who had lower levels of other antibodies, especially Env-specific plasma IgA and neutralizing antibodies (23). Of note, the antibody response waned quickly after 12 months post final immunization, which contributed to decreased protection efficacy over time. This vaccine trial provided valuable information about immune correlates for an HIV vaccine. This study also further suggested that dissecting antibody quality is critical in evaluating a vaccine regimen. Meanwhile, more potent vaccine candidates will presumably be desirable.

In addition, adenovirus vector prime protein boost is also a promising candidate since it can generate balanced immunity. It has been demonstrated that this strategy can induce a high level neutralizing response when Ad26 prime gp140 protein boost was adopted (91).

2.4.3 DNA prime protein boost

Similar to canarypox prime protein boost approach, DNA prime protein boost strategy is also aimed to elicit a balanced antibody and cellular mediated response against HIV-1, which has been extensively studied by our group as well as other groups. Although DNA vaccine alone or gp120 protein alone failed to generate effective antibody

response which is able to neutralize against JR-FL viruses, either rabbit sera from gp120 or gp140 DNA vaccines delivered by gene gun followed by gp120 protein boosting was capable of neutralizing JR-FL virus strain (92). Further, DNA priming plus recombinant protein boosting approach delivering polyvalent primary Env from representative A, B, C, D, and AE was able to compromise the diverse genetic sequence variance, and such vaccine strategy can further expand the neutralized viruses from subtype A, B, C, D and AE (93). Indeed, in a NHP study, DNA vaccines encoding four Env antigens from subtype A, B, C, and AE and HIV-1 Gag antigen from Clade B induced binding antibodies to Envs from multiple HIV-1 isolates that were markedly enhanced following boosting with homologous gp120 proteins. These sera neutralized homologous and, to a lesser degree, heterologous HIV-1 isolates. 75% immunized animals had sterile immunity following rectal challenge with a SHIV encoding Env from HIV-1$_{Ba-L}$, whereas reduced virus load was observed in the infected animals compared to naïve controls (94). Dissection of polyclonal sera showed that the improved neutralization activities might be result from higher antibody avidity, a more diverse and conformational epitope profile (95). Interestingly, antibody responses targeting several peptides that overlap with known CD4 binding area were detected only in DNA-primed sera (96). Further, recent evidence showed that DNA immunization was able to induce higher level of germinal center B cell via T follicular helper cells, which is critical to produce optimally affinity-matured antibody responses(97).

Among a few DNA prime-protein boost studies conducted in healthy human volunteers, the DP6-001 study provided the most comprehensive and promising immunogenicity data (98). In this study, participants received three times priming

immunizations with a polyvalent HIV-1 DNA vaccine, including six DNA plasmids (five expressing different primary gp120 antigens from clades A, B, C, D and E and one expressing a clade C Gag antigen), followed by two times boost with a polyvalent recombinant gp120 protein vaccine (five gp120 proteins matching those used in the DNA prime). Although the DNA vaccine components were administered via intramuscular or intradermal needle injection without using an adjuvant or a physical delivery device (such as gene gun or EP), positive gp120-specific CD4$^+$ T cell responses were detected in all volunteers at the end of three DNA immunizations, and were further boosted by the gp120 protein boost. It was also important to note that these effector memory CD4$^+$ T cells were multifunctional, secreting IFN-γ, IL-2, and TNF-α. The subpopulation positive for CD154 maintained proliferative potential and could rapidly develop into mature effector CD4$^+$ T cells (99). Interestingly, this phenotype was also seen in long-term non-progressors or aviremic HIV-1 infected patients on highly active antiretroviral therapy (HAART). In the higher dose group (1.2 mg for Gag-expressing DNA vaccine component), positive Gag-specific CD4$^+$ T cell responses were also detected at the end of three DNA immunizations, a response that was rare in previous DNA vaccine studies when no adjuvant or EP device was used. Antigen-specific CD8$^+$ T cells were also observed in vaccinated participants (99).

However, the most significant finding was that high-titer gp120-specific antibody responses (end titration titers of 1:10^5, equivalent to Env-specific antibody titers in chronically infected HIV-1 positive patients) were detected in immune sera of 100% of the DP6-001 trial participants following one or two gp120 protein boosts (98). All of these immune sera had a broad reactivity recognizing gp120 antigens from HIV-1

subtypes A to E. High level neutralizing activities were easily detected against pseudotyped viruses expressing Env from the sensitive viruses (TCLA isolates and SF162), activities that were better than observed in a previously reported DNA prime-Ad5 vector boost vaccine trial (100), in which no neutralizing activities were detected even against these sensitive viruses. There are good levels of ADCC activities in vaccinees' sera (95). When DP6-001 trial volunteer immune sera were tested against the more difficult to neutralize pseudotyped viruses from clades A to E and positive NAb was determined as greater than 50% inhibition, sera from approximately 1/3 of the volunteers were able to neutralize 80%–100% of this pseudotyped virus panel; the other 1/3 of the immune sera was able to neutralize 50%–79% tested viruses, and the remaining 1/3 of the immune sera neutralized 25%–49% of the tested viruses; serum from only one volunteer could neutralize only one pseudotyped virus (98). In addition, a neutralization assay was conducted against the most difficult to neutralize Tier 2 viruses, but the neutralizing activities were very low. In summary, the DP6-001 trial raised high level binding antibody and broad neutralizing antibody responses. Additional assays have been done to show high level anti-V2 antibodies in DP6-001 volunteers (unpublished data), similar to RV144 trial results.

The finding of high titer and high quality antibody responses in the DP6-001 trial was supported by another phase I DNA prime-Env protein boost clinical trial. A two-valent DNA vaccine prime, including one expressing an HIV-1 Gag and one expressing a V2-deleted gp140, were formulated in polylactice-coglycolides and delivered by intramuscular needle injection, followed by boost immunization using the recombinant gp140 protein matching that used in DNA prime. Compared to volunteers who received

gp140 protein alone immunizations, DNA priming generated skewed Th1 phenotype polyfunctional Env-specific CD4$^+$ T cells, a higher frequency of Env-specific memory B cells, and a higher titer of neutralizing antibodies and ADCC (101). However, the breadth of neutralizing activities in this trial was limited, presumably due to limited valency of Env immunogens included in the formulation and/or a potential negative impact of V2 deletion to the quality of antibody responses.

In summary, heterologous prime-boost strategy has been demonstrated to not only effectively augment the quantity level of immune response elicited by individual vaccine component alone, but also improve the quality of antibody and T cell responses. It has been a promising approach to combine distinct vaccine components to achieve balanced immune response for HIV-1 vaccine.

3. Env-specific monoclonal antibodies

3.1 Important role for antibodies in HIV prevention

The critical role of antibody in HIV prevention was initially demonstrated by passive immunization studies, during which, administration of single NAbs or a combination of NAbs prior to challenge in non-human primates were both able to prevent viral acquisition or, at least, lower the viral load (102-105). While antibody monotherapy might result in a transient reduction in viral load followed by rebounded viremia, a combination of new generation bNAbs that target different epitopes was able to fully control infection and suppress viral load to an undetectable level (106). In addition to direct antibody administration, vector-mediated gene transfer expressing several new generation bNAbs was also able to fully protect humanized mice from HIV infection (107). This protection was conferred by broad and potent neutralization activities against

viruses, as passive transfer of polyclonal non-NAbs with ADCC function failed to prevent HIV-1 infection (108). Meanwhile, Fc effector domain is also required for *in vivo* capacity for blockage of viral entry and suppression of viremia. For example, binding NAbs with activating Fcγ receptor (FcγR), but not inhibitory FcγR, were able to augment *in vivo* anti-HIV protective activity (109). All of this previous research suggests a pivotal role of both the antigen binding site and the Fc domain in *in vivo* anti-viral protection.

3.2 bNAbs from infected patients

For a long time, only 4 mAbs (b12 (110), 2G12 (111, 112), 2F5 (113, 114)and 4E10 (113, 115)) that could neutralize ~40% of HIV-1 viruses circulating throughout the world were available. Sera from elite neutralizers and new biotechnologies allowing for Env-specific B cell identification and isolation (116-120), have allowed for a considerable amount of bNAb to be isolated in the past 4 years (Table 1.1). Epitopes of novel bNAbs can be categorized into four groups: 1) CD4 binding site on gp120, including VRC01-VRC03 (116), HJ16 (121), VRC-PGV04 (122), CH30-CH34 (119), the HADD motif antibodies (117), CH103 (123). Crystal structure analysis along with deep sequencing of VRC01-like heavy chain variable (VH) region and light chain variable (VL) region showed a convergent mode of epitope recognition despite divergent sequences. Compared to b12, these mAbs can approach its cognate epitope on the functional spike with less steric hindrance. Indeed, it seemed that a restricted set of VH gene families (VH1-46 and VH1-2) was used to generate VRC01-like antibodies. Further, they all have an extraordinarily high number of somatic mutation (~30% for VH gene, ~18% for VL gene) whereas, the average human VH mutation is 5% elicited by immunization; 2) a quaternary epitope dependent upon N160 at V1/V2 region including

PG9, PG16 (124), CH01-CH04 (125) and PGT141-PGT145 (118). These antibodies were isolated through recognition of the conformational V1V2 epitope and shown to have a high degree of somatic mutation, ranging from 11.5% to 16%. Their long CDR3 regions are rich in tyrosines that are frequently sulfated; 3) N332 glycan-dependent V3 epitopes, including PGT121-123 (126), PGT135-PGT137 (118), PGT125-PGT1 (127), and PGT130-PGT131 (37). In contrast to CD4bs mAbs, this group of mAbs can approach Env from several different angles. PGT121-PGT123 bind to the V3 base, N332, and a glycan attached to V1/V2. Using long CDR H1 and CDR H3, PGT135 binds to glycans attached to N332, N392, and N386 as well as to peptide residues at adjacent beta strands between V3 and V4 loops. PGT128, PGT130, and PGT131 recognizes an epitope that includes the C terminal of V3 as well as N-glycan at N332 and N301 positions by adopting a long CDR3 and CDR2 from heavy chain. These antibodies are quite potent, but not as broad as CD4bs antibodies, since they could not neutralize some clade A and clade C viruses; 4) transmembrane protein gp41, including 10E8 and PGT151-PGT152 (128, 129). 10E8 is specific for a linear epitope on the gp41 MPER region (128). Different from previously isolated 2F5 and 4E10, 10E8 is not polyreactive and does not non-specifically bind to lipids but it was able to neutralize 98% of test viruses at IC_{50} below 50ug/ml. PGT151-PGT158 recognize a complex glycan dependent epitope on the both gp120 and gp41, and only recognize a properly formed, cleaved Env trimer(130). PGT151-PGT152 were able to neutralize two thirds of viral isolates at a median IC_{80} 24ng/ml (129).

Newly discovered bNAbs provide valuable information regarding vulnerable regions on the Env spike, which could be used as a guideline for immunogen design.

Table 1.1 Class of broadly neutralizing Env-specific antibodies isolated from infected individuals

Epitope category		antibody Class	representative mAbs	strucutal features	breadth	IC80 (ug/ml)	reference
gp120	CD4bs	HJ16	HJ16	extensive affnity maturaiton	30%	0.77	117
		VRC01	VRC01, NIH45-46	CD4-mimicry by V$_{H}$1-2heavy chain, extnsive affinity maturation	87%	0.98	112
			3BNC117, 3BNC60, 3BNC62		96%	0.3	113
			VRC-PG04		>75%	N/A	118
			CH30-34		>75%	N/A	115
		8ANC131	8ANC37, 8ANC131, 8ANC134	CD4-mimicry by V$_{H}$1-46 heavy chain	57%	4.02	113
		CH103	CH103	heavy chain recognition only	34%	8	119
	V1V2	PG9	PG9, PG16	penerating CDR H3, dependent on N160 glycan	70%	0.31	122
		CH01	CH01-CH04	V2/V3 conformational epitope	36%	2.4	123
		PGT145	PGT141-PGT145	discontiuous conformational epitopes	60%	0.31	114
	V3	PGT121	PGT121-123	recognize V1/V2 and V3 glycan	53%	0.08	120
		PGT128	PGT125-131	penetrating CDR H3, recognize C terminal V3 and V3 glycan (N332 and N301)	56%	0.11	121
		PGT135	PGT135-137	recognize V3 and V4 glycan	<39%	N/A	114
gp41	MPER	10E8	10E8, 7H6	not autoreactive	97%	2.05	124
gp120/gp41	interface of gp41 and gp120	PGT151	PGT151-PGT158	glycan depdent on both gp120 and gp41	66%	0.024	129, 130

N/A: not available in the literature

However, one caveat concerning these bnAbs is that they were isolated from chronically infected individuals. The host environment is very different in HIV-infected patients from that in healthy, uninfected people who are the target population of prophylactic HIV vaccines. First, in a vaccine setting, much lower immunogen dosing and a shorter exposure time are used for healthy populations than for those with chronic HIV-1 infection. Second, the unique features of Env-specific B cells observed in HIV-1-infected patients, such as hyper-activation of B cells and continuously elevated immunoglobin levels (131), which are responsible for the high degree of somatic mutation, long CDR3, and high autoreactivity of Env specific antibodies, are lacking in healthy humans. Therefore, it is not clear whether findings from how HIV and antibodies act in infected humans can be directly translated into developing vaccine-elicited antibodies for non-HIV infected individuals.

3.3. Env-specific animal mAbs from immunization

In order to better understand gp120 structure and function, a large panel of mouse mAbs derived from monomeric gp120 protein immunization has been reported in literature. Mouse mAbs epitopes include neutralizing epitopes against CD4bs, CD4i, C4, V3, V2 as well as non-neutralizing epitopes against C1 and C5 region (132).

Rhesus macaques are often used in the evaluation of immune responses to infection and vaccination. Phylogenetic tree analysis shows that rhesus and human heavy chain Ig loci are highly homologous (133); therefore, rhesus monkey is a desirable animal model to study antibody evolution elicited by vaccination. CD4bs monoclonal antibodies (mAbs) from gp140-F trimer-immunized monkeys have a lower degree of somatic hypermutation and neutralization activity against Tier1 but not Tier 2 viruses (133). Fine

epitope mapping showed these CD4bs epitopes elicited by vaccines overlapped with those of non-broadly neutralizing CD4bs mAbs but remarkably less so with VRC01. Recent developments in deep sequencing will further facilitate an understanding of the B cell repertoire as elicited by immunization.

The llama is also an important animal model for vaccine study as it has only one heavy chain. These unique llama mAbs have a long CDR3 and an additional disulfide bridge between CDR1 and CDR3. A panel of llama CD4bs or CD4i mAbs resulting from gp120 or trimeric gp140 Env immunization has been generated (134-136). Among them, at least three llama mAbs were able to potently neutralize ~96% of HIV-1 strains tested, equivalent to that of the new generation of mAbs from infected patients. This is the first time we have observed such potent and broad mAb induced by experimental immunization. However, the applicability of research in llamas to other animal models or humans is unclear due to the uniqueness of the llama heavy chain only antibody.

Rabbit is also an attractive animal model to study vaccine-elicited antibody response because rabbit is highly immunogenic in responding to various immunization regimens to produce high titer antibody responses. We will present original data from isolated rabbit mAbs using DNA prime protein boost vaccine in Chapter II.

3.4. Env-specific human mAbs from HIV vaccine trials

The first panel of human antibody clonal lineages was derived from HIV vaccine trial, GSK PRO HIV-002; in that trial, gp120 protein immunization was used (137). During affinity maturation, the epitope of one Ab (3491) shifted from the linear C2 region to a conformational epitope. This panel of mAbs showed only sporadic neutralization against one or two Tier 1 sensitive viruses. As expected, protein

immunization induced low level affinity maturation, with only ~3.8% mutation frequency observed.

Several unique mAbs were isolated from the RV144 trial. These antibodies have been critical in dissecting immune-correlate and biological functions of antibody responses. First, two V2-specific mAbs CH58 and CH59 were isolated and considered the immune-correlates in the RV144 trial (90). The antigen-contacting residues of CH59 include four residues (K169, H173, F176 and Y177), while CH58 has larger footprint also around K169 area. Although they bind at or near the site in V2 at which HIV-1 V1-V2 bNAbs (PG9 and CH01) also bind, CH58 and CH59 mAbs recognize a structurally heterogenous site. Increased vaccine efficacy against a virus with a V2 K169 residue was observed among vaccinees, suggesting that the immune pressure observed in the RV144 trial might be mediated by CH58- and CH59-like antibody responses. In addition, four mAbs, CH54, CH57, CH81, and CH91, were also isolated and shown to target at a conformational C1 epitope. Similar to A32, a conformational C1-specific mAb isolated from infected individuals(138), these mAbs also mediated ADCC responses (139). Furthermore, IgA mAb CH38 and CH29 were found to block ADCC activity mediated by C1-specific mAbs (139). This confirmed the previous finding showing that IgA responses correlate with infection risk.

In summary, pursuing vaccine-elicited monoclonal mAbs will not only help understand the antibody development pathway, but will also help us dissect out the most desirable antibody epitopes that have anti-viral activity.

4. **Research Framework and Objectives**

Use of information regarding the quality of vaccine-elicited humoral responses has helped lay a foundation for future vaccine design. Several lines of research including the RV144 trial and animal challenge studies, have provided more evidence suggesting that the coordinated activities of multiple antibody functions, including high affinity binding, neutralizing, and functional non-neutralizing antibodies, may be correlated with protection against acquisition of infection. The goal of the original work described here is to characterize the antibody profiles resulting from several major Env immunogens and regimens.

In first part of dissertation, I aim to determine the quality of antibody response elicited by HIV vaccination by isolating rabbit monoclonal antibodies (mAbs). To meet this goal, first, I expanded a novel rabbit monoclonal antibody platform to isolate antigen-specific mAbs. Second, I determined the binding, cross-reactivity, the degree of affinity maturation, binding specificity, and neutralization activity of these rabbit mAbs. Third, in collaboration with Dr. Xiang-peng Kong from New York University, we studied several representative rabbit mAbs with unique antigen specificities to understand structure-function relationship.

In addition, I evaluated the impact of unique N-glycan patterns on the antigenicity and immunogenicity of gp120 Env proteins. By using genetically engineered yeast cells in collaboration with GlycoFi, a division of Merck, six recombinant HIV-1 gp120 protein immunogens with unique glycan patterns were expressed and purified with high homogeneity. Their antigenic properties have been thoroughly analyzed and their immunogeneity has been determined in rabbits. These novel Envs are promising immunogens capable of inducing high quality antibody profiles.

Moreover, to advance beyond our current gp120 DNA prime gp120 protein boost vaccine strategy, I compared antibody profiles elicited by vaccination using different immunization schedules and immunogen forms. To do this, I compared simultaneous delivery of DNA and protein-based vaccination versus DNA prime protein boost vaccination, and examined the influence of gp120 monomeric Env versus gp160 trimeric Env (generously provided by Dr. Shiu-lok Hu from University of Washington) in the context of Env DNA prime protein boost vaccination. The distinct antibody profiles elicited by such vaccination studies will serve as important guidelines for future vaccine design.

Chapter II Section I

A novel rabbit monoclonal antibody platform to dissect the diverse repertoire of antibody epitopes for HIV-1 Env immunogen design

Introduction

Antibody research in the HIV-1 vaccine field has focused for a long time on the study of neutralizing human monoclonal antibodies (HmAbs) generated from HIV-1-infected patients. While these studies have provided remarkable information on the structural requirements for HmAb, in terms of the breadth and potency of their neutralizing activities, such unusually broad neutralizing HmAbs can only be identified in 2-4% of the infected population and only after two or three years' infection (140-143). In contrast, the role of non-neutralizing antibodies targeting other areas of Env was virtually unknown prior to the study of antibody responses in RV144 volunteers. RV144 provided a rare opportunity to study the quality of antibody responses in immunized individuals and it was shown that antibodies against the V2 region correlated with protection (88). Furthermore, several HmAbs from the RV144 trial that target the V2 region have been produced (90). Since it is a lengthy process to advance a candidate vaccine to human trials, most studies on the diversity and quality of antibody responses will be first conducted in experimental animals during the pre-clinical phase of HIV-1 vaccine development.

Previously, we reported the elicitation of cross-clade neutralizing antibody responses when a DNA prime-protein boost immunization approach was adopted to deliver a polyvalent Env immunogen formulation in animal and human studies (92, 95, 98). Further epitope mapping and antibody competition analyses identified quality

differences between immune sera elicited by the DNA prime-protein boost approach and the protein alone approach (96, 144). However, these studies were conducted using polyclonal sera and results from these studies were unable to link the observed antibody activities with a particular antibody component in a polyclonal serum.

Here we report the development of a recombinant rabbit monoclonal antibody (RmAbs) technology to monitor the specificity and neutralizing activities of antibodies elicited by a candidate HIV-1 Env immunogen. Historically, rabbit has been an attractive animal model for antibody studies and has been used more recently in HIV vaccine research because rabbit is highly immunogenic in responding to various immunization regimens to produce high titer antibody responses. It was shown that only RmAbs were able to provide high quality detection against certain difficult epitopes, such as those in tissue section samples and HIV viral particles (145-147). Rabbit antibodies usually carry limited background reactivity against testing antigens. Rabbits provide a large volume of immune sera for a wide range of antibody assays while the other common experimental animal species, such as mouse or rat, can only provide limited volume of immune sera, usually with high background in functional antibody assays. Moreover, rabbit immune system, but not that from mouse, is able to generate long CDR3 regions, which is important for many neutralizing antibodies against HIV-1 (148, 149).

In the current pilot study, a panel of 12 HIV-1 Env-specific rabbit hybridoma cell lines were produced that can recognize a wide range of Env epitopes. Furthermore, their heavy chain and light chain genes were cloned and their genetic features were analyzed. Recombinant RmAbs were produced from these rabbit Ig clones and their epitope specificity, binding affinity, and neutralization activities were determined.

Results

Generation of HIV-1 Env-specific hybridoma cell lines from a rabbit immunized with the DNA prime-protein boost JR-FL gp120 vaccine

In this pilot study to explore the feasibility of producing recombinant rabbit mAb specific for HIV-1 Env, one NZW rabbit from a previously published immunogenicity study (95) was used for MAb isolation and characterization. During the initial immunogenicity study, this rabbit received three DNA inoculations followed by two inoculations with gp120 protein from HIV-1 JR-FL (Fig. 2.1). By the time we decided to produce RmAb from this rabbit, it had been 16 weeks since the last immunization. Therefore, this rabbit was boosted further with a one-time JR-FL gp120 DNA immunization and a one-time recombinant JR-FL gp120 protein immunization separated by 4 weeks. Four days after the final protein boost, the rabbit spleen was harvested and sent to a subcontractor for production of hybridoma cells (Fig. 2.1).

A total of 57 multi-clonal stage hybridoma cells were screened for their supernatant reactivity against the JR-FL gp120 antigen (Fig. 2.2). Among them, 36 (63%) tested positive by ELISA, including two (R39 and R47) that were considered weakly positive (Fig. 2.2A). Western blot analysis further confirmed that a smaller fraction (17 hybridoma cells, 30%) had various levels of positivity against denatured JR-FL gp120 antigen (Fig. 2.2B). Based on the above screening results, a panel of 12 hybridoma cell lines (13, 15, 20, 27, 28, 31, 35, 41, 43, 52, 53, and 56) was selected for further production of stable monoclonal stage of hybridoma cells.

Diverse epitope profiles of gp120-specific RmAbs elicited by JR-FL gp120 immunogen
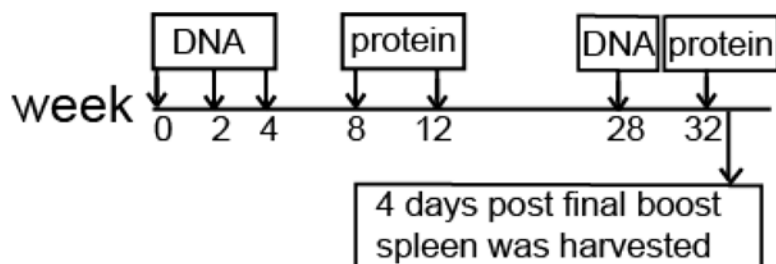
Figure 2.1. Schematic representation of the rabbit immunization schedule. The rabbit was given three times HIV Env encoding DNA at two-week intervals and followed by twice matched protein boost, monthly. After a 16-week resting period, this rabbit was further boosted with 1x DNA and 1x protein boost. The rabbit spleen was harvested 4 days after the final protein boost to generate hybridoma cell lines.
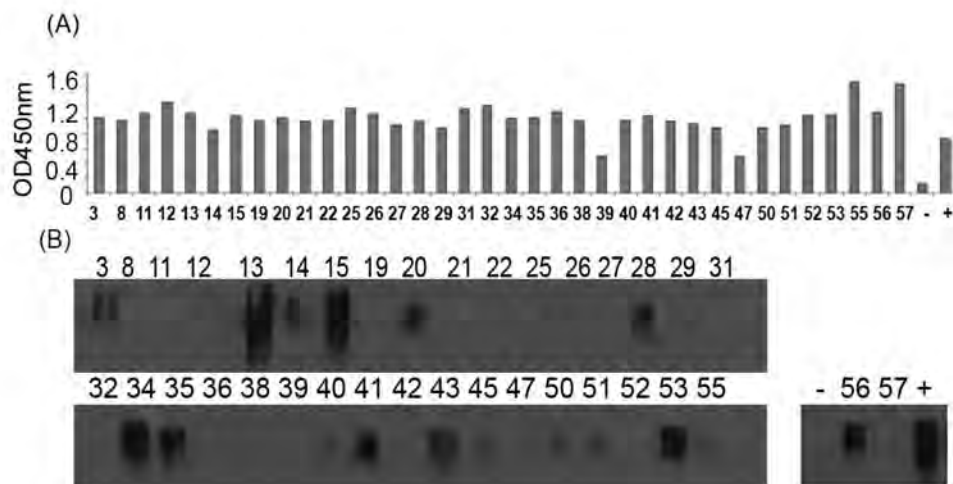
Figure 2.2. Initial screen of 36 multi-clonal stage of hybridoma cell lines by their binding to HIV-1 JR-FL gp120 protein. (A) Binding of rabbit hybridoma supernatants to HIV-1 JR-FL gp120 protein was tested by ELISA. The rabbit sera samples prior to immunization and at week 14 served as the negative control ("-") and positive ("+") control, respectively. (B) Testing hybridoma supernatants against JR-FL gp120 protein by Western blot. The positive and negative controls were same as (A).

The epitope specificity of these RmAbs was determined by an ELISA against linear peptides (15 amino acid (aa) residues each with 11 aa overlapping) spanning the entire length of consensus gp120 from M group of HIV-1. These 12 rabbit hybridoma cell lines could be divided into 5 groups based on their antigen epitope specificity (Fig. 2.3).

(1) V3 specific hybridomas – R20, R43, and R56 (Fig. 2.3A). These hybridomas recognized two different epitopes within V3 region. One hybridoma, R56, recognized the V3 crown, the principal target for most anti-V3 mAbs isolated from patients chronically infected with HIV-1. The other hybridomas R20 and R43 recognized the C terminal portion of the V3 region, an epitope not commonly seen by human mAbs but recently described as part of a key neutralizing epitope for several highly potent human mAbs, such as PGT128 (127).

(2) C4 specific hybridoma – R53 (Fig. 2.3B). Based on the epitope peptide sequence, R53 binds to the bridging sheet of gp120, a rare epitope only reported in a mouse study in early days of HIV-1 research (150, 151). One unique feature of R53 is that it can bind to two discontinuous linear epitopes in the C1 and C4 regions although there is limited sequence homology between these two peptides.

(3) C5 specific hybridoma - R13 (Fig. 2.3C). This hybridoma binds to the far C-terminus of gp120, a region known to be immunodominant (152).

(4) C1 specific hybridomas – R15, R35, and R41 (Fig. 2.3D). Supernatants from these three hybridoma cell lines were able to bind to the same three constitutive peptides in the first constant region of HIV-1 Env.

(5) Hybridoma with unknown epitope - R27, R28, R31, and R52 (Fig. 2.3E). These RmAbs did not bind to any of the peptides included in the overlapping M-group
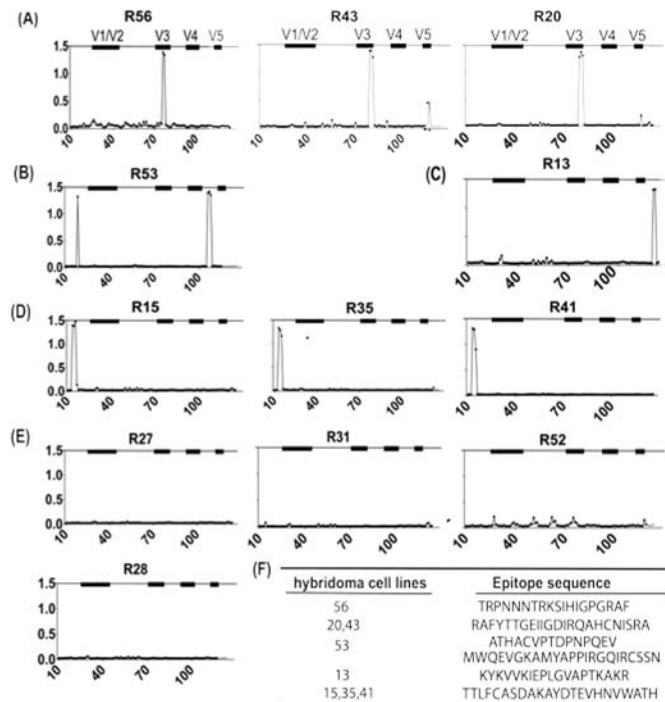
Figure 2.3. Diverse repertoire of gp120-specific rabbit monoclonal hybridoma supernatants revealed by ELISA with plates coated with individual consensus B gp120 overlapping peptides. RmAbs were grouped into the following five groups: (A) V3-specific (R20, R43, and R56); (B) C4-specific (R53); (C) C5-specific (R13); (D) C1-specific (R15, R35, and R41); (E) unknown epitopes (R27, R31, R52, and R28); (F) List of identified epitope sequences for selected rabbit hybridoma cell lines.

Env peptide pool. R27, R31, and R52 may recognize conformational epitopes as they showed positive ELISA binding against ConA-captured JR-FL gp120 (Fig. 2.2A) but no binding as observed by Western blot to the same but denatured gp120 antigen (Fig. 2.2B). For R28, because it showed positive binding by both ELISA and Western blot against JR-FL gp120, it is possible that R28 can only recognize a JR-FL-specific linear peptide that may be different from the sequences of the consensus clade B overlapping peptides.

Crystal structures have been produced for several RmAbs described in the current study. In particular, three RmAbs (R20, R56, and R53) have been co-crystalized with their respective targeted peptides, as described in the above epitope mapping analysis, confirming the accuracy of epitopes mapped by ELISA (153).

Broad binding profile and high affinity of RmAbs against gp120 proteins from different clades of HIV-1

The gene transcripts of the full length IgG heavy chains and light chains from the above RmAbs were cloned from these hybridoma cells by RT-PCR and further subcloned into a mammalian protein expression vector. Individual recombinant RmAbs were produced from 293T cells transiently transfected with these RmAb-expressing molecular clones.

Recombinant RmAbs were individually characterized for their ability to bind to a panel of five recombinant gp120 proteins (92UG037, JR-FL, 93MV965, 92UG021, and consensus AE Env, representing clades A, B, C, D, and E, respectively) (Fig. 2.4). All isolated rabbit mAbs were able to bind well to JR-FL gp120 by ELISA but had different levels of binding against other gp120 antigens. Among the V3-specific RmAbs, R56
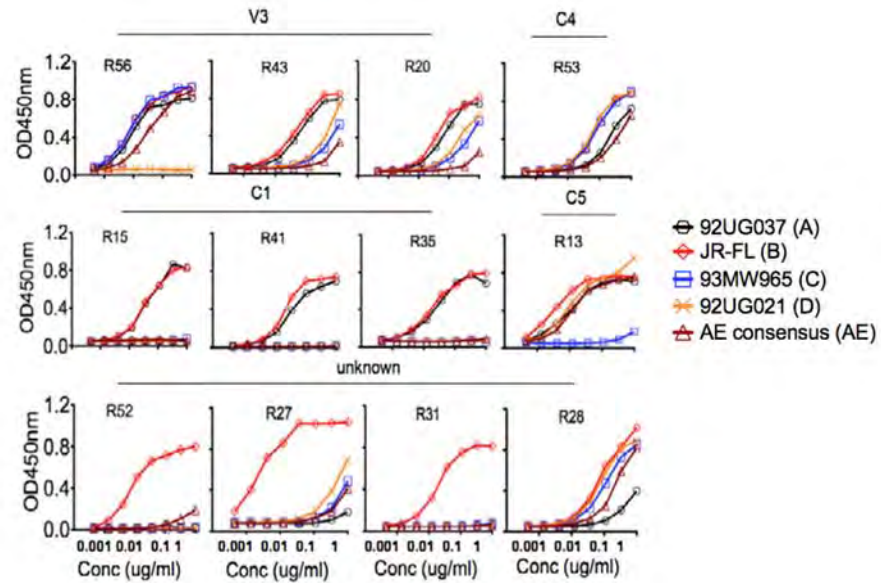
Figure 2.4. The reactivity of 12 RmAbs with a panel of representative gp120 proteins revealed by ELISA. HIV-1 Env gp120 proteins were derived from the following isolates 92UG037, JR-FL, 93MW965, 92UG021, and consensus AE.

binds to four gp120 proteins but not that from the clade D isolate, 92UG021. The tip of V3 loop for clade D gp120, 92UG021, has a very different sequence GVGR vs. the more common GPGR or GPGQ sequences seen with other clades, in addition to unique sequences immediately upstream of the V3 tip (Fig. 2.8). The other two V3 RmAbs, R20 and R43, bind gp120 proteins from JR-FL and clade A isolate, 92UG037, better than other three gp120 proteins from clades C, D, and E isolates. This is also consistent with overlapping peptide ELISA (Fig. 2.3) and phylogenic lineage (Fig. 2.7) results, which showed that R20 and R43 are grouped together in both analyses.

R53 is one RmAb that was broadly reactive with all five gp120 proteins from different clades. In contrast, C1-targeted RmAbs (R15, R41, and R35) uniformly bind to two gp120 proteins from clade B (JR-FL) and clade A (92UG037) with high efficiency.

Three RmAbs recognizing conformational epitopes, R52, R31, and R27, appeared to be highly specific to JR-FL gp120, whereas low to no detectable binding was observed for the other four gp120 proteins tested. R28, which targeted at unknown linear epitope, was broadly reactive to all five gp120 proteins, but the overall binding affinity was low, especially to gp120 protein from clade A isolate, 92UG037.

More detailed binding kinetics, including the binding affinity of these recombinant RmAbs, was further measured using a ForteBio instrument based on recently developed Bio-Layer Interferometry (BLI) technology. This system is similar to the traditional Biacore technology but is more user-friendly and can process a large number of samples simultaneously. Actual measurements for three RmAbs (R15, R53, and R56) are shown in Fig. 2.5. All RmAbs exhibited a considerably high binding affinity to JR-FL gp120 with K_D ranging from 0.02 nM to 4.47 nM (Fig. 2.5).

Gene sequence analysis of HIV-1 gp120-specific RmAbs

The full-length IgG heavy chain and light chain genes of the RmAbs were sequenced. Germline family usage, mutation frequency, and CDR3 length in heavy chain and light chain were determined using IMGT and V-QUEST (Fig. 2.6 and Table 2.1). Consistent with a recent report (154), most of the isolated RmAb heavy chain genes preferentially utilized IGHV1S40*01 (IMGT numbering system) or a3-VH1 (Kabat numbering system) as the germline family gene while only R13 and R31 used IGHV1S45*01 (IMGT numbering system) or a3-VH4 (Kabat numbering system). For light chain, diverse germline gene families were utilized to generate gp120-specific mAbs.

Somatic hypermutation (SHM) is a key parameter in evaluating antibody affinity maturation. In the most studied influenza immunization, the mean VH mutation frequency of human antibodies induced by repeated vaccination is ~5% (155, 156). Among 12 gp120-specific RmAbs identified in the current study, heavy chain V genes exhibited an average SHM of 14.6 ± 9.2% (ranging 5 to 27%) at the amino acid level, while light chain V genes exhibited an average of SHM of 9.25 ± 1.5% (ranging 7 to 12%), indicating that the immunization regimen used in this study was effective in stimulating a high SHM rate of gp120 antigen-specific Ab genes (Table 2.1). The mutated amino acids for heavy chains were mainly distributed in CDR1 and CDR2 region, while SHM occurred across the light chain kappa gene (Fig. 2.6). Examination of the heavy chain CDR3 region revealed an average length of 10.9 ± 6.5 aa (ranging 6 to 23 aa) and the light chain CDR3 region contained an average of 11.5±1.7 aa (ranging from 8 to14 aa) (Table 2.1), compatible with rabbit mAbs elicited from immunization, as
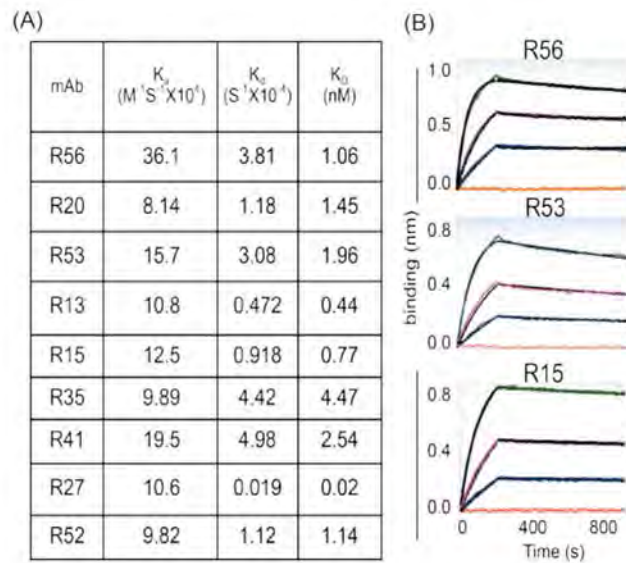
Figure 2.5. Binding affinity of rabbit mAbs to JR-FL Env gp120 protein determined by a ForteBio Octet QK^e system. Rabbit mAbs were immobilized on the chip surface and the JR-FL gp120 proteins were added in the testing solution. (A) The rate constants, K_a, K_d and K_D, for rabbit mAbs binding to JR -FL gp120, which were obtained by global fitting the curves to 1:1 binding model. (B) The binding kinetics of three selected RmAbs, R56, R53, and R15, to three-fold serial dilution of JR-FL gp120 protein.

```
Heavy chain   --------FR1-------------  CDR1  --------FR2------  CDR2  --------FR3--------------------------  CDR3_____  -----FR4---
IGHV1S40*01   QS-LEESGGDLVKPGASLTLTCTASGFSFSSSYYMCWVRQAPGKGLEWIACIYAGSSGSTYYASWAKGRFTISKTSSTVTLQMTSLTAADTATYFCAR
R13           QEQLEESGGGLVKPGTSLTLTCTASGFSFSSSYWIXWVRQAPQKGLEWIACIDVGSSRTTYYASWAKGRFTVSETSSTTVTLQMTSLTAADTATYFCART---------------LNLWGPGTLVTVSS
R15           QEQLVESGGGLVKPGASLTLTCKGSGIDFS-SVGIAWARQAPGKGLEWIAYIWTSTGH-TGYASWAKGRFTVSKTSATTVTLQMTSLTAADTATYFCARN---------------WDLWGPGTLVTVSS
R28           QS-LEESGGGLVKPGGTLTLTCKVSGIDFSVHYYMCWIRQAPGKGLEWIACIVFGGSGSTYYANWAKGRFTISRSSSTTVTLQMTSLTAADTATYFCAR---------------IFDLWGPGTLVTVSS
R35           QS-LEESGGDLVQPEGSLTLTCKGSGIDFS-SVGIAWVRQAPGRGLEWIAYIWTSTGH-TGYASWAKGRFTVSKTSATTVTLQMTSLTAADTATYFCARN---------------WDLWGPGTLVTVSS
R41           QS-LEESGGDLVQPERSLTLTCKGSGIDFS-SAGIAWVRQAPGKGLEWIAYIWTSTGH-AGYASWAKGRFTVSKTSATTVTLQMTSLTAADTATYFCARN---------------WDLWGPGTLVTVSS
R53           QS-LEESGGGPVKPGGTLTLTCKASGIDFSSFYYMCWVRQAPGKGLEWIACIVTDITGESYYATWAKGRFAISKTSSTTVTLQMTSLTAADTATYFCARGDTY------DYGDTVYALNLWGPGTLVTVSS
R52           QS-LEESGGDLVKPGASLTLTCTASGFDLSGYLYMCWVRQPPGKGLEWIACIVTGSSGSTYYASWAKGRFTISQTSSTTVTLQMTGLTVADTATYFCARGDYS---YGGAFLPVAYYFNFWGPGTLVTVSS
R56           QS-LEESGGDLVQPGASLTLTCKASGFSFGNHYDMCWVRQAPGKGLEWIGCIETGSSDSAAYATWAKGRFTISKTSSTTVTLQMTSLTAADTATYFCARN---------------FDLWGPGTLVIVSS

IGHV1S45S*01  QEQLEESGGDLVRPEGSLTLTCTASGFSFSSSYWICWVRQAPGKGLEWIACIYAGSSGSTYYASWAKGRFTISKTSSTTVTLQMTSLTAADTATYFCAR
R20           QS-LEESGGDLVKPGASLTLTCTASGFSFTNHYYMCWVRQAPGKGLEWIACIYGGGRDIVFYATWAKGRFTISKTSSTTVTLQMTSLTAADTATYFCARENFDAVGVGGGTYSTDYYFDLWGPGTLVTVSS
R31           QS-LEESGGGLVQPEGSLTLTCKASGFSFSRTYGICWVRQAPGKGLEWIACIYAGSGR-TYYASWAKGRFTGSKTSSTTVTLQLNSLTAADTATYFCARDMFG---------YGEAAYDLWGPGTLVTVSS


light chain   ---------FR1-------------  CDR1  -----FR2----------  CDR2----------  FR3-------------------  CDR3_____  -----FR4---------
IGKV1S33*01   DPMLTQTASPVSAAVGSTVTISCQASQSVYNNNHLSWYQQKPGQPPKLLIYSASKLATGVPSRFSGSGSGTQFTLTISGVQCDDAATYYC
R15           DPVLTQTPSSVSAAVGSTVTISCQGSSQSVFQNNGLYWYQQKPGQPPKLLIYRASKLESGVPSRFSGSGSGTQFTLTISDLECDDAATYYCAGSYRPN----LYPFGGGTEVVVKGDPVAP

IGKV1S3*01    AQVLTQTPASVSAAVGGTVTINCQASESIS-G-TLGWYQQKLGQPPKLLIYIASTLASGVPSRFNGSGGGTEFTETISGVQCDDASTYYC
R20           DIVMTQTPASVSAAVGGTVTINCQASETI--SNYLAWYQQKPGQPPKLLIYKASTLASGVSSRFKGSGSGTEYTLTISGVQCDDAATYYCQQGY-SIS-DIDNSFGGGTEVVVKGDPVAP
R52           AVVMTQTPASVSAAVGGTVTIHCQASESIG-SHYLSWYQQKPGQPPKLLIYGASTLASGVPSRFKGSGSGTDYTLTISGVQCDDAGTTYCLYGYRSGSS-ADHTFGGGTEMVVKGDPVAP

IGKV1S52*01   DPMLTQTASPVSAAVGGTVTISCQSSQSVYNNNWLSWYQQKPGQPPKLLIYGASTLASGVPSRFKGSGSGTQFTLTINGVQCDDAATYYC
R28           AQVLTQTPASVSAAVGGTVTISCQSSESVAKSNYLSWYQQKPGQPPKQLIYGASTLASGVPSRFKGSGSGTQFTLTISDVQCDDAAAYYCAGQYSFSSDN-FFAFGGGTEVVVKGDPVAP
R31           AAVLTQTPSPVSAAVGGTVTISCQSSQSVHHNRNWLSWYQQKPGQPPKLLIYYASILASGVPSRFKGSGSGTQFTLTISDVQCADAATYYCAGGYIDVSD---TAFGGGTEVVVKGDPVAP
R35           DPVLTQTPSSVSADVGGTVTISCQSSQSVYQSNGLYWYQQKPGQPPKLLIYRASTLESGVPSRFKGNGSGTQFTLTISDLECDDAATYYCAGSYRPN----LYPFGGGTEVVVKGDPVAP
R41           DPVLTQTPSSVSADVGGTVTISCQSSQSVYQSNGLYWYQQKPGQPPKLLIYRASTLESGVPSRFKGSGSGTQFTLTISDLECDDAATYYCAGSYRPN----LYPFGGGSEVVVKGDPVAP

IGKV1S49*01   DPVLTQTPSSACKPVGGTVTTKCQASESIS--SRLAWYQQKPGQSPFLLTISASTLASGVFSRFKGSGSGTEYTLYTSDLECADAATYYC
R53           GFVLTQTPPSASEPVGGTVTIKCQASQAIDEY--LGWYQQKPGQRPKLLMYYASTLASGVPSRFKGSGSGTQPTLTISDLECADAATYYCQNYYVGSSTNYAPTFGGGTEVVVKGDPVAP

IGKV1S15*01   AQGPTQTPSSVSAAVGGTVTINCQTSKSFYSIDNILSWYQQKPGQPPFLLIYDASTLASGVPSRFKGSGSGTQFTLTISDVQCDDAATYYC
R13           AQVLTQTPSPVSAAVGGTVTINCQASESVYSNDRLAWFQQKAGQPPKRLIYGTTSLOSGVSSRFKGSGSGTQFTLTISDVQCDDAATYYCLGGYYSSDWY--FVFGGGTEVVVKGDPVAP
R56           AQVLTQTPSSVSTAVGSAVTINCQSSQHVYSNNHLAWFQQKPGQPPRLLIYDASKLASGVPSRFKGSGSGTQFTFTISDVQCDDAATFYCLGGYDCSSG-DCAAFGGGTEVVVRGDPVAP
```

Figure 2.6. Protein sequences of heavy and light chain variable regions of gp120-specific rabbit mAbs. The sequences are aligned to their corresponding putative germline genes. Framework region (FR) and CDRs are indicated based on IMGT (http://www.imgt.org/) nomenclature. Somatic mutated amino acids compared to the putative germline are in red and CDR3 regions in blue.

Figure 2.7. Phylogenetic tree of heavy chains and light chains gene sequences constructed using maximum likelihood method. V3-specific RmAbs were highlighted in red, C1-specific mAbs in orange, C4-specific mAbs in cyan, C5-specific mAbs in blue, and conformational/unknown RmAbs in black.

Table 2.1 Characteristics of the variable region of heavy chains and light chains of the vaccine-elicited rabbit mAbs.

Epitope	RMAb	Heavy chain					Light chain				
		IGHV		IGHJ		CDR3 length (aa)	IGKV		IGKJ		CDR3 length (aa)
		Germ line	Mutation (%)	Germ line	Mutation (%)		Germ line	Mutation (%)	Germ line	Mutation (%)	
V3	R56	S40*01	6	4*01	9	6	S15*01	9	2*01	10	13
	R20	S40*01	6	4*01	5	23	S3*01	8	2*01	3	12
	R43	S40*01	6	4*01	6	6	S37*01	8	2*01	3	11
C4	R53	S40*01	10	4*01	9	17	S49*01	9	2*01	13	15
C1	R15	S40*01	27	4*01	11	6	S33*01	12	2*01	10	10
	R35	S40*01	26	4*01	11	6	S52*01	10	2*01	3	9
	R41	S40*01	26	4*01	11	6	S52*01	9	2*01	9	10
C5	R13	S45*01	5	4*01	9	6	S15*01	11	2*01	8	12
Conformational/unknown	R27	S40*01	23	4*01	15	15	S10*01	11	2*01	10	10
	R28	S40*01	10	4*01 or 2*01	11	6	S52*01	9	2*01	10	13
	R31	S45*01	22	2*01	12	14	S52*01 or S64*01	7	2*01	5	11
	R52	S40*01	8	4*01 or 4*02	3	20	S3*01	8	2*01	3	12

previously reported (157).

To define the genetic relationship of these RmAbs, phylogenetic trees were constructed based on heavy chain and light chain gene sequences using the maximum likelihood method (Fig. 2.7). Interestingly, RmAbs targeting at the same region of gp120 tend to cluster together to form an independent subtree. For example, heavy chains and light chains from R15, R35, and R41 (all targeting the C1 region) formed independent subtrees. Similarly, the heavy chain from three V3-specific RmAbs, R56, R20, and R43, grouped into another subtree, whereas the light chain genes of R43 and R20 clustered in a subtree but not with R56. This demonstrates a process of clonally-related B cell lineage development and affinity maturation. At the same time, building a phylogenetic tree may help determine the biological relevance of Env-specific RmAbs.

The breadth and potency of neutralizing activities with individual gp120-specific RmAbs

A screening neutralization assay was conducted using an in-house assay at the University of Massachusetts Medical School to first identify those RmAbs with possible neutralizing activities (Table 2). Because this particular rabbit was immunized with a clade B gp120 antigen, a standardized in-house TZM-bl assay was used with a small panel of pseudotyped viruses expressing HIV-1 Env antigens from clade B viruses representing both neutralization-sensitive (Tier 1) and neutralization-resistant (Tier 2) primary isolates. Among 12 isolated RmAbs, 3 showed positive neutralizing activities in this initial screening assay. V3-specific R56 displayed potent neutralizing activity against SF162 (IC$_{50}$=0.02 µg/ml) and to a lesser degree against another sensitive Tier 1

```
                    296                                    332
JR-FL (B)       CTRPNNNTRKSIHIGPGRAFYTTGEIIGDIRQAHC
92UG037(A)      CTRPNNNTRKSVRIGPGQTFYATGDIIGDIRQAHC
93MV965(C)      CTRPNNNTRKSVRIGPGQTFYATGAIIGDIRQAHC
92UG021(D)      CTRPYDKVSYRTPIGVGRASYTT-RIKGDIRQAHC
AE cons(E)      CTRPSNNTRKSITIGPGQVFYRTGDIIGDIRKAYC
```

Figure 2.8. V3 region protein sequences from isolates JR-FL, 92UG037, 93MW965, 92UG021, and consensus AE. The residue position refers to the HXB2 strain. The R56 epitope is highlighted in orange and the R20 epitope is in blue. The amino acids within V3 region that differed from the JR-FL strain are highlighted in red.

Table 2.2 Neutralization IC$_{50}$ (µg/ml) of rabbit MAbs by in-house TZM-bl assay

| | C4 | V3 | | C1 | | C5 | Unknown/Conformation | | | |
	R53	R56	R20	R15	R41	R13	R27	R28	R31	R52
Tier 1										
SF162	0.5	0.02	>50	1.03	>50	>50	>50	>50	>50	42.5
SS1196	31.9	4	>50	28	>50	>50	>50	>50	>50	>50
Tier 2										
JR-FL	>50	>50	>50	>50	>50	>50	>50	>50	>50	>50
QH0692	>50	8.6	>50	>50	>50	>50	>50	>50	>50	>50
6535	>50	>50	>50	>50	>50	>50	>50	>50	>50	>50
aMLV	>50	>50	>50	>50	>50	>50	>50	>50	>50	>50

Table 2.3 Neutralization IC$_{50}$ (µg/ml) of rabbit MAbs by PhenoSense assay at Monogram Biosciences

Tier 1	Clade	R53	R56
SF162	B	<1.9	<1.9
MN-3	B	<1.9	>50
NL4-3	B	<1.9	>50
Tier 2			
92RW020	A	12.2	>50
94UG103	A	10.7	>50
AC10.0.29	B	11.3	>50
JRCSF	B	12.9	>50
PVO.4	B	<5.6	>50
QH0692	B	10.1	12.5
SC422661	B	13.5	>50
93IN905	C	12.7	>50
98CN006	C	8.9	>50
92UG046	D	4.6	>50
94UG114	D	11.0	>50
97TH021	AE	9.4	>50
CMU02	AE	11.3	>50
aMLV		>50	>50

Table 2.4 Neutralization IC$_{50}$ (µg/ml) of rabbit MAbs by TZM-bl assay at CAVIMC

Tier 1 virus	Clade	R53	R56	R15	Tier 2 virus	Clade	R53	R56	R15
SF162.LS	B	6.22	0.10	2.13	JRFL.JB	B	>50	>50	>50
Bal.26	B	>50	2.07	>50	AC10.0.29	B	>50	>50	>50
MN-3	B	>50	>50	>50	REJO4541.67	B	>50	>50	>50
SS1196.1	B	>50	7.18	26.20	CAAN5342.A2	B	>50	>50	>50
Bx.08.16	B	21.16	3.18	23.17	TRO.11	B	>50	>50	>50
BZ167.12	B	>50	>50	>50	Thro4156.18	B	36.7	>50	>50
6535.3	B	>50	>50	>50	Du422.1	C	>50	>50	>50
MW965.26	C	6.62	<0.02	0.27	ZM135M.PL10a	C	>50	>50	8.02
ZM109F.PB4	C	>50	>50	>50	ZM249M.PL1	C	>50	>50	>50
ZM197M.PB7	C	>50	>50	>50	CNE19	BC	>50	>50	>50
00836-2.5	C	>50	>50	>50	CNE20	BC	>50	>50	>50
25710-2.43	C	>50	>50	>50	Q461.e2	A	>50	>50	>50
TV1.21	C	>50	25.63	14.40	Q769.d22	A	>50	>50	>50
Q23.17	A	>50	>50	>50	0330.v4.c3	A	>50	>50	>50
MS208.A1	A	>50	>50	>50	T257-31	AG	>50	>50	>50
TH023.6	AE	>50	18.57	2.22	263-8	AG	>50	>50	>50
DJ263.8	AG	>50	0.64	>50	T250-4	AG	>50	>50	>50
242-14	AG	>50	>50	22.21	R1166.c01	AE	>50	>50	>50
T271-11	AG	>50	15.08	>50	R3265.c06	AE	>50	>50	>50
					C2101.c01	AE	>50	>50	>50
					R2184.c04	AE	>50	>50	>50
					CNE8	AE	>50	>50	>50
					C3347.c11	AE	>50	>50	>50
					X1193_c1	G	>50	>50	>50
					X1254_c3	G	>50	>50	>50

virus SS1196 (IC_{50}=4.0 µg/ml) and a Tier 2 virus QH0692 (IC_{50}=8.6 µg/ml). C4-specific R53 had potent neutralizing activity against SF162 (IC_{50}=0.5 µg/ml) but much less so against SS1196 (IC_{50}= 31.9 µg/ml). It is interesting to see that R15, a C1-specific RmAb, was also able to neutralize SF162 and SS1196, suggesting a novel neutralizing epitope within the C1 region, at least to certain sensitive viruses.

To further map the breadth of neutralizing activities of RmAbs, a high throughput neutralizing assay was conducted at Monogram, Inc. using its PhenoSense[TM] assay system. R53 and R56 were tested against three highly sensitive viruses in addition to 13 primary isolates covering clades A to AE (Table 2.3). V3-specific R56 showed neutralizing activities against SF162 and QH0692, confirming the screening assay results, but was unable to neutralize other pseudotyped viruses. Interestingly, C4-specific R53 neutralized all three sensitive viruses with high potency (IC_{50} < 1.9 µg/ml) and a wide range of primary isolates from various clades although at a low potency.

Because a number of the primary viral isolates used in Monogram's assay were not characterized as either Tier 1 or Tier 2 viruses, final neutralization assays were conducted by the Comprehensive Antibody Vaccine Immune Monitoring Consortium (CAVIMC) of the Collaboration for AIDS Vaccine Discovery (CAVD) program supported by the Bill & Melinda Gates Foundation. RmAb R56, R53, and R15 were tested against a panel of well characterized pseudotyped viruses expressing Env from a wide range of primary HIV-1 isolates, including 19 Tier 1 viruses (2 clade A, 7 clade B, 6 clade C, 1 clade AE, and 3 clade AG) and 25 Tier 2 viruses (3 clade A, 6 clade B, 3 clade C, 3 clade AE, 3 clade AG, 2 clade BC, and 2 clade G) (Table 2.4). V3-specific R56 showed potent neutralizing activities (IC_{50} titer<1 µg/ml) against Tier 1 Clade B viruses

SF162.LS, Clade C viruses MW965.26, and Clade AG viruses DJ263.8; while exhibited moderate to low neutralizing activities against three Tier 1 Clade B viruses (SS1196.1, Bal.26, and Bx.08.16), one Tier 1 Clade C virus (TV1.21), one Clade AE virus (Th023.6) and one Clade AG virus (T271-11). C4-specific R53 was also able to neutralize 3 Tier 1 viruses (SF162.LS, MW965.26 and Bx08.16) and 1 Tier 2 virus (Thro4156.18) at low potency. No other viruses on this panel were neutralized by R53. C1-specific R15 was able to neutralize seven Tier 1 viruses, including SF162.LS, SS1196.1 and Bx.08.16 (Clade B), MW965.26 and TV1.21 (both are Clade C), TH023 (Clade AE), 242-14 (Clade AG) and 1 clade C Tier 2 virus, ZM135M.PL10a.

Discussion

In the past few years, experience in producing high quality HIV-1 Env specific mAb from animal models is limited. Recently, a panel of CD4bs-directed macaque mAbs elicited by an Env vaccine was identified (133) but the high cost of NHP studies prevents the wide adoption of this system. Historically, murine mAbs were unable to achieve good neutralizing activities, partially due to the poor efficacy in generating long CDR3 for mouse mAbs (148, 149). Transgenic mouse systems expressing human antibodies are well established; however, many of these systems are under the control of major pharmaceutical companies, preventing scientists not affiliated with these companies to have easy access to these models due to intellectual property barriers. Newly developed humanized mice models are making progress in HIV infection studies, including the analysis of T cell responses, but their use for B cell and antibody development has not been fully developed (95, 96).

Results presented in this report established the feasibility of producing high quality Env-specific and potentially functional rabbit mAbs. Rabbit is an attractive model to study antibody responses against a wide range of emerging infectious diseases vaccines including HIV-1 (92, 95, 96, 144, 158, 159). Rabbits share common features in B cell development similar to those in mice and human and those of gut-associated lymphoid tissues (GALT) species, such as chickens, sheep, and cows (160). B lymphopoiesis in rabbit occurs similar to that in the human and mice classical pathway in the bone marrow; however, as a member of the GALT species, rabbit B lymphopoiesis terminates during early development (161). The exogenous antigen will further expand and diversify B cell in GALT through somatic hypermutation and gene conversion. Furthermore, phylogenetic analysis showed that human heavy chain variable (VH) genes can be divided into three major groups, A, B, and C; and all rabbit VH genes are closely related to one another and form one monophyletic group, which is included in VH group C (162). Among those VH genes, most rabbit B lineage cells rearranged the same VH gene, VH1, which encodes the VHa allotypic sequence and rabbits preferentially use it to produce functional antibodies (163). The rabbit humoral system can serve as a simplified testing platform to study the evolution pathway of antibody genes, since the rabbit adopted a much less complicated germline usage compared to mouse and human. On the other hand, it was speculated that no VRC01-like antibody will be raised in rabbits due to the lack of an optimal germline VH segment (164).

The phylogenetic analysis suggests that the human and rabbit Ig genes evolved at nearly the same rate. In contrast, most mouse genes evolved considerably faster than human and rabbit genes (162). Gene conversion and somatic hypermutation occur not

only in the germinal center (GC) of the young rabbit appendix, but are also used for diversification during the immune response in secondary lymphoid tissues, such as the spleen (165). Rabbit B cells see antigen in a similar manner as does the human immune system (166). A rabbit hybridoma fusion partner was developed previously (167) and optimization of the traditional rabbit fusion partner cells and fusion methods greatly facilitated the generation of monoclonal antigen-specific rabbit hybrdioma cell lines (US patent No.: US 7,575,896 B2 and US 7,732,168 B2), allowing for relatively efficient production of RmAbs and use in our current study as a contracted service.

In this first report of HIV-1 Env-specific rabbit mAb, a wide diversity of epitopes was identified from a single immunized rabbit, which showed high levels of serum polyclonal antibodies against the autologous JR-FL gp120 antigen. Besides the common V3 loop-specific rabbit mAbs, other rabbit mAbs were produced against both linear epitopes at either N-terminal or C-terminal regions of gp120 and conformational epitopes. Several epitopes were not previously known. At the time of this study, the role of V2-specific antibodies was not known therefore, efforts were not devoted to cloning V2-specific RmAbs in this study. However, serum from this rabbit did show positive antibody responses, recognizing gp70-V1V2 antigen, indicating the presence of V2-specific antibodies.

Three of twelve RmAbs cloned in this pilot study showed positive neutralizing activities. R15 indicated a previously unknown neutralizing epitope in the C1 region of Env as it was able to neutralize several viral isolates across subtypes B, C, AE and AG, although these viruses are from Tier 1 groups and the potency of R15 was low. V3-specific R56 demonstrated high potency against those viral isolates that were sensitive to

V3 neutralization, but the breadth of R56 was limited as would be expected from mAbs recognizing the tip of V3 loop.

The third neutralizing mAb R53 is the only one in this pilot study that was able to bind all five gp120 antigens from subtypes A to E and also showed broad neutralizing activities in Monogram assays despite low potency. Interestingly, previous studies reported that several murine mAb (151), as well as rat mAbs (150), isolated from gp120 protein immunization, were able to prevent gp120 binding to CD4. They mainly bound to a region on aa 430-447 of C4 region which is now known as part of the Env bridging sheet. Crystal structure analysis showed that R53 actually binds to the beta strand 21 region within the bridging sheet (153). R53 was also able to compete with b12, a CD4bs-directed mAb. The bridging sheet, along with the interface of outer domain and inter domain of Env compose the CD4 binding site. Upon CD4 binding, the bridging sheet undergoes a conformational change and enables the formation and exposure of the co-receptor binding site. Given the broad reactivity of R53 against a wide range of primary gp120 proteins across different subtypes and its ability to neutralize multiple Tier 1 pseudoviruses from different clades, future Env vaccine studies should further investigate the protection potential of this class of bridging sheet targeting antibodies.

In this pilot study, RmAbs were first screened by conventional ELISA against recombinant monomer gp120 antigens. Screening based on recognition of viral particles or positive neutralizing antibody activities will improve the chance of identifying more functionally relevant mAbs. Furthermore, limited by the cost restraints associated with the contracted service used, not all gp120-positive hybridomas from the initial screening were further cloned which reduced the understanding on the full spectrum of gp120-

specific RmAb elicited by immunization. Alternative technologies that can isolate individual gp120-positive B cells, similar to those developed for human mAbs, should be applied to RmAbs production in future studies.

Studies of HIV-1-specific human mAbs have suggested that somatic hypermutation and unusually long heavy chain CDR3, as two key indicators for affinity maturation, are usually required for broad and potent neutralizing activities of human mAbs (128, 168-170). Rabbit mAbs identified in the current study showed various levels of hypermutation and length of CDR3, suggesting HIV-1 vaccines delivered in the current prime-boost format were able to initiate the antibody maturation process. It is not known whether the low potency observed in several neutralizing RmAbs could be improved if the affinity maturation process is further enhanced, such as by a different adjuvant. Also, the current study only examined the status of affinity maturation at the end of a full vaccination schedule. Observing the induction of gp120-specific antibody responses throughout the entire process starting from time points before immunization or early in immunization, by using the new RmAb platform, will provide more insight on this process.

As learned from studies following the RV144 trial, antibody activities detected *in vitro* can link to correlates of immune protection, and identifying the effector mAbs would be helpful to evaluate vaccine-elicited humoral immune response. Isolation of mAbs from preclinical vaccine studies using small animal or non-human primate models will help us understand the antibody response and B cell development driven by immunization. The RmAb platform described in the current report will provide a useful tool to achieve such goals.

Chapter II section II

Rabbit Anti-HIV-1 Monoclonal Antibodies Raised by Immunization Can Mimic the Antigen-Binding Modes of Antibodies Derived from HIV-1-Infected Humans

Abstract

Here we present structural analyses of two rabbit monoclonal antibodies (mAbs), R56 and R20, against the third variable region (V3) of HIV-1 gp120. R56 recognizes the well-studied immunogenic region in the V3 crown, while R20 targets a less-studied region at the C terminus of V3. By comparison of the Fab/epitope complex structures of these two antibodies raised by immunization with that of the corresponding human antibodies derived from patients chronically infected with HIV-1, we found that rabbit antibodies can recognize immunogenic regions of gp120 and mimic the binding modes of human antibodies. This result can provide new insight into the use of the rabbit as an animal model in AIDS vaccine development.

The rabbit mAb structural analysis was conducted by Dr. Xiangpeng Kong from New York University School of Medicine. We provided the reagents R56 and R20. The full illustration of this work is in Appendix I.

Chapter II section III

Masking of an immunogenic epitope region in HIV-1 gp120 C4 critical

for receptor and co-receptor binding

Introduction

HIV-1 surface envelope glycoprotein gp120 initiates the virus entry into host cells by engaging its receptor CD4 and co-receptor CCR5/CXCR4, and it is the major target for the AIDS vaccine development. However, gp120 uses many decoys to dodge human immune surveillance, making the development of a protective vaccine very challenging. Conformational masking is one of the decoys gp120 uses to evade the immune responses (171). The variable loops can often adopt different conformations, so that antibodies recognize one conformation will not be able to effectively target another conformation (90, 172, 173). Conformational masking can also protect functionally conserved sites of gp120. For example, the CD4 receptor-binding site is protected by entropy masking (171), and the co-receptor-binding site in the pre-fusion complex is completely buried under the variable loops (19, 20, 24). CD4 receptor binding will expose the co-receptor binding site, which is comprised of various conserved regions including the fourth conserved region (C4). The conformational masking of C4 is the subject of investigation for this manuscript. The C4 region of gp120, consisting of residues 419-448 (numbering in HxB2 scheme (174)), play many important functional roles: it directly involves receptor binding, co-receptor binding and co-receptor selection (tropism) (175, 176). Crystal structures of gp120 complex have revealed that residues Asn[425], Met[426] and Trp[427] in the C4 region have direct contacts with CD4 (13). The C4 region, together in spatial proximity with the base of the third variable loop (V3), also involves co-receptor binding. Early mutagenesis

studies indicated that residues Pro^{438} and Gly^{441} in the C4 region are important for CCR5 binding (177), and later a structural study of gp120 in complex with CD4 and mAb 412d showed that residues Ile^{439}, Arg^{440} and Gly^{441} in the C4 region involve in the binding with the N-terminus of CCR5 (24). A slight conformational change of the C4 region can influence the structure of V3, and even a single amino acid mutation change in the C4 region could increase the neutralization sensitivities of anti-V3 antibodies (178, 179). The C4 region, as well as the V3, also involves in co-receptor selection and mutations of residue 440 in the C4 region can alter co-receptor specificity (180).

The C4 region is highly immunogenic. It can induce T-cell immune response in HIV-1 infected patients and in immunized animal models (181, 182). For example, monomeric gp120 could elicit mouse helper T cell immune responses reactive with a C4 peptide, named T1 (a 16-mer peptide containing the region of residues 428-443), and, vise versa, the T1 peptide could elicit helper T cell immune response reactive with gp120 as well (181). Moreover, recombinant vaccinia virus expressing gp160 gene can elicit human T cell immune response reactive with the T1 peptide. After boosted with the recombinant fragment of gp120 containing the T1 site, the T cell immune response to T1 significant increased (182). The C4 region is thus an antigenic site to T cell immunity.

The C4 region can also induce antibody response (183, 184). A number of animal immune sera and mAbs have been described to target the C4 region. One of the characteristics of these antibody responses is that they can block the binding of CD4 with gp120, thus they were collectively named as CD4-blocking antibodies (185). In fact the CD4 binding region of gp120 was first identified by an anti-C4 mAb 5C2E5, which was raised by immunizing mice with recombinant gp120 and identified by competition with

CD4 binding (175). Since then many antibodies targeting the C4 region have been generated from animal models, including rabbit polyclonal R10-12 and R19-21 raised with poliovirus chimaera S1/env/4 (186), mouse mAbs G3-42, G3-299, G3-508, G3-536 raised with recombinant BH10 gp120 (187, 188), rat mAbs ICR 38.8f and ICR38.1a raised with recombinant BH10 gp120 (150). These reports suggested that the anti-C4 Ab responses can be readily elicited by gp120.

Structurally the C4 region was initially suggested to form amphipathic helices (182), but crystal structures of CD4-bound gp120 showed that the C4 region forms two beta strands, numbered 20 and 21, of the bridging sheet and the following loop F (13). Beta strand 20 involves in CD4 binding while beta strand 21 involves in co-receptor binding. Recent crystal structures of gp120 in complex with various mAbs showed that the C4 region, a sequence-conserved region, could display distinct conformations among the unliganded, CD4-bound and different antibody-bound states (13, 16, 20, 189, 190).

Here we present functional and structural characterizations of a recently generated rabbit anti-C4 mAb R53, which was elicited by JR-FL gp120 using a DNA prime - protein boost regimen (191). We show that R53 has broad cross-clade binding activities against gp120 proteins from clade A, B, C, D and E. It could neutralize sensitive viruses quite potently but was unable to any neutralize Tier 2 viruses. We have determined crystal structures of Fab/epitope complex and Fab alone of R53, and structurally defined R53 epitope and found that this epitope harbors a conserved motif AMYAPPI (residues 433-439) located at the C-terminus of the bridging sheet and loop F. Our data provide a structural understanding of this immunogenic but functionally critical region and how it is protected by conformational masking.

Results

Immunological characterization of rabbit mAb R53

Rabbit mAb R53 is one of the mAbs we generated recently from a New Zealand white rabbit immunized with JR-FL DNA prime followed by a homologous protein boost as previously reported (191). The location of its epitope was mapped to the C4 region of gp120 using a 15-aa overlapping peptide array, and a capture assay was used to identify whether the epitope of R53 overlaps functionally with those of CD4 binding site (CD4bs) mAbs (Table 2.5). CD4bs mAb b12, V3-specific mAb 3074, and glycan specific antibody 2G12 were used as competitive targets. The supernatant of R53 hybridoma was able to prevent 56% virus binding to mAb b12, suggesting that R53 indeed targets the CD4bs region. In contrast, it could not compete against either V3 mAb 3074 or glycan mAb 2G12, further supporting its specific competition against b12. Since previously described mAbs targeting at this C4 region were found to block CD4 binding of gp120 (175, 185), we determined the binding specificity of R53 by competition ELISA (Fig.2.9A). R53, sCD4 and R56 were used to compete with Ig-CD4 for binding to JR-FL gp120. As expected, R53 could inhibit Ig-CD4 binding (IC_{50}=9.8ug/ml), although it is not as effective as the positive control sCD4 (IC_{50}=0.22ug/ml). As a negative control, R56 did not have any impact on Ig-CD4 binding of gp120. These results confirmed that R53 can block CD4 to bind gp120.

To determine the binding breadth of R53 for HIV-1 gp120 from different clades, eight representative gp120s were chosen: 92UG037.8 from clade A; 92US715, BaL, and JR-FL from clade B; 96ZM651 and 93MW965 from clade C; 92US021 from clade D, 93TH976.17 and AE consensus from clade AE. A Western blot analysis showed

Table 2.5 Ability of hybridoma supernatants to outcompete binding to mAbs with known specificities

Competing mAb	Hybridoma cell line ID		
	53	56	15
b12	56%	34%	24%
3074	21%	83%	17%
2G12	39%	22%	11%
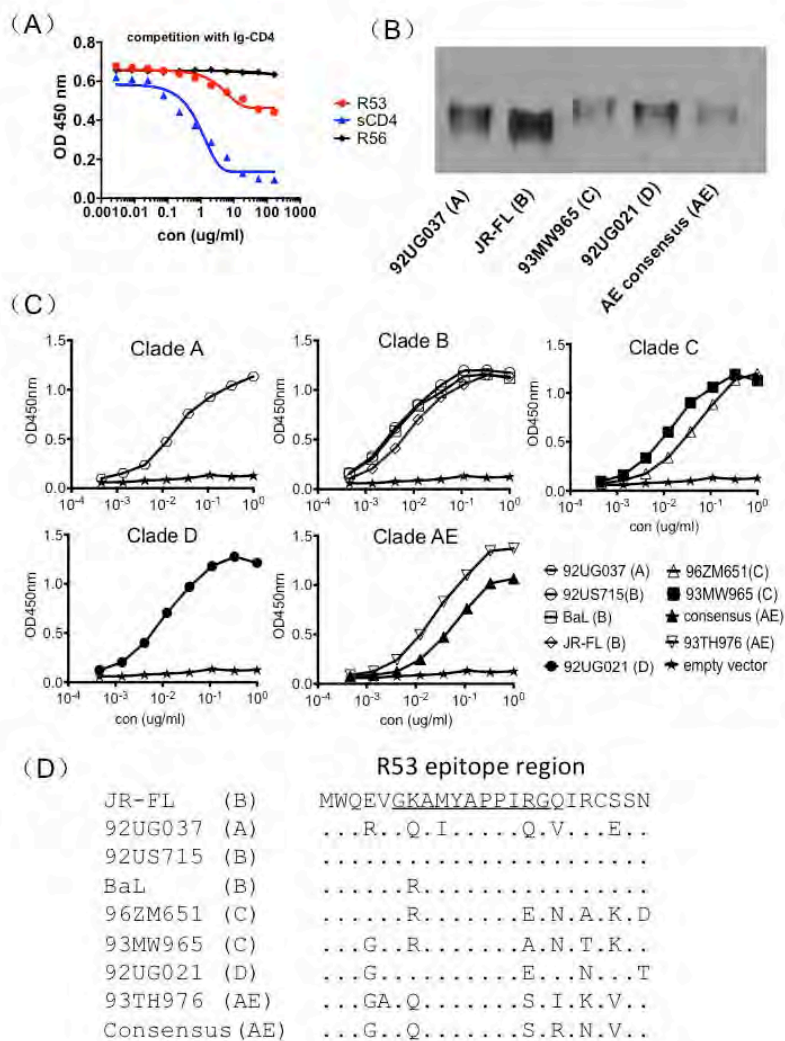
Figure 2.9. **R53 broadly reacts with gp120s of diverse clades.** (A) R53 competition with Ig-CD4 assay. Data from the soluble CD4 (sCD4) and anti-V3 mAb R56 were used as controls. (B) Western blots showed that five selected gp120 proteins from different clades were recognized by R53. (C) R53 binds 10 gp120s from clades A, B, C, D and AE, revealed by ELISA. (D) Protein sequence alignment of R53 epitope region for the 10 gp120s used in panel (C). The R53 epitope is underlined in the JR-FL sequence.

that five representative gp120s from different clades were recognized by R53 in denatured conditions (Fig.2.9B). In addition, R53 was able to recognize all these Env demonstrated by ELISA (Fig. 2.9C). Binding kinetics of R53 with selective five gp120s were further determined using a ForteBio instrument. R53 is shown to have high binding affinities to all five gp120s tested, with K_D ranging from 1.79 nM to 3.98 nM (Table 2.6). A sequence alignment of R53 epitope region revealed that it is highly conserved among clades A, B, C, D and AE (Fig. 2.9D).

Crystal structure of Fab/epitope complex of rabbit mAb R53

We determined the crystal structure of R53 antigen-binding fragment (Fab) in complex with a peptide (VGKAMYAPPIRGQIR, residues 430 to 444 in HXB2 numbering). The complex structure of R53 Fab/epitope was solved by molecular replacement and refined to 2.3 Å resolution with R_{work}/R_{free} of 18.4%/23.0% (Fig. 2.10 and Table 2.7). The crystals grew in the orthorhombic space group $P2_12_12_1$ with two Fab/epitope complexes in the asymmetric unit. The two complexes are highly similar (RMSD = 0.551 Å), we thus chose only one for description here. We numbered the residues following the Kabat and Wu convention (192), with the light and heavy chains preceded by "L" and "H", respectively, and the residues of the epitope by a "P". Although a 15-mer peptide was used in the crystallization, only 11 residues, i.e., GKAMYAPPIRG (residues 431 to 441), were observed in the electron density map. We also determined the structure of Fab alone (Table 2.7); superposition of the two Fab structures showed that R53 Fab appears to have minimal conformational change upon epitope binding (RMSD = 0.772 Å). R53 has a typical rabbit antibody inter-domain disulfide bond between residues 80 and 170 of the light chain, which places a constraint

Table 2.6 R53 binding kinetics to 5 representative Env proteins

gp120 proteins (clade)	K_D (M)	K_{on}(1/Ms)	K_{dis}(1/s)
92UG037 (A)	1.54E-09	3.41E+05	5.24E-04
JR-FL (B)	1.96E-09	1.57E+05	3.09E-04
93MW965 (C)	3.98E-09	3.04E+05	1.21E-03
92UG021 (D)	1.79E-09	3.56E+05	6.38E-04
AE consensus (AE)	2.49E-09	3.91E+05	9.73E-04

on its elbow angle (193).

The epitope of R53 (^{431}GKAMYAPPIRG^{441}) is shaped like a stretched spring, lying across on the top of the light and heavy chains (Fig. 2.10). Its N-terminus sits in a groove formed by the heavy chain while the C-terminus straddles on a saddle formed by R53 light chain residue Asp^{L30}, on one side hanging the side chain of Arg^{P440} and on the other side the side chain of Ile^{P439}. The electrostatic potential analysis shows that the antigen-binding site of R53 is negatively charged (Fig. 2.10D), complementing the positively charged epitope that harbors two positively charged residues, Lys^{P432} and Arg^{P440}. All complementarity determining regions (CDRs) involve in antigen binding except for the second CDR loop of the light chain (CDR L2).

Antigen-antibody interaction of R53

The antigen-antibody interaction of R53 involves extensive hydrophobic contacts, with ~730 Å^2 buried surface areas and multiple potential hydrogen bonds between the antibody and the epitope. The epitope of R53 is comprised of six hydrophobic residues, including Ala^{P433}, Met^{P434}, Ala^{P436}, Pro^{P437}, Pro^{P438} and Ile^{P439}, and they involve in several hydrophobic interactions (Fig.2.11). (1) A small pocket, formed by the phenyl ring of Phe^{H31} and the side chains of Val^{H51} and Thr^{L96}, accommodates the epitope residue Ala^{P433}. (2) Another small pocket, formed by the phenyl rings of three tyrosines, Tyr^{L32}, Tyr^{L92}, Tyr^{H97}, and the backbone of residue Val^{L93}, buries the C$_b$ of Ala^{P436}. (3) The third pocket, formed by the phenyl ring of Tyr^{L92} and a hydrophobic residue Ala^{L28}, buries the side chain of the epitope residue Ile^{P439}. (4) The side chain of Tyr^{H97} of heavy chain stacks against Pro^{P437} of the epitope. Interestingly, the second proline residue in the epitope, Pro^{P438}, has barely any contact with R53 (less than 5 Å^2 of calculated contact
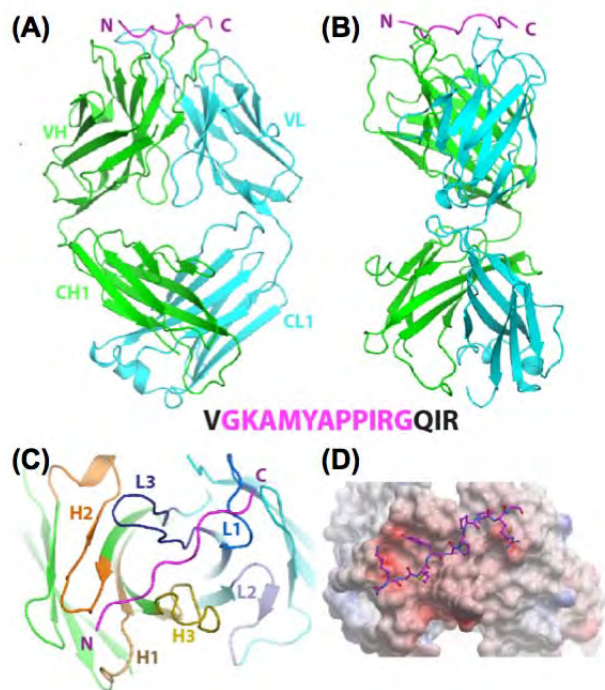
Figure 2.10. Structure of Fab R53/epitope complex. **(A)** A ribbon representation of the Fab R53 in complex with its epitope in a front view. The light, heavy chains, and the V3 epitope were colored cyan, green and magenta, respectively (a coloring scheme kept throughout the manuscript, except where indicated otherwise). **(B)** A side view of the complex. **(C)** A top view of the R53/epitope complex looking at the antigen-binding site. The CDR regions are labeled and colored differently from the rest of Fab. Note that the epitope lies across on top of the light and heavy chains with its N-terminus of the epitope at the heavy chain side and its C-terminus at the light chain side. **(D)** A surface representation of Fab R53 colored according to its electrostatic surface potentials with red as the negatively charged and blue positively charged regions. The inset is the sequence of the peptide used in crystallization and the magenta region indicates the residues visualized in the crystal structure.

areas). (5) The epitope residue Tyr^{P435} has the largest contact with the antibody; its side chain stacks in parallel with the backbone of Ser^{L95A} of CDR L3. There are also hydrogen bonds between the epitope backbone and the antibody: for example, Tyr^{L32} and Tyr^{L92} of light chain with the backbone of the epitope residues Pro^{P437} and Ile^{P439}, respectively; the backbone amide of Ala^{P433} with the side chain of heavy chain residue Asp^{H51B}; the backbone O of Met^{P434} with the amide of Tyr^{H97}; The OH group of epitope residue Tyr^{P435} with the side chain of heavy chain Glu^{H55} (Fig. 2.11).

The epitope of R53 harbors no acidic residues but two basic residues, Lys^{P432} and Arg^{P440}. The side chain of Lys^{P432} is located in an acidic environment formed by Asp^{H51b} and Glu^{H55}, while the side chain of Arg^{P440} forms salt bridges with two heavy chain residues Asp^{L30} and Glu^{L31} of R53 (Fig. 2.11). The R53 contacting residues, AM/IYAPPI, are highly conserved among clades A, B, C, D and AE (Fig. 2.10C).

Spatial location of the R53 epitope in gp120 structures

Examining all currently available gp120 structures in the RCSB Protein Data Bank (PDB), we found that the region of R53 epitope can form four distinct conformations (Fig. 2.12): i) the CD4-bound (represented by the first gp120 core structure; PDB ID 1GC1. The majority of the gp120 structures, including the unbound core structures, belong to this group), ii) the mAb b12-bound (PDB ID 2NY7), iii) the mAb F105-bound (PDB ID 3HI1), and iv) the mAb b13-bound conformations (PDB ID 3IDX) (13, 16, 189, 190). In the CD4-bound conformation, this region extends from strand 21 of the bridging sheet to loop F. In the b12-bound gp120, the conformation of this region is similar to that of the CD4-bound gp120. But the bridging sheet is not completely formed due to the dislocation of the two strands (strands 2 and 3) from the

Figure 2.11. Details of the epitope binding in the Fab R53/epitope complex. **(A)** A stereo view of the antigen-binding site. The side chains of the key residues involved in the hydrogen bonding and van der Waals interactions (with contact areas greater than 10 Å^2) are shown in sticks. Note that (1) three tyrosines and four negatively charged residues on R53 play a key role on binding the epitope, (2) C4 residue Arg^{P440} interacts with two acidic residues Asp^{L30} and Glu^{L31} from the light chain, and (3) the side chain of C4 residue Tyr^{P435} has a Van der Waals stacking with the antibody backbone, and its hydroxyl group forms a hydrogen bond with the side chain of Glu^{H56} of the heavy chain. **(B)** A schematic of the antigen-antibody interaction. Hydrogen-binding interactions are indicated by dashed lines between the residues, while van der Waals contacts by eyelashes. Residues in solid ovals contribute to the interactions by their main chain atoms, and those in dashed ovals by their side chain atoms.

Figure 2.12 Location of the R53 epitope in the gp120 structures. The structure of R53 epitope, together with Fab R53 (only the Fv region is shown), was superimposed onto the epitope region of gp120 structures with distinct C4 conformations, including the CD4-bound **(A)**, b12-bound **(B)**, F105-bound **(C)** and b13-bound **(D)** gp120s (11, 25-27). The R53 epitope is colored in magenta, the gp120 is colored grey. Clashes between the antibody R53 and gp120 are indicated. The R53 epitope is accessible (without clashes between the antibody and gp120) only in the b13-bound conformation of gp120. **(E)** The location of the R53 epitope in the recent BG505 SOSIP.664 trimer. The R53 epitope region, located underneath V1V2/V3, was colored magenta while the rest of the three gp120s were colored grey, yellow, and orange, respectively.

inner domain. In the b13-bound and F105-bound gp120s, this region, as well as the region of strand 20, form coils. Superimposing the R53 epitope with the C4 region in these gp120 structures showed that the epitope is only available in the b13-bound conformation, i.e., R53 binding of the epitope does not cause any clashes with the rest of gp120 molecule. In recently appeared structures of the stabilized BG505 SOSIP.664 trimer (19, 20, 194), the epitope region of R53 is covered under the variable loops V1V2 and V3, thus completely buried in the interior of the trimer (Fig. 2.12E).

Discussion

We have structurally defined for the first time a linear C4 epitope, representative of the epitopes of many CD4 blocking mAbs identified throughout the years. The epitope is located at the C-terminus of the bridging sheet and loop F. This gp120 region plays critical roles in gp120 functions, thus is highly conserved. Residues Tyr^{P435}, Pro^{P438}, Ile^{P439}, Arg^{P440} and Gly^{P441} in the R53 epitope region are critical for co-receptor binding (24, 195). However, this region is also highly immunogenic, as indicated by many mAbs reported in the literature. On the other hand, most of antibodies targeting this region are not neutralizing or have only weak neutralization activities (150, 187, 191, 196, 197), suggesting that this region is masked on gp120 trimer. Our data presented here provide a mechanistic understanding of a conformational masking of this region. In the prefusion complex, this region is buried by V1V2 and V3 loops that lay on top of it; thus this region is sequestered from access of any antibodies. In the CD4 bound state, this region is located on the surface of gp120 and is exposed (not shown). However, in this conformation the epitope of R53 is not available for the mAb to binding (Fig. 2.12), as the side chains of amino acids, such as Tyr^{P435}, that bind to R53 are buried and facing the

core of the molecule. Thus the high immunogenicity of this region may be derived from the side chains that are not accessible in the CD4 bound state, and these side chains are available in gp120 monomer as shown in the b13 bound conformation (Fig. 2.12).

The structure of R53 epitope can explain the mechanism of how this family of mAbs blocks the CD4 binding, i.e., as illustrated in Fig 2.14A, the CD4 bound conformation of gp120 is not compatible with R53 binding. In the other words, the binding of the CD4-blocking mAbs will prevent the correct formation of CD4 binding site, thus preventing CD4 binding to gp120. Structural understanding of R53 epitope also provides a way to design immunogens targeting this highly conserved functionally important epitope region. If an immunogen can induce antibody responses targeting the R53 epitope region from the side available in CD4 bound conformation, it will likely be more effective in neutralization against HIV-1. One way to design such an immunogen is to embed the R53 epitope region by a suitable protein scaffold that can structurally constrain this region in the CD4 bound conformation so that the right side can be presented to the immune system.

Chapter II, Section IV

Structure basis to differentiate a broadly cross-neutralizing V3 mAb

and other V3 mAbs targeting at overlapping epitopes

Introduction

The V3 region is the most immunodominant region on the Env protein. This region was identified in the early stages of HIV research as the "principle neutralizing domain" (PND) of HIV-1 (198). However, this idea was challenged by evidence of extreme sequence diversity within the V3 region. The V3 region usually has 35 residues, and is more conserved in comparison with other variable regions of gp120 (199). A highly conserved motif, Gly-Pro-Gly-Arg/Gln (GPGR/Q), is present at the tip of the V3 region. Structural analysis of V3 in the context of gp120 core showed that it has three regions, including a base, stem, and crown (25).

The V3 crown is around 13 amino acids in the middle of the V3 sequence and adopts a beta-conformation at the distal apex. Detailed structural analysis revealed that the V3 crown has four conserved structural regions, including an arch, a band, a hydrophobic core, and the peptide backbone (172). Interestingly, the majority of human V3 mAbs target the crown, and several of them have shown a 24%-39% breadth of neutralization against a panel of 41 tier 1 and tier 2 pseudoviruses from clades A, B, and C (200). This is quite similar to the breadth of some well-known broadly neutralizing antibodies, such as b12 and 2G12.

Notably, in the RV144 trial, high-level anti-V3 IgG showed a significant inverse correlation with infection risk but only in vaccines that had lower level IgA and neutralizing antibodies (23). Neutralization responses in the RV144 trial were partly

mediated by V3 responses; two V3 crown-specific antibodies, CH22 and CH23, isolated from this trial, showed very potent but limited neutralization activity against tier 1 viruses (87). This new evidence suggests that V3 could also be an appropriate target for HIV vaccine development.

Here we present a panel of V3 crown-specific mAbs, mostly from one immunized rabbit. This panel shows a varying degree of neutralization capabilities, which will be an interesting study template for examining antibody affinity maturation.

Results

Rabbit immunization and generation of rabbit monoclonal antibodies

One New Zealand White rabbit was immunized with three DNA expressing gp120AE through gene gun delivery, followed by a 5-valent protein intramuscular injection, that included UG21-9 from clade A, MW959 from Clade A, JR-FL from Clade B, 92US715 from Clade B, and Th14-12 from Clade B. Eight weeks later, just before termination for mAb production, the rabbit received an additional boost by one-time DNA immunization via gene gun and one-time protein immunization intravenously. The rabbit spleen was harvested at four days post final boost, and sent to a subcontractor for generation of hybridoma cells. 151 hybridoma cell lines were generated, and 11 hybridoma cell lines were further selected to produce a stable monoclonal stage of hybridoma cell lines. Among these 11, we found four that targeted the V3 crown region.

Different binding sites on V3 determined by peptide array

The binding specificities of hybridoma cells were determined by ELISA using overlapping peptides from consensus M as coating antigens. Interestingly, four anti-V3 mAbs were identified, named as R16, R73, R28, and R64 (Table 2.7). Two mAbs, R16

Table 2.7. Linear V3 peptide binding (OD$_{450}$) with V3-specific mAbs determined by ELISA. The positive binding peptides were highlighted.

| Hybridoma ID | V3 peptide# | | | | | | | | | | | | gp120AE |
	72	73	74	75	76	77	78	79	80	81	82	83	
16	0.0537	0.0485	0.8955	0.8414	0.8598	0.0485	0.0502	0.0488	0.0539	0.0480	0.0437	0.0429	1.1087
73	0.0534	0.0525	0.8813	0.8876	0.8836	0.0498	0.0494	0.0490	0.0507	0.0522	0.0439	0.0435	1.1263
64	0.0680	0.0551	0.0605	0.4959	0.3776	0.0509	0.0544	0.0531	0.0524	0.0512	0.0444	0.0445	1.1098
28	0.0617	0.0554	0.0558	0.4122	0.9233	0.0564	0.0558	0.0557	0.0586	0.0571	0.0442	0.0434	1.2343
56	0.0422	0.0621	0.8934	0.8432	0.0487	0.0487	0.0598	0.0534	00507	0.0597	0.0468	0.0469	1.1097

Peptide # ID	sequence
74	CTRPNNNTRKSIRIG
75	NNNTRKSIRIGPGQA
76	RKSIRIGPGQAFYAT

(A)
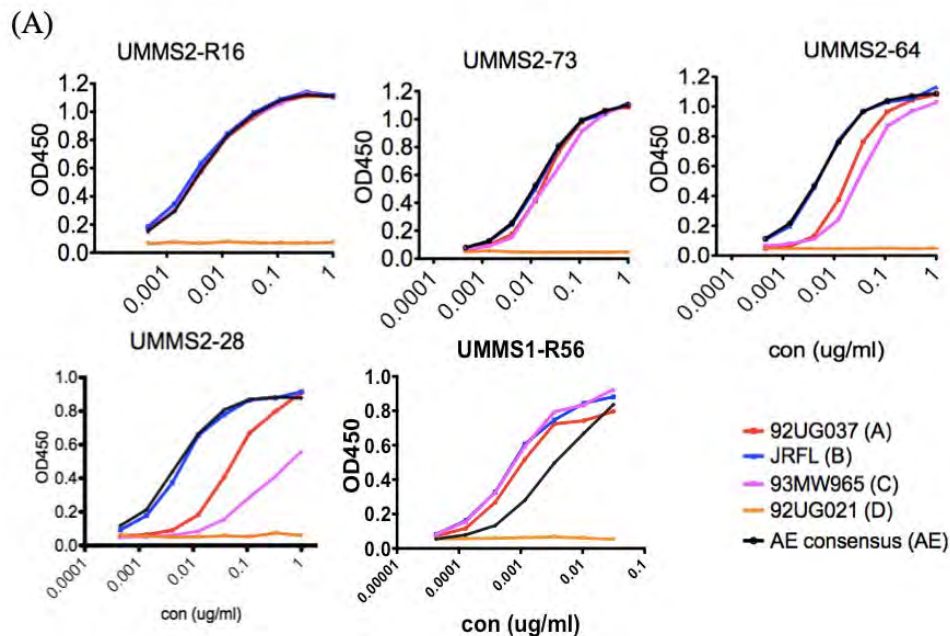
(B) Binding affinity of rabbit MAbs to gp120 proteins of different clades

	92UG037 (A)			JR-FL (B)			93MW965 (C)			92UG021 (D)			AE consensus (AE)		
	K_D (M)	Ka (1/Ms)	Kdis (1/s)	K_D (M)	Ka (1/Ms)	Kdis (1/s)	K_D (M)	Ka (1/Ms)	Kdis (1/s)	K_D (M)	Ka (1/Ms)	Kdis (1/s)	K_D (M)	Ka (1/Ms)	Kdis (1/s)
R16	1.90E-10	1.83E+05	3.48E-05	<1.0E-12	2.28E+05	<1.0E-07	2.65E-10	3.07E+05	8.12E-05	1.04E-08	3.74E+04	3.87E-04	4.75E-11	4.27E+05	2.03E-05
R73	1.12E-09	3.30E+05	3.70E-04	1.71E-09	2.23E+05	3.82E-04	2.21E-09	2.91E+05	6.42E-04		NA		5.18E-10	2.90E+05	1.50E-04
R64	2.19E-09	7.65E+04	1.67E-04	2.40E-09	1.34E+05	3.20E-04	2.42E-09	1.25E+05	3.03E-04		NA		4.29E-09	8.92E+04	3.83E-04
R28	1.24E-09	2.00E+05	2.48E-04	1.07E-09	2.89E+05	3.39E-04	2.31E-09	1.47E+05	3.39E-04		NA		9.17E-10	6.65E+04	6.10E-05
R56	1.20E-09	4.85E+05	5.82E-04	1.06E-09	3.60E+05	3.82E-04	2.72E-09	4.09E+05	1.11E-03	1.20E-09	4.85E+05	5.82E-04	2.39E-09	2.51E+05	6.01E-04

Figure 2.13. The cross reactivity of V3-specific rabbit mAbs with a panel of representative gp120 proteins. (A) ELISA showed RmAbs recognized most of selected Env gp120 proteins, including Clade A 92UG037, Clade B JR-FL, Clade C 93MW965, and consensus AE, but not Clade D 92UG021. (B) Binding affinity of rabbit mAbs to five selected Env protein determined by ForteBio Octet Qk^e system. Rabbit mAbs were immobilized on the chip surface, and the JR-FL gp120 protein was added in the testing solution. Rate constants K_a (equilibrium association constant), K_d (dissociation constant), and K_D for rabbit mAbs binding to Env proteins were obtained by global fitting of the curves to the 1:1 binding model.

and R73, recognized three consecutive peptides, from #74 to #76. R28 recognized

peptides #75 and #76, but bound #76 stronger than #75. Interestingly, R64 recognized

both #75 and #76, albeit in a weak manner, but strongly bound to gp120 Env, suggesting

that conformational dependent epitopes may be involved. R56, another RmAb targeting

the V3 crown, was isolated from another rabbit immunized with JR-FL DNA prime

followed by JR-FL protein boost. R56 equally bound to both #75 and #76 peptides (191).

Distinct binding profiles of V3 mAbs against cross-clade Envs proteins

We cloned out the full-length heavy chain and light chain genes of the above four anti-V3

mAbs and subcloned them into a mammalian protein expression vector. Individual

RmAbs were expressed in 293T cells transiently transfected with these RmAb-expressing

molecular clones. The distinct binding capabilities of RmAbs with cross clade Envs were

observed by ELISA (Fig. 2.13A), although their footprints on the V3 region overlapped

with each other. Both R16 and R73 bound to 92UG037 Env from Clade A, JR-FL Env

from Clade B, 93MW965 Env from Clade C, and AE consensus Env from Clade AE

equally well, but not to 92UG021 from Clade D. R64 showed strong recognition for Envs

from JR-FL and AE consensus, with less recognition for 92UG037 and 93MW965 Envs,

and a failure to recognize 92UG021 Env from clade D. Similarly, R28 recognized both

Clade B and Clade AE Envs quite well but less so for Clade A 92UG037 Envs, and had

no recognition for consensus AE. However, different from the R64 binding profile, R28

recognized Clade C 93MW965 less compared to 92UG037. R56, resulting from JR-FL

immunization, appeared to bind to all four Envs except 92UG021 (191).

Moreover, a more detailed analysis of rabbit mAb binding kinetics with the above

Envs was conducted using Fortebio. Rate constants K_{on}, K_{dis}, and K_D for individual

```
Heavy chain   --------FR1-------------__CDR1__ ------FR2-----__CDR2__ --------FR3------------------------ CDR3 ----FR4----
IGHV1S44*01   QSLEESGGRLVTPGGSLTLTCTVSGIDLTSYAMGWVRQAPGKGLEYIGIISSSGSTYYASWAKGRFTISKTSSTTVDLKMTSLTTEDTATYFCAG
       16H    QSLEESGGRLVTPGGSLTLTCTVSGIDLSSYAVGWVRQAPGKGLEYIGIICEPNKACYANWARGRFTISVTSSTTVELKMTSLTTEDTATYFCGMNLWI-WGPGTLVTVSL
       73H    QSVEESGGRLVTPGGSLTLT-TLSGIDLSRYAIXWVRQAPGKGLEYIGITNEDDIPYYGDWAKGRFTISKTSSTTVDLKMTSLTTEDTATYFCAINIFDPWGLGTLVTVSS
       64H    QSVEESGGRLVTPGGSLTLTCTVSGIDLSGYAIGWVRQAPGKGLEYIGITSDTDIAYYATWAKGRFTISKTSSTTVDLKMTSLTASDTATYFCARNIFDPWGPGTLVTVSS
       28H    QSLEESGGRLVTPGGSLTLTCTVSGIDLSNYAVGWVRQAPGKGLEYIGIIGNIDDTYYANWAKGRFTISKTSSTTVDLKLSSLTIEDTATYFCSTSLY-IWGPGTLVTVSL

IGHV1S40*01   QSLEESGGDLVKPGASLTLTCTASGFSFSSSYYMCWVRQAPGKGLEWIACIYAGSSGSTYYASWAKGRFTISKTSSTTVTLQMTSLTAADTATYFCAR
       56H    QS-LEESGGDLVQPGASLTLTCKASGFSFGNNYDMCWVRQAPGKGLEWIGCIETGSSDSAAYATWAKGRFTISKTSSTTVTLQMTSLTAADTATYFCARNFDLWGPGTLVIVSS


light chain   ---------FR1-------------__CDR1__ -----FR2----------CDR2-----------FR3--------------------__CDR3__ -----FR4---------
IGKV1S16*01   DPMLTQTASPVSAAVGSTVTISCQASQSVYNNNNLAWFQQKPGQPPKLLIYSASTLASGVSSRFKGSGSGTQFTLTISGVQCDDAATYYC
       16H    AQVLTQTPSPVSAAVGGTVTINCQSSQSIYDNNNLAWFQQKPGQPPKGLIHSASTLNSGVPSRFQGSGSGTQFTLTISDVQCDDAATYYCLGGYSDFIYTFGGGTEVVVKGDPVAP

IGKV1S18*01   AAVMTQTPSPVSVAVGGTVTINCQASQSVYNNNYLAWFQQKPGQPPKLLIYSASTLASGVSSRFKGSGSGTQFTLTISGVQCDDAATYYC
       73L    AYDMTQTPSSVSAAVGGTVTVNCQASQSVYNNNNLAWFQQKPGQPPKGLIYSASTLASGVPSRFKGSGSGTQFTLTISDLECDDAATYYCLGGYTDNMFDFGGGTELVVKRDPVAP
       64L    AYDMTQTPSSVSAAVGGTVTINCQASQNVYNNNNLAWFQQKPGQPPKGLIYSASTLASGVPSRFKGSGSGTEYTLTISDLECDDAATYYCLGGYSDNMFTFGGGTELVVKGDPVAP

IGKV1S46*01   DPVLTQTASPVSAAVGGTVTISCQASQSVYNNNYLAWFQQKPGQPPKLLIYSASTLASGVSSRFKGSGSGTQFTLTISGVQCDDAATYYC
       28L    AQVLTQTPSPVSAAVGSTVTITCQSSQSV-DGNNLAWFQKKPGQPPKGLIYSASTLDSGVSPRFSGSGSGTQFTLTIGDVQCDDAATYYCLGGYSGFIYVFGGGTEVVVKGDPVAP

IGKV1S15*01   AQGPTQTPSSVSAAVGGTVTINCQTSESFYSNNILSWYQQKPGQPPKLLIYDASTLASGVPSRFKGSGSGTQFTLTISDVQCDDAATYYCQGSYHSSGWY
       56L    AQVLTQTPSSVSTAVGSAVTINCQSSQNVYSNNNLAWFQQKPGQPPRLLIYDASKLASGVPSRFKGSGSGTQFTFTISDVQCDDAATFYCLGGYDCSSGDCAAFGGGTEVVVRGDPVAP
```

Figure 2.14. Protein sequence alignment of heavy and light chain variable regions of gp120-specific rabbit mAbs. The sequences are aligned to their corresponding putative germline genes. Framework regions (FR) and CDRs are indicated based on IMGT database (http://www.imgt.org/) nomenclature. Somatic mutated amino acids compared to germline sequences are highlighted in red and CDR3 region in blue.

Table 2.8. Characteristics of V gene of heavy chain and light chain of anti-V3 rabbit mAbs elicited by vaccination

Rabbit mAb	IGHV			IGKV		
	Germline	Mutation frequency (%)	CDR H3 (aa)	Germline	Mutation frequency (%)	CDR L3 (aa)
R16	S44*01	9	6	S16*01	12	10
R73	S44*01	10	7	S18*01 or S23*01	10	10
R64	S44*01	8	7	S18*01 or S23*01	10	10
R28	S44*01	7	6	S46*01	11	10
R56	S40*01	6	6	S15*01	12	13

RmAbs with Envs were determined (Fig. 2.13B). Consistent with the ELISA data, R16 had very high affinity for the four Envs proteins from Clade A, B, C and AE, with a K_D ranging from 0.19nM to 0.001nM. Fortebio was more sensitive to detect the interactions of R16 and 92UG021 from clade D, and their affinity was 14.1nM. We also detected strong binding between R73, R64, and R28 with Envs from Clade A, B, C, and AE, with similar binding kinetics. There was no detectable association between these V3 mAbs and Clade D Env.

Genetic analysis and phylogenetic tree analysis for anti-V3 RmAbs

To understand the genetic features of these anti-V3 RmAbs, the full length IgG heavy chain and light chain genes were sequenced. Germline usage, mutation frequency, and CDR3 length of the heavy chain and light chain V genes were determined using IMGT. For the heavy chain V gene, R16, R73, R64, and R28 use S44*01 as their germline; R56 comes from another immunized rabbit, adopting S40*01 as its germline family. Somatic mutation frequency is also critical for antibody affinity maturation. All of these antibodies showed low mutation frequencies, ranging from 7% to 10%, and CDR3 lengths around 6 or 7 amino acids. Light chain germline usage for each mAb is more diverse; distinct germlines were used and the mutation frequencies were 10-12%, with a CDR3 length of 10 amino acids (Table 2.8 and Fig. 2.12).

Neutralization activities of vaccine-elicited anti-V3 RmAbs

We sought to determine the neutralization capabilities for anti-V3 antibodies, including R56, R16, R73, R28, and R64. The RmAbs were sent to the Comprehensive Antibody Vaccine Immune Monitoring Consortium (CAVIMC) of the Collaboration for AIDS Vaccine Discovery (CAVD) (Seaman Lab at Harvard Medical School). A panel of

Table 2.9. Neutralization IC$_{50}$ (µg/ml) of rabbit MAbs by TZM-l assay

	Tier 1 Virus	Clade	R16	R73	R28	R64	R56
Tier 1 viruses	MN-3	B	0.032	3.812	>50	43.196	>50
	SF162.LS	B	<0.023	<0.023	0.179	0.049	0.095
	BaL.26	B	0.191	0.407	0.173	1.860	2.073
	SS1196.1	B	0.924	3.298	1.361	5.210	7.182
	Bx08.16	B	0.189	0.622	0.398	1.440	3.181
	BZ167.12	B	48.057	>50	>50	>50	>50
	6535.3	B	1.505	>50	>50	>50	>50
	MW965.26	C	<0.023	0.622	11.067	14.858	<0.023
	TV1.21	C	0.796	15.531	>50	>50	25.634
	ZM109F.PB4	C	5.369	15.827	>50	>50	>50
	ZM197M.PB7	C	37.772	>50	>50	>50	>50
	00836-2.5	C	42.648	>50	>50	>50	>50
	25710-2.43	C	12.122	>50	22.085	>50	>50
	MS208.A1	A	37.613	>50	>50	>50	>50
	Q23.17	A	>50	>50	>50	>50	>50
	DJ263.8	CRF02_AG	0.111	1.594	>50	>50	0.838
	242-14	CRF02_AG	10.539	>50	20.288	>50	>50
	T271-11	CRF02_AG	0.242	3.301	1.518	5.404	15.083
	TH023.6	CRF01_AE	<0.023	<0.023	<0.023	0.554	18.571
Tier 2 viruses	JR-FL.JB	B	18.128	>50	>50	>50	>50
	REJO4541.67	B	15.955	>50	>50	>50	>50
	ZM135M.PL10a	C	>50	>50	>50	>50	>50
	CNE20	BC	19.120	>50	>50	>50	>50
Breadth			91%	48%	39%	35%	39%
IC$_{50}$ (ug/ml)			2.99	20.2	23.4	27.5	29.8

Legend:
- <0.1ug/ml
- <1ug/ml
- <5 ug/ml
- <25 ug/ml
- <50 ug/ml
- >50 ug/ml

23 well-characterized pseudotyped viruses expressing Env from a wide range of primary HIV-1 isolates, including 19 tier 1 viruses (2 Clade A, 7 Clade B, 6 Clade C, 1 Clade AE, and 3 Clade AG) and 4 tier 2 viruses (2 Clade B, 1 Clade C, 1 Clade BC). Surprisingly, R16 neutralized 91% of the tested viruses at high potency, at geometric IC_{50} of 2.99µg/ml, whereas R73 neutralized 48% of the selected HIV viruses at a geometric IC_{50} of 20.2µg/ml, R28 neutralized 39% of viruses at geometric IC_{50} of 23.3µg/ml, and R64 neutralized 35% of tested viruses at geometric IC_{50} of 27.5µg/ml. R56 neutralized 39% of viruses in the panel at a geometric IC_{50} of 29.8µg/ml.

It is very rare for R16, an antibody resulting from immunization, to have such broad and potent neutralization activities. Further, although peptide mapping suggested these 4 mAbs (R16, R73, R28 and R64) were focused on the V3 crown region, dramatic differences between their neutralization activities were observed.

Structural features of antigen-antibody interactions of mAb R16

To gain a structural understanding of why mAb R16 had such superior neutralization activity, a crystal structure of its Fab in complex with a V3 peptide ($V3_{conA}$) was determined (Fig. 2.14) by our collaborator, Dr. Xiang-peng Kong. The structure revealed that the epitope of R16 consists of 11 residues from Lys^{P305} to Phe^{P317} ($^{305}KSIRIGPGQAF^{317}$) of the V3 crown region (Fig. 2.14A). R16 binds the V3 crown in cradle binding mode (Fig. 2.14B), similar to what was observed for another rabbit mAb, R56 (193). The R16 epitope has seven highly conserved residues, two hydrophobic residue Ile^{p307} and Ile^{p309}, $Gly^{p312}Pro^{P313}Gly^{p314}$ on the crown arch, and Phe^{p317} at C terminus ends of epitope. Three residues, Ile^{P307}, Ile^{P309} and Phe^{P317} play a dominant role
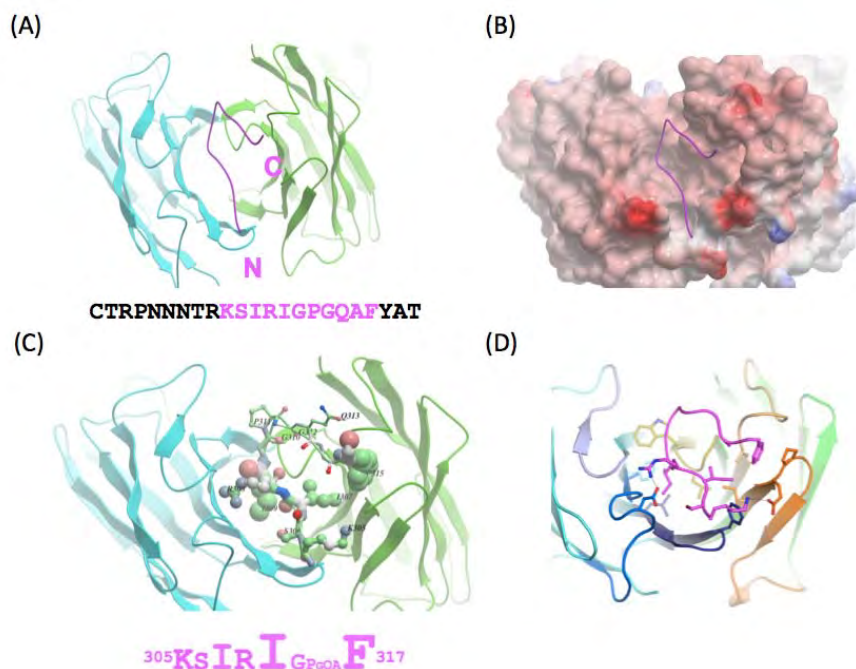
Figure 2.15. Structure of Fab R16 in complex with V3$_{conA}$ peptide. (A) Ribbon representation of a top view looking at the antigen-binding site of R16. The insert peptide sequence was used for crystallization and the residues responsible for interaction with R16 are highlighted in magenta. (B) Surface representation of Fab R16 colored according to its electrostatic surface potentials, with negative charged region in red and the positively charged region in blue. V3 is shown as a ribbon. (C) A top view of looking at the antigen-binding site of R16, with the epitope shown as a sphere with the amino acids noted. The exact epitope sequence is shown in below. The height of the residues is proportional to the binding intensity with R16. (D) Stereo view of the antigen-binding site.

(A)

(B)

R16

R56

R16
(305-317)

KsIRI_{GPGQA}F

R56
(303-314)

_TR_{KS}I_{HI}G_{PG}

Figure 2.16. Structural comparison of epitopes of R16 and R56. (A) Superimposition of V3 epitope bound to R16 (magenta) with that bound to R56 (Red). (B) Sequence alignment of epitopes for R16 and R56. The height of residues was proportional to the binding intensity with corresponding antibodies.

in antigen-antibody interactions of R16 through extensive hydrophobic contacts (Fig.2.14B), which are highly conserved residues. These data provide a structural explanation of the broad recognition of cross-clade of the Envs observed in Fig.2.13.

Structural comparison of mAbs R16 and R56

The superimposition of epitopes from R16 and R56 shows that the majority of epitopes between these two antibodies overlap (Fig. 2.15). Although both antigen-antibody sites adopted a cradle-binding mode, there are two major differences between the complex structure of R16 and R56. First, R16 targets the middle of the V3 crown, spanning 11 residues, ^{305}KSIRIGPGQAF^{317}, while R56 interacts with 10 amino acids at the N-terminal of the V3 crown, with the sequence of ^{303}TRKSIHIGPG^{314}. Second, R16 primarily contacts the V3 crown via hydrophobic interactions, mostly via three hydrophobic residues Ile^{p307}, Ile^{p309}, and Phe^{p317}. In contrast, in addition to hydrophobic binding of Ile^{P307}, Ile^{P309}, R56 also interacts with a side chain, specifically with Arg^{p304} through a salt bridge. Therefore, the dominant residue responsible for this major interaction shifted from Arg^{p304} on epitope of R56 to the highly conserved Phe^{p317} for R16, which explains the broad recognition of variant Envs by R16, and its broad and potent neutralization activities.

Discussion

Here we present four mAbs from one immunized rabbit that target the same V3 crown region but with different Env subtype specificity, binding affinity and neutralization breadth, using another V3 RmAb R56 reported previously as the control (Chapter II Section I). A diverse repertoire of different subspecificities, even within just the V3 region, was observed from antibodies developed from one rabbit. R16 and R73

recognized the tip of the V3 crown, R28 recognized the C terminal of the V3 crown, whereas binding of R64 to Env protein might be more conformational dependent. Genetic analysis showed that all V3 RmAbs had an average degree of affinity maturation in terms of hypermutation and CDR3 length. They bound to cross-clade HIV-1 Envs protein, including Clade A, B, C, and AE, with variant for each mAb, indicating that V3 antibodies tend to have broad recognition and strong binding to a wide range of Env proteins.

Interestingly, R16 showed superior neutralization activity, not only against tier 1 but also selected tier 2 viruses. At a IC_{50} less than 50μg/ml, R16 was able to neutralize 91% of viruses at a concentration that is less than 50μg/ml, and can neutralize three out of four tier 2 viruses tested. In contrast, R56, another V3 crown-specific RmAb isolated from another rabbit, recognized only 39% of tested viruses and could not neutralize any tier 2 viruses. Furthermore, the geometric IC_{50} of R16 was 10-fold lower than that of R56. The structural comparison of R16 and R56 suggested that one amino acid change of their epitopes from charged Arg^{p304} the highly conserved Phe^{p317} might be responsible for this great improvement in neutralization potential. There are two common contacting residues, Ile^{P307} and Ile^{P309}; however, R56 also recognized Arg^{p304} through a salt bridge; in contrast, R16 binds to a highly conserved residue, Phe^{p317} via hydrophobic interaction. This suggests that it is critical for V3-specific mAbs to recognize their cognate epitopes via optimal hydrophobic contacts.

For the first time, we isolated a vaccine-elicited V3-specific mAb that has broad and potent neutralization activities. This suggests that V3 is an appropriate target for an HIV vaccine and our vaccine strategy is effective in generating such high quality

antibodies. Our collaboration study with Zolla-Pazner also succeed in eliciting cross-clade neutralizing responses against tier 1 and tier 2 viruses by a similar approach, namely gp120 DNA prime followed by V3-scaffold protein (201). Furthermore, V3 has become part of key neutralizing epitopes of recently isolated bNAbs. For example, PGT121-PGT123 binds to V3 base and N332 glycan (126); PGT128 recognizes an epitope, including the C terminal of V3 (127). Therefore, given optimal immunogen design and sufficient affinity maturation, elicitation of R16-like antibody responses to prevent HIV acquisition is achievable and potential promising.

Section V
Diverse repertoire of rabbit monoclonal antibodies elicited
by a Clade AE gp120 immunogen

Introduction

HIV-1 subtype AE was initially isolated in Thailand and is currently the predominant circulating isolate in south and southeast Asia. In order to find an immunogen candidate from clade AE, we have screened a number of gp120AE Envs from primary immunogens; however, these Envs could barely induce neutralizing antibody responses. Instead, a consensus clade AE gp120 developed by our lab was found to induce potent neutralizing antibody responses against several tier 1 viruses (Table 2.10). More interestingly, we found that this PG9 was able to bind gp120AE. PG9 is an antibody that preferentially binds to the trimer, suggesting that the quaternary epitope from a conserved region of V1/V2 and V3 presented on the trimer is accessible on this particular gp120AE. To understand the uniqueness of gp120AE and its induced antibody response, a rabbit was primed with a DNA vaccine expressing gp120AE antigen via gene gun and further boosted with a 5-valent gp120 proteins, including 92UG037, JR-FL, 93MV965, 92UG021, and AE consensus. Twelve gp120AE-specific monoclonal antibodies were isolated from this immunized rabbit; four V3-specific mAbs were described in section IV. In this section, we will describe the other eight mAbs, including their binding epitopes, genetic features, binding cross-reactivity, and neutralizing activities.

Results

Different binding epitopes for gp120AE-elicited mAbs as determined through peptide array

mAb binding specificities were determined by overlapping linear peptides ELISA using consensus M gp120 as the coating antigen (Table 2.11). We were able to categorize 10 mAbs into four groups:

1) Four mAbs, UMMS2-R16, UMMS2-R73, UMMS2-R64 and UMMS2-R28, targeted at the most immunogenic V3 crown, which has been discussed in section IV.

2) Three mAbs, UMMS2-R80, UMMS2-R47, and UMMS2-R75, which are specific for the C terminal end of the C1 region. Both R80 and R47 target peptide #27, UMMS2-R80 recognizes the C terminus end of C1, and UMMS2-R47 recognizes peptides spanning #25 to #27. UMMS2-R75 only recognize C1 peptides weakly.

3) Two mAbs, UMMS2-R76 and UMMS2-R7, targeted the middle of the C5 region. The footprint of UMMS2-R7 is slightly larger compared to UMMS2-R76, as UMMS2-R75 recognizes two peptides and UMMS2-R76 only recognize one peptide.

4) There is no detectable positive peptide recognized by two mAbs, UMMS2-R31 and UMMS2-R9. Therefore, they could target conformational epitopes or some unknown linear sequence.

ELISA binding shows broad cross-reactivity against Envs

To determine the binding capacity of vaccine-elicited mAbs, five genetically distinct Envs from subtype A, B, C, D, and AE were used in an ELISA assay where gp120AE was the vaccine strain (Fig.2.17). For C1 mAbs, UMMS2-80 and UMMS2-47 bound to all five Envs quite well, whereas R75 did not bind to all Envs well, especially not to 92UG021 (D). Interestingly, three C1 mAbs isolated from a JR-FL immunized rabbit could bind only to 92UG037(A) and JR-FL (B) (Fig. 2.4), suggesting C1 region from AE immunogen may induce antibody with broader reacting against this region (191).

Table 2.10 Neutralization activity of rabbit sera primed with DNA vaccine expressing gp120AE consensus followed by a five-valent gp120 protein boost

Virus Clade	Pseudovirus Panel	percentage of neutralized virus	IC$_{50}$
Clade B	SF162	99	>7290
	ss1196	96	>270
	QH0692	72	17
	6535	90	71
	SC422	31	NA
Clade C	ZM249	21	NA
	DU172	57	NA
	CAP45	50	NA
	CAP210	0	NA
	DU156	51	11
Clade AE	620345.c01	13	NA
	620345.c10	-32	NA
	703357.c02	21	NA
	427299.c12	34	NA
	816763.c02	24	NA
	356572.c02	31	NA

Table 2.11. Binding specificities of vaccine-elicited mAbs mapped by overlapping peptide ELISA. (A) OD_{450} value of C1-specific mAbs against a panel of C1 linear peptides. The positive peptides were highlighted. (B) OD_{450} value of C5-specific mAbs against a panel of C5 linear peptides. The positive peptides were highlighted.

(A)

peptide #	16	17	18	19	20	21	22	23	24	25	26	27	28	29	30
UMMS2-R80	0.0753	0.0637	0.0741	0.0648	0.0561	0.0574	0.0546	0.0549	0.0614	0.0619	0.0829	0.8880	0.1476	0.2483	0.0884
UMMS2-R47	0.0768	0.0720	0.0736	0.0703	0.0821	0.0821	0.0660	0.0699	0.0719	0.4292	1.0117	0.9997	0.0662	0.0611	0.0984
UMMS2-R75	0.1007	0.0683	0.0664	0.0605	0.0563	0.0607	0.0648	0.0600	0.0598	0.0621	0.0672	0.0900	0.0787	0.1216	0.3356

Peptide # ID	sequence
25	NNMVEQMHEDIISLW
26	EQMHEDIISLWDQSL
27	EDIISLWDQSLKPCV
28	SLWDQSLKPCVKLTP
29	QSLKPCVKLTPLCVT
30	PCVKLTPLCVTLNCT

(B)

	119	120	121	122	123	124
UMMS2-R7	0.0951	0.9451	0.9020	0.0577	0.0520	0.0553
UMMS2-R76	0.0502	0.0572	0.7722	0.0535	0.0539	0.0586

Peptide # ID	sequence
120	KYKVVKIEPLGVAPT
121	VKIEPLGVAPTKAKR
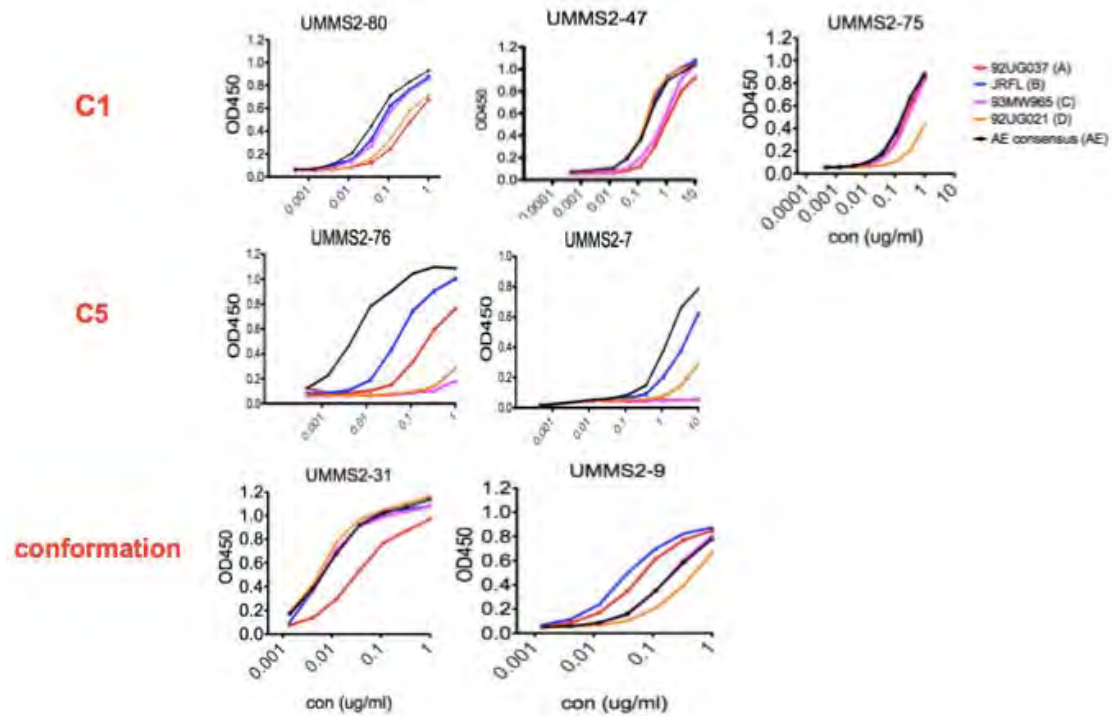
Figure 2.17. Cross reactivity of rabbit mAbs with a panel of representative gp120 proteins. RmAbs recognized most of the selected Env gp120 proteins by ELISA, including Clade A 92UG037, Clade B JR-FL, Clade C 93MW965, and consensus AE, but not Clade D 92UG021.

For C5 mAb, R76 not only strongly recognized gp120 consensus AE, but also bound with gp120 proteins from 92UG037 (A) and JR-FL (B). It could not recognize the other two gp120s of subtype C and D (Fig.2.17). In contrast, R13, another C5 mAb from a JR-FL immunized rabbit, was able to recognize all 4 Envs except Env from Clade C (Fig.2.4). Two conformational mAbs, UMMS2-31 and UMMS2-9, appeared to recognize all five Envs, but UMMS2-9 had lower binding affinity for all Envs compared to UMMS2-31.

Binding kinetics of selective rabbit mAbs for representative Envs

To quantify the binding affinity of rabbit mAbs for different subtype Envs, C1 mAb UMMS2-80, C5 mAb UMMS2-R76, and conformational mAb UMMS2-R31 were selected to determine K_D for five Envs using Fortebio (Table 2.12). Consistent with previous ELISA results, UMMS2-80 showed the highest affinity for JR-FL gp120 and consensus AE gp120, with K_D values of 6.06nM and 5.69nM, respectively. Interestingly, UMMS2-76 had high binding affinity for all five Envs, with highest affinity for JR-FL gp120 (K_D value beyond 0.001nM) and a K_D value of 0.302nM for consensus AE gp120. Conformational mAb UMMS2-31 had high affinity (nM range) for gp120 from B, C, D and AE, while slightly lower binding affinity (16.3nM) for gp120A.

Genetic features of heavy chain and light chain of vaccine-elicited RmAb

To understand the genetic features of these RmAbs, full length IgG heavy chain and light chain genes were sequenced. Germline usage, mutation frequency, and CDR3 length for heavy chain and light chain V genes were determined using IMGT (Table 2.13). In contrast to the observation that S40*01 had mostly germline usage in a JR-FL-immunized rabbit (191), here we see a variety of germlines adopted, including S69*01,

Table 2.12. Binding affinity (M) of rabbit mAbs to five selected Env proteins determined by ForteBio Octet Qk^e.

epitope	mAbs	gp120-A	gp120-B	gp120-C	gp120-D	gp120-AE
C1	umms2-R80	3.24E-08	5.69E-09	1.89E-08	3.33E-08	6.06E-09
C5	umms2-R76	3.28E-10	<1.0E-12	6.24E-11	1.73E-09	3.02E-10
Conformation	umms2-R31	1.63E-08	2.05E-09	3.40E-09	6.13E-09	6.27E-09

Table 2.13. Characteristics of V gene of heavy chain and light chain of anti-V3 rabbit mAbs elicited by vaccine

Epitope	Hybridoma ID#	IGHV			IGKV		
		germline (IMGT)	mutation frequency (%)	CDR3	germline (IMGT)	mutation frequency (%)	CDR3
C5	UMMS2-76	S69*01	21	10	S12*01	6	10
	UMMS2-7	S44*01	8	9	S11*01	10	10
C1	UMMS2-47	S69*01	7	14	S12*01	8	12
	UMMS2-80	S42*01	14	9	S17*01	10	13
	UMMS2-75	S44*01	9	9	S11*01	9	10
Conformation	UMMS2-9	S69*01	8	14	S17*01	10	13
	UMMS2-31	S69*01	5	22	S3*01	6	11

S44*01, and S42*01. This pattern could be the germline preference in individual rabbits, or it could be because different immunization strategies induce activation of different germlines. Interestingly, antibodies with similar epitopes also used different germlines, including two C5 mAbs and three C1 mAbs. Mutation frequency and the length of CDR3 region are important parameters to evaluate the degree of affinity maturation of antibody development. We observed that UMMS2-R76 has a 21% mutation frequency in the heavy chain variable region, indicating a high degree of affinity maturation. Indeed, the affinity of UMMS2-R76 binding with gp120AE reached as high as 0.302nM. Besides, UMMS2-R31 has a long CDR3 (22 residues), which also binds broad gp120s, whereas CDR3 length in other mAbs is typically below 15 residues.

Sporadic neutralization activities measured by TZM-bl assay

To determine the neutralization capabilities of these mAbs, we conducted an in-house TZM-bl neutralization assay using a mini-panel of tier 1 viruses, against which only two mAbs had sporadic neutralization activities. We sent these two mAbs out to the Seaman Lab from the CAVD. A panel of 23 well-characterized pseudotyped viruses expressing Env from a wide range of primary HIV-1 isolates was used, including 19 tier 1 viruses (2 Clade A, 7 Clade B, 6 Clade C, 1 Clade AE, and 3 Clade AG) and 4 tier 2 viruses (2 Clade B, 1 Clade C, 1 Clade BC) (Table 2.14). Similar to what we observed in our in-house assay, C5 mAb R76 neutralized clade AE virus, TH023.6, at a concentration of 8.224μg/ml, clade C virus, MW965.26, at a concentration of 10.071μg/ml, and clade B virus, SF162.LS, at 27.524μg/ml. C1 mAb R75 neutralized Clade AE virus at 0.594μg/ml, Clade B, SF162.LS, at 1.920μg/ml, and Clade C virus, MW965.26, at 23.616μg/ml. Moreover, R75 neutralized Clade B viruses, BaL.26 and Bx08.16, at concentrations of

Table 2.14. Neutralization IC$_{50}$ (µg/ml) of rabbit mAbs by TZM-bl assay

IC50 Titer in TZM.bl cells (ug/ml)			
Tier 1 Virus	Clade	R76	R75
MN-3	B	>50	>50
SF162.LS	B	27.524	1.920
BaL.26	B	>50	36.616
SS1196.1	B	>50	>50
Bx08.16	B	>50	36.065
BZ167.12	B	>50	>50
6535.3	B	>50	>50
MW965.26	C	10.071	23.661
TV1.21	C	>50	>50
ZM109F.PB4	C	>50	>50
ZM197M.PB7	C	>50	>50
00836-2.5	C	>50	>50
25710-2.43	C	>50	>50
MS208.A1	A	>50	>50
Q23.17	A	>50	>50
DJ263.8	CRF02_AG	>50	>50
242-14	CRF02_AG	>50	>50
T271-11	CRF02_AG	>50	>50
TH023.6	CRF01_AE	8.224	0.594
Tier 2 Virus			
JR-FL.JB	B	>50	>50
REJO4541.67	B	>50	>50
ZM135M.PL10a	C	>50	>50
CNE20	BC	NT	>50

36µg/ml (for both). Neither mAbs could neutralize any tier 2 viruses and, overall, they had low level neutralization activities.

Discussion

In this study, we examined humoral responses elicited by a HIV gp120AE vaccine by dissecting the epitopes and biological function of Env-specific monoclonal antibodies. Through gp120 AE vaccination, a diverse array of antibodies targeting different specificities was found, including V3, C5, C1, and conformational epitopes. Other epitopes, such as those in the V2 region, may have been missed since the mAbs were selected based on their potential neutralization capabilities before we learned RV144 study result. These recombinant mAbs have broad cross-reactivity against representative Envs, which not only bind to gp120 Env of the vaccine strain, but also recognize other Envs. This was also confirmed by determining binding affinities using Fortebio. Interestingly, antibodies targeting at the same epitope shared the similar cross-reactivity against representative Envs from different clades. Unfortunately, unlike V3 mAbs, only two out of seven mAbs showed low level neutralization activities and there was no detected neutralization activities for the other five mAbs .

Despite low neutralization activities observed from these mAbs, these rabbit mAbs might also have other important biological functions. First, IgG Fcγ receptor (FcγR)-mediated inhibition of Abs plays an important role in anti-viral function. Abs that recognize an infected target cell via its Fab domain and FcγR on the effector cell via its Fc domain leads to lysis of infected cells, called antibody-dependent cellular cytotoxicity (ADCC). The RV144 trial has shown that low-level IgA and high level ADCC activities inversely correlate with infection risk (88). In addition to ADCC, various antibody

inhibitory functions may also contribute to HIV prevention, including phagocytosis, complement-mediated lysis, and transcytosis inhibition. Further, antibodies also have indirect anti-viral functions. They may modulate inflammatory and immune responses by induction of antiviral cytokines and chemokines and internalization of immune complexes for T cell presentation. Such assay systems to test these other potential biological functions of rabbit mAbs are yet to be established. For example, our lab recently has established a chimeric rabbit Fab-human Fc technology platform which allow us to study above non-neutralizing protective antibody activities.

Chapter III

Immunogenicity of HIV-1 Envelope proteins with

unique N-glycan patterns

Introduction

The modest protection elicited by vaccines in the RV144 trial suggests that Env protein is a key component for HIV vaccine development. Env protein is heavily glycosylated, and nearly 50% of its molecular weight consists of a heterogeneous population of N-glycans with diverse glycoforms. However, the impact of various glycans on Env conformation and on its immunogenicity is still unknown. In particular, the glycoform for optimal immunogenicity of the Env protein is yet to be elucidated. It is current practice to produce GMP-grade Env proteins in CHO cell lines, a process that yields a mixture of different glycoforms that is unknown whether they will be same as that found in humans.

GlycoFi, a biotech company fully owned by Merck & Co., developed a sophisticated glycol-engineering method to control the composition of carbohydrates. In human cells when N-glycans are modified from "high mannose" to the final "complex" pattern, each step is controlled by a unique enzyme. In contrast, in yeast, a different set of host enzymes produces dramatically different patterns of N-glycans. Production of "humanized" yeast cells includes elimination of some yeast endogenous glycosylation pathways by gene knockout and re-creation of the human glycosylation pathway via introduction of heterogeneous essential genes in ER and Golgi in the yeast (*Pichia pastoris*) (Fig.3.1) (202, 203). Based on the specific sets of enzymes used in transfection
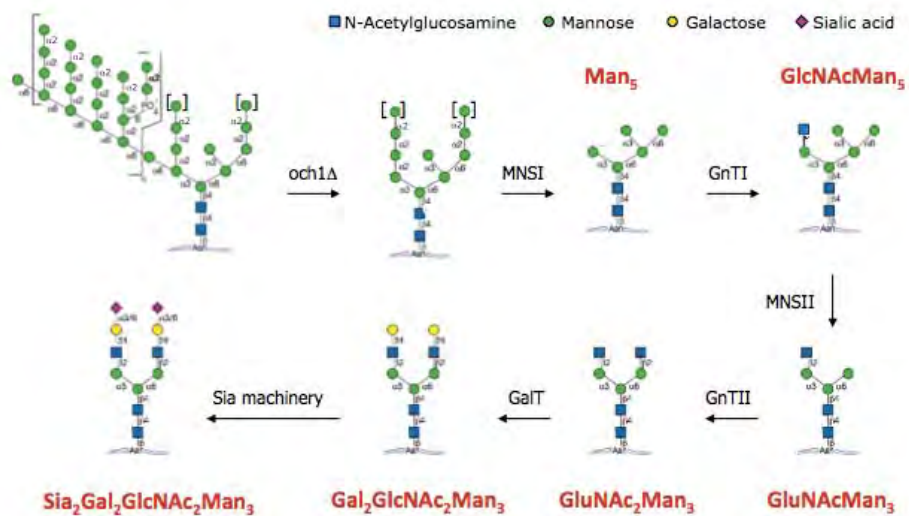
Figure 3.1. A flowchart overview of GlycoFi techonology. Glycoengineered yeast cell lines knocked out and introduced certain enzyme genes to control the glycosylation of protein expression.

with this system, mammalian recombinant proteins can be produced with well defined and more homogeneous patterns of N-linked glycans in yeast cells.

In the current study, we collaborated with scientists at GlycoFi, Inc. to produce and test the immunogenicity of HIV-1 JR-FL Env proteins with well-defined N-glycan patterns. We produced Env protein from five "humanized" yeast cell lines with distinct glycoforms, including Man5, Man8/9, Man3, 2,6 sialic acid and terminal gal (Table 3.1). This will be the first time that the impact of N-glycans on the immunogenicity of HIV-1 Env can be extensively analyzed. Optimal modified N-glycan forms on Env will be identified for the induction of protective antibody responses in animal models.

Results

Glycan analysis of glycan modified Envs produced from glycoengineered yeast cells

Mass spectrometry and high performance liquid chromatography (HPLC)-based quantitative N-glycan analysis for five GFI Envs was performed independently in both GlycoFi and lab of Dr. Lance Well and Dr. Michael Tiemeyer from University of Georgia. Both results are very consistent. GFI materials showed a dominant population of desirable glycoform modification (Fig. 3.2). Man3 Env had 66% of Man3, and 34% of Man4; Man5 Env had 98% of Man5; Man8-9 Env had 68% of Man8 and 27% of Man9; terminal gal Env had a 74% of galactose and 25% Man4-7; 2,6 sialic acid Env had 91% of sialic acid and 9% Man5-7. CHO-producing Env had a mixed population of glycans, which contains fractions of complex and various high mannose forms, none of which constitute more than 30% of the total N-glycan species. This suggested that highly homogenous pattern of N-glycosylation modified Envs have been successfully produced.

Glycan modification may impact the conformation of gp120 protein

Table 3.1 The gp120 proteins expressed from GFI engineered yeast cell lines and their corresponding glycoforms. Symbols used for the structural formulae in this figure: green circle, mannose; blue square, GlcNAc; yellow square, galactose; red square, sialic acid.

GFI cell lines	glycoform	
GFI2.1	Man3	
GFI2.0	Man5	
GFI1.0	Man8/9	
GFI5.0	Terminal Gal	
GFI6.0.6	2,6 Sialic acid	
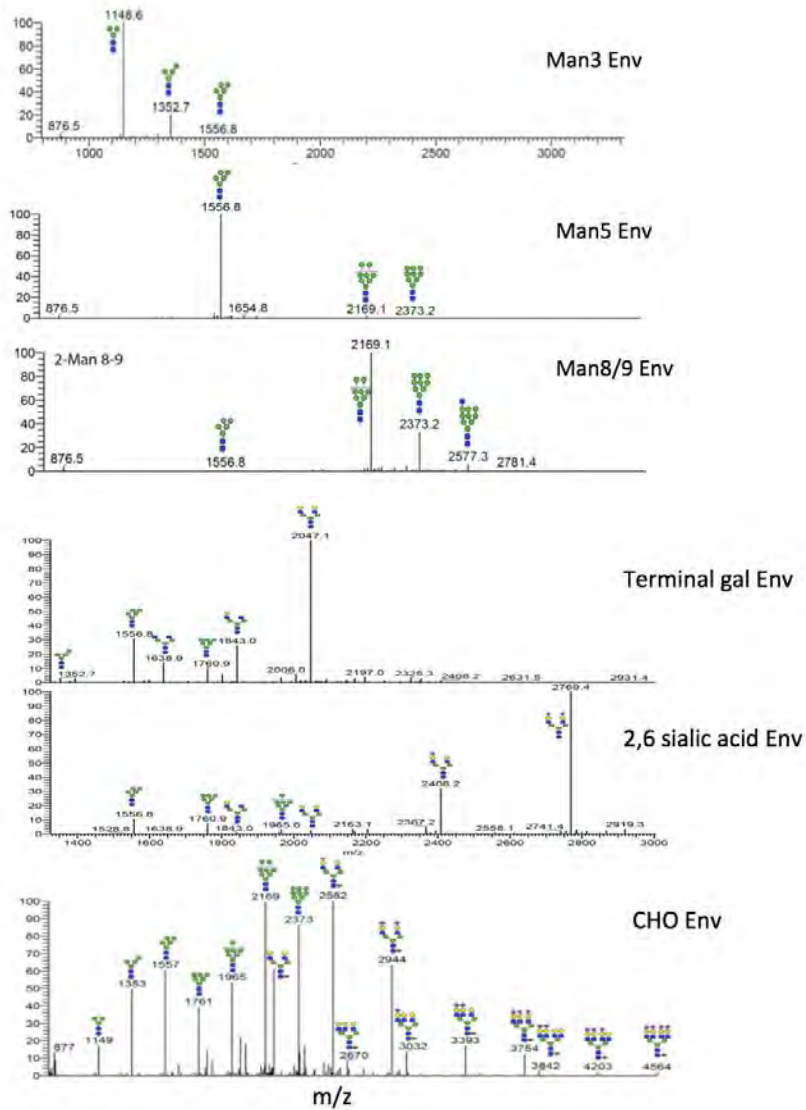
Figure 3.2 MALDI-TOF mass spectrometry analysis of released N-glycans from glycoengineered Pichia and CHO. Symbols used for the structural formulae in this figure: green circle, mannose; blue square, GlcNAc; yellow square, galactose; purple square, sialic acid.
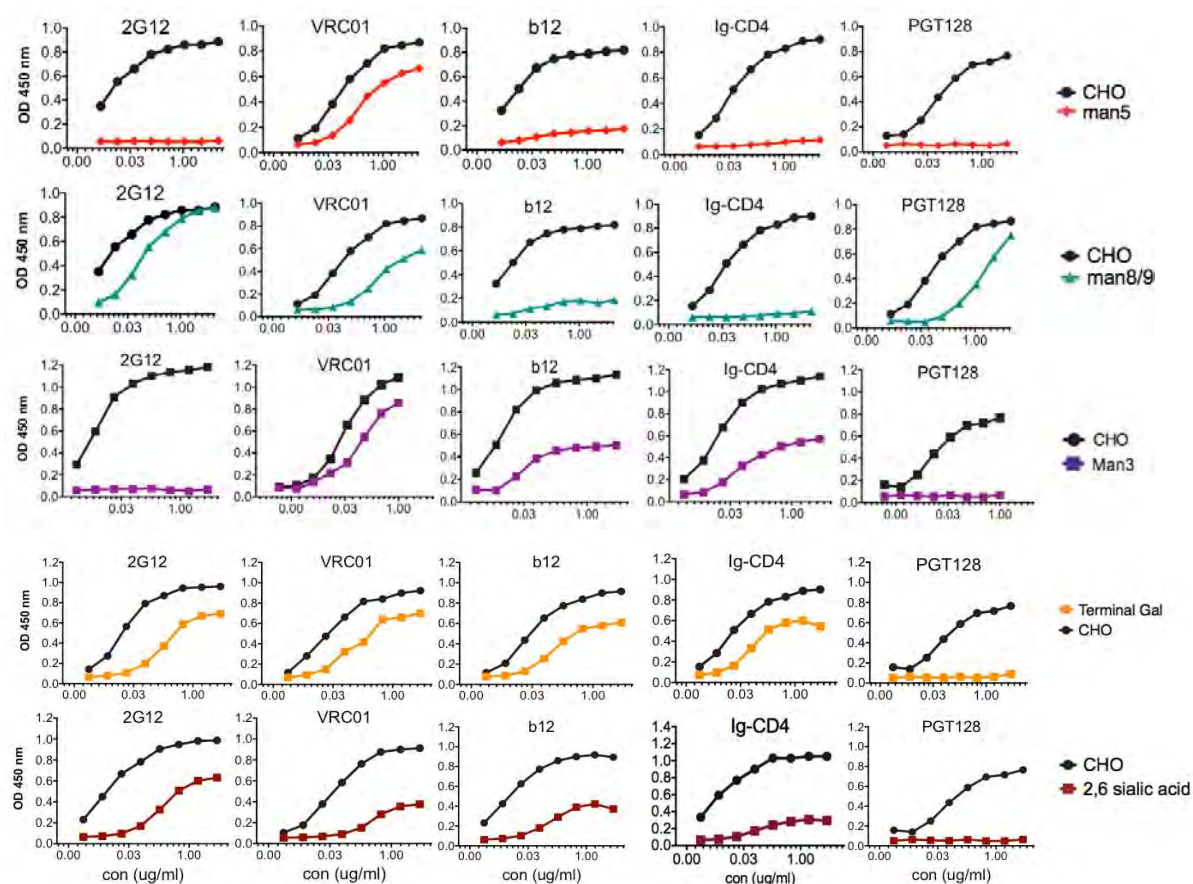
Figure 3.3. The exposure of key neutralizing epitopes on high mannose or complex Env protein. The binding capabilities of five Env modified with a homogenous population of single glycoforms with human mAbs were determined by ELISA. Five human mAbs were included, glycan-specific mAbs, 2G12 and PGT128, and CD4-related mAbs such as VRC01, b12, and Ig-CD4. CHO-producing Env protein was also included as control.
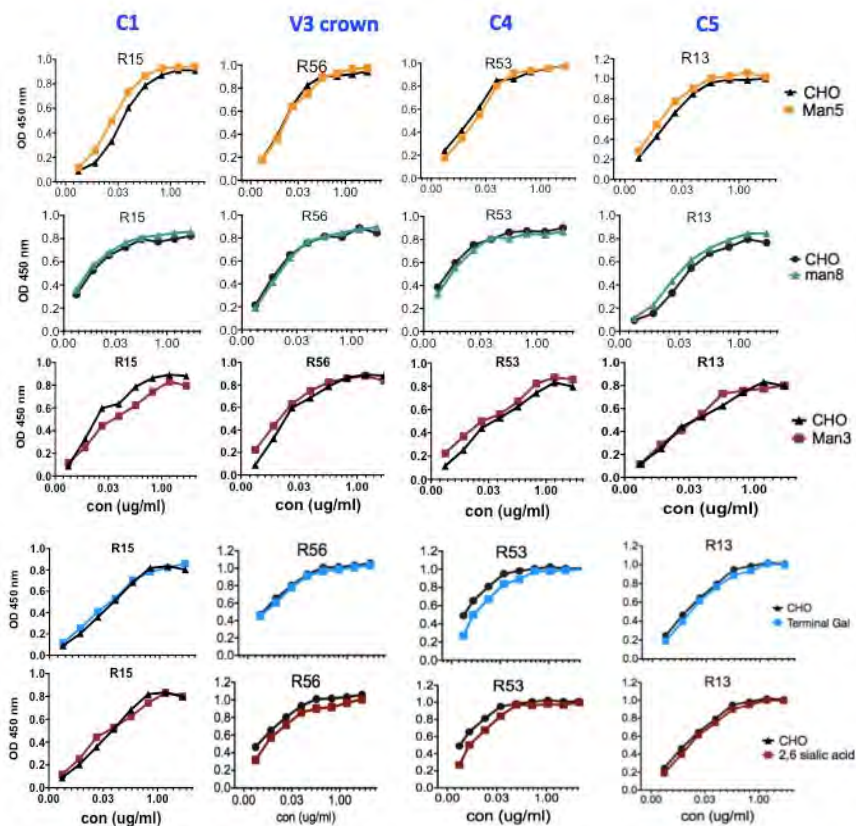
Figure 3.4. The exposure of linear epitopes on high mannose or complex Env protein. The binding capabilities of five Env modified with a homogenous population of single glycoforms with human mAbs were determined by ELISA. Four rabbit mAbs were used, targeting C1, V3 crown, C4 and C5 epitopes, respectively. CHO-producing Env protein was also included as control.

To determine the immunological features of novel Env antigens with modified N-glycosylations, both well-characterized human monoclonal antibodies (mAbs) and rabbit mAbs were utilized to evaluate their binding to Env protein. First, using ELISA, we showed that five N-glycan-modified immunogens have distinct binding profiles (Fig.3.3). Human mAb 2G12, a glycan-specific antibody (Ab), specific for terminal dimannose (Manα1,2Man), was able to bind to Man8/9 gp120, 2,6 sialic acid and terminal galactosylated Env, but failed to bind to Man5 Env. PGT128, the most potent broadly neutralizing antibodies (bNAb) in the PGT family, which specifically recognize the Man8/9 glycans on gp120, was also included into our analysis. As expected, PGT128 only recognized Man8/9 and CHO-produced Env proteins but none of the other GlycoFi (GFI) materials. CD4bs-specific Ab VRC01, a potent neutralizing mAb, was able recognize all of the glycan-modified immunogens, although in a weaker manner compared to Env protein produced from CHO cells. Another CD4bs mAb, b12, which neutralizes 40% of HIV-1 viruses, was able to bind to sialylated and galactosylated Env, but not man5 or man8/9 Env proteins. These differences in binding may be related to the different ways VRC01 approaches the CD4bs. VRC01 can approach its cognate epitope on the functional spike with less steric hindrance than does b12 and, surprisingly, with less hindrance than the soluble form of the virus receptor CD4 itself; while b12 approaches the CD4 contact region by more of a loop-proximal approach (204). Our data indicate that the CD4bs may only be partially conserved on these novel Envs. However, the overall integrity of these novel gp120 proteins are well preserved based on assays using a larger panel of representative rabbit mAbs (discussed in Chapter III), specific for

C1, V3, C4, and C5 regions (Fig.3.4). The rabbit mAbs used in the current study bound to the glycan-modified Envs as effectively as they bind to CHO-producing Env proteins.

To quantify the binding affinity of Env protein and mAbs, we used ForteBio, a powerful and user-friendly assay system; specifically, ForteBio Octet, was used for high throughput measurement of intermolecular interactions, including determination of association, dissociation, and K_D values down to a picomolar range. ForteBio Octet uses the natural phenomenon of biolayer interferonmetry analysis; it is label free, and provides a rapid, real-time record of biomolecule interactions. This technology made it possible to further determine the binding kinetics of human mAbs and glycan-modified Envs (Fig. 3.5). Glycan-specific mAb 2G12 showed higher affinity binding to Man8/9 Env protein (K_D =0.0263nM), compared to CHO Env protein (K_D =2.45nM), while its binding affinities to man5 and man3 Env protein were below detection. 2G12 bound to complex glycan (terminal gal and 2,6 sialic acid)-modified Env with ~10 fold lower affinity, compared to CHO protein. Consistent with our ELISA results, CD4bs-related mAb, VRC01, bound to all N-glycan-modified Env with slightly lower affinity, ranging from 2- to 20-fold, suggesting that the VRC01 epitope is preserved on these novel Envs. b12, another CD4bs mAb, bound Man8/9 protein with 18-fold lower affinity compared to CHO protein, and it failed to bind to Man5 protein. For complex carbohydrate-modified Envs, such as terminal gal and sialic acid Envs, b12 could bind with 13-fold and 16-fold weaker affinity, respectively, compared to CHO protein. For Ig-CD4, the binding affinities of Ig-CD4 to Man5, Man8/9, and Man3 proteins were 60-fold, 80-fold and 12-fold lower, respectively, compared to that of CHO (K_D=2.64nM). For complex glycans,

(A)

(B)
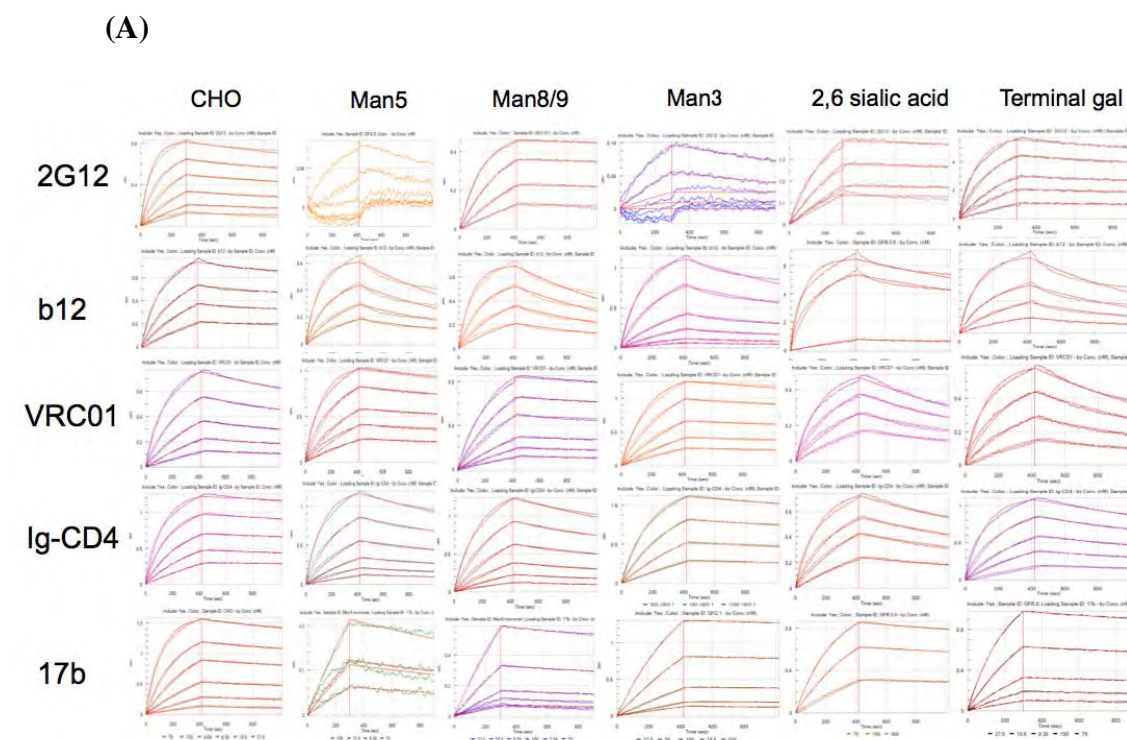
Binding affinity K_D (nM) of glycan modified Envs with key human mAbs

mAbs	CHO	Man5	Man8/9	Man3	2,6 sialic acid	terminal gal
2G12	2.45	NB	0.0263	NB	18.8	19.1
b12	1.43	14.1	26.4	23.3	20.4	18.6
VRC01	16	26.8	63.4	27.2	312	132
Ig-CD4	2.64	128.8	163.2	32.3	89	44.4
17b	2.82	58.8	28	5.42	10	4.32

Figure 3.5. Binding affinity for GFI Envs to key human Env-specific mAbs determined by ForteBio Octet QK^e. Human mAbs were immobilized on the chip surface; GFI Env or CHO Env was added to the testing solution. (A) The binding kinetics of five human mAbs to serially diluted glycan-modified Env protein. (B) Summary of binding affinity K_D for human mAbs binding to Envs, which were obtained by global fitting of the curves to 1:1 binding models. NB indicates "no binding".

Ig-CD4 binds to terminal gal and sialic acid Env protein with 20-fold and 40-fold lower affinity, respectively, compared to CHO-Env protein.

We further examined epitope exposure of CD4i antibody, 17b, on these novel Envs. To measure its affinity, first soluble CD4 (sCD4) was incubated with Env protein for 1 hour, and then 17b was used to test its ability to bind to Env protein after exposure to sCD4. We found that 17b binds to CHO, Man3, terminal gal, and 2,6-sialic acid Envs with similar affinities (K_D=2.82nM, 5.42nM, 4.32nM, and 10nM, respectively). However, 17b recognizes Man5 and Man8/9 with 25- and 10-fold lower affinity, respectively, compared to CHO Envs. The lower affinity with Man5 and Man8/9 may be due to their poor binding ability toward sCD4.

In summary, the data presented here indicates that the 2G12 epitope was preserved with Man 8/9, sialylated, and galactosylated Env, but not with Man5 or Man3 Env. The CD4bs was partially preserved on glycan-modified Env proteins, but may not take the same conformation as CHO-produced gp120 protein.

Evaluation of the quantity and quality of gp120-specific antibody responses elicited by different glycan modified gp120s

The immunogenicity of the above novel glycan-modified Envs was tested. In this study, only protein immunizations were used so that we could compare the immunogenicity of Env proteins directly without the interference of DNA priming. In pilot study, R-MK-01, Man5 formulated with alum was used to establish a baseline for our future study. Man5 Env and CHO-Env protein were formulated with adjuvant aluminum hydroxide and intramuscularly injected into rabbits four times, two weeks apart. Serum was collected at 2 weeks post the fourth immunization.

The antibody profile of immune sera was carefully examined. First, all gp120 protein immunogens elicited comparable levels of gp120-specific IgG antibody titer as detected by ELISA (Fig. 3.6). When CHO-Env was used as coating antigen, rabbit sera immunized with CHO-Env has slightly higher titer compared to Man5 immunized sera, while when using Man5 and deglysoylated Env as coating antigen, both groups had similar level of binding titer, suggesting that CHO-Env immune sera preferentially bind to homologous sugar modified Env protein. To determine the neutralization activities of immunized rabbit sera, a panel of tier 1 and tier 2 HIV-1 pseudoviruses produced from 293T cells was tested in a standard TZM-bl assay. The rabbit sera were sent to the Comprehensive Antibody Vaccine Immune Monitoring Consortium (CAVIMC) of the Collaboration for AIDS Vaccine Discovery (CAVD) (Seaman Lab at Harvard Medical School). A panel of eight Tier 1 and seven Tier 2 pseudovirus isolates covering different clades were chosen (Table 3.2). Data from the Seaman lab revealed that different neutralizing activities could be seen between sera elicited by Man5 gp120 protein and CHO-gp120 protein (Fig.3.7). Using alum as an adjuvant, Man5 gp120 protein was able to induce neutralizing antibodies against some sensitive isolates, but at a lower potency compared to CHO-gp120 protein-elicited sera. Tier 1B 6535.3 (Clade B), Tier 2 TRO.11 (Clade B), AC10.0.29 (Clade B), Du422.1 (Clade C), ZM53M.PB12 (Clade C), 0260.v5.c36 (Clade A), Q259.d22.17 (Clade A) and vaccine strain JRFL.JB (Clade B) were also included in the analysis but without neutralization any activity.

However, the above data could not rule out the possibility that all pseudoviruses were produced from 293T cells, in which the N-glycosylation pattern is more similar to that from a CHO cell expression system. The following studies were designed to
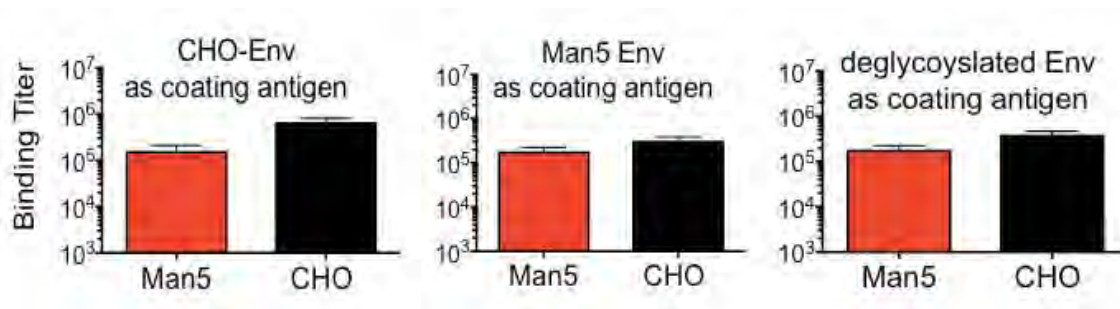
Figure 3.6. Env-specific binding titer in rabbits immunized with either Man5 Env or CHO Env. Total gp120-specific IgG was measured by ELISA in sera collected 14 days after the final protein boost, using CHO Envs, Man5 Env, and deglycosylated Env as coating antigens. There is no statistical significance between groups by student's t-test.

Tier 1A	Tier 1B	Tier 2
MW965.26-C	ss11961.1-B	TRO.11-B
SF162.LS-B	Bx08.1-B	AC10.0.29-B
	Bal.26-B	Du422.1-C
	BZ167.12-B	0260.v5.c36-A
	6535.3-B	Q259.d22.17-A
	DJ263.8-B	JR-FL.JB-B
		ZM53M.PB12-C

Table 3.2. A representative panel of 15 pseudoviruses used for evaluating neutralization activities of immune sera. The viruses included two tier 1A, six tier 1B, and seven tier 2 viruses. The corresponding subtype of each pseudovirus is noted, ranging from subtype A to subtype C.
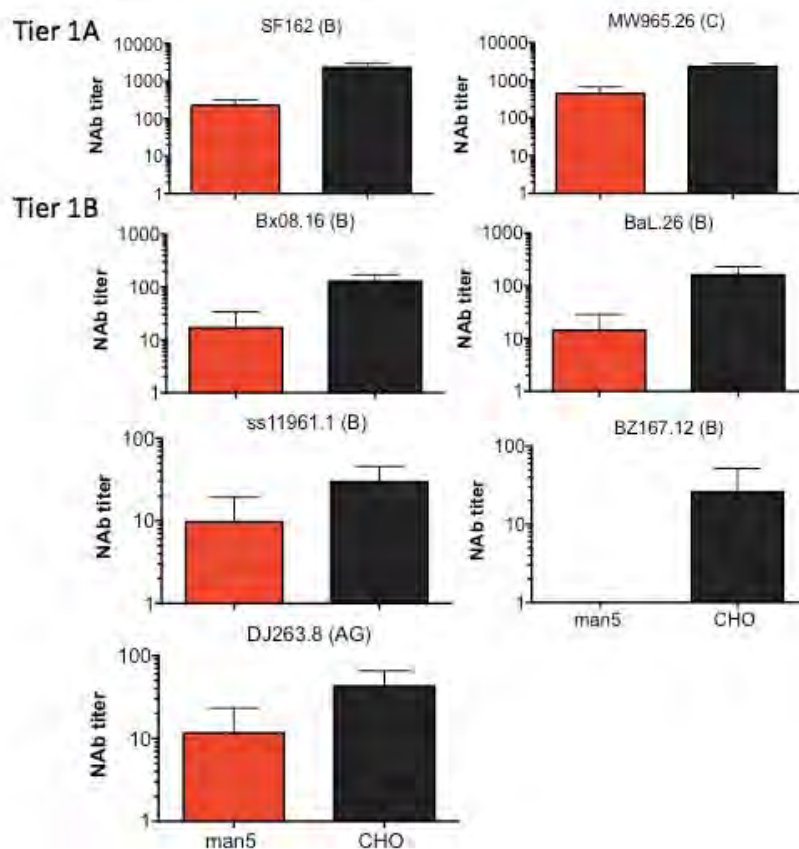
Figure 3.7. Neutralization activity of sera elicited by either Man5 or CHO-Env protein formulated with alum-based immunization against sensitive HIV isolates. Rabbit sera collected at two weeks post final protein immunization was tested for its ability to neutralize HIV isolates in a TZM-bl assay system, performed by CAVD Seaman laboratory. There is no statistical significance between groups by student's t-test.
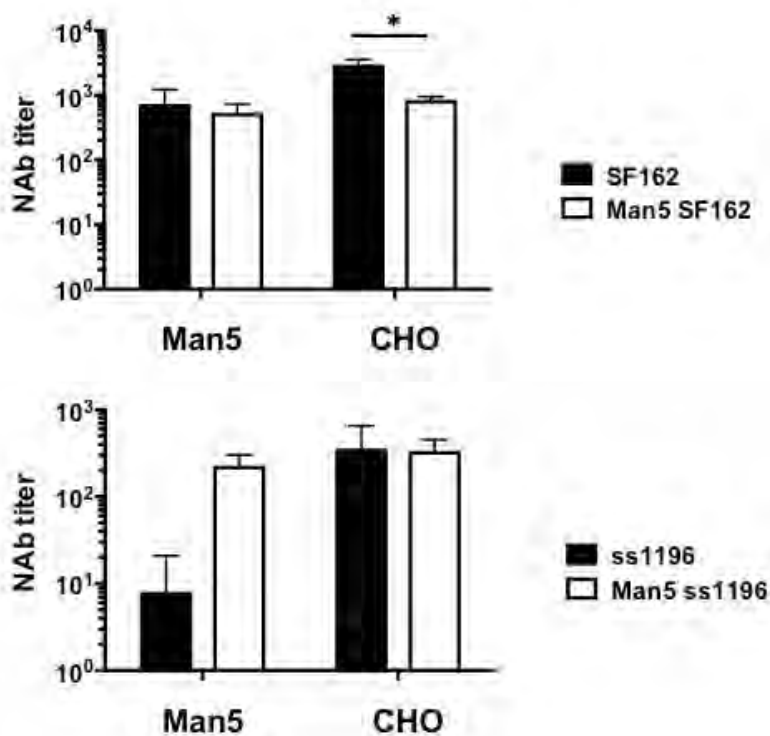
Figure 3.8. Neutralization activity of immune sera elicited by either Man5 or CHO Env protein formulated with alum-based immunization against glycan-modified HIV isolates. Rabbit sera collected two weeks post final protein immunization were tested for their ability to neutralize HIV isolates in TZM-bl assay system. The pseudoviruses SF162 and ss1196 were produced from 293T cells, and Man5 SF162 and Man5 ss1196 viruses were produced from GnTI-293S cells. *: $p<0.05$ by Student's t-test.

(A)

(B)
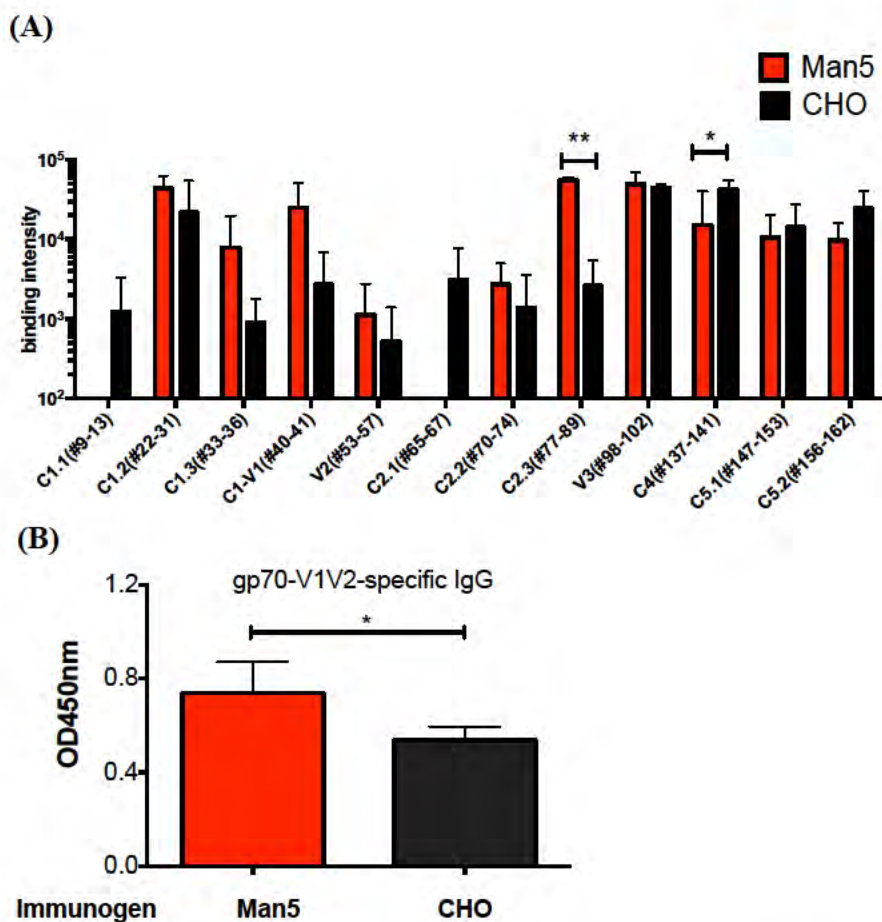
Figure 3.9. Epitope specificity of immune sera elicited by either Man5 or CHO Env protein. Rabbit sera collected two weeks post final protein immunization were tested for their epitope specificity, particularly against linear epitopes and the V1V2 region. (A) Maximum binding intensity of immune sera, Man5 Env (red) and CHO Env (black) against gp120 linear overlapping peptides. (B) V1V2-specific IgG response for immune sera from Man5 Env and CHO Env group. Statistical analysis was performed with Student's t-test (* : $p<0.05$ and ** : $p<0.005$).

investigate this possibility. To determine whether pseudoviruses containing modified N-glycosylation may be more sensitive to neutralization by rabbit sera elicited from high mannose gp120 proteins, we produced a series of pseudoviruses expressing only modified Man5, which are produced from GnTI$^{-/-}$ 293S cells. For the SF162 isolate, a significant reduction in NAb titer against Man5 SF162 relative to SF162 was seen with rabbit sera from the CHO-gp120; while the neutralizing potency of sera from the Man5-gp120 group was similar for N-glycan-processed SF162 as observed for the normal 293T-producing SF162 virus. More dramatically, sera from the Man5-gp120 group showed significantly increased NAb titers against GnTI-ss1196, compared to 293T-ss1196; whereas sera from CHO-gp120 immunized rabbits exhibited similar NAb titers against GnTI-ss1196 as it did against 293T-ss1196 (Fig. 3.8). Similar results were observed with the NL4-3 isolate. These observations suggest that Man5-gp120 protein immunogens may preferentially induce NAb against high mannose-modified viruses.

Epitope mapping with overlapping peptides for R-MK-01 rabbit immune sera

Distinct epitope specificities were observed between Man5-Env and CHO-Env proteins by using JPT high throughput peptide microarray technology, conducted by Dr. Tomaras's Lab, which is part of the CAVIMC in the CAVD (23). Binding specificity of rabbit sera was tested against seven types of consensus HIV Env peptide pools and against six vaccine strains. Figure 3.9A shows the maximum binding of each region of Env protein, indicating the highest binding intensity to a single peptide within a specific epitope region. First, all rabbits developed strong cross-clade anti-V3 responses. Second, distinct antibody repertoire were identified between the Man5 protein groups and the CHO protein group. In particular, Man5 Env protein generated strong antibody responses

(A)
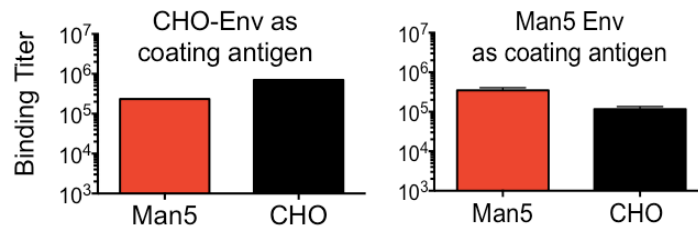
(B)
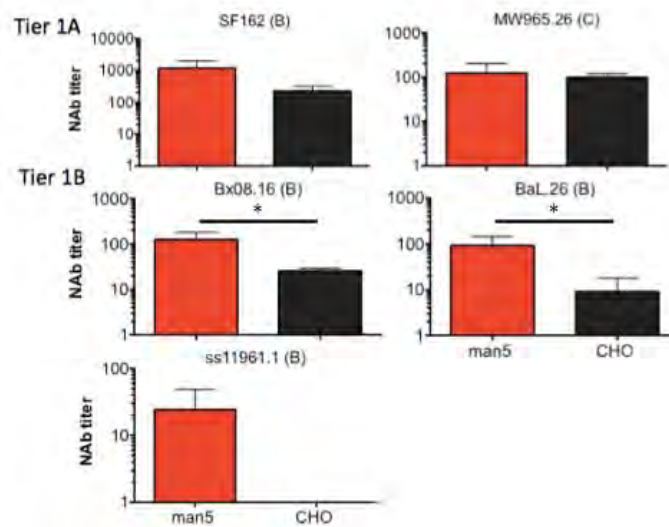
Figure 3.10. Neutralization activity of sera against sensitive HIV isolates elicited by either Man5 or CHO Env protein formulated with ISCOMATRIX^{TM} based immunization. Rabbit sera collected at two weeks post final protein immunization were tested for their ability to neutralize HIV isolates in TZM-bl assay, performed by CAVD Seaman laboratory (* : $p<0.05$ by student's t-test).

against C1.3, C1-V1 and C2.3 epitopes, responses that were weak in CHO-Env immunized rabbit sera; whereas CHO-Env was able to elicit a higher level of C4-specific antibody responses compared to the Man5-Env group.

We also detected low level V1V2 positive responses on peptide microarray, likely due to the fact that V2-specific recognition is conformational dependent. To further confirm whether we elicited a V1V2-specific response, scaffold protein gp70 derived from Feline leukemia virus envelope fused with V1V2 was used as a coating antigen in an ELISA assay. Man5 gp120 elicited higher JRFL V1V2-specific antibody responses, compared to CHO cell-derived gp120 (Fig. 3.9B).

ISCOMATRIX^TM enhanced GFI Env protein for induction of higher neutralizing antibody responses

For this study, we sought to determine whether an alternative adjuvant, ISCOMATRIX^TM, could further improve the immunogenicity of Man5 Env protein. ISCOMATRIX^TM adjuvant is by nature both a particulate and a saponin, which has been observed *in vivo* to induce IL-1B responses (205, 206). This adjuvant was also selected for our next generation HIV-1 polyvalent vaccine due to its ability to elicit higher titer bNAb with improved breadth against more primary HIV-1 viruses. Therefore, in our second animal study, we gave rabbits four immunizations of Man5 Env protein formulated with ISCOMATRIX^TM to see whether this adjuvant might be optimal for glycan-modified materials. For Env-specific binding titers, we found that immune sera was more preferentially bound to each homologous N-glycan modified antigen. (Fig.3.10A). Similar to R-MK-01, CHO-Env immune sera had a higher binding titer against CHO-Env compared to Man5 Env immune sera. In addition, different from our

(A)

(B)
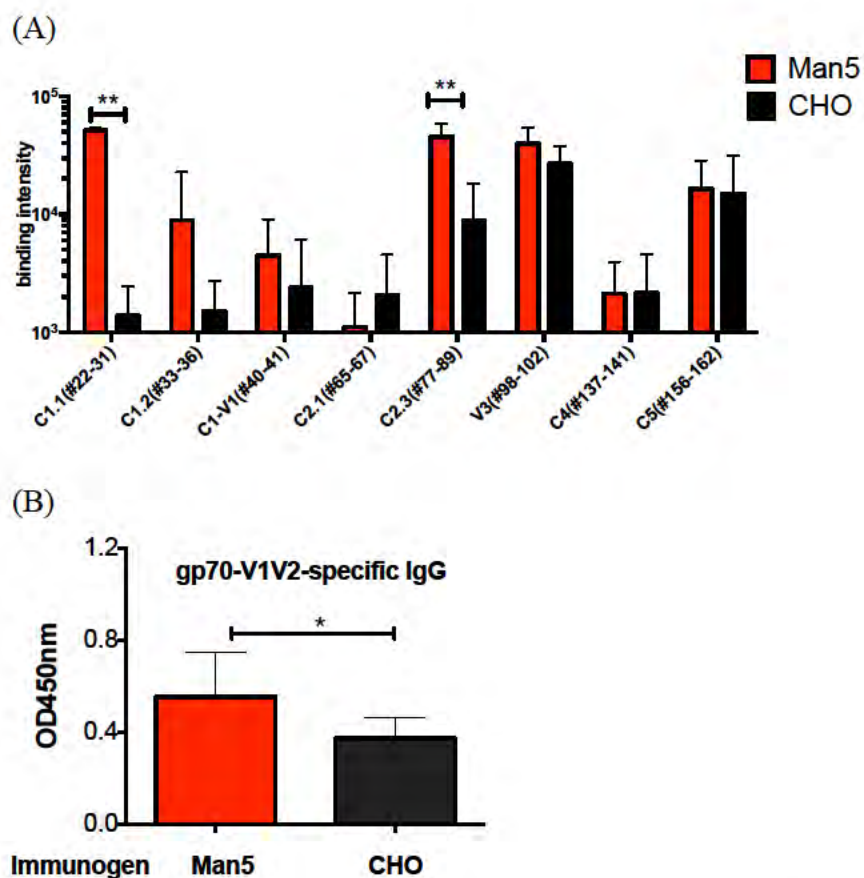
Figure 3.11. Epitope specificity of immune sera elicited by either Man5 or CHO Env protein. Rabbit sera collected two weeks post final protein immunization were tested for their epitope specificity, especially against linear epitope and V1V2 region. (A) Maximum binding intensity of immune sera, Man5 Env (red) and CHO Env (black) against gp120 linear overlapping peptides. **: $p<0.005$ by Student's t-test. (B) V1V2-specific IgG response for immune sera from Man5 Env and CHO Env group. * : $p<0.05$ by student's t-test.

observation from R-MK-01, Man5 immune sera also had a higher binding titer against Man5 Env compared to CHO-Env immune sera, suggesting that this adjuvant did improve the immunogenicity of Man5 Env. Furthermore, there was a clear improvement in NAb activities with the rabbit sera that were elicited by Man5 gp120 proteins (Fig.3.10B).

Rabbit sera elicited by Man5 JRFL gp120 elicited higher titer NAb against tier 1 viruses (SF162, ss1196, and NL4-3) compared to the CHO-Env protein group. Meanwhile, one rabbit from Man5 gp120 generated NAb against tier 2 virus, SC422.8, at low titer, while rabbit sera from the CHO-gp120 group failed to elicit any neutralization activities against tier 2 viruses. Our data confirmed that the glycan-modified gp120 proteins produced in yeast cells are equal or more immunogenic than the original gp120 protein produced in CHO cells, especially with the help of an optimal adjuvant such as ISCOMATRIX[TM].

Fig. 3.11A shows the maximum binding intensity for each epitope from the R-MK-02 study using JPT technology. First, similar to the R-MK-01 study, we observed that all animals developed strong cross-clade anti-V3 responses. Second, using ISCOMATRIX[TM] adjuvant, Man5-Env protein elicited higher IgG responses against additional regions compared to the CHO Env group, including C1.1, C1.2 and C2.3,. Moreover, Man5 protein elicited a higher level of V1V2-specific Ab responses than sera from the CHO-gp120 group (Fig.3.11).

Man8/9 Env protein-induced glycan-specific humoral responses

In this set of studies, we further explored the immunogenicity of other high mannose Env proteins. Man8/9 Env proteins formulated with ISCOMATRIX[TM] were
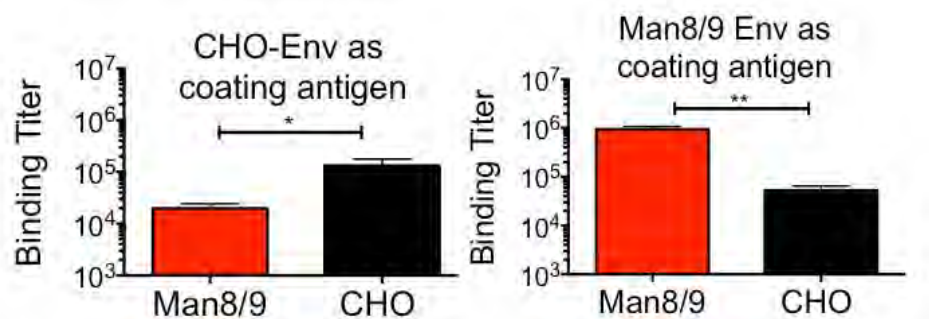
Figure 3.12. Env-specific binding titer in rabbits immunized with either Man8/9 Env or CHO Env. Total gp120-specific IgG was measured by ELISA in sera collected 14 days after the final protein boost, using CHO Envs and Man8/9 Env as coating antigen. *: $p<0.05$ and **: $p<0.005$ by Student's t-test.
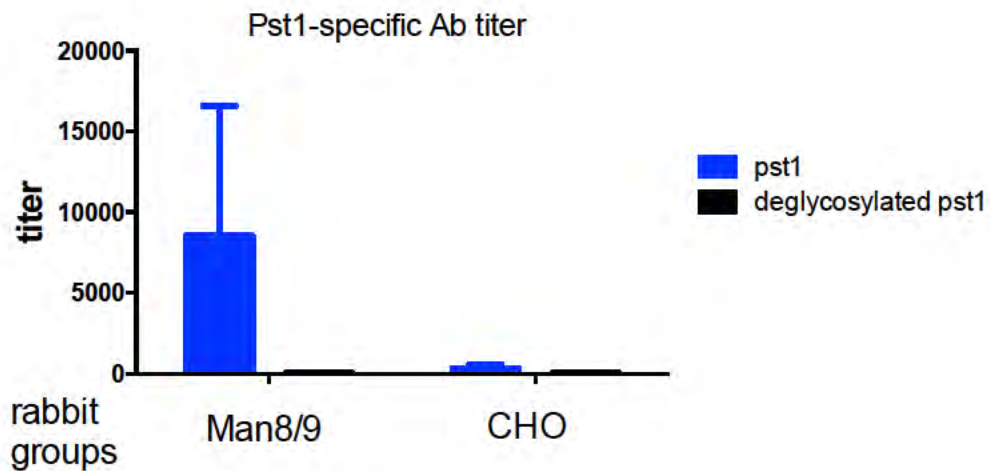
Figure 3.13. Man8/9 specific IgG responses from Man8/9 Env immunized rabbit sera. Man8/9-specific IgG were measured by ELISA in sera collected 14 days after the final protein boost, using pst1 and deglycosylated pst1 as coating antigen, respectively.

(A)
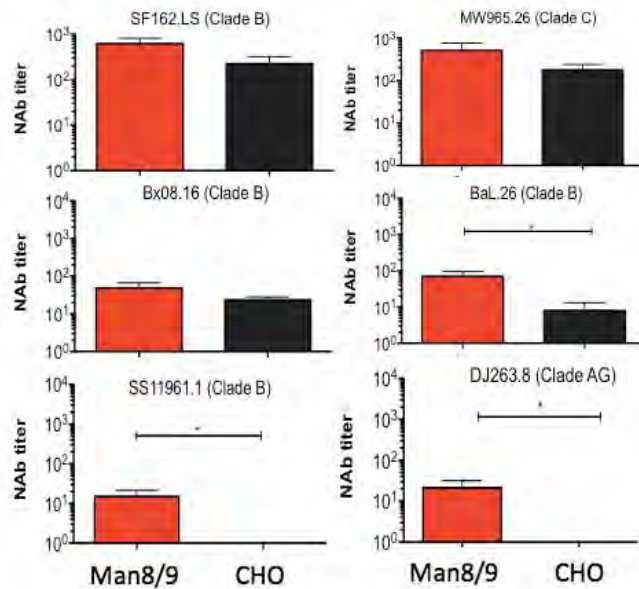
(B)
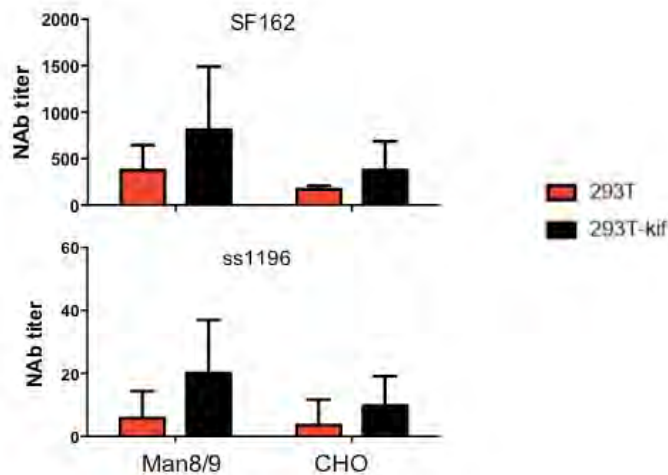
Figure 3.14. Neutralization activity of sera elicited by either Man8/9 or CHO Env protein immunization against sensitive HIV isolates. (A) Rabbit sera collected two weeks post final protein immunization were tested for their ability to neutralize HIV isolates in TZM-bl assay system, performed by CAVD Seaman laboratory. * : $p<0.05$ by Student's t-test. (B) Neutralization activities of immune sera against either 293T-producing viruses or with treatment with sugar inhibitor kifunensine.

injected into rabbits four times, one month apart. All proteins elicited comparable levels of gp120-specific IgG antibody titer as detected by ELISA (Fig. 3.12). Interestingly, gp120 protein with Man8/9 Env protein induced the highest binding titer in rabbit sera against the Man8/9 Env, while CHO-Env immunized rabbit sera had the highest binding titer against the CHO-Env protein. This suggests that N-glycan modification on Env may influence glycan-specific antibody responses.

To determine whether any specific Man8/9 humoral responses were generated, a $Man_8GlcNAc_2$ heavily glycosylated protein, Pst1, was used as the coating antigen in an ELISA binding assay (207). Pst1 is a non-HIV related yeast membrane protein that shows high affinity for 2G12(208). More importantly, although it cannot neutralize pseudoviruses produced from regular 293T cells, it is able to generate antibody that can neutralize Man8/9-modified pseudoviruses in rabbit. Fig. 3.13 shows that Man8/9 Env protein generated pst1-specific IgG responses, whereas hardly any detectable pst1-specific Ab responses could be observed with CHO-Env immunized rabbits. Deglycosylation of pst1 abrogated binding of rabbit sera immunized with Man8/9 proteins were used as a control.

To determine the neutralization activities of immunized rabbit sera, a panel of tier 1 HIV-1 pseudoviruses produced from 293T cells was tested in a standard TZM-bl assay, conducted by the CAVD Seaman Lab (Fig. 3.14A). The sera of rabbits immunized with Man8/9 Env had the higher titer against sensitive viruses SF162 (Clade B) and MW965.26 (Clade C) when compared to rabbit sera induced by CHO-Env. Man8/9 also elicited decent levels of neutralizing activities against Tier 1b viruses, including Bx08.16 (Clade B), BaL.26 (Clade B), ss11961.1 (Clade B), but reduced level of neutralizing
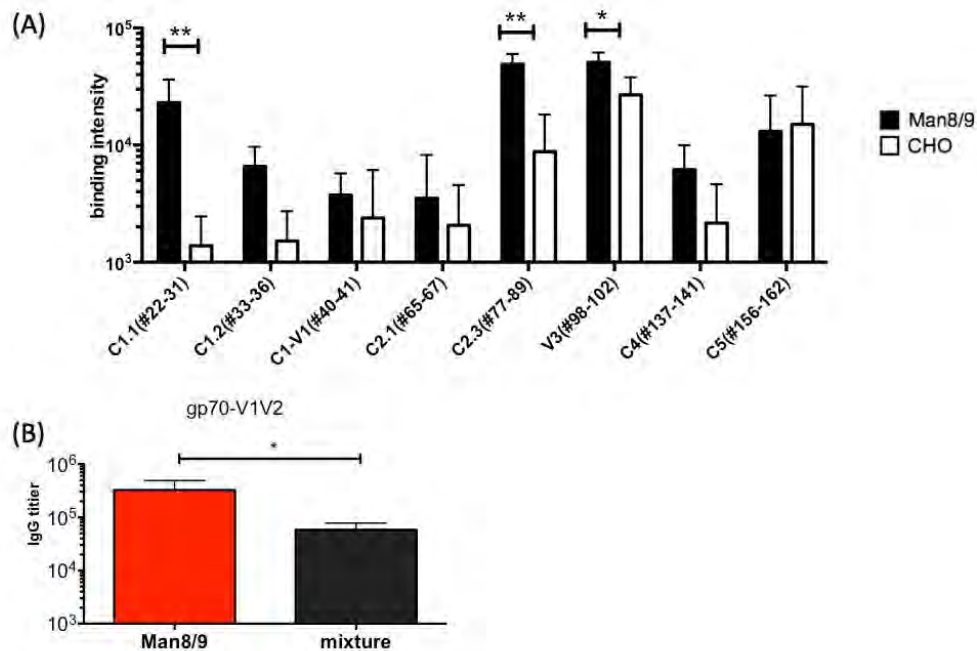
Figure 3.15. Epitope specificity of immune sera elicited by either Man8/9 or CHO Env protein. Rabbit sera collected two weeks post final protein immunizations were tested for their epitope specificity, especially against linear epitope and V1V2 region. (A) Maximal binding intensity of immune sera, Man8/9 Env (black) and CHO Env (white) against gp120 linear overlapping peptides. *: $p<0.05$ and **: $p<0.005$ by Student's t-test. (B) V1V2-specific IgG response for immune sera from Man8/9 Env and CHO Env group ($p<0.05$).

antibodies was observed in CHO-Env induced rabbit group. Man8/9 was even able to neutralize Clade AG DJ263.8 at very low level while the other groups failed to do so.

To further determine whether rabbit sera could become more sensitive to neutralize Man8/9 glycan-modified pseudoviruses, the above pseudoviruses were produced from 293T cells treated with α-mannosidase inhibitor Kifunensine (Kif). Kif inhibits $Man_9GlcNAc_2$ into $Man_5GlcNAc_2$, so that all pseudoviruses have only $Man_9GlcNAc_2$ at all utilized N-linked glycosylation sites (209). All rabbit sera showed increased neutralizing titers against both Kif-treated SF162 and ss1196 when compared to those from 293T cells (Fig. 3.14). This suggests that key neutralizing epitopes might be easily accessible due to a decreased presence of protective sugars.

Peptide microarray data performed by the CAVD showed a wide range of cross-clade responses against gp120 epitopes including C1, C2, V3, C4, and C5. In particular, strong N-terminal C1 region- and C terminal of C2 region-specific responses occurred in the Man8/9 Env group compared to the CHO-group. Man8/9 also induced higher N-terminal C5-specific responses compared to CHO-Env groups (Fig. 3.12A). Further, Man8/9 immunized sera showed strong IgG responses against the V1V2 region compared to CHO-Env protein (Fig. 3.15B).

Complex glycan-modified Env induced higher neutralizing activities

In addition to high mannose, complex and hybrid sugar is also a target of bNAbs (129). In this set of studies, we determined the immunogenicity of the remaining GFI Env proteins, including Man3, terminal gal, and 2,6-sialic acid Env protein. Using CHO-Env and three other GFI Envs in ELISA, I was able to detect the binding titer of Envs (Fig. 3.16). Either CHO-Env or GFI Envs produced overall comparable levels of binding titer
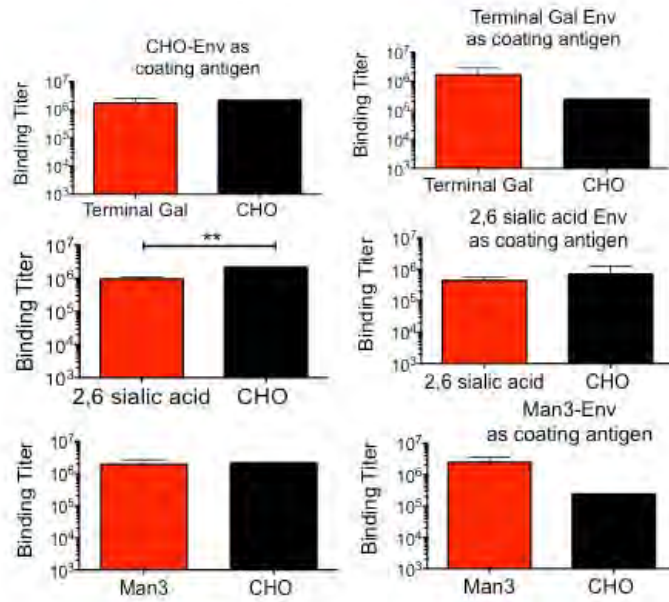
Figure 3.16. Env-specific binding titer in rabbits immunized with terminal gal, 2,6 sialic acid, Man3, and CHO Env. Total gp120-specific IgG was measured by ELISA in sera collected 14 days after the final protein boost, using each immunogen as a coating antigen (**: $p<0.005$ by Student's t-test).
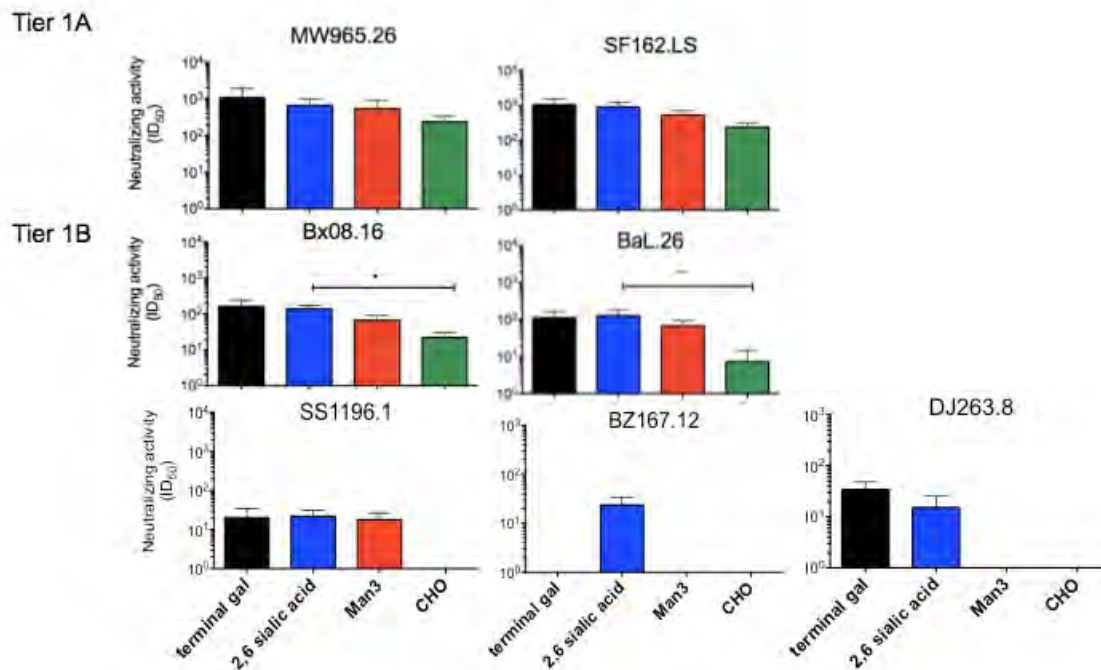
Figure 3.17. Neutralization activity of sera elicited by terminal gal, 2,6 sialic acid, Man3, and CHO Env protein immunization against sensitive HIV isolates. Rabbit sera collected two weeks post final protein immunization were tested for their ability to neutralize HIV isolates in TZM-bl assay system, performed by the CAVD Seaman laboratory. * : $p < 0.05$ and ** : $p < 0.005$ by Student's t-test.
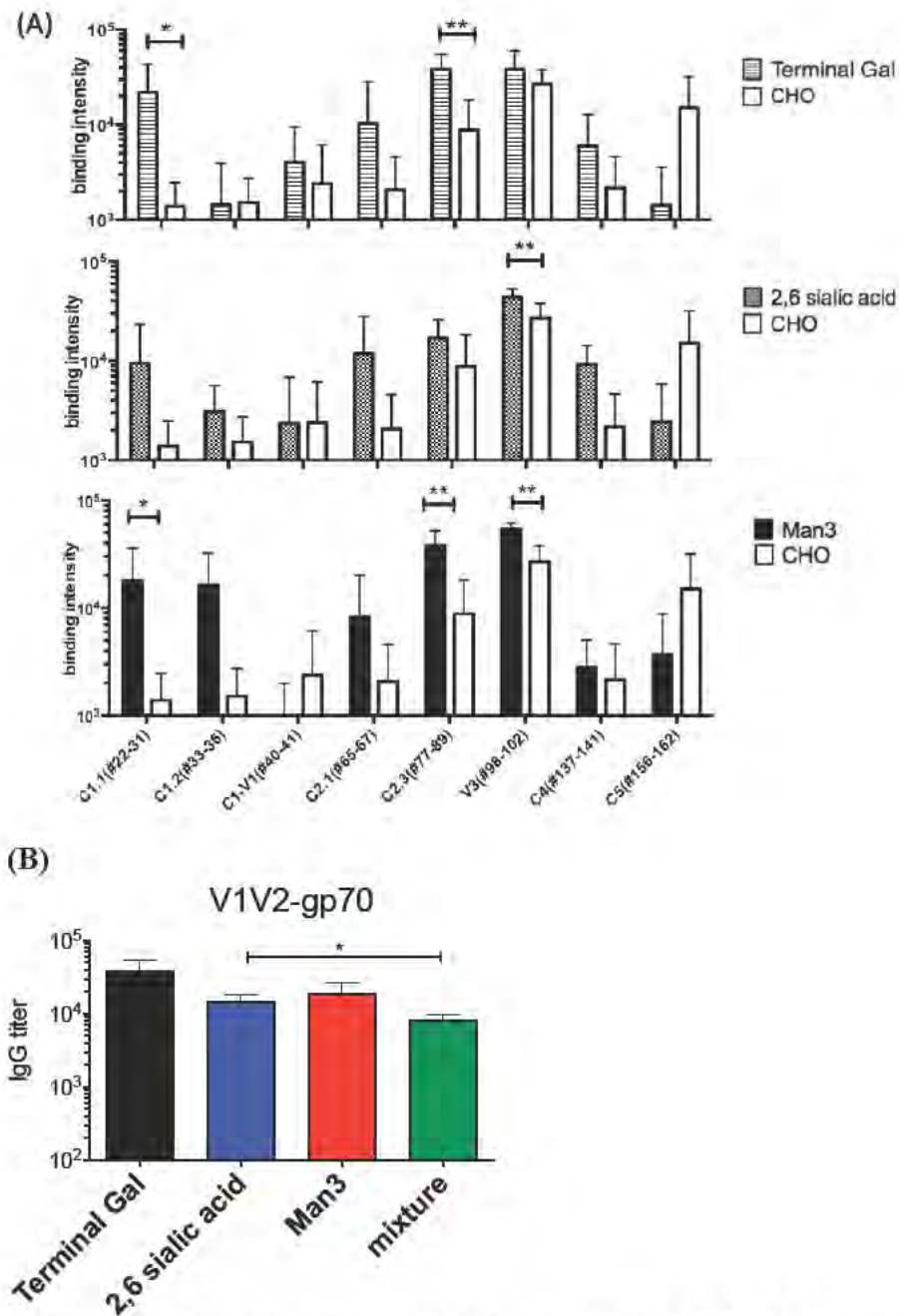
Figure 3.18. Epitope specificity of immune sera elicited by terminal gal, 2,6 sialic acid, Man3 Env, or CHO Env. Rabbit sera collected two weeks post final protein immunization were tested for their epitope specificity, particularly against linear epitopes and the V1V2 region. (A) Maximum binding intensity of immune sera against gp120 linear overlapping peptides. (B) V1V2-specific IgG response for immune sera (* : $p<0.05$ and ** : $p<0.005$ by Student's t-test).

(no statistical difference), using either CHO-Env or GFI Env as coating antigen. CHO-Env induced significantly higher binding titer compared to that from 2,6 sialic acid Envs, if using CHO-Env as coating antigen (p=0.001).

Further, we determined the neutralization activities of immunized rabbit sera. All groups showed a high level of neutralizing responses against Tier 1a viruses SF162.LS and MW965.26 (Fig. 3.17). Three GFI Env proteins induced significantly higher neutralizing titers against four tier 1b viruses, including Bx08.16, BaL.26, ss11961.1, and DJ263.8 compared to the CHO-Env group. Only the 2,6 sialic acid Env group was able to neutralize the BZ167.12 virus. Interestingly, complex glycan-modified Envs (2,6 sialic acid and terminal gal) induced the highest level of NAb responses compared to other GFI cell line modified Envs, despite a lack of statistical significance. All immunized groups failed to neutralize tier 2 viruses, indicating that protein alone immunization still is not an effective approach to induce potent neutralization activities.

Similar to previous observations from Man5 and Man8/9 Envs, Man3, terminal gal, and 2,6 sialic acid Envs also induced antibody repertoire with diverse specificities, especially higher level of antibody against N terminal of C1, C terminal of C2, and V3 region. Moreover, higher level of V1V2-specific antibody responses was also generated compared to CHO produced Envs (Fig. 3.18).

Discussion

Given the significant demand for recombinant Env proteins for HIV vaccine development, a solid understanding of the quality of Env proteins with an optimal glycosylation pattern will guide the production of Env immunogens. In this study, we established a yeast-based expression system for functional Env proteins with humanized

N-glycosylation, which provide a highly efficient and less costly expression system for the production of more affordable HIV vaccines.

In this study, five different glycoform-modified Env proteins were evaluated for their antigenicity and immunogenicity. Three high mannose carbohydrates were included. The first, $Man_5GlcNAc_2$ (Man5), is a biosynthetic intermediate in the N-link glycosylation pathway. HIV-1 Env-derived infected PBMCs are almost entirely oligomannose ($Man_{5-9}GlcNAc_2$) with a predominant population of $Man_5GlcNAc_2$ (33), indicating a lack of processing by GnTI or any of the subsequent Golgi-resident glycan processing enzymes. Therefore, Man5 is the native glycoform when viruses are propagated in infected PBMC (210). The second glycoform is Man8/9, composed of the epitope of a few glycan-dependent broadly NAbs. 2G12 binds terminal Manα1,2 Man-linked sugars moieties of high-mannose ($Man_{8-9}GlcNAc_2$) with high affinity. PG9 and PG16 also depend on Man8/9 oligomannose, due to the fact that they show decreased neutralization sensitivity against pseudoviruses produced from GnTI-deficient 293S cells while showing enhanced neutralization with Kifunesine treatment (209). Further, PGT family antibodies (PGT125-128 and 130-131) bind specifically to Man8/9 glycans on gp120 and potently neutralize cross clade viruses. The third glycoform, Man3, is the simplest glycan and has the minimal core structure for oligomannose. With a homogenous population of Man3, Envs have lower glycan "layer" compared to hybrid or complex glycan-modified Envs, which may allow for potential exposure sites for broadly NAb epitopes.

Two complex N-glycan types were also included. The first is a complex human biantennary structure with terminal galactose. One study showed increased neutralization

activity and T cell responses elicited by gp120 by enzymatic replacement of sialic acid on these carbohydrate chains with alpha-gal epitopes (211, 212). Anti-gal epitopes can bind the natural anti-Gal antibody (present in all humans as 1% of IgG), and thus form immune complexes, when injected as a vaccine into humans. It was considered that gp120 expressing alpha-gal epitopes lead to enhanced effective antigen uptake by antigen-presenting cells, due to the interaction between the Fc portion of the antibody and Fcγ receptor on antigen presentation cells (APC). The other is α-linked 2,6 sialic acid, which is a human type N-glycan and is negatively charged with a relative large size. These two N-glycans are the end products during N-glycosylation biosynthesis; CHO-produced Env protein has a dominant population of these complex N-glycans.

Antigenicity results from current studies suggest that CD4bs might not be exposed on glycan-modified Envs or if they are present, that may take on an alternative conformation since GFI Envs do not typically have high affinity for either Ig-CD4 or b12, especially when compared to CHO-derived Envs. However, this did not necessarily translate to poor immunogenicity for the CD4bs. For example, L40 and B33 are Env isolated from a single patient; they have low affinity for CD4 and high affinity for CD4, respectively. Surprisingly, L40 elicited broader NAb responses than B33 due to the recognition of CD4bs of Env (213). Indeed, all GFI Envs showed broader and more potent NAb responses compared to CHO-Envs. Epitope mapping indicated that GFI Envs tend to have a diverse range of linear epitope specificities, whereas there is a dominant population of V3-specific antibody responses from the CHO-Env protein immunized group. Further, GFI Envs also induced glycan-specific antibody responses, which might also enhance neutralization activities.

Interestingly, the majority of GFI Envs induced higher V1V2-specific antibody responses than those induced by CHO-Env. This is also consistent with epitope microarray data, which showed comprehensive humoral responses generated against diverse linear epitopes. In particular, high mannose Envs (Man5 and Man8/9 Env) elicited the highest level of V1V2-specific response, which might be due to a decreased sugar lattice on the Env protein, leading to increased exposure of the V2 region. The V1V2 region gained much attention lately due to its correlation with vaccine efficacy in the RV144 trial (85).

Another exciting finding was that carbohydrate-specific responses were also detected from GFI immunized sera. Carbohydrate is often considered poorly immunogenic (214). However, recent evidence shows that the human immune system can target either the glycan shield or specific N-glycan sites, followed by further affinity maturation and refinement to bNAbs, such as 2G12, PGT128, and PGT121 (37, 126, 127, 215). In our study, we also found carbohydrate-specific antibody responses from Man8/9 Env immunized sera, demonstrated by a strong recognition for pst1, an exclusively Man8/9 coated yeast cell membrane protein. Meanwhile, the deglycosylation of pst1 leads to a loss of recognition by immune sera. Moreover, Man8/9-modified psedoviruses were more sensitive to Man8/9 Env immunized sera, but not to CHO-Env-induced sera. Evidence has showed that HIV-1 viruses produced from infected PBMC are high mannose (33). All of these studies indicate that glycoforms play a critical role in vaccine design, and an optimal N-glycan form would be able to induce strong carbohydrate-specific antibody responses, which might further enhance neutralization activities *in vitro* and *in vivo*.

Several glycoforms of interest have been identified. We showed that Envs with a homogenous population of certain glycoforms are immunogenic and can even elicit high NAb responses and V1V2 responses. In particular, Man8/9 Envs is capable of inducing glycan-specific IgG responses, which was shown to play an important role in virus defense. Further, complex glycans, such as 2,6 sialic acid and terminal gal, have superior neutralization activities and induce V1V2 responses better than CHO-producing Envs. It will be of great interest to explore the immunogenicity of a polyvalent vaccine that combines Envs with several distinct glycoforms in non-human primate models.

Chapter IV

Sequential versus concomitant delivery of DNA and protein vaccines

Introduction

Initial work in our lab has shown that DNA prime-protein boost was more effective to elicit cross-clade neutralizing antibody responses compared to protein alone or DNA alone approaches (95, 96). Heterologous DNA prime-protein boost delivery not only may induce higher quantity antigen-specific humoral responses, but also generated an improved humoral response with broad neutralizing activity and higher avidity. Moreover, sera specificity against the CD4 binding domain of Env was more prevalent in the DNA prime-protein boost group whereas little was seen in the protein alone group. This result suggested that different immunization modalities lead to distinct antibody repertoires, allowing us to design new immunization delivery strategies to maximize the protective immune response.

Given our previous findings, in the current set of studies we sought to determine whether there is any beneficial impact to delivery both DNA and protein components at the same time throughout the entire immunization course, Recent studies from the Pavlakis group suggest that, compared to DNA prime-protein boost, co-immunization of DNA and viral particles might be more beneficial in generating a protective immune response against HIV acquisition (216). Further, they showed that co-immunization of DNA and protein induced similar cellular responses, but that these humoral immune reponses were of higher magnitude and greater longevity compared to those induced by DNA prime-protein boost in both mice and macaques (217, 218). However, there is a potential caveat in their study: their comparison was not based on equal amount of

immunogens throughout the immunization, as the co-delivery group received double dose of DNA and protein compared to those receiving sequential DNA prime-protein boost.

In this study, we attempted to address these caveats by making a more stringent comparison of humoral responses elicited by different delivery regimens in both mouse and rabbit. To complete our questions about the impact of immunization order on the humoral response, in addition to a co-immunization DNA-protein group and DNA prime-protein boost group, we also included a protein prime-DNA boost immunization regimen and also simultaneous delivery of vector DNA and protein. The primary outcomes of these studies were binding antibody titer at immunogenicity peak time point, long-term immunity, epitope specificity, and neutralization capability of immunized sera. These analyses indicated that the DNA prime-protein boost strategy was able to induce superior antibody responses with unique protective epitopes and better neutralizing activities against sensitive viruses compared to the other vaccination regimens.

Results

DNA prime-protein boost elicited high IgG binding titers in mice

Five different immunization regimens were designed to study the impact of the delivery sequence of different immunogens on the humoral response upon in mice (Fig. 4.1). Either DNA encoding JR-FL Env gp120 protein or matched JR-FL Env gp120 protein were used as vaccines. Immunizations were given twice at four weeks apart, and either DNA or protein vaccines were injected intramuscularly (5 mice per group). The first group received 100μg DNA prime followed by 5μg protein boost, where the protein immunization was formulated with the adjuvant, alum. The second group received

	Prime (0 wks)	Boost (4 wks)
A	100µg DNA	5µg protein/alum
B	50µg DNA 2.5µg protein/alum	50µg DNA 2.5µg protein/alum
C	50µg DNA 2.5µg protein	50µg DNA 2.5µg protein
D	100µg DNA	100µg DNA
E	5µg protein/alum	5µg protein/alum

Figure 4.1.Study design and immunization schedule for mice receiving JR-FL gp120-based immunizations. Mice were intramuscularly immunized with one of six vaccine regimens: A) once 100µg DNA prime plus once 5µg gp120 protein boost; B) twice simultaneous delivery of 50µg DNA and 2.5µg protein formulated with alum; C) twice simultaneous delivery of 50µg DNA and 5µg protein formulated with alum; D) twice 100µg DNA encoding Env gp120 protein; E) twice 5µg protein formulated with alum. "Priming" immunizations were administered at week 0, "boosting" immunizations were given at week 4.

simultaneous immunization of 50µg DNA and 2.5µg protein adjuvanted with alum twice. To prevent a chemical interaction between DNA and protein, we specifically injected the two vaccines into different legs of the animal. These two groups allowed for a direct comparison of humoral immune responses given the same vaccine dose during the immunization course. The third group received simultaneous delivery of 50µg DNA and 2.5µg protein but without adjuvant twice. This helps address the question of whether DNA alone could function as adjuvant of protein. The other two control groups were twice 100µg DNA immunization and twice 5µg protein adjuvanted with alum, which were also used as controls in previous studies from our lab (95, 96). Blood was collected and the humoral immune responses were assessed at two and four weeks after the final immunization.

At two weeks after the final immunization, the DNA prime-protein boost group (group A) showed higher titers compared to the protein alone group and the DNA-protein co-immunization without adjuvant group (Fig. 4.2A) ($p=0.029$ and $p=0.032$, respectively); however, the DNA prime-protein boost group showed a similar magnitude of binding as the co-delivery of DNA and protein with alum group, suggesting a critical role for adjuvant in the protein-based vaccine. Interestingly, DNA alone generated significantly higher antibody responses compared to protein/alum alone ($p=0.044$), suggesting that the DNA vaccine is highly immunogenic in mice. The humoral immune responses were further analyzed at week 8, 4 weeks post final immunization (Fig. 4.2B). Interestingly, each immunization regimen produced a unique antibody response profile. Three immunization groups, including the DNA prime-protein boost group, the
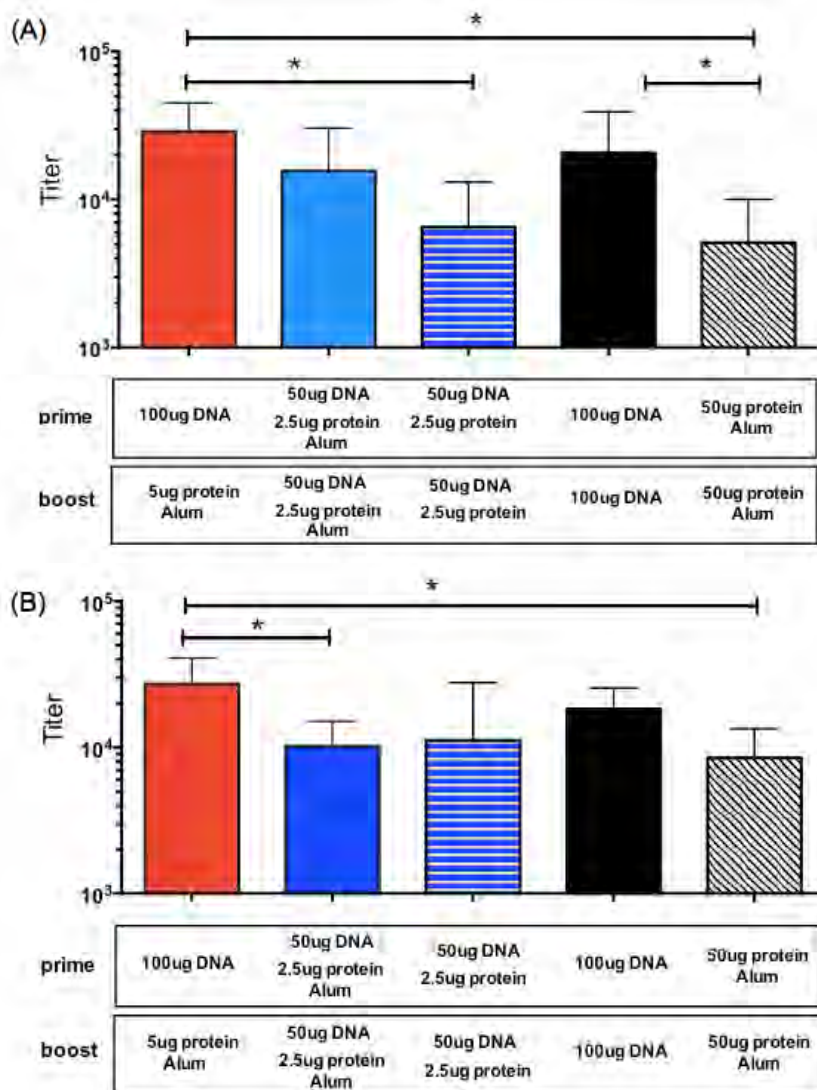
Figure 4.2. Env-specific binding titers in mice elicited by different vaccine regimens.
(A) JR-FL gp120-specific binding IgG titer of rabbit sera collected 2 weeks after the final boost titer was measured by ELISA. (B) JR-FL gp120-specific binding IgG titer of rabbit sera collected 4 weeks post final boost were measured by ELISA. Statistical differences were determined using Student's t test (*: $p<0.05$).

simultaneous delivery of DNA and protein adjuvanted with alum group, and the DNA alone group, showed a slightly decreased antibody titer (0.94-, 0.65-, and 0.88-fold decrease, respectively) at week 8 compared to week 6. However, the protein/alum immunization group had a 1.65-fold increase in Env-specific humoral immune response at week 8 compared to that observed at week 6 and simultaneous delivery of DNA and protein without alum resulted in a 1.7-fold higher antibody response. DNA prime-protein boost had a significantly higher antibody response compared to DNA and protein/alum co-immunization (p=0.030) and compared to protein/alum alone (p=0.016).

DNA prime-protein boost elicited comparable magnitudes of IgG binding titer in rabbit

We further tested the impact of delivery sequence of DNA and protein-based vaccines on the humoral immune response of rabbits. To be consistent, JR-FL gp120 protein was used as the model antigen. In this rabbit study, five groups were included: A) twice 100μg protein prime followed by three times 200μg DNA boost; B) three times 200μg DNA protein prime twice 100μg protein boost; C) five times simultaneous immunization of 120μg DNA and 40μg protein/alum; D) five times simultaneous immunization of 120μg empty DNA vector and 40μg protein/alum; E) five times simultaneous immunization of 200μg DNA vector and 100μg protein/alum (Fig. 4.3). Of note, for immunization groups A-D, the same amount of protein and DNA encoding JR-FL gp120 protein or empty DNA vector was given during the entire immunization period. Consistent with our previous study in mice, DNA and protein were intramuscularly injected at two different muscle sites. Group E was included as control to compare with previously published results.

	Prime (0,4 wks)	Boost (8,10,12 wks)
A	100µg protein/alum	200µg DNA
	Prime (0,2,4 wks)	Boost (8,12 wks)
B	200µg DNA	100µg protein/alum

	Simultaneous delivery (0, 2, 4, 8, 12 wks)
C	120µg DNA and 40µg protein/alum
D	120µg empty DNA vector and 40µg protein/alum
E	200µg DNA and 100µg protein/alum

Figure 4.3. Study design and immunization schedule for rabbit receiving JR-FL gp120-based immunizations. Rabbit were immunized with one of four vaccine regimens: A) Twice 100µg protein, followed by three times 200µg DNA encoding gp120 protein boost; B) Three times 200µg DNA encoding Env gp120 protein prime, followed by 100µg gp120 protein; C) five times simultaneous delivery of 120µg DNA and 40µg protein; D) five times simultaneous delivery of 120µg empty DNA vector and 40µg protein; E）five times simultaneous delivery of 200ug DNA and 100ug protein.

Figure 4.4. Env-specific binding IgG titer elicited by different orders of DNA and protein-based immunizations in rabbits. Env-specific endpoint binding titer at week 14, 2 weeks post final boost. Statistical differences were determined using Student's t test (*: $p<0.05$; **: $p<0.005$).

Peak immunogenicity antibody responses for individual rabbits were examined (Fig. 4.4). Specifically, geometric mean Env-binding titers for rabbits receiving protein prime-DNA boost had the lowest endpoint binding IgG titer (1:209499); while DNA prime-protein boost and co-delivery of DNA and protein had geometric mean Env-specific IgG titers of 1: 452029. For co-delivery of empty vector and protein and co-delivery of a double dose of DNA and protein, similar geometric mean Env-specific antibody titers were observed (1: 362863). This suggests that protein prime-DNA boost only induced transient high-titer antibody responses, which quickly diminished. Furthermore, DNA prime-protein boost was able to induce a similar magnitude of Env-specific binding titers as co-delivery of DNA and protein/adjuvant when given the same antigen amount. Interestingly, increasing the amount of antigen given during co-delivery of DNA and protein impaired Env-specific antibody titers, suggesting that an optimal amount of antigen is critical to eliciting high magnitude of antibody titers.

Longevity of HIV Env-specific humoral responses in rabbits

We monitored the humoral immune response for an additional 12 weeks after the last vaccination. We observed persistent, high-level Env-specific antibody responses even after a long rest period after the last immunization. The DNA prime-protein boost group maintained high-level Env-specific binding geometric titers (1: 103849), which were significantly higher than observed in the co-delivery of DNA and protein group (1:52195) and the co-delivery of double dose DNA and protein group (1:52195) (Fig. 4.5). Further, we determined differences in the longevity of the Env responses among the groups by comparing the decline of the antibody titers from week 2 to week 14 after the final

12 weeks post final immunizations

Y-axis: Env-specific binding titer (10^2 to 10^7)

X-axis categories: DNA prime protein boost; co-delivery of DNA and protein; co-delivery of double dose DNA and protein
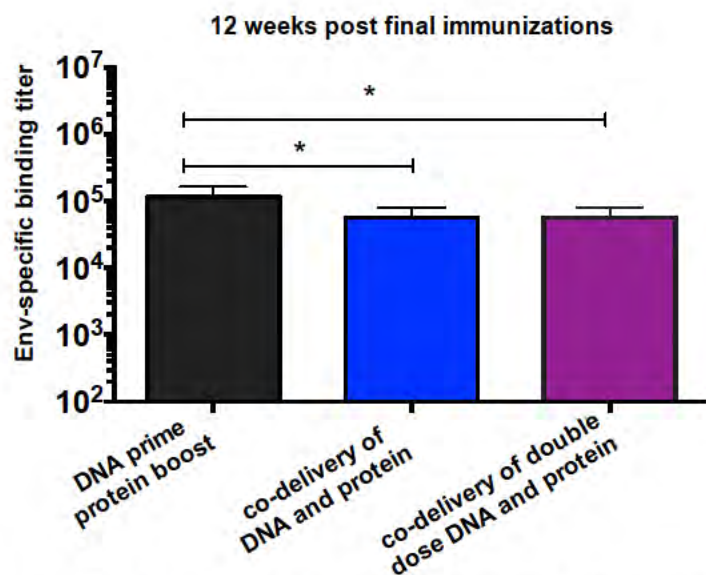
Figure 4.5 Long-term humoral responses of immunized sera from varying order of DNA and protein immunizations. Total gp120-specific IgG were measured by ELISA in sera collected week 24, 12 weeks after the final boost. Statistical differences were determined using Student's t test (*: $p<0.05$; **: $p<0.005$).

immunization. Humoral immune responses from the DNA prime-protein boost group showed only a 0.64 log reduction; co-delivery of vector and protein showed a similar level of decline (0.75 log), while protein prime-DNA boost and co-delivery of DNA and protein had greater declines (0.89 log and 0.94 log, respectively) over a 12-week period.

Avidity of elicited antibody responses

Avidity is an important property of an immune response to evaluate antibody quality. Non-neutralizing antibodies with high avidity contribute to protective efficacy against SHIV challenge in a non-human primate challenge study (219, 220). In the current study, the avidity of rabbit immune sera elicited by each immunization group was measured by how tightly the serum could bind the gp120 antigen in an ELISA assay (95). We found that serum avidity differed greatly between immunization regimens (Fig. 4.6). In the ELISA, we ran bound IgG from our test animals against an IgG standard and were able to calculate the amount of IgG displaced by increasing concentrations of sodium thiocynate (NaSCN). NaSCN most easily displaced sera from animals that received co-delivery of vector and protein. Half of all bound IgG was displaced with an average of 2.4M solution of NaSCN. When co-delivery of vector or protein was given, 50% of bound sera remained bound to the plate in 3.1M solution of NaSCN. Serum avidity increased further with the administration of co-delivery of DNA and protein immunization with 50% of sera remaining bound at a concentration of 3.8M NaSCN. Interestingly, co-delivery of a double dose of DNA-prime protein boost induced antibody with less avidity (3.0M NaSCN). The use of a DNA prime-protein boost approach improved this further to an average of 50% displacement at 4.8M NaSCN. Although a similar level of antibody quantity was detected, the quality of antibody responses varied.
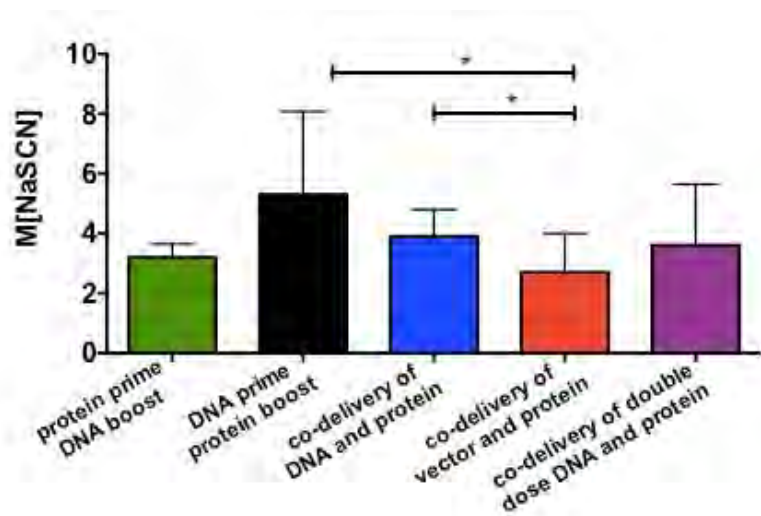
Figure 4.6 Measurement of serum avidity elicited by varying order of DNA and protein-based immunizations. Sera were evaluated for their ability to be displaced from gp120 protein by increased molar concentration of sodium thiocynate (NaSCN). The minimal concentration of NaSCN to displace 50% of bound IgG was determined. Statistical differences were determined using Student's t test (*: $p < 0.05$).

The heterologous prime-boost strategy appears to induce Env-specific humoral responses with higher avidity.

Epitope mapping of polyclonal sera using linear overlapping peptides

To determine different antibody specificities among groups receiving different HIV-1 vaccines, linear 15-mer peptides with an 11-residue overlap derived from clade B consensus gp120 sequence were used. Fig. 4.7A shows a heatmap of binding intensities against gp120 peptides for serum obtained at 2 weeks after the final immunization. Among them, V3 loop, C1 and C5 region of gp120 are the major targets for IgG responses in immunized animals. Interestingly, these three regions were also observed as the dominant response sites in the RV144 trial (23). Further, the DNA prime-protein boost group exhibited unique positive binding against the N terminal of C2, a site that was poorly recognized by the other three immunization groups (Fig.4.7B). In addition, the DNA prime-protein boost group elicited a less dominant V3-specific response compared to the other three groups (Fig.4.7C), with a significant difference compared to the co-delivery of vector and protein group (p=0.044). Further, the DNA prime-protein boost group induced higher-level antibody responses against the C1/V1 conjunction region when compared to protein prime-DNA boost and co-delivery of double dose DNA and protein group (p=0.004 and p=0.004, respectively). To our surprise, co-delivery of double dose of DNA and protein induced the lowest level of IgG response against several linear peptides compared to the other groups, including C1, C2, and C5 region, suggesting that repeated boosting of large dose of antigens might prevent the elicitation of diverse immune repertoire. Overall, the DNA prime-protein boost regimen induced responses with diverse specificities.

(A)

Group	C1.1 (#18-20)	C1.2 (#23-25)	C1/V1 (#40-42)	C2.1 (#64-68)	C2.2 (#82-86)	V3 (#98-106)	V4 (#126-129)	C5.1 (#148-150)	C5.2 (#157-162)
protein prime DNA boost	5200	10590	149	715	9963	42060	496	4920	35716
	1634	31765	558	72	734	62059	2027	6870	50319
	3663	37422	578	347	33149	51303	34289	21701	25747
	63	26514	893	1	4526	65249	3360	1228	65301
	1	29249	1	3995	25581	51683	4642	502	11565
DNA prime protein boost	203	33558	6875	9386	2275	65132	3373	8806	43241
	3187	6435	5774	10600	15042	49787	9909	27408	48252
	2805	59089	11397	12131	5173	29652	9922	2269	12409
	116	36669	3215	13904	40808	29306	2161	63981	65303
	1212	231	2517	4219	43924	18354	16345	350	49307
co-delivery of DNA and protein	565	1699	1322	2758	2215	47187	3021	1325	62213
	978	50853	658	17267	32773	49536	1195	1050	49432
	17824	46874	22597	725	2290	34690	22756	41264	4544
	14287	6322	655	433	3266	53993	1144	175	16468
	1339	34916	3252	1338	22131	58781	8281	14987	9511
co-delivery of double dose DNA and proten	902	505	1	81	249	46639	2241	452	12334
	630	1	289	113	798	28315	5713	828	2635
	4766	221	140	291	16176	46831	991	2445	7634
	423	174	67	568	507	30080	969	19	3059
	8937	1062	1251	2601	1593	46589	39200	26481	4941
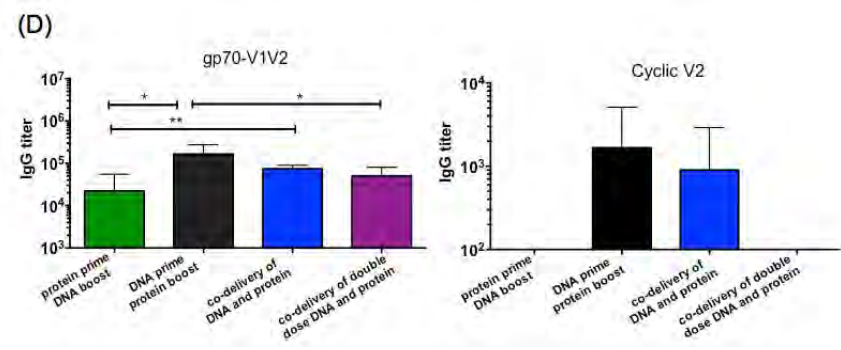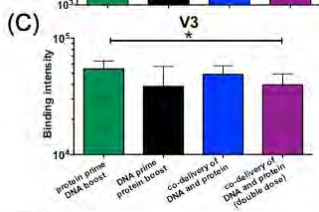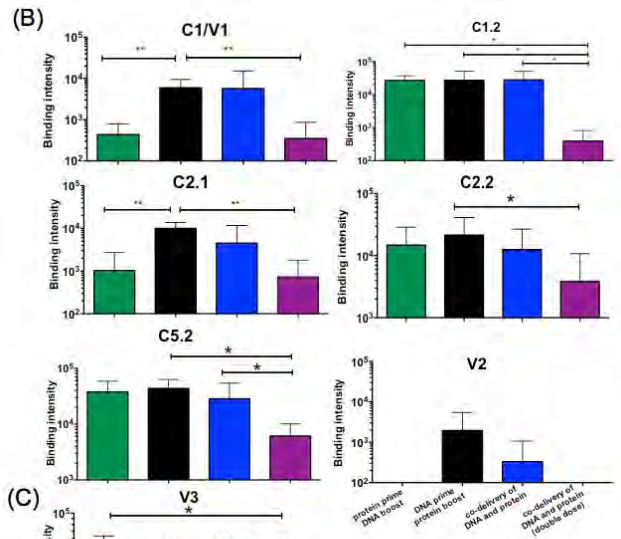
Figure 4.7. Distinct epitope specificities of immune sera elicited by varying order of DNA and protein-based immunizations. Rabbit sera collected two weeks after the final protein immunizations were tested for their epitope specificity, especially against linear epitope and the V1V2 region. (A) Maximum binding intensity of immune sera against single peptide within an epitope region from individual immune rabbit sera. Regions that were strongly recognized by immune sera are shown in red. (B) Quantitative comparisons of epitope specificities against C1, C1/V1, C2, V2 and C5 region using immune sera. (C) Quantitative comparisons of IgG against V3 region (D) IgG response against gp70-V1V2 and cyclic V2 region. Statistical differences were determined using Student's t test (*: $p<0.05$ and **: $p<0.005$).

Strong V2-specific humoral responses observed with DNA prime-protein boost

In the RV144 clinical vaccine trial, which showed modest protection efficacy, extensive analysis demonstrated a positive correlation of protection with the presence of serum IgG binding Ab to variable region 2 (V2) (88). Since limited linear V2-specific humoral responses were detected in our overlapping peptide assay, we reasoned that antibody might preferentially recognize the conformational V2 region presented on Env. Therefore, we included fusion protein JR-FL gp70-V1V2 and A244 cyclic V2 peptides to determine V2 reactivity in rabbit sera. gp70-V1V2 is the scaffold protein carrying the first and second variable regions of the HIV Env glycoprotein fused with murine leukemia virus (MLV) glycoprotein 70 (gp70) (221), which helps to present V1V2 in its native conformation. Cyclic V2 is derived from isolate Case A2, a subtype B strain, which was used for the RV144 immune correlation analysis (222). As seen in Fig. 4.7D, the DNA prime-protein boost group generated the highest gp70-V1V2 IgG titer compared to the other four groups, significantly compared to protein prime-DNA boost (p=0.01) and the co-delivery of double dose DNA and protein (p=0.02). Further, both co-delivery of DNA and protein and co-delivery of vector and protein induced significantly higher gp70-V1V2-specific antibody responses compared to protein prime-DNA boos immunization (p=0.006 and p=0.03 respectively).

Neutralization activities of primary HIV isolates

To evaluate the neutralization activities of rabbit sera elicited by different vaccine regimens, rabbit sera was sent to Comprehensive Antibody Vaccine Immune Monitoring Consortium (CAVIMC), part of the Collaboration for AIDS Vaccine Discovery (CAVD) program supported by the Bill & Melinda Gates Foundation. The rabbit sera was tested

against a panel of 15 well-characterized pseudotyped viruses expressing Env from a wide range of primary HIV-1 isolates, including SF162.LS (Clade B), MW965.26 (Clade C), BaL.26 (Clade B), Bx08.16 (Clade B), DJ263.8 (Clade AG), and ss1196 (Clade B) for Tier 1 HIV viruses as well as TRO.11 (Clade B), AC10.0.29 (Clade B), Du422.1 (Clade C), ZM53M.PB12 (Clade C), 0260.v5.c36 (Clade A), A259.d22.17 (Clade A), and JR-FL (Clade B) for tier 2 viruses (Fig.4.8). For Tier 1a SF162.LS, DNA prime-protein boost had a geometric mean neutralization titer of 1:395; co-delivery of DNA and protein elicited an average neutralization titer of 1:308; the geometric mean NAb titer for co-delivery of double dose DNA and protein was 1:195; while the other two immunization regimens, co-delivery of empty DNA vector and protein and protein prime-DNA boost induced neutralization titers of 1:128.4 and 1:155.2, respectively. For another tier 1a virus, MW965.26 from Clade C, DNA prime-protein boost still had the highest neutralization titer (1:726.6) followed by co-delivery of double dose DNA and protein (1:639.2). This suggests that both DNA prime-protein boost and co-delivery of double dose DNA and protein were able to induce effective humoral responses against sensitive tier1a viruses.

For Tier 1b viruses, sporadic neutralization activities against Clade B viruses Bal.26 and Bx08.16 were observed. For Bal.26, DNA prime-protein boost still induced the highest mean neutralizing titer (1:72.4) among the groups; while co-delivery of DNA and protein, co-delivery of vector and protein, and protein prime-DNA boost had neutralizing titers of 1:40, 1:56 and 1:29.8, respectively. Only 1 out of 5 rabbits from the co-delivery of double dose DNA and protein group was able to neutralize the Bal.26 virus. For Bx08.16, protein prime-DNA boost elicited a significantly higher neutralizing

titer (1:76.4) compared to co-delivery of DNA and protein (1:10.6). DNA prime-protein boost and co-delivery of vector and protein had average neutralizing titers of 1:26.6 and 1:28.8, respectively. Again, only 1 rabbit from the co-delivery of double dose DNA and protein group was able to neutralize Bx08.16. This suggests that co-delivery of double dose DNA and protein failed to generate effective humoral responses against relatively difficult to neutralize viruses. Previously observed high titer neutralizing activities against SF162 and MW965.26 may be mostly mediated by V3-specific antibodies. Only 1 rabbit from the DNA prime-protein boost group and 1 from the protein prime-DNA boost group elicited weak neutralizing titers against virus DJ263.8 from Clade AG (1:21 and 1:21, respectively). For ss1196, only weak neutralization activities were observed from 2 rabbits sera from the DNA prime -rotein boost group and 1 rabbit from the co-delivery of double dose DNA and protein group.

Among 8 tier 1 viruses, DNA prime-protein boost neutralized 75% of tier 1 viruses, more compared to any other group. Both protein prime-DNA boost and double dose of DNA and protein neutralized 67.5% of tier 1 viruses, and co-delivery of DNA and protein and co-delivery of empty DNA vector and protein neutralized 50% of tier 1 viruses. This suggests that DNA prime-protein boost was able to induce broad neutralizing activities against tier 1 viruses.

Little neutralization activity was detected against tier 2 viruses. Only 1 rabbit from the co-delivery of DNA and protein group was able to neutralize homologous virus JR-FL at very low titer (1:21) (data not shown).

Discussion

Outcome after vaccination is influenced by a variety of factors due to the
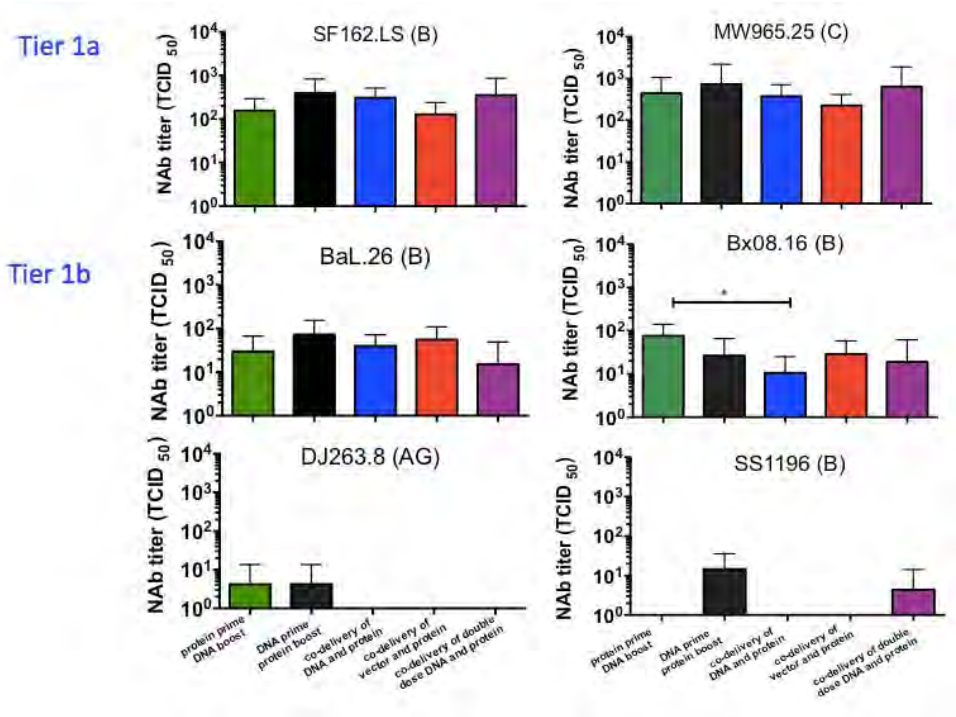
Figure 4.8. Neutralization activity of sera elicited by varying order of DNA and protein-based immunizations against sensitive HIV isolates. Rabbit sera collected two weeks after the final protein immunization were tested for their ability to neutralize HIV isolates in TZM-bl assay, performed by CAVD's Seaman laboratory. Statistical differences were determined using Student's t test (*: $p<0.05$ and **: $p<0.005$).

comprehensive interplay between host immunity and each vaccine inoculation. For example, the order of administration of heterologous vaccines has a great impact on quantity and quality of antibody generation. Indeed, heterologous prime-boost could be considered a cause of "original antigen sin" (223). The initial priming events elicited by a foreign antigen appear to be imprinted permanently on host immune system. As a priming immunogen, DNA vaccine transduces a low level of antigen into the host cell, which can present naïve B cells with more authentic epitope structure *in vivo*. Later protein immunization, due to its high immunogenicity, can robustly drive and expand pre-existing epitope-specific memory B cells, during which, somatic hypermutation and affinity maturation occur and high affinity of boosted antibody responses with efficient antiviral functions are induced. In contrast, protein prime can induce robust primary immune responses, while DNA vaccine as a boost component, did not have a sufficient amount of antigen and therefore, cannot stimulate pre-existing memory B cells. Therefore, the protein prime-DNA boost regimen appears courter-productive since it might inhibit the efficacy of a boost vaccine. Indeed, this hypothesis is quite compatible with what we observed. In mice, at 2 weeks after the final immunization, we did not see any improvement in terms of antibody quantity from co-administration of DNA and protein compared to the traditional DNA prime-protein boost approach. At 4 weeks post final immunization, we found that DNA prime-protein boost had even higher antibody responses compared co-delivery of DNA and protein. Analysis of rabbit immunized sera suggested that DNA prime-protein boost induced high quality Env-specific antibody responses. Although they all induced a similar magnitude of Env-specific binding titers, more sustainable humoral immunity was observed after DNA prime-protein boost

immunization compared to other vaccination regimens. Moreover, antibody responses with higher avidity were observed after DNA prime-protein boost immunization. Further, a diverse repertoire of linear epitopes was found in the DNA prime-protein boost group, including C1, C1/V1 junction, V2, C2, and V3 regions. Interestingly, the RV144 clinical trial also showed robust antibody responses against the above regions (23). In the protein prime-DNA boost group, twice protein immunizations induced transient high titer antibody responses; however, three times DNA boost failed to further improve the magnitude of antibody responses. Long-term humoral immunity also waned quickly probably due to the low affinity of the Env-generated antibody response. As expected, antibody specificity predominantly focused on the V3 region by protein prime DNA boost approach, as V3 loop is the most immunodominant region when protein only was used in the priming phase. There was no detectable cyclic V2 specific-antibody response; neutralization potency was also quite low.

We also looked at co-delivery of DNA and protein. Given the same amount of antigen, we found that, different from protein prime-DNA boost, this regimen was able to sustain high-level antibody responses throughout the immunization. It induced a similar magnitude of binding titer at peak immunogenicity as was observed in the DNA prime-protein boost group; however, the binding titer quickly waned at 12 weeks after the final immunization and was significantly lower than that observed in the DNA prime-protein boost group. Co-delivery of DNA and protein elicited a similar epitope profile of antibody specificity as DNA prime-protein boost, but a lower level of C terminal of C1- and N terminal of C2-specific antibody responses were seen. Furthermore, this regimen elicited immune sera with limited breadth of neutralization. This further confirms that the

overwhelming robust immune response at the priming phase failed to generate a high-quality antibody response.

DNA vaccine may have a dual role as both an adjuvant through innate immune pathways and as a vector to deliver a subunit antigen. Therefore, in this study, we also included co-delivery of empty DNA vector and protein, in comparison with co-delivery of DNA and protein. We showed that co-delivery of DNA vector and protein induced similar peak level antibody responses and long-term humoral responses. However, antibody avidity was significantly lower compared to DNA prime-protein boost and co-delivery of DNA and protein. Co-delivery of DNA vector and protein could only neutralize 50% tier 1 viruses, suggesting that an empty DNA empty could not improve the quality of antibody response compared to DNA vaccine.

Antigen dose also impacted the immunogenicity of vaccine regimens. It was previously reported that high-dose priming antigen can hinder a response to the boost inoculation and further impair long-term T cell memory response (224, 225). This may also apply to humoral immune responses. Co-delivery of double dose of antigen did not further improve either the quality or quantity of antibody responses. Env-specific binding titers diminished quickly at week 4 post final immunization, and only neutralized 67% of tier 1 viruses, compared to 75% neutralizing breadth with co-delivery of DNA and protein. Furthermore, the antibody specificity mapped by linear peptide microarray also showed the minimum IgG titer against C1, C2 and C5 region, with the only exception of V3 region.

More importantly, we did not see any benefit for simultaneous delivery of DNA and protein, as reported by the Pavlakis group, which showed that co-immunization of DNA

and protein induced humoral immune responses with a higher magnitude and greater avidity and longevity compared to DNA prime-protein boost in mice and macaques (217, 218). Several factors might be responsible these divergent results. First, intramuscular injection of DNA vaccine was used in our study, and previous studies used electroporation to deliver DNA vaccines. Electroporation allows for more direct delivery of DNA molecules to target tissues so as to improve the efficiency of the DNA vaccine. It is possible that electroporation delivery of DNA could synergistically improve the immunogenicity of the protein immunization. Second, in our study, to prevent further chemical interference of DNA and adjuvanted protein, we injected DNA into one leg of the animal, and administered protein into the other leg. Pavlakis' group administered two different vaccine components at the same injection site. Whether this has any effect on the fate of the immune outcome is yet to be determined. Third, in our study, the same amount of antigen was used for DNA prime-protein boost group and co-delivery of DNA and protein group. While in other study co-delivery of DNA and protein group, double dose antigen amount was used, which might be responsible for higher magnitude of antibody response. However, we also included double dose co-delivery group, and there was still no improvement in terms of both magnitude and quality of antibody response. Fourth, animal species might also make a difference. In this study, both mice and rabbit were used as animal model, while other groups used non-human primate as animal model. Whether different animal models will have any impact on antibody response is yet to be investigated.

Overall, among all vaccine regimens we tested here, we found that the DNA prime-protein boost regimen induced the best quality antibody response, in terms of broad

antibody specificities, avidity, longevity, and neutralization activities. Indeed, we have found that DNA priming resulted in a markedly more robust germinal center (GC) reaction compared to priming with protein alone, and that DNA priming also increased the percentage of GC-derived memory B cells that have undergone sufficient affinity maturation and Ig isotype switching (97). Such an underlying mechanism may be responsible for superior humoral responses induced by the heterologous DNA prime-protein boost regimen.

Chapter V

**Antigenicity and immunogenicity of gp120 and gp160 in the context
of heterologous DNA prime-protein boost**

Introduction

Optimal envelope glycoprotein form for induction of HIV-1-specific neutralizing antibodies (NAbs) and functional antibodies is still yet to be elucidated. A major objective in the HIV vaccine field has been to develop a trimer Env mimicking the nature Env on HIV-1 viral particles. The recently reported BG505 SOSIP trimer has been shown to mimic the native state of the Env spike, which has high reactivity with all Env-specific broadly neutralizing antibodies (bNAb) but no detectable binding with non-NAb against CD4bs, CD4i, or the gp41 region (24). However, there was a disconnection between antigenicity and immunogenicity as this perfect trimer failed to induce Nab against heterologous viruses, as it had transient, positive NAbs against autologous Tier 2 but not other Tier 2 viruses. There are additional designs of novel and modified Env immunogens. A unique one is the "full length single chain gp120-CD4 complex" (FLSC)–which was designed based on the idea that a conformationally constrained and stabilized gp120 Env is capable induce immune response against highly conserved gp120 epitopes (221-223). Currently this novel Env immunogen is moving forward to be tested in humans.

Historically, there are three major Env forms being tested for HIV vaccine research. The first is monomeric gp120 protein, which was included as a critical component in the RV144 trial, the first HIV-1 efficacy trial with modest success. It is safe and relatively easy to manufacture compared to other Env forms. The second Env form often employed is the gp140, the ectodomain of entire Env. Previous studies have

shown that both the gp120 and gp140 forms of envelope proteins have comparable immunogenicity, but gp140 trimers failed to induce stronger NAb responses compared to monomeric gp120 (224, 225). Lately, a gp140 trimer with C-terminal T4 bacteriophage fibritin trimerization domains and polyhistidine motifs was produced from insect cells (226). These stable, homogenous trimmers have antigenic properties markedly different from those of monomeric gp120s derived from the same sequences (227). It has been tested in small animals and will be included in formulations moving into human studies. However there is no convincing data to support that neutralizing antibodies elicited by this gp140 timer is significantly improved against sera elicited by gp120 immunogens, because there is no significant Nab against tier 2 viruses (87, 227).

The third, gp160 protein, is the native form of Env on the HIV-1 viral spike. It is unstable and technically difficult to produce as a recombinant product. Dr. Shiu-lok Hu group used the recombinant vaccinia virus system to express and further purified full-length, membrane bound gp160 protein with cleavage site intact (228-230). Substantial gp160-specific antibody titers and neutralization activities were observed from gp160-immunized rabbit sera. Further, priming with vaccinia recombinant expressing HIV Env gp160 followed by gp160 protein boost induced both a high magnitude of humoral and cellular responses in human (231). However, how to further optimize the immunogenicity of gp160 in the context of DNA prime and protein boost is yet to be determined.

This prompted us to compare the immunogenicity of gp120 and gp160 Env in the context of DNA-protein vaccination. gp160 protein was generously provided by Dr. Shiu-lok Hu group. In the present study, we sought to do a comparative immunogenicity study using gp120 and gp160 (in both DNA and protein forms) derived from the JR-FL

isolate alternatively either as the priming or boosting immunogen. We evaluated the quantity of binding antibody against Env protein as well as other functional subregions at 2 weeks post DNA prime and 2 weeks post final protein boost. Further, the neutralizing antibody titers against a panel of Tier 1 and Tier 2 HIV-1 viruses were determined. To elucidate the serum specificity elicited by different vaccine regimens, linear overlapping epitope mapping, V3 peptide absorption as well as CD4 binding site mapping were performed.

Results

Antigenic properties of trimeric Env gp160 and monomeric gp120 protein

To determine any significant antigenic differences between gp160 and gp120 proteins, glycan-specific mAbs, CD4 binding site (CD4bs)-specific mAbs, and rabbit mAbs targeting linear and conformational epitopes were employed in ELISA and ForteBio assay to test their binding to either gp120 or gp160 proteins. First, glycan-specific mAb 2G12 targets at a specific high mannose patch. ELISA showed stronger 2G12 binding to gp160 compared to gp120 (Fig. 5.1A). BLI assay using ForteBio instrument showed that 2G12 bound to gp160 with an affinity of 0.029nM, while it bound to gp120 with an affinity of 0.53nM, 24-fold lower compared to that of gp160. PGT128 is another bNAb that was able to recognize and penetrate the V3 glycan shield. It bound to gp160 protein more potently compared to gp120 demonstrated by ELISA (Fig. 5.1A). Binding kinetics also showed that PGT128 bound to gp160 with an affinity of 0.0192 nM, and to gp120 with a 61-fold lower affinity (1.18nM) (Fig. 5.1B). Although gp120 and gp160 had similar level of association rate when bound to PGT128, a slower dissociation rate of gp160 with PGT128 was observed compared to that of gp120.

CD4 binding site (CD4bs) is one of the most conformation-dependent regions of the Env protein, which is also a key neutralizing epitope for a vaccine target. The first probe we used was fusion protein Ig-CD4, which consists of the first two N-terminal domains of the CD4 molecules and the Fc region of human IgG1. The second mAb probe was b12, a moderate neutralizing antibody that can neutralize 40% of global circulating viruses. The third probe was VRC01, a recently isolated CD4bs bNAb. ELISA showed that all three CD4bs probes were capable of binding to gp160 with greater affinity compared to gp120 (Fig. 5.1A). Compatible with this ELISA result, the ForteBio Qk^e assay suggested that the binding affinities of these CD4bs probes interacting with gp160 were higher compared to that of gp120. Ig-CD4 bound gp160 protein with very high affinity of 0.56nM while Ig-CD4 interacted with gp120 protein with 13-fold lower affinity. b12 reacted with gp160 with a high affinity of 0.163 nM, while b12 binding to gp120 had a 32-fold lower affinity (5.63 nM). VRC01 bound to both gp160 and gp120 tightly, with affinities of 4.56nM and 16nM, respectively. The high binding affinity of these CD4bs probes bound to gp160 results from the slower off-rate of the gp160-CD4bs interaction, which could due to the avidity effect of the gp160 trimer (Fig.5.1B).

We also looked at exposure of linear or conformational epitopes on either gp160 or gp120 proteins. A panel of rabbit mAbs including V3 mAb R56, C4 mAb R53, conformational-dependent mAb R52, and C1-specific mAb R13 was used. ELISA showed that they could bind to both gp160 and gp120 proteins with equal strength.

Overall, we found that these mAb targeting key neutralizing epitopes bound to gp160 trimer with higher affinity compared to gp120, ranging from 3- to 61-fold higher. On the other hand, rabbit mAbs with low to no neutralizing activities reacted with both

gp160 and gp120 proteins equally well, no matter whether they target either linear or conformational epitopes.

gp120 DNA priming induced higher binding and neutralizing titers compared to gp160 DNA primng.

To investigate the immunogenicity of gp120 and gp160 as DNA priming immunogens, New Zealand White rabbits were immunized 3 times with either gp120 or gp160 DNA vaccines via gene gun (Fig. 5.2). Sera were collected 2 weeks after the third immunization to evaluate Env-specific IgG and NAb responses. Despite having 3 immunizations, rabbits that received gp120 as a prime (group A and group B) had significantly higher endpoint titers against gp120 Env protein (p=0.001) and gp70-V1V2 protein (p=0.031) compared to gp160 DNA prime (Fig. 5.3A and Fig. 5.3B). As expected, low-level gp41-specific binding titers were significantly higher in rabbits immunized with gp160 DNA vaccines compared to those who had only gp120 DNA priming (p=0.0001) (Fig. 5.3C). Further, we were able to detect modest neutralization activities against the sensitive virus, SF162, and the less sensitive virus, SS1196, suggesting that DNA priming is very effective (Fig. 5.3D). Interestingly, after only three DNA priming immunizations, gp120 DNA priming elicited significantly higher neutralization titers against SS1196 than gp160 priming (p=0.049).

gp120 DNA prime elicited higher endpoint binding titers against gp120-based Env protein compared to gp160 DNA prime

Following the completion of three DNA priming immunizations, rabbits were boosted twice by either gp120 or gp160 Env protein (Fig. 5.2). Here we compare the immunogenicity of different combinations of gp120 or gp160 either as priming or
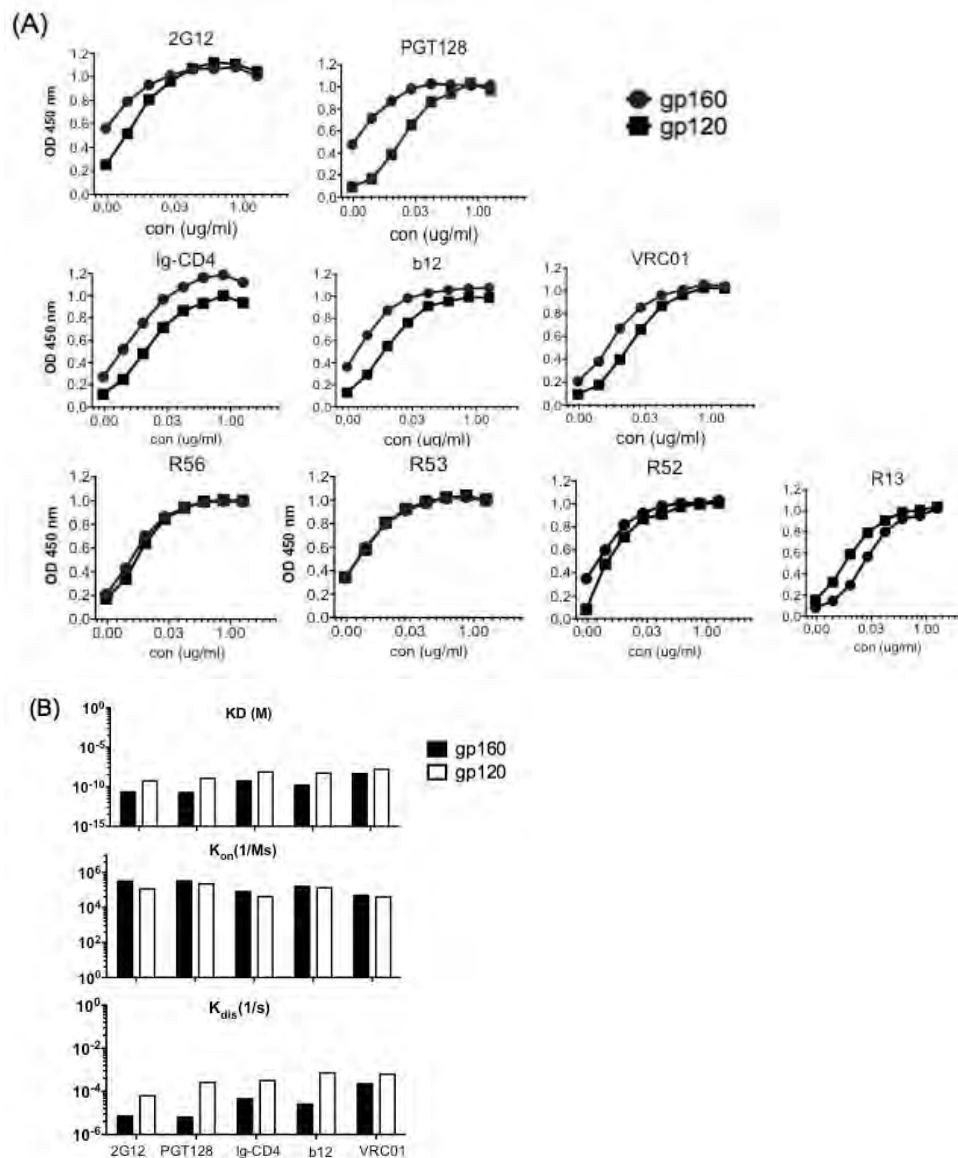
Figure 5.1. Antigenicity of gp160 and gp120 probed by key human and rabbit mAbs. (A) Head-to-head comparison of a panel of mAbs binding to gp160 and gp120 by ELISA. The antibody panel includes glycan-specific mAbs (2G12 and PGT128), CD4bs-related human mAbs (Ig-CD4, b12, and VRC01), rabbit V3 mAb (R56), C4 mAb (R53), conformational mAb (R52) and C1 mAb (R13). (B) Binding affinity, K_{on} (equilibrium association constant) and K_{off} (dissociation constant) for key human mAbs binding to gp160 and gp120, determined by a ForteBio Octect QK^e system.

boosting immunogens (Fig. 5.4). First, gp120 prime-gp120 boost and gp120 prime-gp160 boost induced significantly higher endpoint titers against JR-FL gp160 Env protein compared to the other two groups (Fig.5.4A). Further, we analyzed antibody response specificity by dissecting the different regions on the gp160 Env protein. gp120 prime-gp160 boost group elicited the highest gp120-specific endpoint binding titers when compared to all other groups (Fig.5.4B). Significantly higher gp120 core-specific antibody responses were observed in the gp120 prime-gp120 boost group and the gp120 prime-gp160 boost group compared to the other two groups (Fig.5.4C). Similarly, gp120 prime-gp160 boost induced higher V1V2-specific endpoint binding titers compared to the two groups that received a gp160 prime. Moreover, gp160 prime-gp160 boost generated the highest level of gp41-specific antibodies, followed by gp120 prime-gp160 boost and gp160 prime-gp120 boost group.

gp120 DNA prime elicited higher neutralizing titers against gp120-based Env protein compared to gp160 DNA prime

To elucidate the capability of vaccines to elicit NAbs, neutralization assays with rabbit sera from 2 weeks post final protein immunization were conducted by the Comprehensive Antibody Vaccine Immune Monitoring Consortium (CAVIMC) of the Collaboration for AIDS Vaccine Discovery (CAVD) program supported by the Bill & Melinda Gates Foundation. A panel of 14 well-characterized pseudotyped viruses expressing Env from a wide range of primary HIV-1 isolates, including 6 Tier 1 viruses and 8 Tier 2 viruses (Fig. 5.5A). Both gp120 DNA primed groups followed either by gp120 protein boost or gp160 protein boost showed the broadest neutralization

	Prime (0, 2, 4 wks)	Boost (8, 12 wks)
A	gp120 DNA	gp120 protein
B	gp120 DNA	gp160 protein
C	gp160 DNA	gp120 protein
D	gp160 DNA	gp160 protein

Figure 5.2. Study design and immunization schedule for rabbits. Rabbits were immunized with one of four prime-boost regimens: 1) JR-FL gp120 DNA prime plus JR-FL gp120 protein boost; 2) JR-FL gp160 DNA plus JR-FL gp120 protein boost; 3) JR-FL gp120 DNA prime plus JR-FL gp160 protein boost; and 4) JR-FL gp160 DNA prime followed by JR-FL gp160 protein boost.
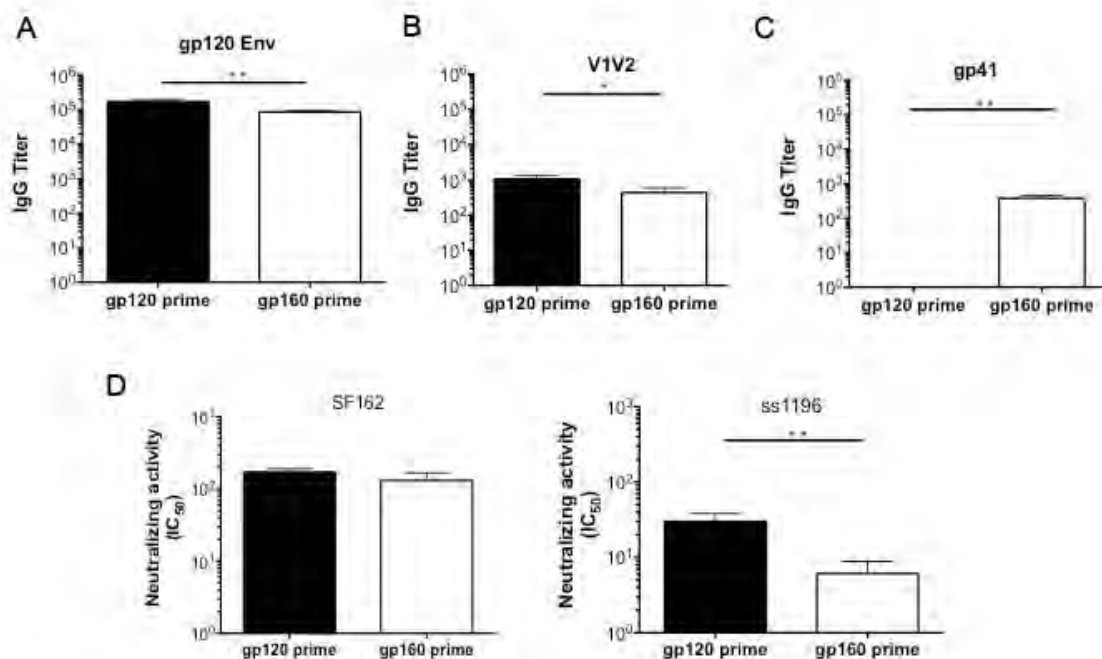
Figure 5.3. gp120 DNA prime alone elicited higher endpoint binding titers and neutralization titers compared to gp160 DNA prime. Rabbit sera were collected at two weeks post three times DNA immunization. Endpoint binding IgG titers against gp120 protein (A), V1V2 region (B), gp41 region (C) and neutralization titers against Tier 1a virus SF162 and Tier 1b virus ss1196 (D) were measured by ELISA. Statistical differences between groups were determined by Student's t-test (*$p<0.05$, **$p<0.005$).
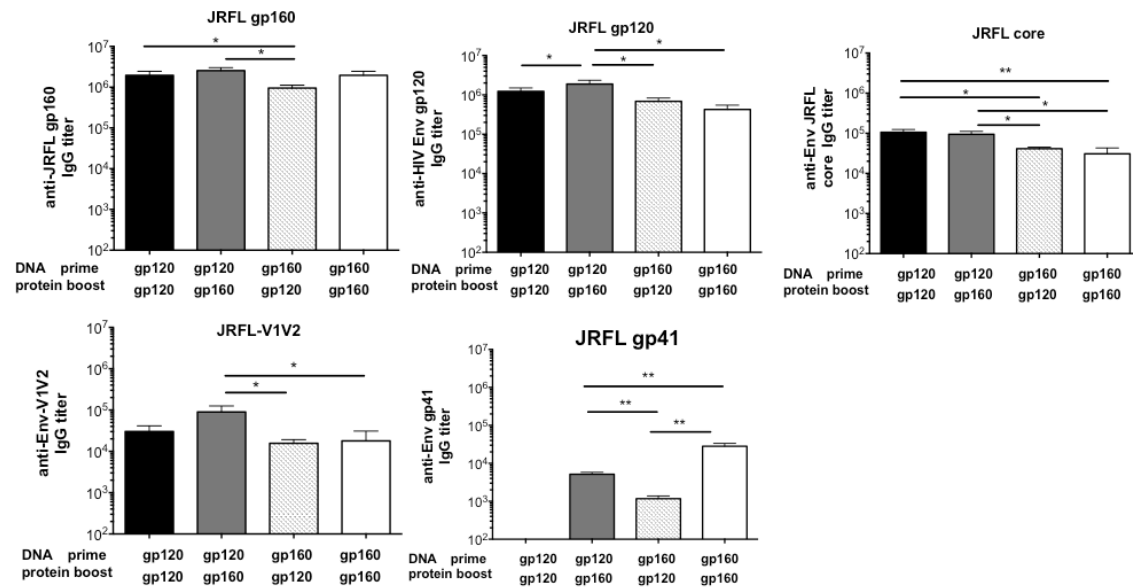
Figure 5.4. Both gp120 DNA primes elicited higher binding titer compared to both gp160 DNA primes. Rabbit sera were collected at two weeks post final immunization. Endpoint binding IgG titers against gp160 protein, gp120 protein, JR-FL core, V1V2 region, gp41 region were determined by ELISA. Statistical differences between groups were determined by Student's t-test (*: $p<0.05$, **: $p<0.005$).

activities (57%), among which, they can neutralize all Tier 1-tested viruses, and 25% of Tier 2-tested viruses (Fig. 5.5B). gp160 DNA prime-gp160 protein boost was able to neutralized 50% of viruses, while gp160 DNA prime-gp120 protein boost only neutralized 35.7% of viruses (Fig. 5.5B).

Both groups receiving gp120 DNA prime followed by either gp120 protein boost or gp160 protein boost showed higher NAbs against Tier 1a virus, SF162, with geometric titer of 1:6199 and 1:13329, respectively, while gp160 DNA prime followed by gp120 protein boost or gp160 protein boost had a geometric neutralizing titer of 1:2777 and 1:866, respectively. The four groups also showed a similar trend of sensitivity to SF162 and other Tier 1b viruses tested here, including SS1196.1, BZ167.12, Bx08.16, Bal.26, and 6535.3. Of note, the form of Env immunogen used in the priming stage appeared to determine the final outcome of neutralization. Interestingly, if the neutralization capabilities between groups receiving gp120 DNA prime (group A and B) and groups receiving gp160 DNA prime (group C and D) were further compared, significantly higher neutralizing titers were observed in the gp120 priming groups compared to the gp160 priming groups against most of the tested Tier 1 viruses except BZ167.12 (Fig. 5.5C). However, there was no significant difference between the groups receiving gp120 protein as boost (group A and C) and the groups boosted with gp160 protein (group B and group D), in terms of neutralization ability of the Tier 1 viruses mentioned above.

Further, only few rabbit sera showed low level neutralization activities against 3 out of 8 Tier 2 viruses tested, including JR-FL, QH0692.42, and TRO.11, but not the

(A)

Tier	Clade	Virus ID
1A		SF162.LS
1B		Bx08.16
		BaL.26
		SS11961.1
		BZ167.12
		6535.3
	B	TRO.11
		QH0692.42
		AC10.0.29
2		SC422661.8
		RHPA4259.7
		REJO4541.67
		CAAN5342.A2
		JRFL.JB

>50% IC50 at serum dilution 1:10
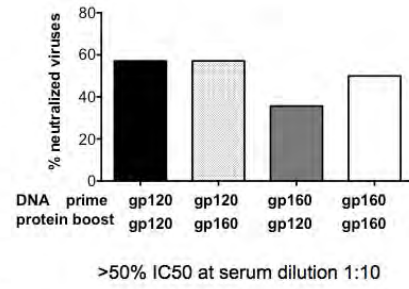
(B)
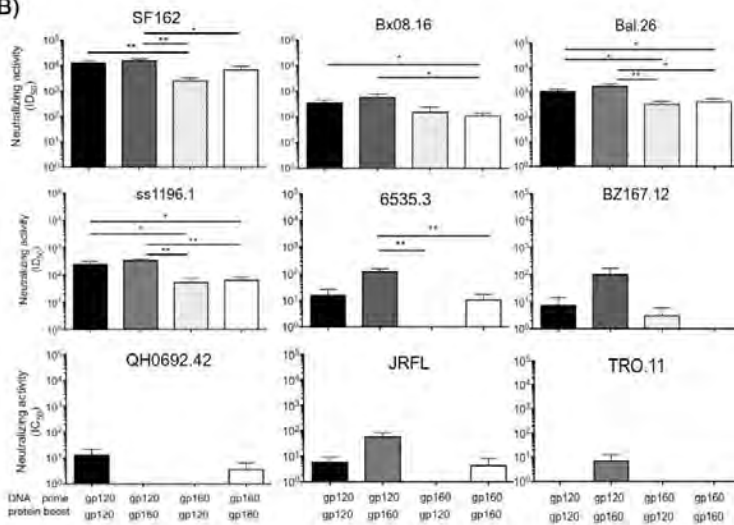
(C)
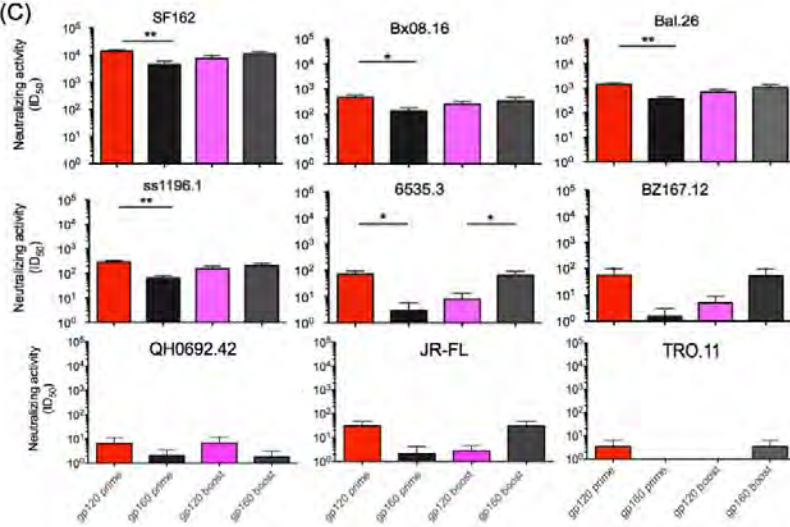
Figure 5.5. gp120 DNA prime elicited higher neutralizing titers compared to gp160 DNA prime. Rabbit sera collected two weeks after the final boost immunization were tested for neutralization ability in TZM-bl assay system. (A) Neutralization activities of immunized sera were determined against a panel of 14 viruses covering Tier 1 and Tier 2 (left panel). Right panel is an overview of the percentage of total neutralized viruses given the different immunization regimens. (B) Neutralization titers against specific viruses for groups receiving different immunization regimens. (C) Neutralization activities of groups receiving either gp120 prime or gp160 prime and groups receiving gp120 boost and gp160 boost. Statistical differences between groups were determined by Student's t-test (*: $p<0.05$, **: $p<0.005$).

other viruses tested, including AC10.0.29, SC422661.8, RHPA4259.7, REJO4541.67, and CAAN5342.A2. For homologous virus JR-FL, 4 out of 5 rabbit sera from the gp120 prime-gp160 boost group had neutralization activities with average neutralizing titer of 1:56.2; 2 out of 5 rabbits in the gp120 prime-gp120 boost group were able to neutralize JR-FL with an average neutralizing titer of 1:5.6. Between the two groups receiving gp160 DNA prime, only 1 out of 5 rabbit sera from the gp160 prime-gp160 boost group could neutralize JR-FL viruses while no rabbit sera from the gp160 prime-gp120 boost group could neutralize this virus. For QH0692.42, two rabbits from the gp120 prime-gp120 boost group were able to neutralize this virus with a mean neutralizing titer of 1:13, while two rabbits from the gp160 prime-gp160 boost group were able to neutralize QH069.42 with a mean neutralizing titer of 1:3.6. Another Tier 2 virus, TRO.11, was neutralized by only 2 out of 5 rabbit sera from the gp120 prime-gp160 boost group, while remaining resistant to all other immunized sera.

Epitope mapping of polyclonal sera using linear overlapping peptide microarrays

To understand the linear epitope specificities of immunized serum, peptide microarrays were performed. Each array contained 1431 overlapping 15 amino acid peptides representing Env gp160 sequences from clades A, B, C, D, M, CRF1, and CRF2 consensus and vaccine strains, which include 1.A244, 1.TH023, B.MN, C.1086, C.TV1 and C.ZM651. The highest binding intensity to a single peptide within a specific epitope region was used as maximum binding value of each region of Env protein.

First, all animals from all groups developed strong IgG responses to epitopes in the C1 and V3 regions of HIV-1 gp120 of the different clades tested (Fig. 5.7A). There was no difference in total gp160 IgG linear epitope binding (sum of maximum binding

intensity for all epitopes) responses among groups (data not shown). Second, as expected, we observed a different IgG response against the gp41 subregion. Kennedy sequence is a loop at the C-terminal tail of gp41, and an early study showed that an antibody response against this region was able to neutralize viruses (226). Here we saw that gp160 DNA prime-gp160 protein boost and gp120 DNA prime-gp160 protein boost had the higher IgG response against gp41 Kennedy Sequence (Fig.5.6), compared to gp120 DNA prime-DNA boost and gp160 DNA prime-gp120 boost. Beyond the gp41 region, to our surprise, we also noticed that gp160 DNA prime-gp160 protein boost group induced highest IgG response against the conjunction of the V4-C5 region, especially compared to gp160 DNA prime-gp120 protein boost and gp120 DNA prime-gp160 protein boost (p=0.032 and p=0.018, respectively). Further, a decreased C5-specific IgG response was elicited in gp160 DNA prime gp160 protein boost group when compared to other groups. Interestingly, anti-C5 IgG responses and gp41 Kennedy Sequence-specific IgG responses were discordant (Fig. 5.6B). Of note, we did not detect any positive signals against the V2 region using the linear peptide microarray (Fig. 5.6A), but when gp70-V1V2 scaffold proteins were used, V1V2-specific antibody responses was detected in all four groups (Fig. 5.4D). This assay outcome difference could be due to preferential recognition of the conformational antigen by V2-specific antibodies.

Effect of V3 peptide adsorption on serum neutralization

Linear peptide microarray demonstrated robust cross-reactive V3-specific antibody responses among four groups, and V3-specific antibodies that were sensitive to several Tier 1 viruses, such as SF162. Therefore, we decided to determine neutralization capabilities of rabbit sera mediated by non-V3-specific antibodies. We addressed this
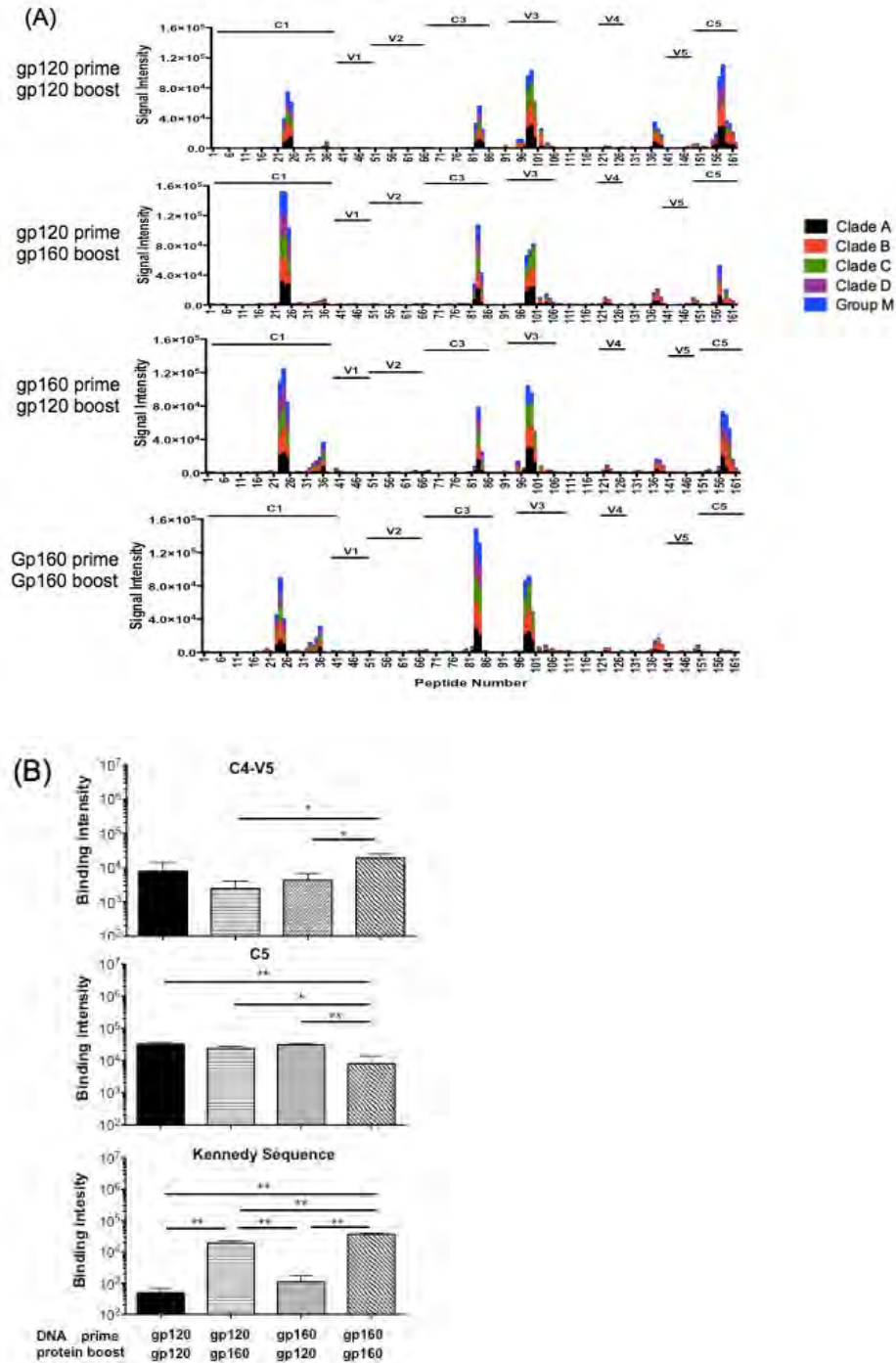
Figure 5.6. Linear overlapping peptide mapping for immunized sera. (A) Accumulative signal intensity against Clade A, B, C, D, and AE consensus Env for immunized sera in HxB2 alignment for immunized sera. (B) Maximum binding intensity for IgG antibody responses against V4-C4, C5 and Kennedy sequence region. Statistical differences between groups were determined by Student's t-test (*: $p<0.05$, **: $p<0.005$).

question by absorbing the V3-specific antibodies by incubating sera with 15-mer clade B

consensus peptides spanning the entire V3 region. V3 peptide absorption of this serum

resulted in overall reduction in neutralization activities against SF162, a virus very

sensitive to V3-mediated neutralization (Fig. 5.8). After V3 absorption, previously

superior neutralization activities against SF162 in the gp120 prime-gp160 boost group

disappeared compared to the other three groups. Only the gp120 prime-gp120 boost

group showed higher neutralization titers against SF162 compared to the gp160 prime

gp120-boost group, suggesting gp120 Env might have induced other neutralizing

antibodies that were absent from the other three groups. We also repeated the V3 peptide

absorption in an attempt to neutralize two other clade B primary isolates, SS1196, and

NL4-3 (Fig 5.8). We still observed a substantial reduction in neutralization activities

against SS1196 and NL4-3. Different from SF162, the overall trend of neutralization

among four groups remained the same as was observed prior to V3 absorption. This

indicates that in addition to V3-specific antibodies, there were other functional antibodies,

such as CD4bs antibodies or other conformational antibodies, that play an important role

in the neutralization of more resistant primary isolates.

High prevalence of CD4 binding site antibodies with gp120 DNA prime

In our previous studies, we found that the DNA prime-protein boost regimen

induced significant levels of CD4 binding domain-specific antibodies (95, 96). Here we

used a similar pseudoviral-based competitive binding assay to determine the presence of

CD4 binding site-specific antibodies, as previously reported. When the neutralizing mAb,

b12, was used as a competitive binding target, all five rabbits from the gp120 prime-

gp120 boost group were able to outcompete binding to b12 with highest mean dilution
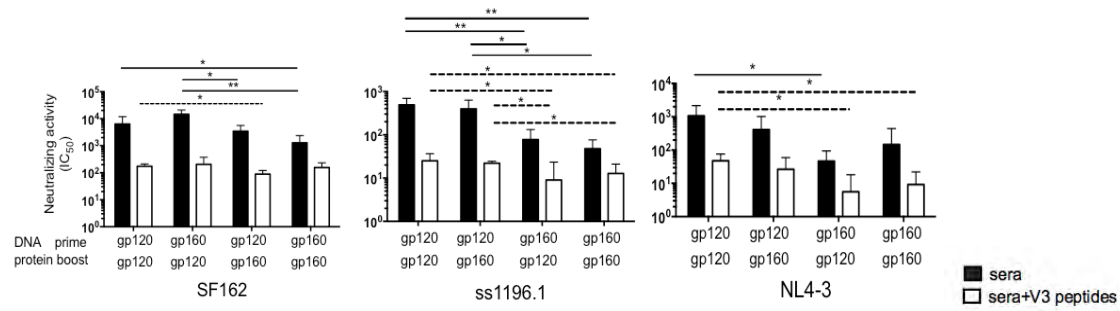
Figure 5.7. Neutralization of Tier 1 viruses with V3 absorption. Neutralization activities of rabbit immune sera with or without pooled V3 peptide incubation. Black bar showed in-house neutralization activities in TZM-bl system. White bar showed pooled V3 peptides were incubated with rabbit immune sera for 1 hour and neutralization activities were measured.

titer of 1:64, while animals in the other three groups (gp120 DNA prime gp160 protein boost, gp160 DNA prime gp120 protein boost, and gp160 DNA prime gp160 protein boost) only sporadically elicited antibodies targeted to the CD4 binding site with a low titer (Fig. 5.9A). Again, 3 out of 5 animals from the gp120 DNA prime-gp160 protein boost and gp160 DNA prime-gp120 protein boost groups could outcompete with b12 with a mean titer of 1:27 and 1:17.8, respectively. Finally, 2 out of 5 rabbits from the gp160 prime-gp160 boost group outcompeted with b12 with a lowest titer of 1:13.6.

To further confirm the presence of CD4bs-specific antibodies in immunized sera, we determined binding titers using immunized sera against either resurfaced, stabilized core (RSC3) protein or delta RSC3 (dRSC3) protein by ELISA. dRSC3 is modified based on RSC3 protein with a mutation that eliminates CD4 binding (RSC3delta371I) (116). This pair of reagents were used to identify the CD4bs broadly Nab VRC01. Using sera collected at 2 weeks after three times DNA prime, there were no differences in terms of antibody binding titers against RSC3 or dRSC3. However, both gp120 priming followed by either gp120 protein or gp160 protein boost induced significantly higher binding titers against RSC3 compared to dRSC3 (Fig 5.9B). Specifically, gp120 prime-gp120 boost had 1.84-fold higher binding titers against RSC3 compared to dRSC3 (p=0.037), while gp160 prime-gp120 boost elicited 1.54-fold higher binding titer against RSC3 compared to dRSC3 (p=0.019). There was no significant difference in binding to RSC3 or dRSC3 for the two gp160-primed groups. This suggests that gp120 DNA prime followed by protein boost (either gp120 or gp160) leads to a higher population of CD4bs-specific binding antibodies, which may further be responsible for the higher neutralizing titer.
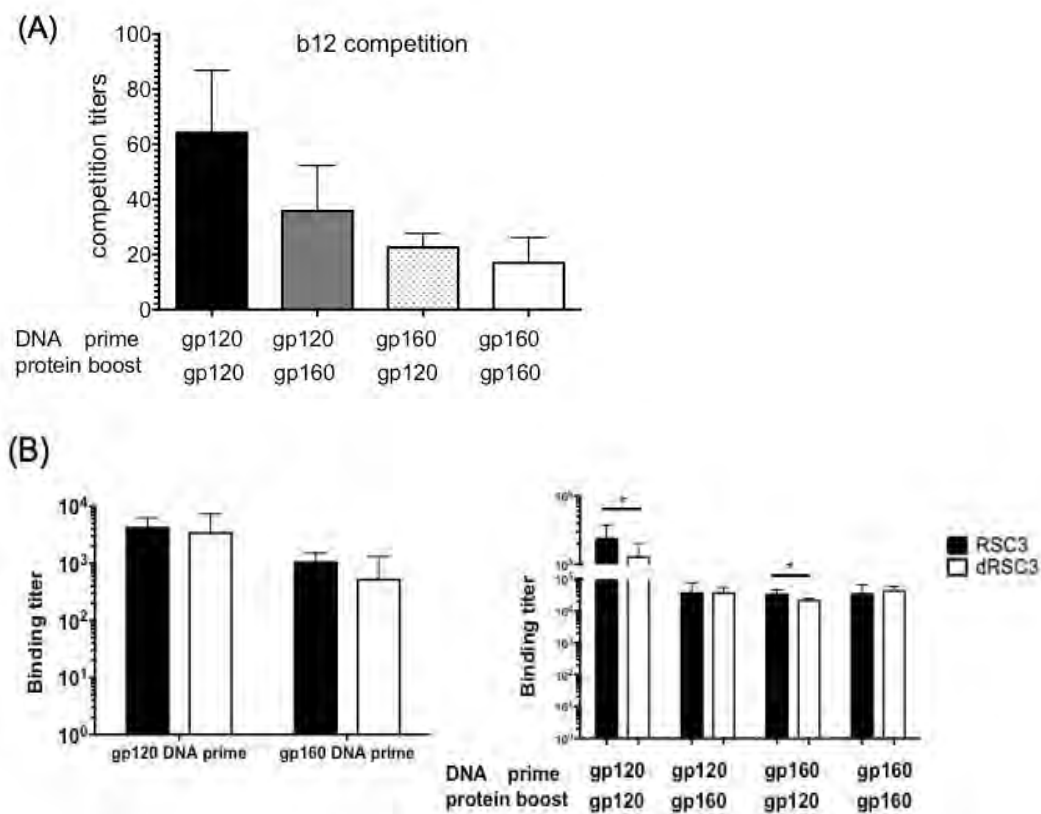
Figure 5.8. High prevalence of CD4 binding site antibodies in gp120 DNA primed groups. (A) The ability of serially diluted rabbit immune serum to outcompete binding of CD4bs mAb b12 to a JR-FL and VSV-G pseudotyped virus was measured. Competition titer is the serum dilution preventing 50% of pseudoviral binding to b12. (B) Binding antibody titer against RSC3 and dRSC3, a CD4bs mutant. Statistical differences between groups were determined by Student's t-test (*: $p<0.05$, **: $p<0.005$).

Discussion

In this study, we assessed the impact of HIV Env form, either gp160 or gp120, based upon viral isolate JR-FL, to elicit humoral responses in rabbits. We inoculated the rabbits with DNA expressing cleavage site intact, cell surface presented gp160 trimer via gene gun for priming. As a control, we also included DNA priming groups that encoded gp120 protein. First, the DNA vaccination approach was able to express *in vivo* genetically encoded membrane-anchored gp160 or secreted gp120 protein, which maintained the native conformation of sensitive Env proteins compared to recombinant Env proteins manufactured by the traditional *in vitro* production and purification process (227). Second, as one of our boost immunogens, we were able to express full-length, membrane-bound Env gp160 protein with natural cleavage site intact in recombinant vaccina virus-infected cells. This way, we were able to mimic the natural form of full-length Env spike to a larger degree compared to using a gp140 protein. Indeed, uncleaved gp140 trimers have been shown to be less stable and display aberrant conformations compared to the newly cleaved BG505 SOSIP.664 gp140 trimer (28). Two weeks after the DNA prime, higher antibody titers against gp120 and V1V2 region were observed in the gp120 DNA priming group when compared to the gp160 DNA prime group. In addition to binding antibody, the gp120 DNA priming group also elicited higher NAb against SS1196. This is consistent with previous reports, when gp120, gp140, and gp160 DNA vaccines were compared directly in a rabbit study, gp120 was the most immunogenic in eliciting antibodies against Env protein, gp140 was less effective, and gp160 was the least immunogenic (228).

Further, we boosted the DNA-primed Env-specific antibody responses by two additional intramuscular inoculations of either gp120 or gp160 protein, formulated with Incomplete Freund's adjuvant (IFA). Interestingly, the quantity and quality of humoral responses elicited by four different vaccination regimens depended upon the form of DNA used during the priming stage. Compared to the two gp160 DNA primed groups, both gp120 DNA primed groups, generated higher antibody response against gp160, gp120, gp120 core as well as the V1V2 region, independent of the form of Env immunogens they were later boosted with. Moreover, gp120 DNA prime groups elicited higher neutralizing titers against Tier 1 viruses, compared to gp160 DNA-primed groups. For the first time, this evidence suggests that when using a heterologous prime boost strategy, DNA encoding gp120 protein, instead of gp160 protein, at an early stage directly impacts the fate of the immune response. It could be that DNA priming is more effective in eliciting memory B cells targeting corresponding conformational epitopes of priming immunogens. This is similar to the observation of "original antigen sin", in which the immune system preferentially utilizes immunological memory based on the priming immunogen when a second slightly different version of a boosting immunogen is encountered.

Our earlier study showed that DNA prime followed by protein boost induces high frequency of CD4bs-directed antibodies compared to protein alone (96). Here we also sought to determine epitope specificity within immunized sera that might contribute to superior neutralization capabilities of gp120 DNA prime compared to the gp160 DNA prime. First, epitope mapping by virus capture assay suggested that gp120 DNA prime-gp120 protein boost selectively elicited b12 competing binding antibodies. This was

further verified by determining binding titers against RSC3 and dRSC3 using immunized sera. The gp120 DNA-primed groups showed high RSC3 binding titers compared to dRSC3 binding titers, suggesting that CD4 binding site-specific antibodies were generated in gp120 DNA-primed groups but less so in gp160 DNA-primed groups. Interestingly, there is no detected difference for CD4 binding site-specific binding titers among groups at DNA priming phase, suggesting that protein boost is essential to amplify such CD4 binding site-directed binding antibody response.

It is intriguing to see that DNA prime with gp160 immunogen expressed *in vivo* which should mimic an Env trimer, did not elicit superior NAbs, compared to DNA primed with gp120, a monomer. Meanwhile, several studies suggested that immunogens designed to expose conserved regions did not enhance generation of bNAbs compared to immunogens that failed to expose those regions. For example, gp140 trimer used for solving trimer cystal structures is selectively recognized by bNAbs, but not by non-broadly Nabs. However, it only induced transient, positive neutralization activities against autologous Tier 2 but not other Tier 2 viruses (29). The RSC3 probe, which was specifically designed to fish out CD4bs-specific monoclonal antibodies, failed to detect CD4-binding site NAbs. Another study used two closely related Env antigens with different antigenic properties to compare their immunogenicity (213). The Env with low CD4 affinity turned out to elicit broader NAbs with higher titer compared to the Env with high CD4 affinity. Moreover, superior NAb abilities were pinpointed to limited residues within or flanking the CD4 binding site. Coincidentally, all these data suggest a disconnection between antigenicity and immunogenicity.

To summarize, this study provides key information to guide the design of optimal form of Env in the context of DNA prime and protein boost. Our data demonstrate that DNA priming was a critical stage that determined the immunogenicity outcome. Furthermore, gp120 DNA priming was able to effectively induce a high quantity of binding antibodies that recognized diverse linear and conformational epitopes on HIV-1 Env, thus might contribute to superior neutralization activities.

Chapter VI

Materials and Methods

HIV-1 gp120 DNA vaccine

Gene segment coding for the gp120 region of HIV-1 isolate JR-FL was produced by PCR from parental full length JR-FL *env* genes (229). JR-FL gp120 gene was then subcloned into the pJW4303 DNA vaccine vector for the DNA priming phase of the immunization, as previously reported (92). JR-FL gp120 DNA plasmid was produced in the HB101 strain of *E. coli* then purified using the Qiagen Plasmid Mega Kit (cat.no. 12183).

HIV-1 gp120 protein vaccines

Recombinant HIV-1 gp120 protein vaccine was produced from Chinese Hamster Ovary (CHO) cells. Secreted gp120 proteins from stably transfected CHO cell lines were harvested and purified over a lectin column.

Rabbit Immunizations

New Zealand White rabbits (6-8 weeks of age) were purchased from Millbrook Farm (Amherst, MA) and housed in the animal facility managed by the Department of Animal Medicine at the University of Massachusetts Medical School.

For Chapter II mAb project, each rabbit was immunized with three times gp120 DNA vaccine via a Bio-Rad Helios gene gun to the shaved abdominal skin (36 µg/immunization), followed by twice intramuscularly boosted with gp120 recombinant proteins formulated with incomplete Freund's adjuvant (IFA). After a 4-month resting period post three times DNA prime-twice protein boost, one rabbit from the study group

was boosted again with the same JR-FL gp120 DNA vaccine at week 28, followed by an intravenous 400 µg JR-FL gp120 protein immunization at week 32.

In Chapter III, the rabbits were intramuscularly immunized with four times JR-FL gp120 proteins formulated with ISCOMATRIX™ adjuvant (CSL Ltd.). In Chapter IV, the rabbits were either intramuscularly immunized with JR-FL gp120 DNA or gp120 protein formulated with aluminum hydroxide. In Chapter V, the rabbits were immunized with three times either gp120 or gp160 JR-FL DNA vaccine via gene gun, and boosted with twice either gp120 or gp160 JR-FL protein formulated with IFA. The JR-FL gp160 protein was generously provided by Dr. Shiu-lok Hu from University of Washington. The gp160 protein expression and purification was described previously (75, 230).

Rabbit hybridoma production

Spleens were collected from sacrificed rabbits 4 days after the final protein boost and sent to a subcontractor (Epitopmics) for the production of hybridoma cells, according to the company's established procedure.

Enzyme Linked Immunosorbent Assay (ELISA)

Supernatant from hybridoma culture was sent back to UMMS for screening of gp120-specific antibodies. ELISA was conducted in 96-well microtiter plates (Corning, NY), which were first incubated with concanavalin A (ConA) (5 µg per well in 100 µl of PBS, pH 7.2) for 1 hour then coated with 100 µl of gp120 antigen (1 µg/ml) from transiently transfected 293T cell supernatant. Plates were washed five times with ELISA Washing Buffer (EWB, PBS containing 0.1% Triton-X), and blocked overnight at 4°C in PBS containing whey dilution buffer (4% whey by weight) and 5% powdered milk. The following morning, plates were washed five times in EWB. Hybridoma supernatants or

serially diluted rabbit monoclonal antibodies were added to the wells in a volume of 100 µL. Plates were washed five times in EWB and incubated with 100 µL of biotinylated anti-rabbit secondary antibody (Vector Labs BA-1000) at 1.5 µg/mL for 1 hr at room temperature. Plates were washed five times with EWB and incubated with 100 µL of a streptavidin-conjugated horseradish peroxidase (Vector Labs, cat.no. SA-5004) at 500 ng/mL. Plates were washed five times with EWB and developed for 3 min in 100 µL of a 3,3'5,5'-tetramethylbenzidine substrate solution (Sigma, cat.no. T3405). The reaction was stopped with 25 µL of 2N H_2SO_4.

For the peptide epitope assay, 96-well microtiter plates were coated with overlapping peptides of HIV-1 consensus subtype B Env at 4 µg/mL for one hour and blocked overnight. Hybridoma supernatants (100 µl) were then added to the peptide wells. Bound antibody was detected using an anti-rabbit IgG secondary antibody, as described above.

Western Blot

The JR-FL gp120 antigen used in the Western blot analysis was obtained from 293T cells transiently transfected with JR-FL gp120 expressing DNA vaccine, as previously reported (96). The gp120 antigens were subjected to SDS-PAGE and blotted onto a PVDF membrane, as previously described (98). Blocking of the PVDF membrane was done with 0.1% I-Block (Tropix, Bedford, MA). The membranes were incubated with hybridoma supernatants at 1:100 dilution for 45 min and subsequently reacted with AP-conjugated goat anti-rabbit IgG (Tropix, Bedford, MA) at 1:5000 dilution for 30 min. Membranes were washed with blocking buffer after each step. Western-light substrate

was then applied to the membranes for 5 min. Once the membranes were dry, X-ray films were exposed to the membrane and developed using a Kodak processor.

Cloning and Expression of rabbit mAb IgG genes

Full length heavy chain and light chain gene transcripts of rabbit mAb were isolated by one-step RT-PCR amplification of hybridoma cell RNA using primers specific to conserved regions of rabbit IgG genes. Antibody heavy chain and light chain gene products were separately cloned into a mammalian expression vector, pJW4303. For expression, equal amounts of heavy- and light-chain plasmid DNAs were transfected with 293Fectin into Freestyle 293F cells (Invitrogen). The cell culture supernatant containing the secreted rabbit IgG was harvested 2 days after transfection and purified using protein A-Sepharose columns (GE healthcare).

Analysis of rabbit mAb heavy chain and light chain sequences

The cloned full-length heavy chain and light chain DNA fragments were sequenced by Gene-Wiz, North Brunswick, NJ. Sequencing analysis was conducted with the rabbit heavy chain and light chain genes of rabbit mAb. ClustalW was used and the multiple sequence alignments were done to construct phylogenetic trees using maximum likelihood methods. The trees were then graphically edited (231). Antibody germline usage, mutation frequency, and CDR3 length were determined by means of IMGT/V-QUEST (232).

Neutralization Assays

In-house neutralization assays were done as previously described (233). HIV pseudoviruses were first produced and titrated. Briefly, equimolar quantities of a plasmid expressing gp160 from the HIV-1 Env of interest and the pSG3ΔEnv HIV backbone were

co-transfected into HEK 293T cells. At 48 hours after transfection, supernatants were harvested and cleared of cell debris by low speed centrifugation. Produced pseudoviruses were titrated on TZM-bl cells using a two-fold increase above background levels of luciferase activity as a positive cutoff.

For in-house neutralization assay, 200 $TCID_{50}$ of pseudovirus was incubated with the rabbit sera or rabbit mAb for 1 hr at 37°C. The virus/mAb mix was then added to 10^5 TZM-bl cells in a final concentration of 20 µg/mL DEAE Dextran. Plates were incubated at 37°C for 48 hours and developed with luciferase assay reagent according to the manufacturer's instruction (Promega). Neutralization was calculated as the percent change in luciferase activity in the presence of preimmune sera versus that of luciferase activity in the presence of immune sera [(Preimmune RLUs – Immune RLUs)/(Preimmune RLUs)] X100.

Selected RmAbs were tested in a high throughput neutralization assay using the PhenoSense assay at Monogram Biosciences as previously reported (South San Francisco, CA) (96).

Additional neutralization assays were conducted at Duke University, and Beth Israel Deaconess Medical Center, Harvard Medical School, according to their established protocols as described in previous reports (92).

Binding kinetics of rabbit mAbs

The binding kinetics of rabbit mAb to five representative gp120s from HIV-1 clades A to E were studied using a ForteBio Octet QK^e instrument based on the Biolayer Interferometry (BLI) measurement in a 96-well format following the manufacturer's instructions. Protein A coated tips (ForteBio) were loaded with rabbit mAbs at 10 µg/ml

diluted in the buffer of PBS/0.1%BSA/0.002%Tween 20. After capture, a 1-min wash in loading buffer removed excess unbound Ab to establish a new baseline signal. The biosensor tip was then put into wells containing the selected gp120 proteins at three-fold serially diluted concentrations from 100 to 11 nanomolar (nM), in loading buffer.

Rabbit mAb-gp120 association on-rate was measured given a 3-min interval, followed by putting the sensor in wells containing regenerating buffer (500mM phosphoric acid) to measure dissociation rate (off-rate) over a 10-min interval. K_D values were calculated as the ratio of off-rate/on-rate. The sensorgrams were corrected with the blank reference and fit with the software ForteBio Data Analysis package 7.0 using a 1:1 binding model with the global fitting function (grouped by color, R_{max}).

Competitive binding assays

The sheep gp120 C5-specific mAb, D3742 (Aalto Bio Reagents), was used at 2 µg/ml to coat ELISA plates. The plates were washed for five times and blocked with PBS containing 4% whey and 5% powdered milk, and gp120 proteins were then added to these pre-coated plates. After a five-time wash, the competitor rabbit mAbs or sCD4 were diluted in the blocking buffer and plated at 3-fold serial dilutions, starting at 500 µg/ml. After a 30-min incubation, 10 µl Ig-CD4 at 0.1 µg/ml was added to wells. Bound Ig-CD4 was performed as ELISA assay described above.

Virus capture competition.

Virus Capture competition assay was performed as previously described (Vaine et al, Vaccine, 2010). Pseudovirions bearing the JR-FL Env and vesicular stomatitis virus (VSV) glycoprotein were produced with the pSG3ΔEnv backbone in 293T cells. Microtiter plates were coated with 50µl of monoclonal antibodies b12, 3074 and 2G12 at

5 µg/ml for 1 h at room temperature. Plates were then blocked in PBS with 3% bovine serum albumin overnight at 4°C. Rabbit hybridoma supernatants were incubated with pseudovirus correlating to 2.5 ng of p24/well for 1 h prior to the addition to the virus-sera mixture to the ELISA wells. The pseudovirus-sera mixture was then incubated in the ELISA wells for 3 h at room temperature. Plates were washed 5 times with sterile PBS and overlaid with 10,000 TZM-bl cells per well. Plates were then incubated for 48 h at 37°C. Luciferase activity was determined per the manufacturer's instructions (Promega). The percentage inhibition is reported when compared to PBS as negative control.

The ability of rabbit sera to inhibit the capture of pseudovirions by CD4bs specific monoclonal antibody (mAb) b12 was investigated as described above. The capture of pseudovirions by HIV-1 monoclonal antibodies will be blocked if there is a competing antibody in the rabbit sera. Briefly, microwells were coated with mAb b12 (5 µg/ml) overnight and were then washed and blocked with 3% bovine serum albumin in PBS. Graded dilutions of rabbit sera were added to the virus, and the virus-serum mixtures were then added to b12-coated ELISA wells for 3 h, followed by washing with TMZ-BL cells were overlaid, and 2 days later infection was measured by assaying luciferase. The reciprocal serum dilution that inhibited b12-mediated virus capture by 50% was recorded.

NaSCN Displacement

JR-FL gp120 was coated onto 96 well microtiter plates (Costar) at 1 µg/mL in 100 µL of PBS for 1 hr at room temperature. Plates were then washed 5 times in PBS containing 0.1% Triton-X (EWB) and blocked overnight at 4°C in PBS containing 4% by weight whey (whey dilution buffer) and 5% powdered milk. Rabbit sera were then added

to the plate at either a 1:30,000 or 1:100,000 dilution and incubated at room temperature for 1 hr. Plates were then washed 5 times in EWB. NaSCN was then added at various (0, 1, 2, 3, 4, 5 M) concentrations in PBS for 15 min followed by 5 washes in EWB. Bound IgG was detected as described above. Determination of IgG quantity remaining on the plates was done using linear regression analysis of a standard IgG curve (Southern Biotech). Data is reported as the NaSCN concentration required to displace 50% of IgG initially bound on the plate.

Fab production and purification

Details of the rabbit mAb R53 productions and antigenicity characterizations have been published (191). The Fab fragment of R53 was prepared by papain digestion as described previously (234). Briefly, the IgG molecule was mixed with papain (Worthington) at a 20:1 ratio and 100 mM Tris (pH 6.8) with 1 mM cysteine hydrochloride and 4 mM EDTA. The mixtures were incubated for 1 hour at 37°C and the reaction was stopped by adding 10 mM iodoacetamide. The Fab fragment was separated from Fc and the undigested IgG by a protein A column and further purified by size exclusion chromatography. The concentration of the Fab fragment for crystallization is about 10 mg/ml.

Crystallization, data collection, structure determination and refinement

The C4 peptide was synthesized by Biomatik (Wilmington, DE) and dissolved in water to a concentration of 10 mg/ml. Preliminary crystals of Fab in complex with/without peptide were obtained by robot screening using the vapor diffusion hanging drop method. Well-diffracted crystals of R53 Fab in complex with peptide were obtained in a solution of 24% polyethylene glycol 6000, 0.1 M citric acid pH 5.0, and 0.02% NaN$_3$.

Crystals of R53 Fab alone were obtained in a solution of 14% polyethylene glycol 8000,

0.1 M HEPES pH 7.5, and 8% ethylene glycol. Crystals of Fab R53/epitope complex and

Fab R53 alone were first soaked in the mother liquor with additional 20% glycerol (v/v)

and 20% ethylene glycol, respectively, before placed in the X-ray beam. X-ray diffraction

data of the crystals of Fab R53/epitope complex were collected at beam line X6A,

National Synchrotron Light Source (NSLS), Brookhaven National Laboratory. Data of

the crystals of R53 Fab alone were collected at the synchrotron beamline GM/CA CAT at

the Advanced Photo Source (APS), Argonne National Laboratory. All data sets were

processed using the HKL 2000 package (235), and structures were determined by

molecular replacement, using as the starting model the structure of another rabbit mAb

R56 we previously determined (PDB ID 4JO1). Cycles of refinement for each model

were carried out in COOT and Phenix (236, 237). Contact areas were calculated by ICM

(238). Final structural analysis was carried out using ICM and figures were generated

using Pymol (239) and ICM.

Linear peptide microarray

Peptide microarray was performed at Duke University according to their

established protocols as described in previous reports (23, 240). Peptide libraries

(designed by Dr. Bette Korber) consist of 15-mers overlapped by 12 amino acids were

printed on glass slides, covering the full length of consensus gp160 Env from clade A, B,

C, D, M, CRF01_AE, and CRF02_AE as well as gp120 derived from vaccine strain,

including 1. A244, 1.TH023, MN, C.1086, C.TV1, and C.ZM651. Briefly, the peptide

microarray was performed using a Tecan HS4000 Hybridization WorkStation. All arrays

were blocked with Superblock T20 PBS blocking buffer for 0.5 hour at 30°C with heat

inactivated plasma diluted 1:100 in SuperBlock T20. The arrays were incubated for 45 minutes at 30°C with anti-IgG Cy5 secondary antibody (1.5ug/ml final concentration). PBS containing 0.1% Tween was used for each washes between all steps. Arrays were scanned at 635 nm using an Axon Genepix 4300 Scanner (Molecular Devices, Sunnyvale, CA, USA) at a PMT setting of 600, 50% laser power. Images were analyzed using Genepix Pro 7 software (Molecular Device).

Chapter VII

Final comments and Conclusions

An effective prophylactic AIDS vaccine is still urgently needed to control the current HIV pandemic. The unprecedented, albeit modest, protection elicited in the RV144 trial suggested that substantial effort is still necessary to improve the vaccine efficacy. However, it remains unknown what are the desirable immune responses capable of providing protection against virus acquisition. Evidence from the recent immune correlate study of RV144 trial not only confirmed the importance of antibody responses, but also suggested that a successful HIV vaccine should induce a broad repertoire of HIV-1 epitope specificity and antibody subclasses with a wide range of antiviral mechanisms. Therefore, well-characterized vaccine-elicited antibody response in terms of magnitude and quality will be essential for rational design of HIV vaccines.

I started to characterize the antibody response by isolation of vaccine elicited Env-specific rabbit monoclonal antibodies (RmAbs). Two dozens of RmAbs were isolated from immunized rabbits primed with DNA vaccines expressing gp120 protein following recombinant gp120 protein boost. They showed a broad diversity of Env epitopes focusing on C1, V3, C4, C5 and unknown conformational regions. Overall, these RmAbs showed high binding affinities, and a majority of them could cross-react with multiple clades of gp120 antigens, and several had quite potent and broad neutralizing activities against Tier 1 sensitive viruses. Specifically, RmAb R56 recognized the immunodominant region in V3 crown, the epitope previously identified in HIV infected individuals. R16 shared a similar antigen-binding region of R56, with merely one amino acid shift from charged to hydrophobic residue. However, such

structural shift led to great improvement in neutralization activities in both potency and breadth. R20 targeted at C-terminal region of V3 region that overlaps the epitope of human broadly neutralizing Ab PGT128. The epitope of R53 within C4 region is a representative of CD4 blocking mAbs identified in mouse model during early HIV research. Overall, the rabbit mAb platform has provided us a great tool to dissect the specificity, biochemical and biological function of vaccine-induced antibody response at molecular level.

The traditional hybridoma fusion technology was used to isolate antigen-specific rabbit monoclonal antibodies. This protocol requires around 3 month, and I only obtained two dozens of gp120-specific rabbit hybridoma cell lines. With current advancement of single B cell labeling and cloning technology, in future florescence labeled protein or peptide probes could be used to isolate the antigen-specific B cells by flow cytometry and the immunoglobulin genes could be cloned in a high throughput manner. These cloned mAbs will be further carefully characterized for their biochemical and biophysical properties and anti-viral functions. Further, development of next generation sequencing (NGS) technology also allows monitoring the selection, enrichment and maturation of immunoglobulin genes with sequences that have been identified as potentially yielding anti-viral functions. Such combination of single B cell identification as well as NGS of antigen-specific B cell heavy chain and light chain genes will provide valuable information about the quality of antibody response driven by vaccine. Moreover, if longitudinal samples at key time points post each immunization are collected, this will help understand the molecular pathway of affinity maturation of antigen-specific B cells. Such information will be highly useful to further guide us in designing better

immunogens and an optimal immunization schedule.

In addition, with a variety of assay systems to evaluate the magnitude and quality of antibody response within polyclonal sera, we attempted to evaluate novel immungens or immunization regimens. Since heavily glycosylated gp120 Env protein is one of the critical components in HIV vaccine, we want to determine the impact of glycan shield of HIV Env on antibody responses. Six Env proteins modified with homogenous population of distinct glycoforms were produced from humanized glycoengineered yeast cell lines. The selective glycoforms are as follows: Man3, Man5, Man8/9, terminal galactose, and 2,6 sialic acid. Antigenicity analysis showed that glycoforms did impact the exposure of key neutralizing epitope on these glycan modified Envs if compared to Env protein produced from traditional Chinese Hamster Ovary (CHO) cells. Specifically, glycan-specific mAb 2G12 could not recognize Man3 and Man5-modified Env proteins, but the binding affinity of 2G12 to Man8/9 Env was improved compared to that of Env from CHO cells. CD4bs related mAbs also has decreased binding affinity with most of these glycan-modified Envs compared to CHO-derived Envs. Rabbit studies tested the immunogenicity of that these novel immunogens and Env protein produced from traditional CHO cells was used as control. The glycan-modified Envs are highly immunogenic and elicited gp120-specific antibody response. Most significantly, sera elicited by glycan modified gp120 protein immunogens revealed better neutralizing activities and an increased diversity of epitopes than sera elicited by traditional gp120 produced in CHO cells.

It is intriguing to observe that relative homogenous glycan modification on Env can improve the immunogenicity of Env. The mechanism of how N-glycans manipulate

the immune system and generate high quality of antibody response is yet to be determined. First, a comparison needs to be performed regarding glycan site occupancies for Envs produced from CHO cells and from glycoengineered yeast cells. If fewer glycan occupancy sites were observed from GlycoFi Envs, this might expose more critical epitopes, such as V1/V2 region, to immune system. Further, a dense shield of the uniform N-glycans might be capable of inducing antibody responses against the particular glycoform, as we observed from Man8/9 Env immune sera. It is not known that whether these glycan-specific antibodies contributed to better neutralization activities. It will be helpful if we can identify and further characterize the biological function of gp120-specific monoclonal antibodies that involve glycan recognition.

In present study, all the Envs modified with different glycans were based on JR-FL gp120 backbone. To verify my findings, Env from other isolates could also be tested to see whether Env produced from glyco-engineered yeast cell strains still have a superior immunogenicity compared Envs produced from CHO cells. Further, several glycoforms of interest were identified, such as Man8/9 and 2,6 sialic acid. They both induce significantly higher neutralization activities and V1/V2-specific antibody response. It will be interesting to test the immunogenicity of a polyvalent vaccine consisting of several GlycoFi Envs modified with different glycoforms. I would expect that such a polyvalent vaccine might have synergistic effects to further improve humoral response compared to monovalent GlycoFi Env vaccine.

RV144 trial has demonstrated the improved vaccine efficacy by the combination of two vaccines via distinct mechanisms. We aimed to define the impact of the varying delivery order of DNA and protein-based vaccine on the antibody response. In particular,

DNA prime-protein boost, co-delivery of DNA and protein, and protein prime-DNA boost were analyzed. In murine model, we showed that DNA prime protein boost was able to elicit highest level of Env-specific binding Abs compared to co-delivery DNA and protein. The immune rabbit sera further suggested the presence of quality differences of antibody response among groups. DNA prime protein boost group induced Env-specific persistent antibody response with high avidity and a broad repertoire of specificity. Although immunized group induced comparable level of neutralizing antibodies, DNA prime protein boost neutralized the most viruses compared to other group. All of these parameters indicated that DNA prime-protein boost regimen is a promising strategy for future vaccine development.

While we have demonstrated that sequential delivery of DNA and protein-based vaccine generated the most effective antibody response, the optimal form of HIV-1 Env, either gp120 or gp160, at the prime and boost phase is still not clear. Our data confirmed that at prime stage, DNA vaccine expressing gp120 protein was more immunogenic and induce higher magnitude of neutralizing antibodies against ss1196. This further directly determined the final immune outcome. At the peak immunogenicity point after final boost, both groups receiving gp120 DNA vaccines showed higher level of binding antibody against gp160 Env, gp120 Env, V1V2 region and CD4 binding site than gp160 DNA primed groups. Further, gp120 DNA primed groups showed C4, C5, and V5 focused humoral response, which is lacking in the sera from gp160 DNA primed and gp160 protein boost group. Moreover, both gp120 DNA primed groups showed broader and more potent neutralizing activities compared to gp160 DNA primed groups. Indeed, a collaboration study with us showed that DNA prime was able to re-orchestrate germinal

center response by rapidly developing T follicular helper cells and further recruit B cells into germinal center, a crucial process for antibody somatic mutation and affinity maturation (97). These results suggested that appropriate stimulation of immune cells at the early immunization event is essential and pivotal to generate high quality of antibody responses.

While we have learned the uniqueness of DNA vaccine in induction of high quality of antibody response from this thesis work, the mechanisms of DNA vaccine priming immune system are not well understood. Indeed, priming with DNA activates more CD4+ T cells into T follicular helper (Tfh) cells and directs more germinal center (GC) B cells into memory cells, if compared to priming with protein-based immunization (97). This might be due to several reasons. First, similar to viral vector-based vaccine, DNA vaccine transfected into host cell, producing endogenous antigens which could be effectively presented to immune system by MHC class I and class II pathway. This will effectively induce both CD4+ and CD8+ T cell responses. Second, DNA vaccination also activates innate signaling pathways to regulate the antigen-specific adaptive immune responses, including AIM2 (absent in melanoma 2) inflammasome, a DNA sensor responsible for maturation of IL-1 and IL18 (241). Therefore, DNA vaccine is capable of providing a favorable microenvironment with sufficient Tfh cells and inflammatory cytokines, thus facilitating the affinity maturation of B cells. Future work should further understand how DNA vaccine orchestrates high frequency of Tfh cells and GC B cells, whether this process involves any well-characterized innate signaling pathways and the serum cytokine profile after DNA immunization.

In conclusion, in my thesis I characterized the quality of antibody response induced by different immunogens and immunization schedules, in the context of either mAbs or polyclonal sera. Through DNA prime-protein boost vaccination, a panel of antibody repertoire with diverse specificities and anti-viral function is observed. Further, I found that glycan modification on HIV-1 Env protein and appropriately priming the immune system have a great impact on the quality of antibody responses. The data presented here will be the guideline for rational design of next generation HIV-1 vaccine.

Preface to Appendix I

Appendix I were taken from the following publication:

Ruimin Pan, Jared M Sampson, Yuxin Chen, Michael Vaine, Shixia Wang, Shan Lu, Xiang-Peng Kong. *Rabbit anti-HIV-1 monoclonal antibodies raised by immunization can mimic the antigen-binding modes of antibodies derived from HIV-1 infected humans.* J.Virol. 2013, 87(18):10221.

In this collaboration study, we provided the reagents rabbit monoclonal antibodies R56 and R20. Dr. Ruimin Pan and Dr. Xiang-Peng Kong conducted the rabbit mAb structural analysis.

Appendix I

Rabbit anti-Env monoclonal antibodies raised by immunization can mimic the

antigen-binding modes of antibodies derived from HIV-1-Infected humans

Introduction

Here we present structural analyses of two rabbit monoclonal antibodies (mAbs) against the third variable region (V3) of HIV-1 gp120. V3 plays a key role in virus entry into the host cell, participating in the binding of the CCR5 or CXCR4 co-receptor (14, 242). V3 is about 35 amino acids in length, and the structure of full-length V3 in the context of the gp120 core showed that it can be divided into three regions, the base in the gp120 core (residues 296 to 300 and 326 to 331), the flexible stem (residues 301 to 303 and 319 to 325), and the crown at the distal apex (304 to 318) (25, 172). The V3 crown can be further divided into three smaller regions, the arch of the beta hairpin of the V3 crown (consisting of residues 312 to 315), the band (residues 304 to 305 and 317 to 318), and the circlet between the arch and the band, which is more genetically diverse than the other two regions (172). The amino acid sequence of the arch is often GPGR in clade B strains and GPGQ in non-clade B strains.

There are many anti-V3 mAbs derived from human patients, as well as from animal models other than the rabbit (243, 244). Most of the known anti-V3 mAbs are against the V3 crown; only a few of them target the C-terminal region, including a mouse mAb raised by immunization with a synthetic peptide (245). Several recently described highly potent human mAbs, including PGT128, are also against the C-terminal region of V3, as well as its associated glycans (118). Many of the anti-V3 mAbs are characterized by structural methods, including protein crystallography and the nuclear magnetic

resonance (NMR) method (118, 172, 246, 247). These structural studies of mAbs against the V3 crown showed that they have, in general, two antigen-binding modes. (i) In the "ladle" mode, the antibodies have a long CDR H3 (the handle of the ladle) interacting with the main chain of the N-terminal beta strand of the V3 crown and a pocket at the base of the CDR H3 (the bowl of the ladle) interacting with the apex beta turn of the V3 crown. (ii) In the "cradle" mode, the antigen lies along a long binding groove resembling a cradle (172, 248, 249). The former is represented by human mAb 447-52D, and the latter is represented by several human mAbs, including mAb 2557, encoded by germline IGHV5-51 (172).

We present here several Fab/epitope complex structures of rabbit anti-V3 mAbs R56 and R20 that had been raised by immunization with gp120 of clade B strain JR-FL by using the DNA prime-protein boost regimen. The epitopes of R56 and R20 have been mapped to the V3 crown and the V3 C-terminal region, respectively. By analyzing the antigen-antibody interactions of these mAbs and comparing them with those of human and mouse anti-V3 antibodies, we showed that immunization of rabbits with HIV-1 gp120 can elicit anti-V3 crown antibodies with a binding mode similar to that of human IGHV5-51 antibodies and that this immunization can also produce rabbit antibodies that target an epitope in the C-terminal region that overlaps the epitope of human mAb PGT128.

Results

Determination of the structures of Fabs R56 and R20.

We first determined the crystal structures of Fab R56 in complex with its
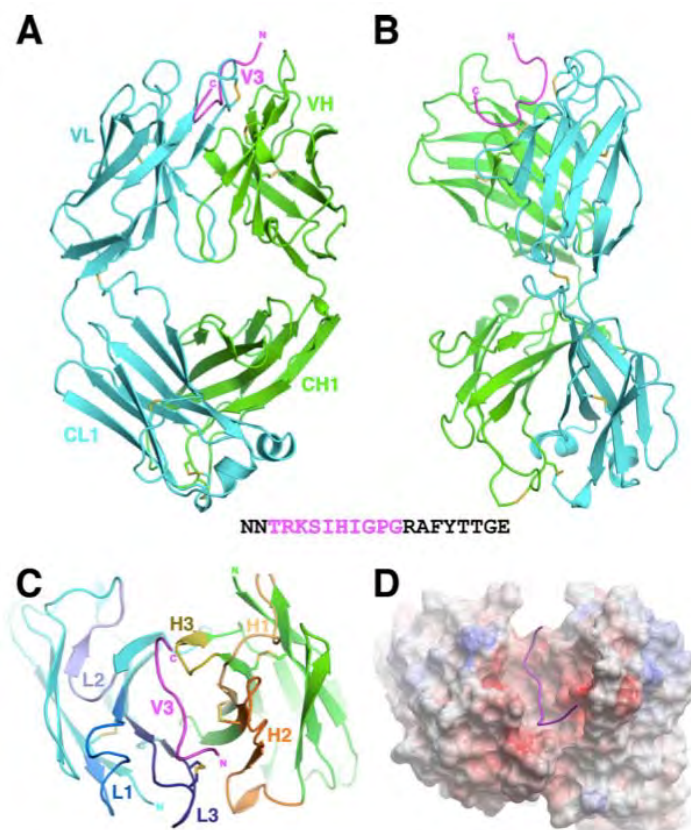
Figure AI.1 Structure of Fab R56 in complex with V3$_{\text{JR-FL}}$. (A) Ribbon representation of a front view of the Fab R56/V3$_{\text{JR-FL}}$ complex with the light and heavy chains and the V3 epitope colored cyan, green, and magenta, respectively (a coloring scheme kept throughout this report, except where indicated otherwise). Disulfide bonds are shown by side chain sticks. (B) Side view of the complex. (C) Top view of the complex looking at the antigen-binding site of Fab R56. The CDRs are labeled and colored differently from the rest of the Fab. (D) Surface representation of Fab R56 colored according to its electrostatic surface potentials, with the negatively charged region in red and the positively charged region in blue. V3 is shown as a ribbon. The inset is the sequence of the peptide used for crystallization, and the magenta residues are those visualized in the crystal structure.

Table AI.1 Crystallization data collection and refinement statistics

Parameter	Result(s)[a] for Fab:			
	R56/V3$_{JRFL}$	R56/V3$_{conA}$	R20/V3$_{conB}$	R20/PEG
Data collection				
Space group	P2$_1$	P2$_1$	P2$_1$2$_1$2$_1$	P2$_1$2$_1$2$_1$
Cell dimensions				
a, b, c (Å)	70.51, 74.34, 84.43	69.84, 74.35, 84.96	70.223, 118.977, 134.946	70.649, 119.690, 135.337
α, β, γ (°)	90, 90, 90	90, 90, 90	90, 90, 90	90, 90, 90
Resolution (Å)	2.03 (2.07–2.03)	2.50 (2.54–2.50)	2.60 (2.64–2.60)	2.27 (2.31–2.27)
R$_{merge}$	8.5 (45.0)	16.1 (58.7)	15.9 (66.4)	10.7 (59.3)
I/σI ratio	18.8 (2.4)	8.9 (2.6)	11.1 (2.7)	22.5 (3.8)
% Completeness	99.5 (94.2)	93.7 (89.9)	97.6 (95.4)	99.9 (99.5)
Redundancy	4.2 (3.8)	3.9 (4.0)	5.7 (5.6)	8.2 (8.1)
Refinement				
Resolution (Å)	36.23–2.03	26.46–2.50	38.05–2.60	38.27–2.27
No. of reflections	56,014	30,171	34,658	53,548
R$_{work}$/R$_{free}$ ratio	18.13/22.32	18.95/26.54	18.45/23.45	18.43/22.64
No. of atoms				
Protein	6,447	6,336	6,670	6,566
Solvent	805	479	369	730
B factors				
Protein	27.9	24.11	41.1	29.1
Solvent	34.9	22.08	31.3	34.3
RMSD				
Bond lengths (Å)	0.008	0.008	0.009	0.008
Bond angles (°)	1.168	1.147	1.188	1.088

[a] Values in parentheses are for the outer resolution shell.

epitope, which was mapped to the crown region of V3 (Fig. AI.1 and Table AI.1). We crystallized Fab R56 in complex with two different V3 peptides, NNTRKSIHIG PGRAFYTTGE IIG (V3$_{JR-FL}$), derived from the clade B strain JR-FL, and NNTRKSIRIG PGQAFY ATGD IIG (V3$_{conA}$), derived from the consensus A sequence of gp120. These two peptides were selected because JR-FL gp120 was the one used to immunize the rabbit and the consensus A sequence has a GPGQ motif in the crown arch, representing non- clade B HIV-1 strains. We determined the Fab R56/V3$_{JR-FL}$ and Fab R56/V3$_{conA}$ complex structures by molecular replacement and refined them to 2.0 Å and 2.5 Å resolutions, respectively (Fig.AI.1; Table AI.1). The crystals of both complexes belong to monoclinic space group P2$_1$ with essentially the same unit cell parameters. The two Fab/V3 complexes in the asymmetry unit are highly similar (for example, the root mean square deviation [RMSD] for super- imposition of all of the C-α atoms is 0.16 Å in the R56/V3$_{JR-FL}$ complex). We therefore, for simplicity, refer to only one of the complexes. We assigned the chain identities (IDs) L, H, and P, respectively, to the light and heavy chains and the epitope of the first Fab/V3 complex in the asymmetric unit. We numbered the residues of the light and heavy chains by following the Kabat and Wu convention, applied to the coordinates with the Abnum server (250), and the residues of V3 in the HXB2 numbering scheme (251). A residue is referred to by its number preceded by its chain ID, for example, Arg^{P315} refers to arginine residue 315 of the V3 epitope. Although 23-mer peptides were used for crystallization, only 10 residues, from Thr^{P303} to Gly^{P314} of the V3 crown region, with the sequence TRKSIHIGPG for V3$_{JR-FL}$ or TRKSIRIGPG for V3$_{conA}$, were observed in the electron densities and have thus been built into the final

structures (Fig. AI.1). Since the R56/V3$_{conA}$ structure has a slightly twinned data set with a lower resolution (Table AI.1) and is essentially the same as that of Fab R56/V3$_{JR-FL}$, we have not included it here but the atomic coordinates have been deposited in the PDB.

We then determined the crystal structure of Fab R20 in complex with its epitope, which was mapped to the C-terminal region of V3 (Fig. AI.2 and Table AI.1). We crystallized the Fab fragment of R20 in complex with a 15-mer V3 peptide of the consensus B sequence, TTGEIIGDIRQAHCN (V3$_{conB}$). The complex structure was determined by molecular replacement and refined to 2.6 Å resolution (Fig. AI.1 and Table AI.1). The crystals belong to the orthorhombic space group P2$_1$2$_1$2$_1$ with two Fab/V3 complexes in the asymmetric unit. Again we refer to only one of the complexes in this report, as the structures of the two complexes are highly similar (RMSD of superimposition of all C-α 0.55 Å). We have numbered the residues of the Fab R20/V3 complex in the same way as those of the R56/V3 complex. Although a 15-mer peptide was used for crystallization, only nine residues, Glu^{P322} to Ala^{P329} of the V3 C-terminal region, with the sequence EIIGDIRQA, were observed.

Antigen-binding mode of R56

The structures of R56/V3 complexes showed that R56 binds the V3 crown by using the cradle-binding mode (Fig. AI.1 and Fig.AI.3), similar to that of the human anti-V3 IGHV5-51 mAbs (172, 249). Its antigen-binding site is shaped like a cradle between the light and heavy chains ~14 Å deep and ~10 Å wide with CDR L3 at one end of the cradle and CDR H3 at the other end (Fig. AI.1C and Fig.AI.5A). Similar to that of the human anti-V3 crown mAbs, the antigen-binding site of R56 has a negative charge contributed
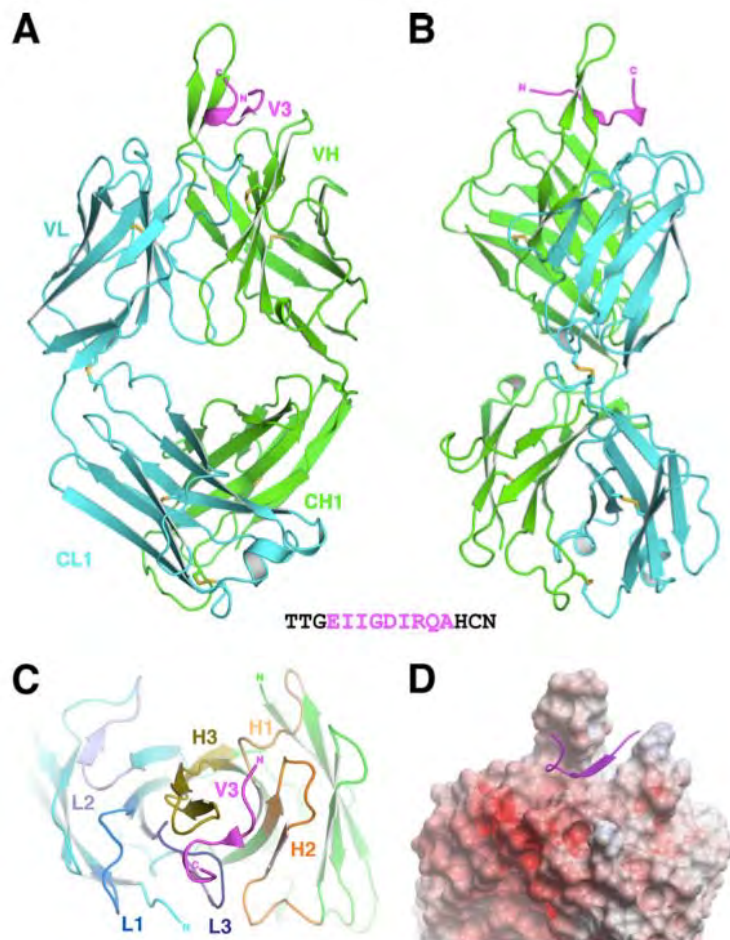
Figure AI.2 Structure of Fab R20 in complex with V3$_{conB}$. (A) Ribbon representation of a front view the Fab R20/V3$_{conB}$ complex. (B) Side view of the complex. (C) Top view of the complex looking at the antigen-binding site of Fab R20 with the CDRs labeled and colored differently from the rest of the Fab. (D) Surface representation of Fab R20 colored according to its electrostatic surface potentials. The inset is the sequence of the peptide used for crystallization, and the magenta residues are those visualized in the crystal structure.

Figure AI.3 Antigen-antibody interactions in the Fab R56/V3$_{JR-FL}$ complex. (A) Stereo view of the antigen-binding site. Side chains are displayed for key residues involved in the hydrogen bonding and van der Waals interactions (with contact areas greater than 10 Å^2). For simplicity, the chain IDs are not shown in residue labels because the chains are already indicated by the coloring scheme. (B) Schematic illustration of antigen-antibody interactions. Hydrogen-binding interactions are indicated by dashed lines between the residues, while van der Waals contacts are indicated by eyelashes. Residues in solid ovals contribute to the interactions by their main chain atoms, and those in dashed ovals contribute by their side chain atoms.

in part by three CDR residues from the light chain (Asp^{L50}, Asp^{L93}, and Asp^{L95C}) and

three CDR residues from the heavy chain (Asp^{H34}, Glu^{H52}, and Asp^{H101}), all located at the

periphery of the cradle. The bottom of the cradle is very hydrophobic and is formed by

residues Ala^{L34}, Leu^{L49}, Leu^{L89}, Cys^{L94}, Cys^{L95D}, and Ala^{L96} from the light chain and

residues Cys^{H50} and Phe^{H96} from the heavy chain (Fig.AI.3). The aforementioned two

noncanonical disulfide bonds (Cys^{H35A}-Cys^{H50} and Cys^{L94}-Cys^{L95D}) in the CDRs both

contribute to this hydrophobic base. Interestingly, the epitope of R56 superimposed well

on that of mAb 447-52D (RMSD ~0.75 Å with the superimposed C-α atoms of eight

residues [P305 to P314]), even though the latter belongs to the ladle V3-binding mode.

Our Fab R56/V3 complex structures showed that the epitope recognized by

R56 consists of 10 amino acids (P303 to P314) in the N-terminal half of the V3 crown

(Fig. AI.1 and Fig.AI.3). The N terminus of the epitope harbors two highly conserved

positively charged band residues (Arg^{P304} and Lys^{P305}), and the C terminus ends with the

highly conserved Gly^{P312} Pro^{P313} Gly^{P314} sequence of the crown arch. The epitope lies

along the cradle with its N terminus sitting on top of the disulfide bond (Cys^{L94}-Cys^{L95D})

of CDR L3 and its C terminus extending toward CDR H3. The antigen-antibody

interactions buried a total surface area of 750 Å^2 with 356 Å^2 from the antibody and 394

Å^2 from the epitope. There are three key components of the antigen-antibody interactions

(Fig.AI.3). The first is a salt bridge between band residue Arg^{P304} of the epitope and

Asp^{H34} of CDR H1. Negatively charged Glu^{H52} sits on the top of Arg^{P304}, leaving the salt

bridge largely buried. The second is the hydrophobic interactions between highly

Figure AI.4. Antigen-antibody interactions in the Fab R20/V3$_{conB}$ complex. (A) Stereo view of the antigen-binding site. Side chains are displayed for key residues. (B) Schematic illustration of the antigen-antibody interactions. The short beta strand in the epitope is indicated by a pink arrow, and the short 3$_{10}$ G turn is indicated by a pink shed.

conserved circlet residues Ile^{P307} and Ile^{P309} of the epitope and the hydrophobic base of the antigen-binding site, burying these two isoleucines in the center of the cradle. The third is Pro^{P313} at the GPG beta turn stacking with the side chain of Tyr^{L49} in CDR L2. Interestingly, the side chain of circlet residue His^{P308} (Arg^{P308} in V3$_{conA}$) in the center of the epitope points away from the antibody toward the solvent; thus, it does not contribute to the antigen-antibody interaction. Therefore, R56 does not distinguish the sequence difference between JR-FL and consensus A (data not shown). There are at least two facts explaining the broad reactivity of R56. (i) The interacting residues in the three key components are highly conserved among HIV-1 strains, and (ii) the side chain of variable residue His^{P308}/Arg^{P308} is not involved in the antigen-antibody interaction. It is also clear from the structures that R56 will not be able to bind gp120 of 92UG021, a clade D strain with the sequence VSYRTPIGVG (from 303 to 314) in the epitope region of R56. In particular, the region of the antigen-binding site that fits Ser^{P306} in JR-FL will not be able to accommodate the long side chain of an Arg in the case of 92UG021. Similarly, R56 will not bind gp120 of the MN strain, which also has an Arg at position P306. In addition, R56 does not neutralize commonly used strain IIIB because it has a QR insertion in the V3 crown just before the GPG turn, and Gln has a large side chain, which does not fit the space that is occupied by Gly^{P312} in the JR-FL/conA complex structures.

Antigen-binding mode of R20

R20 has a long CDR H3 of 21 amino acids, unlike R56, which has a short CDR H3 of only 4 amino acids (Kabat definition). CDR H3 of R20 forms a beta hairpin standing tall at the center of its antigen-binding site (Fig. AI.2). This conformation is
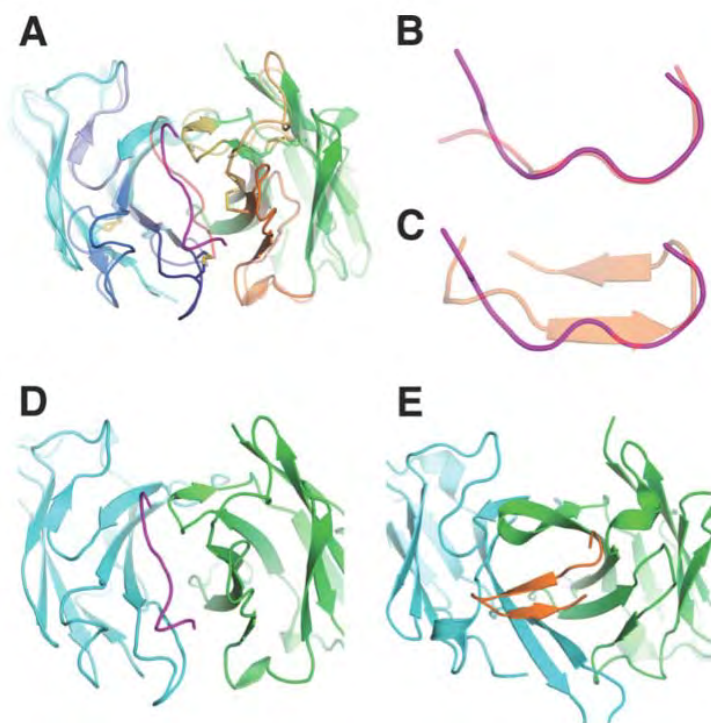
FIG AI.5. Structural comparison of R56 with mouse and human anti-V3 mAbs. (A) Superimposition of the Fv region of R56 on that of mouse anti-V3 mAb 50.1. The RMSD of the superimposed C-α is 0.73 Å. (B) Superimposition of the V3$_{JR\text{-}FL}$ epitope bound to R56 (magenta) with that bound to mouse mAb 50.1 (salmon). The RMSD of the superimposed C-α of the eight atoms (P305 to P314) is 0.57 Å. (C) Superimposition of V3$_{JR\text{-}FL}$ (magenta) bound to R56 with V3$_{NY5}$ (orange) bound to human mAb 2557. The RMSD of the superim- posed 10 C-α atoms (P303 to P314) is 1.7 Å. The antigen-binding modes of mAb R56 and human IGHV5-51 mAb 2557 are shown in panels D and E, respectively.

similar to that of several human and rhesus mAbs, such as quaternary neutralizing epitope mAbs 2909 and 2.5B (252). Residues at the top of the other CDR loops form a pedestal-like structure. This pedestal is roughly 30 Å long and 10 Å wide and is contributed about equally by the light chain at one end and the heavy chain at the other end. The antigen-binding site of R20 runs across the light chain and heavy chain; this is again different from that of R56, whose antigen-binding site groove is the chasm between the light and heavy chains.

Our Fab R20/V3$_{conB}$ complex structure showed that the epitope recognized by R20 consists of nine amino acids (P322 to P329, including a numbering insertion for Ile^{P322A} in the HXB2 scheme) of the C-terminal region of V3 (Fig. AI.2 and Fig. AI.4). This epitope is shaped like a fishhook lying on the top of the pedestal of the antigen-binding site. A short two-residue beta strand (Gly^{P324} and Asp^{P326}) in the N-terminal half of the epitope—the shank of the fishhook—forms a parallel beta sheet with the C-terminal strand of the CDR H3 hairpin. This beta-sheet-type interaction is similar to the ladle antigen-binding mode described for anti-V3 mAbs 447-52D and 537 (248). Following the beta strand, a short 3_{10} G helical turn (Ile^{P326}, Arg^{P327}, and Gln^{P328})—the bend of the fish hook—extends toward the light-chain side of the pedestal. Interestingly, it was previously predicted by sequence analysis that the C-terminal region of V3 has a tendency to form a short alpha helix (253), and it was reported that the V3 C-terminal strand could form a helical conformation in an NMR study of a cyclic V3 peptide (254). However, this region of the full-length V3 structures in the context of the gp120 core does not contain any helical conformation (24, 25). Taken together, these data suggest that this region of V3 is very flexible and it can have many different conformations.

The antigen-antibody interactions buried a total of 804 Å^2 of surface area with

344 Å^2 from the antibody and 460 Å^2 from the epitope. Tyr^{H100G} on the C-terminal strand

of the CDR H3 hairpin bisects the antigen-antibody interactions (Fig. AI.4). The antigen-

antibody interactions at the N terminus of the epitope have two components centered at

residues Glu^{P322} and Ile^{P322A}, respectively (Fig. AI.4). First, negatively charged residue

Glu^{P322} interacts with Arg^{H54}, forming a hydrogen bond with its amide group. Second, the

side chain of hydrophobic residue Ile^{P322A} is buried by the side chains of Tyr^{H52} and Ile^{H56}

on one side and by the backbones of Tyr^{H100G} and Ser^{H100H} on the other side. The antigen-

antibody interactions at the C terminus of the epitope have three components centered at

residues Asp^{P325}, Ile^{P326}, and Arg^{P327}, respectively (Fig. AI.4). First, Asp^{P325} near the

middle of the epitope is buried in the center of the antigen-binding site and its side chain

can form hydrogen bonds with the side chains of Ser^{L92} and Tyr^{H100K} and the backbone

amide of Ile^{L94}. Second, the side chain of hydrophobic Ile^{P326} is buried by the side chain

of Tyr^{L92} on the one side and by the side chains of Val^{H100} and Tyr^{H100G} on the other side.

Third, positively charged Arg^{P327} (shaped like the bait on the fishhook) forms a salt

bridge with Asp^{L1}, the first residue of the light chain. Three negatively charged residues

in the light chain, Asp^{L1}, Glu^{L27}, and Asp^{L95A}, encircle the side chain of Arg^{P327}, holding

it at the center of this highly negatively charged environment.

Comparison with the binding modes of mouse and human anti-V3 mAbs.

By comparing the antigen-binding mode of R56 with those of all of the

available complex structures of anti-V3 mAbs, we found that the antigen-binding mode

of mouse mAb 50.1 (IgG2a) is the most similar one (Fig. AI.5). Mouse mAb 50.1, although also produced by immunization, was induced by using the disulfide-linked 40-mer cyclic peptide RP70 (INCTRPNYNKRKRIHIGPGRAFYTTKNIIGTIRQAHCNIS), which contains the V3 sequence of strain MN of HIV-1 gp120 (243). The complex structure of mAb 50.1 was resolved to 2.8 Å resolution by co-crystallizing its Fab with another cyclic peptide, MP1 (CKRIHIGPGRAFYTTC) (246). The N-terminal nine amino acids of the peptide were observed in the structure, including the first Cys, a non-HIV-1 amino acid. Only the N-terminal half of the crown hairpin was observed in the 50.1 complex structure, as in the case of R56, although a cyclic peptide was used. Notably, the sequences of the epitopes of mAbs 50.1 and R56 are derived from the same region of the V3 crown, and the structures of the epitopes have the same 3D shape (Fig. AI.5B), with an RMSD of 0.57 Å for superimposition of the C-α atoms of P305 to P314. The Fv domains of mAbs 50.1 and R56 also superimpose well, with an RMSD of 0.73 Å for the C-α atoms. The details of the antigen-antibody interactions of the two mAbs have several similarities. First, both mAbs have an antigen-binding site shaped like a cradle running along the interface between the light and heavy chains (Fig. AI.5A). Second, both antigen-binding sites have a hydrophobic base, burying highly conserved Ile^{P307} and Ile^{P309}. Third, mAb 50.1 also harbors Tyr^{L49} in its CDR L2 and stacks Pro^{P313} in the same manner as that of mAb R56.

Some human anti-V3 mAbs also have a binding mode similar to that of R56. The best example is the family of anti-V3 mAbs encoded by IGHV5-51 germ line genes, including mAbs 1006, 2219, 2557, 2558, and 4025 (249, 255). The binding mode of this human mAb family has a couple of similarities to that of R56 and 50.1. First, all of these

mAbs have a cradle-shaped antigen-binding site with a hydrophobic base that binds conserved N-terminal circlet residues Ile^{P307} and Ile^{P309} of the V3 crown. Structure superimposition showed that the epitope of R56 and the N termini of the epitopes of IGHV5-51 anti-V3 mAbs are very similar; e.g., the structure superimposition of V3$_{JR\text{-}FL}$ bound to R56 with the N terminus of V3$_{NY5}$ bound to human mAb 2557 has an RMSD of 1.7 Å (Fig. AI.5C). Second, Pro^{P313} in the GPG turn of the V3 epitopes bound by the IGHV5-51 anti-V3 mAbs is stacked by a van der Waals interaction against the side chain of a tyrosine (Tyr^{L32}) from the CDR L1 region (172), although in the case of R56, Pro^{P313} is packed against a tyrosine from the CDR L2 region, Tyr^{L49}. How- ever, the binding mode of the human IGHV5-51 anti-V3 mAbs also has a couple of differences from that of mAbs R56 and 50.1. First, the whole beta hairpin of the V3 crown is visible in all of the Fab/epitope complex structures of human IGHV5-51 mAbs, while only the N-terminal half of the V3 crown hairpin could be observed in the complex structures of R56 and 50.1. The C-terminal half of the V3 crown hairpin was also observed in the complex structure of mouse mAb 0.5β determined by an NMR study (256). Interestingly mAb 0.5β was raised by immunization of IIIB gp120, which is different from mouse mAb 50.1, which was raised by a cyclic peptide. Thus, gp120 itself may be able to elicit in mice antibody responses with a more complex epitope. Second, the orientation of the antigen-binding cradle of the IGHV5-51 mAbs is perpendicular to that of R56 and 50.1. In the human case, the epitope bridges the two chains, with the arch of the V3 crown binding the light chain and the band binding the heavy chain (Fig. AI.5D and E).

The recently identified highly potent human mAb PGT128 has an epitope

region that overlaps that of R20. PGT128 binds the mannose glycans harbored by two glycosylation sites (Asn^{P301} and Asn^{P332}) at the base of V3 (127). It also engages amino acids in the C-terminal region of V3 through its CDR H3 by a beta-sheet-type interaction. The key interacting V3 amino acids are residues P323 to P327 (IGDIR), which are at the core of the R20 epitope. Nevertheless, the conformation of the PGT128 epitope is rather different from that of the R20 epitope, reflecting the flexibility of the V3 stem. Interestingly, PGT128 also has a noncanonical disulfide bond between CDRs H1 and H2 that plays a critical role in antigen binding; removing it will make PGT128 lose its gp120-binding activity (127).

Discussion

We present Fab/epitope complex structures of two rabbit mAbs, R56 and R20, raised by immunization with gp120 of HIV-1 clade B strain JR-FL with a DNA prime-protein boost regimen. These structures show that they recognize two V3 regions known to be immunogenic in humans—the crown located at the apex and the C-terminal region, including residues from both the V3 stem and base regions (257, 258). R56 has a cradle antigen-binding mode similar to that of a panel of human anti-V3 antibodies encoded by IGHV5-51 germ line genes. Antibodies with this binding mode focus their antigen binding on the highly conserved residues at the N terminus of the V3 crown, consistent with their broad antigen-binding activities. Our analyses further support the notion that the V3 crown has a shape that naturally fits the cradle-binding mode of antibodies. Antibodies with this binding mode are preferentially encoded in humans by the IGHV5-51 germ line genes, making it possible to design a vaccine that elicits antibodies encoded by a specific germ line to target the highly immunogenic V3 crown.

R20 recognizes an epitope consisting of amino acids P322 to P329, just preceding the disulfide bond at the V3 base (Cys^{P296} - Cys^{P331}). This region is spatially close to the two highly conserved glycosylation sites (Asn^{P301} and Asn^{P332}) near the V3 base. The glycans harbored by these two sites have been shown to be part of the epitope of hyperpotent human mAb PGT128 and related mAbs (118). Unlike PGT128, which has broadly potent neutralization activity, R20 does not neutralize the strains tested. There are several potential reasons for this difference. First, the epitope of R20 has a shape very different from that of the V3 region bound by PGT128. Superimposition of the two epitopes showed that only the last five residues of the R20 epitope adopt a conformation similar to that of the PGT128 epitope. Second, the epitope of PGT128 consists mainly of glycans harbored by N301 and N332 while our mutagenesis study suggested that R20 does not need glycan for binding (data not shown). Third, R20 approaches the V3 base from an angle tilted about 20° from that of PGT128; this lower approach angle likely hinders its ability to bind gp120 in the trimeric conformation. Nevertheless, the overlapping of the epitopes of mAbs R20, IIIB-V3-01, and PGT128 suggests that this V3 C-terminal region is immunogenic and a target of first immune responses (257). Structurally designed immunogens that target this V3 C-terminal region may induce precursor antibodies with a potential to mature into antibodies that can recognize the glycans at the V3 base in a way that mimics that of PGT128.

There are clearly differences between the epitopes recognized by the rabbit mAbs raised by immunization and those recognized by human mAbs derived from chronically infected patients. This can best be understood in the case of R56, as we have for comparison many structures of human anti-V3 mAbs with the same antigen-binding

mode. Previous structural data showed that the C- terminal residues of the V3 crown are visible in the complex structures of the human anti-V3 mAbs because these residues engage the antibody by specific interactions sufficient to stabilize the C terminus of the V3 crown (172, 249, 259). For rabbit antibody R56, on the contrary, only the N-terminal half of the V3 crown can be observed in the complex structures. Since the V3 crown tends to have a beta hairpin structure, its C-terminal half must be spatially close to the N-terminal half. However, R56 did not develop contacts with the C terminus of the V3 crown or the contacts were not sufficiently strong to stabilize the C-terminal half to be observable in the crystal structure. This is also the case for mouse mAb 50.1, which was raised by immunization as well. Thus, we hypothesize that, because of the limited time intervals and insufficient antigen stimulation in immunization, the immunization-derived antibodies do not have the necessary affinity maturation to develop strong contacts with the C terminus of the V3 crown.

Our structural analyses of R56 and R20 show from several aspects the suitability of using the rabbit as an animal model for AIDS vaccine development. First, the rabbit immune system is able to respond to gp120 immunogens and recognizes immunogenic regions similar to those recognized by the human immune system, such as the crown and C-terminal regions of V3. Second, antibodies elicited by gp120 immunogens in rabbits can mimic the binding modes of human antibodies. This is most clear in the case of antibodies that target the V3 crown. Third, rabbits can produce antibodies with CDR H3s with a wide length range, including antibodies with very long CDR H3s, a hallmark increasingly found in potent human mAbs. Fourth, the long CDR H3s of rabbit antibodies can engage antigen through a beta-sheet-type interaction, a feature often observed in

human mAbs with long CDR H3s. Taken together, our data show that the rabbit is a useful animal model in which to test immunogens and immunization regimens in AIDS vaccine development.

Chapter VIII

Bibliography

1. **WHO.** 2013. http://www.who.int/hiv/en/.
2. **Gray RH, Li X, Kigozi G, Serwadda D, Nalugoda F, Watya S, Reynolds SJ, Wawer M.** 2007. The impact of male circumcision on HIV incidence and cost per infection prevented: a stochastic simulation model from Rakai, Uganda. Aids **21:**845-850.
3. **Pinkerton SD, Abramson PR.** 1997. Effectiveness of condoms in preventing HIV transmission. Social science & medicine **44:**1303-1312.
4. **Wodak A, Cooney A.** 2006. Do needle syringe programs reduce HIV infection among injecting drug users: a comprehensive review of the international evidence. Substance use & misuse **41:**777-813.
5. **Abdool Karim Q, Abdool Karim SS, Frohlich JA, Grobler AC, Baxter C, Mansoor LE, Kharsany AB, Sibeko S, Mlisana KP, Omar Z, Gengiah TN, Maarschalk S, Arulappan N, Mlotshwa M, Morris L, Taylor D, Group CT.** 2010. Effectiveness and safety of tenofovir gel, an antiretroviral microbicide, for the prevention of HIV infection in women. Science **329:**1168-1174.
6. **Grant RM, Lama JR, Anderson PL, McMahan V, Liu AY, Vargas L, Goicochea P, Casapia M, Guanira-Carranza JV, Ramirez-Cardich ME, Montoya-Herrera O, Fernandez T, Veloso VG, Buchbinder SP, Chariyalertsak S, Schechter M, Bekker LG, Mayer KH, Kallas EG, Amico KR, Mulligan K, Bushman LR, Hance RJ, Ganoza C, Defechereux P, Postle B, Wang F, McConnell JJ, Zheng JH, Lee J, Rooney JF, Jaffe HS, Martinez AI, Burns DN, Glidden DV, iPrEx Study T.** 2010. Preexposure chemoprophylaxis for HIV prevention in men who have sex with men. The New England journal of medicine **363:**2587-2599.
7. **Baeten JM, Donnell D, Ndase P, Mugo NR, Campbell JD, Wangisi J, Tappero JW, Bukusi EA, Cohen CR, Katabira E, Ronald A, Tumwesigye E, Were E, Fife KH, Kiarie J, Farquhar C, John-Stewart G, Kakia A, Odoyo J, Mucunguzi A, Nakku-Joloba E, Twesigye R, Ngure K, Apaka C, Tamooh H, Gabona F, Mujugira A, Panteleeff D, Thomas KK, Kidoguchi L, Krows M, Revall J, Morrison S, Haugen H, Emmanuel-Ogier M, Ondrejcek L, Coombs RW, Frenkel L, Hendrix C, Bumpus NN, Bangsberg D, Haberer JE, Stevens WS, Lingappa JR, Celum C, Partners Pr EPST.** 2012. Antiretroviral prophylaxis for HIV prevention in heterosexual men and women. The New England journal of medicine **367:**399-410.
8. **Thigpen MC, Kebaabetswe PM, Paxton LA, Smith DK, Rose CE, Segolodi TM, Henderson FL, Pathak SR, Soud FA, Chillag KL, Mutanhaurwa R, Chirwa LI, Kasonde M, Abebe D, Buliva E, Gvetadze RJ, Johnson S, Sukalac T, Thomas VT, Hart C, Johnson JA, Malotte CK, Hendrix CW, Brooks JT, Group TDFS.** 2012. Antiretroviral preexposure prophylaxis for heterosexual HIV transmission in Botswana. The New England journal of medicine **367:**423-434.

9.   **Van Damme L, Corneli A, Ahmed K, Agot K, Lombaard J, Kapiga S, Malahleha M, Owino F, Manongi R, Onyango J, Temu L, Monedi MC, Mak'Oketch P, Makanda M, Reblin I, Makatu SE, Saylor L, Kiernan H, Kirkendale S, Wong C, Grant R, Kashuba A, Nanda K, Mandala J, Fransen K, Deese J, Crucitti T, Mastro TD, Taylor D, Group FE-PS.** 2012. Preexposure prophylaxis for HIV infection among African women. The New England journal of medicine **367:**411-422.

10.   **Cremin I, Alsallaq R, Dybul M, Piot P, Garnett G, Hallett TB.** 2013. The new role of antiretrovirals in combination HIV prevention: a mathematical modelling analysis. Aids **27:**447-458.

11.   **Chan DC, Fass D, Berger JM, Kim PS.** 1997. Core structure of gp41 from the HIV envelope glycoprotein. Cell **89:**263-273.

12.   **Weissenhorn W, Dessen A, Harrison SC, Skehel JJ, Wiley DC.** 1997. Atomic structure of the ectodomain from HIV-1 gp41. Nature **387:**426-430.

13.   **Kwong PD, Wyatt R, Robinson J, Sweet RW, Sodroski J, Hendrickson WA.** 1998. Structure of an HIV gp120 envelope glycoprotein in complex with the CD4 receptor and a neutralizing human antibody. Nature **393:**648-659.

14.   **Wyatt R, Kwong PD, Desjardins E, Sweet RW, Robinson J, Hendrickson WA, Sodroski JG.** 1998. The antigenic structure of the HIV gp120 envelope glycoprotein. Nature **393:**705-711.

15.   **Kong L, Huang CC, Coales SJ, Molnar KS, Skinner J, Hamuro Y, Kwong PD.** 2010. Local conformational stability of HIV-1 gp120 in unliganded and CD4-bound states as defined by amide hydrogen/deuterium exchange. Journal of virology **84:**10311-10321.

16.   **Chen L, Kwon YD, Zhou T, Wu X, O'Dell S, Cavacini L, Hessell AJ, Pancera M, Tang M, Xu L, Yang ZY, Zhang MY, Arthos J, Burton DR, Dimitrov DS, Nabel GJ, Posner MR, Sodroski J, Wyatt R, Mascola JR, Kwong PD.** 2009. Structural basis of immune evasion at the site of CD4 attachment on HIV-1 gp120. Science **326:**1123-1127.

17.   **Liu J, Bartesaghi A, Borgnia MJ, Sapiro G, Subramaniam S.** 2008. Molecular architecture of native HIV-1 gp120 trimers. Nature **455:**109-113.

18.   **White TA, Bartesaghi A, Borgnia MJ, Meyerson JR, de la Cruz MJ, Bess JW, Nandwani R, Hoxie JA, Lifson JD, Milne JL, Subramaniam S.** 2010. Molecular architectures of trimeric SIV and HIV-1 envelope glycoproteins on intact viruses: strain-dependent variation in quaternary structure. PLoS pathogens **6:**e1001249.

19.   **Lyumkis D, Julien JP, de Val N, Cupo A, Potter CS, Klasse PJ, Burton DR, Sanders RW, Moore JP, Carragher B, Wilson IA, Ward AB.** 2013. Cryo-EM structure of a fully glycosylated soluble cleaved HIV-1 envelope trimer. Science **342:**1484-1490.

20.   **Julien JP, Cupo A, Sok D, Stanfield RL, Lyumkis D, Deller MC, Klasse PJ, Burton DR, Sanders RW, Moore JP, Ward AB, Wilson IA.** 2013. Crystal structure of a soluble cleaved HIV-1 envelope trimer. Science **342:**1477-1483.

21.   **Arthos J, Cicala C, Martinelli E, Macleod K, Van Ryk D, Wei D, Xiao Z, Veenstra TD, Conrad TP, Lempicki RA, McLaughlin S, Pascuccio M, Gopaul R, McNally J, Cruz CC, Censoplano N, Chung E, Reitano KN,**

Kottilil S, Goode DJ, Fauci AS. 2008. HIV-1 envelope protein binds to and signals through integrin alpha4beta7, the gut mucosal homing receptor for peripheral T cells. Nature immunology **9:**301-309.

22. **Cicala C, Martinelli E, McNally JP, Goode DJ, Gopaul R, Hiatt J, Jelicic K, Kottilil S, Macleod K, O'Shea A, Patel N, Van Ryk D, Wei D, Pascuccio M, Yi L, McKinnon L, Izulla P, Kimani J, Kaul R, Fauci AS, Arthos J.** 2009. The integrin alpha4beta7 forms a complex with cell-surface CD4 and defines a T-cell subset that is highly susceptible to infection by HIV-1. Proceedings of the National Academy of Sciences of the United States of America **106:**20877-20882.

23. **Gottardo R, Bailer RT, Korber BT, Gnanakaran S, Phillips J, Shen X, Tomaras GD, Turk E, Imholte G, Eckler L, Wenschuh H, Zerweck J, Greene K, Gao H, Berman PW, Francis D, Sinangil F, Lee C, Nitayaphan S, Rerks-Ngarm S, Kaewkungwal J, Pitisuttithum P, Tartaglia J, Robb ML, Michael NL, Kim JH, Zolla-Pazner S, Haynes BF, Mascola JR, Self S, Gilbert P, Montefiori DC.** 2013. Plasma IgG to linear epitopes in the V2 and V3 regions of HIV-1 gp120 correlate with a reduced risk of infection in the RV144 vaccine efficacy trial. PloS one **8:**e75665.

24. **Huang CC, Lam SN, Acharya P, Tang M, Xiang SH, Hussan SS, Stanfield RL, Robinson J, Sodroski J, Wilson IA, Wyatt R, Bewley CA, Kwong PD.** 2007. Structures of the CCR5 N terminus and of a tyrosine-sulfated antibody with HIV-1 gp120 and CD4. Science **317:**1930-1934.

25. **Huang CC, Tang M, Zhang MY, Majeed S, Montabana E, Stanfield RL, Dimitrov DS, Korber B, Sodroski J, Wilson IA, Wyatt R, Kwong PD.** 2005. Structure of a V3-containing HIV-1 gp120 core. Science **310:**1025-1028.

26. **Zolla-Pazner S, Cardozo T.** 2010. Structure-function relationships of HIV-1 envelope sequence-variable regions refocus vaccine design. Nature reviews. Immunology **10:**527-535.

27. **Merk A, Subramaniam S.** 2013. HIV-1 envelope glycoprotein structure. Current opinion in structural biology **23:**268-276.

28. **Sanders RW, Derking R, Cupo A, Julien JP, Yasmeen A, de Val N, Kim HJ, Blattner C, de la Pena AT, Korzun J, Golabek M, de Los Reyes K, Ketas TJ, van Gils MJ, King CR, Wilson IA, Ward AB, Klasse PJ, Moore JP.** 2013. A next-generation cleaved, soluble HIV-1 Env Trimer, BG505 SOSIP.664 gp140, expresses multiple epitopes for broadly neutralizing but not non-neutralizing antibodies. PLoS Pathog **9:**e1003618.

29. **W.Sanders R, Derkling R, Cupo A, Ketas TJ, Gils MJv, Burger JA, Schief WR, King CR, Wilson IA, Ward AB, Labranche CC, Montefior DC, Klasse PJ, Burton DR, Dean H, Moore JP.** 2013. HIV-1 neutralizing antibodies induced by native-like BG505 SOSIP.664 trimer in animals. HIV vaccines Keystone 2014 **X3 3016**.

30. **Go EP, Chang Q, Liao HX, Sutherland LL, Alam SM, Haynes BF, Desaire H.** 2009. Glycosylation site-specific analysis of clade C HIV-1 envelope proteins. Journal of proteome research **8:**4231-4242.

31. **Go EP, Irungu J, Zhang Y, Dalpathado DS, Liao HX, Sutherland LL, Alam SM, Haynes BF, Desaire H.** 2008. Glycosylation site-specific analysis of HIV envelope proteins (JR-FL and CON-S) reveals major differences in glycosylation

site occupancy, glycoform profiles, and antigenic epitopes' accessibility. Journal of proteome research **7:**1660-1674.

32. **Jenkins N, Parekh RB, James DC.** 1996. Getting the glycosylation right: implications for the biotechnology industry. Nature biotechnology **14:**975-981.

33. **Doores KJ, Bonomelli C, Harvey DJ, Vasiljevic S, Dwek RA, Burton DR, Crispin M, Scanlan CN.** 2010. Envelope glycans of immunodeficiency virions are almost entirely oligomannose antigens. Proceedings of the National Academy of Sciences of the United States of America **107:**13800-13805.

34. **Eggink D, Melchers M, Wuhrer M, van Montfort T, Dey AK, Naaijkens BA, David KB, Le Douce V, Deelder AM, Kang K, Olson WC, Berkhout B, Hokke CH, Moore JP, Sanders RW.** 2010. Lack of complex N-glycans on HIV-1 envelope glycoproteins preserves protein conformation and entry function. Virology **401:**236-247.

35. **Depetris RS, Julien JP, Khayat R, Lee JH, Pejchal R, Katpally U, Cocco N, Kachare M, Massi E, David KB, Cupo A, Marozsan AJ, Olson WC, Ward AB, Wilson IA, Sanders RW, Moore JP.** 2012. Partial enzymatic deglycosylation preserves the structure of cleaved recombinant HIV-1 envelope glycoprotein trimers. The Journal of biological chemistry **287:**24239-24254.

36. **Binley JM, Ban YE, Crooks ET, Eggink D, Osawa K, Schief WR, Sanders RW.** 2010. Role of complex carbohydrates in human immunodeficiency virus type 1 infection and resistance to antibody neutralization. J Virol **84:**5637-5655.

37. **Moore PL, Gray ES, Wibmer CK, Bhiman JN, Nonyane M, Sheward DJ, Hermanus T, Bajimaya S, Tumba NL, Abrahams MR, Lambson BE, Ranchobe N, Ping L, Ngandu N, Abdool Karim Q, Abdool Karim SS, Swanstrom RI, Seaman MS, Williamson C, Morris L.** 2012. Evolution of an HIV glycan-dependent broadly neutralizing antibody epitope through immune escape. Nature medicine **18:**1688-1692.

38. **Walker LM, Sok D, Nishimura Y, Donau O, Sadjadpour R, Gautam R, Shingai M, Pejchal R, Ramos A, Simek MD, Geng Y, Wilson IA, Poignard P, Martin MA, Burton DR.** 2011. Rapid development of glycan-specific, broad, and potent anti-HIV-1 gp120 neutralizing antibodies in an R5 SIV/HIV chimeric virus infected macaque. Proceedings of the National Academy of Sciences of the United States of America **108:**20125-20129.

39. **Flynn NM, Forthal DN, Harro CD, Judson FN, Mayer KH, Para MF, rgp HIVVSG.** 2005. Placebo-controlled phase 3 trial of a recombinant glycoprotein 120 vaccine to prevent HIV-1 infection. The Journal of infectious diseases **191:**654-665.

40. **Gilbert PB, Ackers ML, Berman PW, Francis DP, Popovic V, Hu DJ, Heyward WL, Sinangil F, Shepherd BE, Gurwith M.** 2005. HIV-1 virologic and immunologic progression and initiation of antiretroviral therapy among HIV-1-infected subjects in a trial of the efficacy of recombinant glycoprotein 120 vaccine. The Journal of infectious diseases **192:**974-983.

41. **Gilbert PB, Peterson ML, Follmann D, Hudgens MG, Francis DP, Gurwith M, Heyward WL, Jobes DV, Popovic V, Self SG, Sinangil F, Burke D, Berman PW.** 2005. Correlation between immunologic responses to a recombinant glycoprotein 120 vaccine and incidence of HIV-1 infection in a

phase 3 HIV-1 preventive vaccine trial. The Journal of infectious diseases **191:**666-677.

42. **Johnson RP, Desrosiers RC.** 1998. Protective immunity induced by live attenuated simian immunodeficiency virus. Current opinion in immunology **10:**436-443.

43. **Tenner-Racz K, Stahl Hennig C, Uberla K, Stoiber H, Ignatius R, Heeney J, Steinman RM, Racz P.** 2004. Early protection against pathogenic virus infection at a mucosal challenge site after vaccination with attenuated simian immunodeficiency virus. Proceedings of the National Academy of Sciences of the United States of America **101:**3017-3022.

44. **Wyand MS, Manson KH, Garcia-Moll M, Montefiori D, Desrosiers RC.** 1996. Vaccine protection by a triple deletion mutant of simian immunodeficiency virus. Journal of virology **70:**3724-3733.

45. **Johnson RP, Lifson JD, Czajak SC, Cole KS, Manson KH, Glickman R, Yang J, Montefiori DC, Montelaro R, Wyand MS, Desrosiers RC.** 1999. Highly attenuated vaccine strains of simian immunodeficiency virus protect against vaginal challenge: inverse relationship of degree of protection with level of attenuation. Journal of virology **73:**4952-4961.

46. **Buchbinder SP, Mehrotra DV, Duerr A, Fitzgerald DW, Mogg R, Li D, Gilbert PB, Lama JR, Marmor M, Del Rio C, McElrath MJ, Casimiro DR, Gottesdiener KM, Chodakewitz JA, Corey L, Robertson MN, Step Study Protocol T.** 2008. Efficacy assessment of a cell-mediated immunity HIV-1 vaccine (the Step Study): a double-blind, randomised, placebo-controlled, test-of-concept trial. Lancet **372:**1881-1893.

47. **McElrath MJ, De Rosa SC, Moodie Z, Dubey S, Kierstead L, Janes H, Defawe OD, Carter DK, Hural J, Akondy R, Buchbinder SP, Robertson MN, Mehrotra DV, Self SG, Corey L, Shiver JW, Casimiro DR, Step Study Protocol T.** 2008. HIV-1 vaccine-induced immunity in the test-of-concept Step Study: a case-cohort analysis. Lancet **372:**1894-1905.

48. **Ledford H.** 2007. HIV vaccine may raise risk. Nature **450:**325.

49. **Zak DE, Andersen-Nissen E, Peterson ER, Sato A, Hamilton MK, Borgerding J, Krishnamurty AT, Chang JT, Adams DJ, Hensley TR, Salter AI, Morgan CA, Duerr AC, De Rosa SC, Aderem A, McElrath MJ.** 2012. Merck Ad5/HIV induces broad innate immune activation that predicts CD8(+) T-cell responses but is attenuated by preexisting Ad5 immunity. Proceedings of the National Academy of Sciences of the United States of America **109:**E3503-3512.

50. **O'Brien KL, Liu J, King SL, Sun YH, Schmitz JE, Lifton MA, Hutnick NA, Betts MR, Dubey SA, Goudsmit J, Shiver JW, Robertson MN, Casimiro DR, Barouch DH.** 2009. Adenovirus-specific immunity after immunization with an Ad5 HIV-1 vaccine candidate in humans. Nature medicine **15:**873-875.

51. **Barouch DH, Pau MG, Custers JH, Koudstaal W, Kostense S, Havenga MJ, Truitt DM, Sumida SM, Kishko MG, Arthur JC, Korioth-Schmitz B, Newberg MH, Gorgone DA, Lifton MA, Panicali DL, Nabel GJ, Letvin NL, Goudsmit J.** 2004. Immunogenicity of recombinant adenovirus serotype 35 vaccine in the presence of pre-existing anti-Ad5 immunity. Journal of immunology **172:**6290-6297.

52.	**Fitzgerald JC, Gao GP, Reyes-Sandoval A, Pavlakis GN, Xiang ZQ, Wlazlo AP, Giles-Davis W, Wilson JM, Ertl HC.** 2003. A simian replication-defective adenoviral recombinant vaccine to HIV-1 gag. Journal of immunology **170:**1416-1422.

53.	**Abbink P, Lemckert AA, Ewald BA, Lynch DM, Denholtz M, Smits S, Holterman L, Damen I, Vogels R, Thorner AR, O'Brien KL, Carville A, Mansfield KG, Goudsmit J, Havenga MJ, Barouch DH.** 2007. Comparative seroprevalence and immunogenicity of six rare serotype recombinant adenovirus vaccine vectors from subgroups B and D. Journal of virology **81:**4654-4663.

54.	**Baden LR, Liu J, Li H, Johnson JA, Walsh SR, Kleinjan JA, Engelson BA, Peter L, Abbink P, Milner DA, Jr., Golden KL, Viani KL, Stachler MD, Chen BJ, Pau MG, Weijtens M, Carey BR, Miller CA, Swann EM, Wolff M, Loblein H, Seaman MS, Dolin R, Barouch DH.** 2014. Induction of HIV-1-Specific Mucosal Immune Responses Following Intramuscular Recombinant Adenovirus Serotype 26 HIV-1 Vaccination of Humans. The Journal of infectious diseases.

55.	**Liu Y, Duan DL, Peng H, Tang HL, Liu S, Zhang N, Wang N, Liu JY, Shao YM.** 2004. [Immunogenicity analysis of HIV vaccine based on replicating vaccinia virus Tiantan vector]. Zhonghua shi yan he lin chuang bing du xue za zhi = Zhonghua shiyan he linchuang bingduxue zazhi = Chinese journal of experimental and clinical virology **18:**281-283.

56.	**Vazquez Blomquist D, Green P, Laidlaw SM, Skinner MA, Borrow P, Duarte CA.** 2002. Induction of a strong HIV-specific CD8+ T cell response in mice using a fowlpox virus vector expressing an HIV-1 multi-CTL-epitope polypeptide. Viral immunology **15:**337-356.

57.	**Zanotto C, Pozzi E, Pacchioni S, Volonte L, De Giuli Morghen C, Radaelli A.** 2010. Canarypox and fowlpox viruses as recombinant vaccine vectors: a biological and immunological comparison. Antiviral research **88:**53-63.

58.	**Belshe RB, Stevens C, Gorse GJ, Buchbinder S, Weinhold K, Sheppard H, Stablein D, Self S, McNamara J, Frey S, Flores J, Excler JL, Klein M, Habib RE, Duliege AM, Harro C, Corey L, Keefer M, Mulligan M, Wright P, Celum C, Judson F, Mayer K, McKirnan D, Marmor M, Woody G, National Institute of A, Infectious Diseases AVEG, Trials HIVNfP.** 2001. Safety and immunogenicity of a canarypox-vectored human immunodeficiency virus Type 1 vaccine with or without gp120: a phase 2 study in higher- and lower-risk volunteers. The Journal of infectious diseases **183:**1343-1352.

59.	**Vasan S, Schlesinger SJ, Chen Z, Hurley A, Lombardo A, Than S, Adesanya P, Bunce C, Boaz M, Boyle R, Sayeed E, Clark L, Dugin D, Boente-Carrera M, Schmidt C, Fang Q, LeiBa, Huang Y, Zaharatos GJ, Gardiner DF, Caskey M, Seamons L, Ho M, Dally L, Smith C, Cox J, Gill D, Gilmour J, Keefer MC, Fast P, Ho DD.** 2010. Phase 1 safety and immunogenicity evaluation of ADMVA, a multigenic, modified vaccinia Ankara-HIV-1 B'/C candidate vaccine. PloS one **5:**e8816.

60.	**Harari A, Bart PA, Stohr W, Tapia G, Garcia M, Medjitna-Rais E, Burnet S, Cellerai C, Erlwein O, Barber T, Moog C, Liljestrom P, Wagner R, Wolf H, Kraehenbuhl JP, Esteban M, Heeney J, Frachette MJ, Tartaglia J,**

McCormack S, Babiker A, Weber J, Pantaleo G. 2008. An HIV-1 clade C DNA prime, NYVAC boost vaccine regimen induces reliable, polyfunctional, and long-lasting T cell responses. The Journal of experimental medicine **205:**63-77.

61. **Hansen SG, Ford JC, Lewis MS, Ventura AB, Hughes CM, Coyne-Johnson L, Whizin N, Oswald K, Shoemaker R, Swanson T, Legasse AW, Chiuchiolo MJ, Parks CL, Axthelm MK, Nelson JA, Jarvis MA, Piatak M, Jr., Lifson JD, Picker LJ.** 2011. Profound early control of highly pathogenic SIV by an effector memory T-cell vaccine. Nature **473:**523-527.

62. **Hansen SG, Piatak M, Jr., Ventura AB, Hughes CM, Gilbride RM, Ford JC, Oswald K, Shoemaker R, Li Y, Lewis MS, Gilliam AN, Xu G, Whizin N, Burwitz BJ, Planer SL, Turner JM, Legasse AW, Axthelm MK, Nelson JA, Fruh K, Sacha JB, Estes JD, Keele BF, Edlefsen PT, Lifson JD, Picker LJ.** 2013. Immune clearance of highly pathogenic SIV infection. Nature **502:**100-104.

63. **Egan MA, Chong SY, Rose NF, Megati S, Lopez KJ, Schadeck EB, Johnson JE, Masood A, Piacente P, Druilhet RE, Barras PW, Hasselschwert DL, Reilly P, Mishkin EM, Montefiori DC, Lewis MG, Clarke DK, Hendry RM, Marx PA, Eldridge JH, Udem SA, Israel ZR, Rose JK.** 2004. Immunogenicity of attenuated vesicular stomatitis virus vectors expressing HIV type 1 Env and SIV Gag proteins: comparison of intranasal and intramuscular vaccination routes. AIDS research and human retroviruses **20:**989-1004.

64. **Forsell MN, McInerney GM, Dosenovic P, Hidmark AS, Eriksson C, Liljestrom P, Grundner C, Karlsson Hedestam GB.** 2007. Increased human immunodeficiency virus type 1 Env expression and antibody induction using an enhanced alphavirus vector. The Journal of general virology **88:**2774-2779.

65. **Strang BL, Takeuchi Y, Relander T, Richter J, Bailey R, Sanders DA, Collins MK, Ikeda Y.** 2005. Human immunodeficiency virus type 1 vectors with alphavirus envelope glycoproteins produced from stable packaging cells. Journal of virology **79:**1765-1771.

66. **MacGregor RR, Boyer JD, Ugen KE, Lacy KE, Gluckman SJ, Bagarazzi ML, Chattergoon MA, Baine Y, Higgins TJ, Ciccarelli RB, Coney LR, Ginsberg RS, Weiner DB.** 1998. First human trial of a DNA-based vaccine for treatment of human immunodeficiency virus type 1 infection: safety and host response. The Journal of infectious diseases **178:**92-100.

67. **MacGregor RR, Ginsberg R, Ugen KE, Baine Y, Kang CU, Tu XM, Higgins T, Weiner DB, Boyer JD.** 2002. T-cell responses induced in normal volunteers immunized with a DNA-based vaccine containing HIV-1 env and rev. Aids **16:**2137-2143.

68. **Gao F, Li Y, Decker JM, Peyerl FW, Bibollet-Ruche F, Rodenburg CM, Chen Y, Shaw DR, Allen S, Musonda R, Shaw GM, Zajac AJ, Letvin N, Hahn BH.** 2003. Codon usage optimization of HIV type 1 subtype C gag, pol, env, and nef genes: in vitro expression and immune responses in DNA-vaccinated mice. AIDS research and human retroviruses **19:**817-823.

69. **Ramakrishna L, Anand KK, Mohankumar KM, Ranga U.** 2004. Codon optimization of the tat antigen of human immunodeficiency virus type 1 generates strong immune responses in mice following genetic immunization. Journal of virology **78:**9174-9189.

70.   **Andre S, Seed B, Eberle J, Schraut W, Bultmann A, Haas J.** 1998. Increased immune response elicited by DNA vaccination with a synthetic gp120 sequence with optimized codon usage. Journal of virology **72:**1497-1503.

71.   **Deml L, Bojak A, Steck S, Graf M, Wild J, Schirmbeck R, Wolf H, Wagner R.** 2001. Multiple effects of codon usage optimization on expression and immunogenicity of DNA candidate vaccines encoding the human immunodeficiency virus type 1 Gag protein. Journal of virology **75:**10991-11001.

72.   **Chapman BS, Thayer RM, Vincent KA, Haigwood NL.** 1991. Effect of intron A from human cytomegalovirus (Towne) immediate-early gene on heterologous expression in mammalian cells. Nucleic acids research **19:**3979-3986.

73.   **Cheng L, Ziegelhoffer PR, Yang NS.** 1993. In vivo promoter activity and transgene expression in mammalian somatic tissues evaluated by using particle bombardment. Proceedings of the National Academy of Sciences of the United States of America **90:**4455-4459.

74.   **Ulmer JB, Donnelly JJ, Parker SE, Rhodes GH, Felgner PL, Dwarki VJ, Gromkowski SH, Deck RR, DeWitt CM, Friedman A, et al.** 1993. Heterologous protection against influenza by injection of DNA encoding a viral protein. Science **259:**1745-1749.

75.   **Hu SL, Abrams K, Barber GN, Moran P, Zarling JM, Langlois AJ, Kuller L, Morton WR, Benveniste RE.** 1992. Protection of macaques against SIV infection by subunit vaccines of SIV envelope glycoprotein gp160. Science **255:**456-459.

76.   **Hu SL, Stallard V, Abrams K, Barber GN, Kuller L, Langlois AJ, Morton WR, Benveniste RE.** 1993. Protection of vaccinia-primed macaques against SIVmne infection by combination immunization with recombinant vaccinia virus and SIVmne gp160. Journal of medical primatology **22:**92-99.

77.   **Hammer SM, Sobieszczyk ME, Janes H, Karuna ST, Mulligan MJ, Grove D, Koblin BA, Buchbinder SP, Keefer MC, Tomaras GD, Frahm N, Hural J, Anude C, Graham BS, Enama ME, Adams E, DeJesus E, Novak RM, Frank I, Bentley C, Ramirez S, Fu R, Koup RA, Mascola JR, Nabel GJ, Montefiori DC, Kublin J, McElrath MJ, Corey L, Gilbert PB, Team HS.** 2013. Efficacy trial of a DNA/rAd5 HIV-1 preventive vaccine. The New England journal of medicine **369:**2083-2092.

78.   **Dorrell L, Williams P, Suttill A, Brown D, Roberts J, Conlon C, Hanke T, McMichael A.** 2007. Safety and tolerability of recombinant modified vaccinia virus Ankara expressing an HIV-1 gag/multiepitope immunogen (MVA.HIVA) in HIV-1-infected persons receiving combination antiretroviral therapy. Vaccine **25:**3277-3283.

79.   **Wee EG, Patel S, McMichael AJ, Hanke T.** 2002. A DNA/MVA-based candidate human immunodeficiency virus vaccine for Kenya induces multi-specific T cell responses in rhesus macaques. The Journal of general virology **83:**75-80.

80.   **Goonetilleke N, Moore S, Dally L, Winstone N, Cebere I, Mahmoud A, Pinheiro S, Gillespie G, Brown D, Loach V, Roberts J, Guimaraes-Walker A, Hayes P, Loughran K, Smith C, De Bont J, Verlinde C, Vooijs D, Schmidt C, Boaz M, Gilmour J, Fast P, Dorrell L, Hanke T, McMichael AJ.** 2006.

Induction of multifunctional human immunodeficiency virus type 1 (HIV-1)-specific T cells capable of proliferation in healthy subjects by using a prime-boost regimen of DNA- and modified vaccinia virus Ankara-vectored vaccines expressing HIV-1 Gag coupled to CD8+ T-cell epitopes. Journal of virology **80:**4717-4728.

81. **Hanke T, McMichael AJ, Samuel RV, Powell LA, McLoughlin L, Crome SJ, Edlin A.** 2002. Lack of toxicity and persistence in the mouse associated with administration of candidate DNA- and modified vaccinia virus Ankara (MVA)-based HIV vaccines for Kenya. Vaccine **21:**108-114.

82. **Jaoko W, Karita E, Kayitenkore K, Omosa-Manyonyi G, Allen S, Than S, Adams EM, Graham BS, Koup RA, Bailer RT, Smith C, Dally L, Farah B, Anzala O, Muvunyi CM, Bizimana J, Tarragona-Fiol T, Bergin PJ, Hayes P, Ho M, Loughran K, Komaroff W, Stevens G, Thomson H, Boaz MJ, Cox JH, Schmidt C, Gilmour J, Nabel GJ, Fast P, Bwayo J.** 2010. Safety and immunogenicity study of Multiclade HIV-1 adenoviral vector vaccine alone or as boost following a multiclade HIV-1 DNA vaccine in Africa. PloS one **5:**e12873.

83. **Goepfert PA, Elizaga ML, Sato A, Qin L, Cardinali M, Hay CM, Hural J, DeRosa SC, DeFawe OD, Tomaras GD, Montefiori DC, Xu Y, Lai L, Kalams SA, Baden LR, Frey SE, Blattner WA, Wyatt LS, Moss B, Robinson HL, National Institute of A, Infectious Diseases HIVVTN.** 2011. Phase 1 safety and immunogenicity testing of DNA and recombinant modified vaccinia Ankara vaccines expressing HIV-1 virus-like particles. The Journal of infectious diseases **203:**610-619.

84. **Peters BS, Jaoko W, Vardas E, Panayotakopoulos G, Fast P, Schmidt C, Gilmour J, Bogoshi M, Omosa-Manyonyi G, Dally L, Klavinskis L, Farah B, Tarragona T, Bart PA, Robinson A, Pieterse C, Stevens W, Thomas R, Barin B, McMichael AJ, McIntyre JA, Pantaleo G, Hanke T, Bwayo J.** 2007. Studies of a prophylactic HIV-1 vaccine candidate based on modified vaccinia virus Ankara (MVA) with and without DNA priming: effects of dosage and route on safety and immunogenicity. Vaccine **25:**2120-2127.

85. **de Souza MS, Ratto-Kim S, Chuenarom W, Schuetz A, Chantakulkij S, Nuntapinit B, Valencia-Micolta A, Thelian D, Nitayaphan S, Pitisuttithum P, Paris RM, Kaewkungwal J, Michael NL, Rerks-Ngarm S, Mathieson B, Marovich M, Currier JR, Kim JH, Ministry of Public Health-Thai AVEGC.** 2012. The Thai phase III trial (RV144) vaccine regimen induces T cell responses that preferentially target epitopes within the V2 region of HIV-1 envelope. Journal of immunology **188:**5166-5176.

86. **Rerks-Ngarm S, Pitisuttithum P, Nitayaphan S, Kaewkungwal J, Chiu J, Paris R, Premsri N, Namwat C, de Souza M, Adams E, Benenson M, Gurunathan S, Tartaglia J, McNeil JG, Francis DP, Stablein D, Birx DL, Chunsuttiwat S, Khamboonruang C, Thongcharoen P, Robb ML, Michael NL, Kunasol P, Kim JH, Investigators M-T.** 2009. Vaccination with ALVAC and AIDSVAX to prevent HIV-1 infection in Thailand. The New England journal of medicine **361:**2209-2220.

87. **Montefiori DC, Karnasuta C, Huang Y, Ahmed H, Gilbert P, de Souza MS, McLinden R, Tovanabutra S, Laurence-Chenine A, Sanders-Buell E, Moody**

MA, Bonsignori M, Ochsenbauer C, Kappes J, Tang H, Greene K, Gao H, LaBranche CC, Andrews C, Polonis VR, Rerks-Ngarm S, Pitisuttithum P, Nitayaphan S, Kaewkungwal J, Self SG, Berman PW, Francis D, Sinangil F, Lee C, Tartaglia J, Robb ML, Haynes BF, Michael NL, Kim JH.** 2012. Magnitude and breadth of the neutralizing antibody response in the RV144 and Vax003 HIV-1 vaccine efficacy trials. The Journal of infectious diseases **206:**431-441.

88. **Haynes BF, Gilbert PB, McElrath MJ, Zolla-Pazner S, Tomaras GD, Alam SM, Evans DT, Montefiori DC, Karnasuta C, Sutthent R, Liao HX, DeVico AL, Lewis GK, Williams C, Pinter A, Fong Y, Janes H, DeCamp A, Huang Y, Rao M, Billings E, Karasavvas N, Robb ML, Ngauy V, de Souza MS, Paris R, Ferrari G, Bailer RT, Soderberg KA, Andrews C, Berman PW, Frahm N, De Rosa SC, Alpert MD, Yates NL, Shen X, Koup RA, Pitisuttithum P, Kaewkungwal J, Nitayaphan S, Rerks-Ngarm S, Michael NL, Kim JH.** 2012. Immune-correlates analysis of an HIV-1 vaccine efficacy trial. The New England journal of medicine **366:**1275-1286.

89. **Rolland M, Edlefsen PT, Larsen BB, Tovanabutra S, Sanders-Buell E, Hertz T, deCamp AC, Carrico C, Menis S, Magaret CA, Ahmed H, Juraska M, Chen L, Konopa P, Nariya S, Stoddard JN, Wong K, Zhao H, Deng W, Maust BS, Bose M, Howell S, Bates A, Lazzaro M, O'Sullivan A, Lei E, Bradfield A, Ibitamuno G, Assawadarachai V, O'Connell RJ, deSouza MS, Nitayaphan S, Rerks-Ngarm S, Robb ML, McLellan JS, Georgiev I, Kwong PD, Carlson JM, Michael NL, Schief WR, Gilbert PB, Mullins JI, Kim JH.** 2012. Increased HIV-1 vaccine efficacy against viruses with genetic signatures in Env V2. Nature **490:**417-420.

90. **Liao HX, Bonsignori M, Alam SM, McLellan JS, Tomaras GD, Moody MA, Kozink DM, Hwang KK, Chen X, Tsao CY, Liu P, Lu X, Parks RJ, Montefiori DC, Ferrari G, Pollara J, Rao M, Peachman KK, Santra S, Letvin NL, Karasavvas N, Yang ZY, Dai K, Pancera M, Gorman J, Wiehe K, Nicely NI, Rerks-Ngarm S, Nitayaphan S, Kaewkungwal J, Pitisuttithum P, Tartaglia J, Sinangil F, Kim JH, Michael NL, Kepler TB, Kwong PD, Mascola JR, Nabel GJ, Pinter A, Zolla-Pazner S, Haynes BF.** 2013. Vaccine induction of antibodies against a structurally heterogeneous site of immune pressure within HIV-1 envelope protein variable regions 1 and 2. Immunity **38:**176-186.

91. **Nkolola JP, Peng H, Settembre EC, Freeman M, Grandpre LE, Devoy C, Lynch DM, La Porte A, Simmons NL, Bradley R, Montefiori DC, Seaman MS, Chen B, Barouch DH.** 2010. Breadth of neutralizing antibodies elicited by stable, homogeneous clade A and clade C HIV-1 gp140 envelope trimers in guinea pigs. Journal of virology **84:**3270-3279.

92. **Wang S, Arthos J, Lawrence JM, Van Ryk D, Mboudjeka I, Shen S, Chou TH, Montefiori DC, Lu S.** 2005. Enhanced immunogenicity of gp120 protein when combined with recombinant DNA priming to generate antibodies that neutralize the JR-FL primary isolate of human immunodeficiency virus type 1. J Virol **79:**7933-7937.

93. **Wang S, Pal R, Mascola JR, Chou TH, Mboudjeka I, Shen S, Liu Q, Whitney S, Keen T, Nair BC, Kalyanaraman VS, Markham P, Lu S.** 2006. Polyvalent HIV-1 Env vaccine formulations delivered by the DNA priming plus protein boosting approach are effective in generating neutralizing antibodies against primary human immunodeficiency virus type 1 isolates from subtypes A, B, C, D and E. Virology **350:**34-47.

94. **Pal R, Kalyanaraman VS, Nair BC, Whitney S, Keen T, Hocker L, Hudacik L, Rose N, Mboudjeka I, Shen S, Wu-Chou TH, Montefiori D, Mascola J, Markham P, Lu S.** 2006. Immunization of rhesus macaques with a polyvalent DNA prime/protein boost human immunodeficiency virus type 1 vaccine elicits protective antibody response against simian human immunodeficiency virus of R5 phenotype. Virology **348:**341-353.

95. **Vaine M, Wang S, Hackett A, Arthos J, Lu S.** 2010. Antibody responses elicited through homologous or heterologous prime-boost DNA and protein vaccinations differ in functional activity and avidity. Vaccine **28:**2999-3007.

96. **Vaine M, Wang S, Crooks ET, Jiang P, Montefiori DC, Binley J, Lu S.** 2008. Improved induction of antibodies against key neutralizing epitopes by human immunodeficiency virus type 1 gp120 DNA prime-protein boost vaccination compared to gp120 protein-only vaccination. J Virol **82:**7369-7378.

97. **Hollister K, Chen Y, Wang S, Wu H, Mondal A, Clegg N, Lu S, Dent A.** 2014. The role of follicular helper T cells and the germinal center in HIV-1 gp120 DNA prime and gp120 protein boost vaccination. Human vaccines & immunotherapeutics **10**.

98. **Wang S, Kennedy JS, West K, Montefiori DC, Coley S, Lawrence J, Shen S, Green S, Rothman AL, Ennis FA, Arthos J, Pal R, Markham P, Lu S.** 2008. Cross-subtype antibody and cellular immune responses induced by a polyvalent DNA prime-protein boost HIV-1 vaccine in healthy human volunteers. Vaccine **26:**3947-3957.

99. **Bansal A, Jackson B, West K, Wang S, Lu S, Kennedy JS, Goepfert PA.** 2008. Multifunctional T-cell characteristics induced by a polyvalent DNA prime/protein boost human immunodeficiency virus type 1 vaccine regimen given to healthy adults are dependent on the route and dose of administration. Journal of virology **82:**6458-6469.

100. **Graham BS, Koup RA, Roederer M, Bailer RT, Enama ME, Moodie Z, Martin JE, McCluskey MM, Chakrabarti BK, Lamoreaux L, Andrews CA, Gomez PL, Mascola JR, Nabel GJ, Vaccine Research Center 004 Study T.** 2006. Phase 1 safety and immunogenicity evaluation of a multiclade HIV-1 DNA candidate vaccine. The Journal of infectious diseases **194:**1650-1660.

101. **Spearman P, Lally MA, Elizaga M, Montefiori D, Tomaras GD, McElrath MJ, Hural J, De Rosa SC, Sato A, Huang Y, Frey SE, Sato P, Donnelly J, Barnett S, Corey LJ, NIAID HIVVTNo.** 2011. A trimeric, V2-deleted HIV-1 envelope glycoprotein vaccine elicits potent neutralizing antibodies but limited breadth of neutralization in human volunteers. The Journal of infectious diseases **203:**1165-1173.

102. **Mascola JR, Lewis MG, Stiegler G, Harris D, VanCott TC, Hayes D, Louder MK, Brown CR, Sapan CV, Frankel SS, Lu Y, Robb ML, Katinger H, Birx**

DL. 1999. Protection of Macaques against pathogenic simian/human immunodeficiency virus 89.6PD by passive transfer of neutralizing antibodies. Journal of virology **73:**4009-4018.

103. **Emini EA, Schleif WA, Nunberg JH, Conley AJ, Eda Y, Tokiyoshi S, Putney SD, Matsushita S, Cobb KE, Jett CM, et al.** 1992. Prevention of HIV-1 infection in chimpanzees by gp120 V3 domain-specific monoclonal antibody. Nature **355:**728-730.

104. **Mascola JR, Stiegler G, VanCott TC, Katinger H, Carpenter CB, Hanson CE, Beary H, Hayes D, Frankel SS, Birx DL, Lewis MG.** 2000. Protection of macaques against vaginal transmission of a pathogenic HIV-1/SIV chimeric virus by passive infusion of neutralizing antibodies. Nature medicine **6:**207-210.

105. **Veazey RS, Shattock RJ, Pope M, Kirijan JC, Jones J, Hu Q, Ketas T, Marx PA, Klasse PJ, Burton DR, Moore JP.** 2003. Prevention of virus transmission to macaque monkeys by a vaginally applied monoclonal antibody to HIV-1 gp120. Nature medicine **9:**343-346.

106. **Klein F, Halper-Stromberg A, Horwitz JA, Gruell H, Scheid JF, Bournazos S, Mouquet H, Spatz LA, Diskin R, Abadir A, Zang T, Dorner M, Billerbeck E, Labitt RN, Gaebler C, Marcovecchio PM, Incesu RB, Eisenreich TR, Bieniasz PD, Seaman MS, Bjorkman PJ, Ravetch JV, Ploss A, Nussenzweig MC.** 2012. HIV therapy by a combination of broadly neutralizing antibodies in humanized mice. Nature **492:**118-122.

107. **Balazs AB, Chen J, Hong CM, Rao DS, Yang L, Baltimore D.** 2012. Antibody-based protection against HIV infection by vectored immunoprophylaxis. Nature **481:**81-84.

108. **Dugast AS, Chan Y, Hoffner M, Licht A, Nkolola J, Li H, Streeck H, Suscovich TJ, Ghebremichael M, Ackerman ME, Barouch DH, Alter G.** 2014. Lack of protection following passive transfer of polyclonal highly functional low-dose non-neutralizing antibodies. PloS one **9:**e97229.

109. **Bournazos S, Klein F, Pietzsch J, Seaman MS, Nussenzweig MC, Ravetch JV.** 2014. Broadly Neutralizing Anti-HIV-1 Antibodies Require Fc Effector Functions for In Vivo Activity. Cell **158:**1243-1253.

110. **Burton DR, Pyati J, Koduri R, Sharp SJ, Thornton GB, Parren PW, Sawyer LS, Hendry RM, Dunlop N, Nara PL, et al.** 1994. Efficient neutralization of primary isolates of HIV-1 by a recombinant human monoclonal antibody. Science **266:**1024-1027.

111. **Trkola A, Pomales AB, Yuan H, Korber B, Maddon PJ, Allaway GP, Katinger H, Barbas CF, 3rd, Burton DR, Ho DD, et al.** 1995. Cross-clade neutralization of primary isolates of human immunodeficiency virus type 1 by human monoclonal antibodies and tetrameric CD4-IgG. Journal of virology **69:**6609-6617.

112. **Calarese DA, Scanlan CN, Zwick MB, Deechongkit S, Mimura Y, Kunert R, Zhu P, Wormald MR, Stanfield RL, Roux KH, Kelly JW, Rudd PM, Dwek RA, Katinger H, Burton DR, Wilson IA.** 2003. Antibody domain exchange is an immunological solution to carbohydrate cluster recognition. Science **300:**2065-2071.

113. **Muster T, Steindl F, Purtscher M, Trkola A, Klima A, Himmler G, Ruker F, Katinger H.** 1993. A conserved neutralizing epitope on gp41 of human immunodeficiency virus type 1. Journal of virology **67:**6642-6647.

114. **Ofek G, Tang M, Sambor A, Katinger H, Mascola JR, Wyatt R, Kwong PD.** 2004. Structure and mechanistic analysis of the anti-human immunodeficiency virus type 1 antibody 2F5 in complex with its gp41 epitope. Journal of virology **78:**10724-10737.

115. **Cardoso RM, Zwick MB, Stanfield RL, Kunert R, Binley JM, Katinger H, Burton DR, Wilson IA.** 2005. Broadly neutralizing anti-HIV antibody 4E10 recognizes a helical conformation of a highly conserved fusion-associated motif in gp41. Immunity **22:**163-173.

116. **Wu X, Yang ZY, Li Y, Hogerkorp CM, Schief WR, Seaman MS, Zhou T, Schmidt SD, Wu L, Xu L, Longo NS, McKee K, O'Dell S, Louder MK, Wycuff DL, Feng Y, Nason M, Doria-Rose N, Connors M, Kwong PD, Roederer M, Wyatt RT, Nabel GJ, Mascola JR.** 2010. Rational design of envelope identifies broadly neutralizing human monoclonal antibodies to HIV-1. Science **329:**856-861.

117. **Scheid JF, Mouquet H, Ueberheide B, Diskin R, Klein F, Oliveira TY, Pietzsch J, Fenyo D, Abadir A, Velinzon K, Hurley A, Myung S, Boulad F, Poignard P, Burton DR, Pereyra F, Ho DD, Walker BD, Seaman MS, Bjorkman PJ, Chait BT, Nussenzweig MC.** 2011. Sequence and structural convergence of broad and potent HIV antibodies that mimic CD4 binding. Science **333:**1633-1637.

118. **Walker LM, Huber M, Doores KJ, Falkowska E, Pejchal R, Julien JP, Wang SK, Ramos A, Chan-Hui PY, Moyle M, Mitcham JL, Hammond PW, Olsen OA, Phung P, Fling S, Wong CH, Phogat S, Wrin T, Simek MD, Protocol GPI, Koff WC, Wilson IA, Burton DR, Poignard P.** 2011. Broad neutralization coverage of HIV by multiple highly potent antibodies. Nature **477:**466-470.

119. **Wu X, Zhou T, Zhu J, Zhang B, Georgiev I, Wang C, Chen X, Longo NS, Louder M, McKee K, O'Dell S, Perfetto S, Schmidt SD, Shi W, Wu L, Yang Y, Yang ZY, Yang Z, Zhang Z, Bonsignori M, Crump JA, Kapiga SH, Sam NE, Haynes BF, Simek M, Burton DR, Koff WC, Doria-Rose NA, Connors M, Program NCS, Mullikin JC, Nabel GJ, Roederer M, Shapiro L, Kwong PD, Mascola JR.** 2011. Focused evolution of HIV-1 neutralizing antibodies revealed by structures and deep sequencing. Science **333:**1593-1602.

120. **Zhou T, Georgiev I, Wu X, Yang ZY, Dai K, Finzi A, Kwon YD, Scheid JF, Shi W, Xu L, Yang Y, Zhu J, Nussenzweig MC, Sodroski J, Shapiro L, Nabel GJ, Mascola JR, Kwong PD.** 2010. Structural basis for broad and potent neutralization of HIV-1 by antibody VRC01. Science **329:**811-817.

121. **Corti D, Langedijk JP, Hinz A, Seaman MS, Vanzetta F, Fernandez-Rodriguez BM, Silacci C, Pinna D, Jarrossay D, Balla-Jhagjhoorsingh S, Willems B, Zekveld MJ, Dreja H, O'Sullivan E, Pade C, Orkin C, Jeffs SA, Montefiori DC, Davis D, Weissenhorn W, McKnight A, Heeney JL, Sallusto F, Sattentau QJ, Weiss RA, Lanzavecchia A.** 2010. Analysis of memory B cell responses and isolation of novel monoclonal antibodies with neutralizing breadth from HIV-1-infected individuals. PloS one **5:**e8805.

122. **Falkowska E, Ramos A, Feng Y, Zhou T, Moquin S, Walker LM, Wu X, Seaman MS, Wrin T, Kwong PD, Wyatt RT, Mascola JR, Poignard P, Burton DR.** 2012. PGV04, an HIV-1 gp120 CD4 binding site antibody, is broad and potent in neutralization but does not induce conformational changes characteristic of CD4. Journal of virology **86:**4394-4403.

123. **Liao HX, Lynch R, Zhou T, Gao F, Alam SM, Boyd SD, Fire AZ, Roskin KM, Schramm CA, Zhang Z, Zhu J, Shapiro L, Program NCS, Mullikin JC, Gnanakaran S, Hraber P, Wiehe K, Kelsoe G, Yang G, Xia SM, Montefiori DC, Parks R, Lloyd KE, Scearce RM, Soderberg KA, Cohen M, Kamanga G, Louder MK, Tran LM, Chen Y, Cai F, Chen S, Moquin S, Du X, Joyce MG, Srivatsan S, Zhang B, Zheng A, Shaw GM, Hahn BH, Kepler TB, Korber BT, Kwong PD, Mascola JR, Haynes BF.** 2013. Co-evolution of a broadly neutralizing HIV-1 antibody and founder virus. Nature **496:**469-476.

124. **Walker LM, Phogat SK, Chan-Hui PY, Wagner D, Phung P, Goss JL, Wrin T, Simek MD, Fling S, Mitcham JL, Lehrman JK, Priddy FH, Olsen OA, Frey SM, Hammond PW, Protocol GPI, Kaminsky S, Zamb T, Moyle M, Koff WC, Poignard P, Burton DR.** 2009. Broad and potent neutralizing antibodies from an African donor reveal a new HIV-1 vaccine target. Science **326:**285-289.

125. **Bonsignori M, Hwang KK, Chen X, Tsao CY, Morris L, Gray E, Marshall DJ, Crump JA, Kapiga SH, Sam NE, Sinangil F, Pancera M, Yongping Y, Zhang B, Zhu J, Kwong PD, O'Dell S, Mascola JR, Wu L, Nabel GJ, Phogat S, Seaman MS, Whitesides JF, Moody MA, Kelsoe G, Yang X, Sodroski J, Shaw GM, Montefiori DC, Kepler TB, Tomaras GD, Alam SM, Liao HX, Haynes BF.** 2011. Analysis of a clonal lineage of HIV-1 envelope V2/V3 conformational epitope-specific broadly neutralizing antibodies and their inferred unmutated common ancestors. Journal of virology **85:**9998-10009.

126. **Julien JP, Sok D, Khayat R, Lee JH, Doores KJ, Walker LM, Ramos A, Diwanji DC, Pejchal R, Cupo A, Katpally U, Depetris RS, Stanfield RL, McBride R, Marozsan AJ, Paulson JC, Sanders RW, Moore JP, Burton DR, Poignard P, Ward AB, Wilson IA.** 2013. Broadly neutralizing antibody PGT121 allosterically modulates CD4 binding via recognition of the HIV-1 gp120 V3 base and multiple surrounding glycans. PLoS pathogens **9:**e1003342.

127. **Pejchal R, Doores KJ, Walker LM, Khayat R, Huang PS, Wang SK, Stanfield RL, Julien JP, Ramos A, Crispin M, Depetris R, Katpally U, Marozsan A, Cupo A, Maloveste S, Liu Y, McBride R, Ito Y, Sanders RW, Ogohara C, Paulson JC, Feizi T, Scanlan CN, Wong CH, Moore JP, Olson WC, Ward AB, Poignard P, Schief WR, Burton DR, Wilson IA.** 2011. A potent and broad neutralizing antibody recognizes and penetrates the HIV glycan shield. Science **334:**1097-1103.

128. **Huang J, Ofek G, Laub L, Louder MK, Doria-Rose NA, Longo NS, Imamichi H, Bailer RT, Chakrabarti B, Sharma SK, Alam SM, Wang T, Yang Y, Zhang B, Migueles SA, Wyatt R, Haynes BF, Kwong PD, Mascola JR, Connors M.** 2012. Broad and potent neutralization of HIV-1 by a gp41-specific human antibody. Nature **491:**406-412.

129. **Falkowska E, Le KM, Ramos A, Doores KJ, Lee JH, Blattner C, Ramirez A, Derking R, van Gils MJ, Liang CH, McBride R, von Bredow B, Shivatare SS, Wu CY, Chan-Hui PY, Liu Y, Feizi T, Zwick MB, Koff WC, Seaman MS, Swiderek K, Moore JP, Evans D, Paulson JC, Wong CH, Ward AB, Wilson IA, Sanders RW, Poignard P, Burton DR.** 2014. Broadly neutralizing HIV antibodies define a glycan-dependent epitope on the prefusion conformation of gp41 on cleaved envelope trimers. Immunity **40:**657-668.

130. **Blattner C, Lee JH, Sliepen K, Derking R, Falkowska E, de la Pena AT, Cupo A, Julien JP, van Gils M, Lee PS, Peng W, Paulson JC, Poignard P, Burton DR, Moore JP, Sanders RW, Wilson IA, Ward AB.** 2014. Structural delineation of a quaternary, cleavage-dependent epitope at the gp41-gp120 interface on intact HIV-1 Env trimers. Immunity **40:**669-680.

131. **Moir S, Fauci AS.** 2009. B cells in HIV infection and disease. Nature reviews. Immunology **9:**235-245.

132. **Moore JP, Sodroski J.** 1996. Antibody cross-competition analysis of the human immunodeficiency virus type 1 gp120 exterior envelope glycoprotein. Journal of virology **70:**1863-1872.

133. **Sundling C, Li Y, Huynh N, Poulsen C, Wilson R, O'Dell S, Feng Y, Mascola JR, Wyatt RT, Karlsson Hedestam GB.** 2012. High-resolution definition of vaccine-elicited B cell responses against the HIV primary receptor binding site. Science translational medicine **4:**142ra196.

134. **Forsman A, Beirnaert E, Aasa-Chapman MM, Hoorelbeke B, Hijazi K, Koh W, Tack V, Szynol A, Kelly C, McKnight A, Verrips T, de Haard H, Weiss RA.** 2008. Llama antibody fragments with cross-subtype human immunodeficiency virus type 1 (HIV-1)-neutralizing properties and high affinity for HIV-1 gp120. Journal of virology **82:**12069-12081.

135. **Matz J, Kessler P, Bouchet J, Combes O, Ramos OH, Barin F, Baty D, Martin L, Benichou S, Chames P.** 2013. Straightforward selection of broadly neutralizing single-domain antibodies targeting the conserved CD4 and coreceptor binding sites of HIV-1 gp120. Journal of virology **87:**1137-1149.

136. **McCoy LE, Quigley AF, Strokappe NM, Bulmer-Thomas B, Seaman MS, Mortier D, Rutten L, Chander N, Edwards CJ, Ketteler R, Davis D, Verrips T, Weiss RA.** 2012. Potent and broad neutralization of HIV-1 by a llama antibody elicited by immunization. The Journal of experimental medicine **209:**1091-1103.

137. **Moody MA, Yates NL, Amos JD, Drinker MS, Eudailey JA, Gurley TC, Marshall DJ, Whitesides JF, Chen X, Foulger A, Yu JS, Zhang R, Meyerhoff RR, Parks R, Scull JC, Wang L, Vandergrift NA, Pickeral J, Pollara J, Kelsoe G, Alam SM, Ferrari G, Montefiori DC, Voss G, Liao HX, Tomaras GD, Haynes BF.** 2012. HIV-1 gp120 vaccine induces affinity maturation in both new and persistent antibody clonal lineages. Journal of virology **86:**7496-7507.

138. **Ferrari G, Pollara J, Kozink D, Harms T, Drinker M, Freel S, Moody MA, Alam SM, Tomaras GD, Ochsenbauer C, Kappes JC, Shaw GM, Hoxie JA, Robinson JE, Haynes BF.** 2011. An HIV-1 gp120 envelope human monoclonal antibody that recognizes a C1 conformational epitope mediates potent antibody-dependent cellular cytotoxicity (ADCC) activity and defines a common ADCC epitope in human HIV-1 serum. Journal of virology **85:**7029-7036.

139. **Tomaras GD, Ferrari G, Shen X, Alam SM, Liao HX, Pollara J, Bonsignori M, Moody MA, Fong Y, Chen X, Poling B, Nicholson CO, Zhang R, Lu X, Parks R, Kaewkungwal J, Nitayaphan S, Pitisuttithum P, Rerks-Ngarm S, Gilbert PB, Kim JH, Michael NL, Montefiori DC, Haynes BF.** 2013. Vaccine-induced plasma IgA specific for the C1 region of the HIV-1 envelope blocks binding and effector function of IgG. Proceedings of the National Academy of Sciences of the United States of America **110:**9019-9024.

140. **Doria-Rose NA, Klein RM, Manion MM, O'Dell S, Phogat A, Chakrabarti B, Hallahan CW, Migueles SA, Wrammert J, Ahmed R, Nason M, Wyatt RT, Mascola JR, Connors M.** 2009. Frequency and phenotype of human immunodeficiency virus envelope-specific B cells from patients with broadly cross-neutralizing antibodies. J Virol **83:**188-199.

141. **Gray ES, Madiga MC, Hermanus T, Moore PL, Wibmer CK, Tumba NL, Werner L, Mlisana K, Sibeko S, Williamson C, Abdool Karim SS, Morris L, and the CST.** 2011. The neutralization breadth of HIV-1 develops incrementally over four years and is associated with CD4+ T cell decline and high viral load during acute infection. J Virol **85:**4828-4840.

142. **Simek MD, Rida W, Priddy FH, Pung P, Carrow E, Laufer DS, Lehrman JK, Boaz M, Tarragona-Fiol T, Miiro G, Birungi J, Pozniak A, McPhee DA, Manigart O, Karita E, Inwoley A, Jaoko W, Dehovitz J, Bekker LG, Pitisuttithum P, Paris R, Walker LM, Poignard P, Wrin T, Fast PE, Burton DR, Koff WC.** 2009. Human immunodeficiency virus type 1 elite neutralizers: individuals with broad and potent neutralizing activity identified by using a high-throughput neutralization assay together with an analytical selection algorithm. J Virol **83:**7337-7348.

143. **Sather DN, Armann J, Ching LK, Mavrantoni A, Sellhorn G, Caldwell Z, Yu X, Wood B, Self S, Kalams S, Stamatatos L.** 2009. Factors associated with the development of cross-reactive neutralizing antibodies during human immunodeficiency virus type 1 infection. J Virol **83:**757-769.

144. **Vaine M, Wang S, Liu Q, Arthos J, Montefiori D, Goepfert P, McElrath MJ, Lu S.** 2010. Profiles of human serum antibody responses elicited by three leading HIV vaccines focusing on the induction of Env-specific antibodies. PloS one **5:**e13916.

145. **Puri R, Suzuki T, Yamakawa K, Ganesh S.** 2009. Hyperphosphorylation and aggregation of Tau in laforin-deficient mice, an animal model for Lafora disease. J Biol Chem **284:**22657-22663.

146. **Hellerstein M, Xu Y, Marino T, Lu S, Yi H, Wright ER, Robinson HL.** 2012. Co-expression of HIV-1 virus-like particles and granulocyte-macrophage colony stimulating factor by GEO-D03 DNA vaccine. Hum Vaccin Immunother **8**.

147. **Shaftel SS, Kyrkanides S, Olschowka JA, Miller JN, Johnson RE, O'Banion MK.** 2007. Sustained hippocampal IL-1 beta overexpression mediates chronic neuroinflammation and ameliorates Alzheimer plaque pathology. J Clin Invest **117:**1595-1604.

148. **Burton DR, Desrosiers RC, Doms RW, Koff WC, Kwong PD, Moore JP, Nabel GJ, Sodroski J, Wilson IA, Wyatt RT.** 2004. HIV vaccine design and the neutralizing antibody problem. Nat Immunol **5:**233-236.

149. **Gao F, Scearce RM, Alam SM, Hora B, Xia S, Hohm JE, Parks RJ, Ogburn DF, Tomaras GD, Park E, Lomas WE, Maino VC, Fiscus SA, Cohen MS, Moody MA, Hahn BH, Korber BT, Liao HX, Haynes BF.** 2009. Cross-reactive monoclonal antibodies to multiple HIV-1 subtype and SIVcpz envelope glycoproteins. Virology **394:**91-98.

150. **Cordell J, Moore JP, Dean CJ, Klasse PJ, Weiss RA, McKeating JA.** 1991. Rat monoclonal antibodies to nonoverlapping epitopes of human immunodeficiency virus type 1 gp120 block CD4 binding in vitro. Virology **185:**72-79.

151. **Sun NC, Ho DD, Sun CR, Liou RS, Gordon W, Fung MS, Li XL, Ting RC, Lee TH, Chang NT, et al.** 1989. Generation and characterization of monoclonal antibodies to the putative CD4-binding domain of human immunodeficiency virus type 1 gp120. J Virol **63:**3579-3585.

152. **Palker TJ, Matthews TJ, Clark ME, Cianciolo GJ, Randall RR, Langlois AJ, White GC, Safai B, Snyderman R, Bolognesi DP, et al.** 1987. A conserved region at the COOH terminus of human immunodeficiency virus gp120 envelope protein contains an immunodominant epitope. Proc Natl Acad Sci U S A **84:**2479-2483.

153. **Pan R, Sampson JM, Chen2 Y, Vaine M, Wang S, Lu S, Kong X-P.** 2013. Rabbit anti-HIV-1 monoclonal antibodies raised by immunization can mimic the antigen-binding modes of antibodies derived from HIV-1 infected humans. submitted.

154. **Cheung WC, Beausoleil SA, Zhang X, Sato S, Schieferl SM, Wieler JS, Beaudet JG, Ramenani RK, Popova L, Comb MJ, Rush J, Polakiewicz RD.** 2012. A proteomics approach for the identification and cloning of monoclonal antibodies from serum. Nat Biotechnol **30:**447-452.

155. **Moody MA, Zhang R, Walter EB, Woods CW, Ginsburg GS, McClain MT, Denny TN, Chen X, Munshaw S, Marshall DJ, Whitesides JF, Drinker MS, Amos JD, Gurley TC, Eudailey JA, Foulger A, DeRosa KR, Parks R, Meyerhoff RR, Yu JS, Kozink DM, Barefoot BE, Ramsburg EA, Khurana S, Golding H, Vandergrift NA, Alam SM, Tomaras GD, Kepler TB, Kelsoe G, Liao HX, Haynes BF.** 2011. H3N2 influenza infection elicits more cross-reactive and less clonally expanded anti-hemagglutinin antibodies than influenza vaccination. PLoS One **6:**e25797.

156. **Wrammert J, Smith K, Miller J, Langley WA, Kokko K, Larsen C, Zheng NY, Mays I, Garman L, Helms C, James J, Air GM, Capra JD, Ahmed R, Wilson PC.** 2008. Rapid cloning of high-affinity human monoclonal antibodies against influenza virus. Nature **453:**667-671.

157. **Popkov M, Mage RG, Alexander CB, Thundivalappil S, Barbas CF, 3rd, Rader C.** 2003. Rabbit immune repertoires as sources for therapeutic monoclonal antibodies: the impact of kappa allotype-correlated variation in cysteine content on antibody libraries selected by phage display. J Mol Biol **325:**325-335.

158. **Wang S, Taaffe J, Parker C, Solorzano A, Cao H, Garcia-Sastre A, Lu S.** 2006. Hemagglutinin (HA) proteins from H1 and H3 serotypes of influenza A viruses require different antigen designs for the induction of optimal protective

antibody responses as studied by codon-optimized HA DNA vaccines. J Virol **80:**11628-11637.

159.   **Wang S, Chou TH, Sakhatskyy PV, Huang S, Lawrence JM, Cao H, Huang X, Lu S.** 2005. Identification of two neutralizing regions on the severe acute respiratory syndrome coronavirus spike glycoprotein produced from the mammalian expression system. J Virol **79:**1906-1910.

160.   **Mage RG, Lanning D, Knight KL.** 2006. B cell and antibody repertoire development in rabbits: the requirement of gut-associated lymphoid tissues. Dev Comp Immunol **30:**137-153.

161.   **Jasper PJ, Zhai SK, Kalis SL, Kingzette M, Knight KL.** 2003. B lymphocyte development in rabbit: progenitor B cells and waning of B lymphopoiesis. J Immunol **171:**6372-6380.

162.   **Su C, Nei M.** 1999. Fifty-million-year-old polymorphism at an immunoglobulin variable region gene locus in the rabbit evolutionary lineage. Proc Natl Acad Sci U S A **96:**9710-9715.

163.   **Knight KL, Becker RS.** 1990. Molecular basis of the allelic inheritance of rabbit immunoglobulin VH allotypes: implications for the generation of antibody diversity. Cell **60:**963-970.

164.   **West AP, Jr., Diskin R, Nussenzweig MC, Bjorkman PJ.** 2012. Structural basis for germ-line gene usage of a potent class of antibodies targeting the CD4-binding site of HIV-1 gp120. Proc Natl Acad Sci U S A **109:**E2083-2090.

165.   **Mage RG, Sehgal D, Schiaffella E, Anderson AO.** 1999. Gene-conversion in rabbit B-cell ontogeny and during immune responses in splenic germinal centers. Vet Immunol Immunopathol **72:**7-15.

166.   **McClain MT, Lutz CS, Kaufman KM, Faig OZ, Gross TF, James JA.** 2004. Structural availability influences the capacity of autoantigenic epitopes to induce a widespread lupus-like autoimmune response. Proc Natl Acad Sci U S A **101:**3551-3556.

167.   **Spieker-Polet H, Sethupathi P, Yam PC, Knight KL.** 1995. Rabbit monoclonal antibodies: generating a fusion partner to produce rabbit-rabbit hybridomas. Proc Natl Acad Sci U S A **92:**9348-9352.

168.   **Wu X, Zhou T, Zhu J, Zhang B, Georgiev I, Wang C, Chen X, Longo NS, Louder M, McKee K, O'Dell S, Perfetto S, Schmidt SD, Shi W, Wu L, Yang Y, Yang ZY, Yang Z, Zhang Z, Bonsignori M, Crump JA, Kapiga SH, Sam NE, Haynes BF, Simek M, Burton DR, Koff WC, Doria-Rose N, Connors M, Program NCS, Mullikin JC, Nabel GJ, Roederer M, Shapiro L, Kwong PD, Mascola JR.** 2011. Focused Evolution of HIV-1 Neutralizing Antibodies Revealed by Structures and Deep Sequencing. Science.

169.   **Haynes BF, Fleming J, St Clair EW, Katinger H, Stiegler G, Kunert R, Robinson J, Scearce RM, Plonk K, Staats HF, Ortel TL, Liao HX, Alam SM.** 2005. Cardiolipin polyspecific autoreactivity in two broadly neutralizing HIV-1 antibodies. Science **308:**1906-1908.

170.   **Bonsignori M, Alam SM, Liao HX, Verkoczy L, Tomaras GD, Haynes BF, Moody MA.** 2012. HIV-1 antibodies from infection and vaccination: insights for guiding vaccine design. Trends Microbiol **20:**532-539.

171. **Kwong PD, Doyle ML, Casper DJ, Cicala C, Leavitt SA, Majeed S, Steenbeke TD, Venturi M, Chaiken I, Fung M, Katinger H, Parren PW, Robinson J, Van Ryk D, Wang L, Burton DR, Freire E, Wyatt R, Sodroski J, Hendrickson WA, Arthos J.** 2002. HIV-1 evades antibody-mediated neutralization through conformational masking of receptor-binding sites. Nature **420:**678-682.

172. **Jiang X, Burke V, Totrov M, Williams C, Cardozo T, Gorny MK, Zolla-Pazner S, Kong XP.** 2010. Conserved structural elements in the V3 crown of HIV-1 gp120. Nature structural & molecular biology **17:**955-961.

173. **Killikelly A, Zhang HT, Spurrier B, Williams C, Gorny MK, Zolla-Pazner S, Kong XP.** 2013. Thermodynamic signatures of the antigen binding site of mAb 447-52D targeting the third variable region of HIV-1 gp120. Biochemistry **52:**6249-6257.

174. **Ratner L, Fisher A, Jagodzinski LL, Mitsuya H, Liou RS, Gallo RC, Wong-Staal F.** 1987. Complete nucleotide sequences of functional clones of the AIDS virus. AIDS research and human retroviruses **3:**57-69.

175. **Lasky LA, Nakamura G, Smith DH, Fennie C, Shimasaki C, Patzer E, Berman P, Gregory T, Capon DJ.** 1987. Delineation of a region of the human immunodeficiency virus type 1 gp120 glycoprotein critical for interaction with the CD4 receptor. Cell **50:**975-985.

176. **Rizzuto C, Sodroski J.** 2000. Fine definition of a conserved CCR5-binding region on the human immunodeficiency virus type 1 glycoprotein 120. AIDS Res Hum Retroviruses **16:**741-749.

177. **Rizzuto CD, Wyatt R, Hernandez-Ramos N, Sun Y, Kwong PD, Hendrickson WA, Sodroski J.** 1998. A conserved HIV gp120 glycoprotein structure involved in chemokine receptor binding. Science **280:**1949-1953.

178. **Moore JP, Thali M, Jameson BA, Vignaux F, Lewis GK, Poon SW, Charles M, Fung MS, Sun B, Durda PJ, et al.** 1993. Immunochemical analysis of the gp120 surface glycoprotein of human immunodeficiency virus type 1: probing the structure of the C4 and V4 domains and the interaction of the C4 domain with the V3 loop. J Virol **67:**4785-4796.

179. **Wyatt R, Thali M, Tilley S, Pinter A, Posner M, Ho D, Robinson J, Sodroski J.** 1992. Relationship of the human immunodeficiency virus type 1 gp120 third variable loop to a component of the CD4 binding site in the fourth conserved region. J Virol **66:**6997-7004.

180. **Hoffman NG, Seillier-Moiseiwitsch F, Ahn J, Walker JM, Swanstrom R.** 2002. Variability in the human immunodeficiency virus type 1 gp120 Env protein linked to phenotype-associated changes in the V3 loop. J Virol **76:**3852-3864.

181. **Cease KB, Margalit H, Cornette JL, Putney SD, Robey WG, Ouyang C, Streicher HZ, Fischinger PJ, Gallo RC, DeLisi C, et al.** 1987. Helper T-cell antigenic site identification in the acquired immunodeficiency syndrome virus gp120 envelope protein and induction of immunity in mice to the native protein using a 16-residue synthetic peptide. Proc Natl Acad Sci U S A **84:**4249-4253.

182. **Berzofsky JA, Bensussan A, Cease KB, Bourge JF, Cheynier R, Lurhuma Z, Salaun JJ, Gallo RC, Shearer GM, Zagury D.** 1988. Antigenic peptides

recognized by T lymphocytes from AIDS viral envelope-immune humans. Nature **334:**706-708.

183. **Morrow WJ, Williams WM, Whalley AS, Ryskamp T, Newman R, Kang CY, Chamat S, Kohler H, Kieber-Emmons T.** 1992. Synthetic peptides from a conserved region of gp120 induce broadly reactive anti-HIV responses. Immunology **75:**557-564.

184. **Li H, Chien PC, Jr., Tuen M, Visciano ML, Cohen S, Blais S, Xu CF, Zhang HT, Hioe CE.** 2008. Identification of an N-linked glycosylation in the C4 region of HIV-1 envelope gp120 that is critical for recognition of neighboring CD4 T cell epitopes. Journal of immunology **180:**4011-4021.

185. **Nakamura GR, Byrn R, Wilkes DM, Fox JA, Hobbs MR, Hastings R, Wessling HC, Norcross MA, Fendly BM, Berman PW.** 1993. Strain specificity and binding affinity requirements of neutralizing monoclonal antibodies to the C4 domain of gp120 from human immunodeficiency virus type 1. Journal of virology **67:**6179-6191.

186. **McKeating JA, Moore JP, Ferguson M, Marsden HS, Graham S, Almond JW, Evans DJ, Weiss RA.** 1992. Monoclonal antibodies to the C4 region of human immunodeficiency virus type 1 gp120: use in topological analysis of a CD4 binding site. AIDS Res Hum Retroviruses **8:**451-459.

187. **Coussens PM, Tieber VL, Mehigh CS, Marcus M.** 1991. Identification of a novel transcription factor, ACF, in cultured avian fibroblast cells that interacts with a Marek's disease virus late gene promoter. Virology **185:**80-89.

188. **Sun NC, Ho DD, Sun CR, Liou RS, Gordon W, Fung MS, Li XL, Ting RC, Lee TH, Chang NT, et al.** 1989. Generation and characterization of monoclonal antibodies to the putative CD4-binding domain of human immunodeficiency virus type 1 gp120. Journal of virology **63:**3579-3585.

189. **Kwon YD, Finzi A, Wu X, Dogo-Isonagie C, Lee LK, Moore LR, Schmidt SD, Stuckey J, Yang Y, Zhou T, Zhu J, Vicic DA, Debnath AK, Shapiro L, Bewley CA, Mascola JR, Sodroski JG, Kwong PD.** 2012. Unliganded HIV-1 gp120 core structures assume the CD4-bound conformation with regulation by quaternary interactions and variable loops. Proc Natl Acad Sci U S A **109:**5663-5668.

190. **Zhou T, Xu L, Dey B, Hessell AJ, Van Ryk D, Xiang SH, Yang X, Zhang MY, Zwick MB, Arthos J, Burton DR, Dimitrov DS, Sodroski J, Wyatt R, Nabel GJ, Kwong PD.** 2007. Structural definition of a conserved neutralization epitope on HIV-1 gp120. Nature **445:**732-737.

191. **Chen Y, Vaine M, Wallace A, Han D, Wan S, Seaman MS, Montefiori D, Wang S, Lu S.** 2013. A novel rabbit monoclonal antibody platform to dissect the diverse repertoire of antibody epitopes for HIV-1 Env immunogen design. Journal of virology **87:**10232-10243.

192. **Kabat EA, Wu TT, Perry HM, Gottesman KS.** 1991. Sequences of Proteins of Immunological Interest, 5th ed. National Institutes of Health, Bethesda, MD.

193. **Pan R, Sampson JM, Chen Y, Vaine M, Wang S, Lu S, Kong XP.** 2013. Rabbit anti-HIV-1 monoclonal antibodies raised by immunization can mimic the antigen-binding modes of antibodies derived from HIV-1-infected humans. Journal of virology **87:**10221-10231.

194. **Pancera M, Zhou T, Druz A, Georgiev IS, Soto C, Gorman J, Huang J, Acharya P, Chuang GY, Ofek G, Stewart-Jones GB, Stuckey J, Bailer RT, Joyce MG, Louder MK, Tumba N, Yang Y, Zhang B, Cohen MS, Haynes BF, Mascola JR, Morris L, Munro JB, Blanchard SC, Mothes W, Connors M, Kwong PD.** 2014. Structure and immune recognition of trimeric pre-fusion HIV-1 Env. Nature.

195. **Xiang SH, Wang L, Abreu M, Huang CC, Kwong PD, Rosenberg E, Robinson JE, Sodroski J.** 2003. Epitope mapping and characterization of a novel CD4-induced human monoclonal antibody capable of neutralizing primary HIV-1 strains. Virology **315:**124-134.

196. **Nakamura GR, Byrn R, Rosenthal K, Porter JP, Hobbs MR, Riddle L, Eastman DJ, Dowbenko D, Gregory T, Fendly BM, et al.** 1992. Monoclonal antibodies to the extracellular domain of HIV-1IIIB gp160 that neutralize infectivity, block binding to CD4, and react with diverse isolates. AIDS Res Hum Retroviruses **8:**1875-1885.

197. **Kelker HC, Itri VR, Valentine FT.** 2010. A strategy for eliciting antibodies against cryptic, conserved, conformationally dependent epitopes of HIV envelope glycoprotein. PLoS One **5:**e8555.

198. **Javaherian K, Langlois AJ, McDanal C, Ross KL, Eckler LI, Jellis CL, Profy AT, Rusche JR, Bolognesi DP, Putney SD, et al.** 1989. Principal neutralizing domain of the human immunodeficiency virus type 1 envelope protein. Proceedings of the National Academy of Sciences of the United States of America **86:**6768-6772.

199. **LaRosa GJ, Davide JP, Weinhold K, Waterbury JA, Profy AT, Lewis JA, Langlois AJ, Dreesman GR, Boswell RN, Shadduck P, et al.** 1990. Conserved sequence and structural elements in the HIV-1 principal neutralizing determinant. Science **249:**932-935.

200. **Hioe CE, Wrin T, Seaman MS, Yu X, Wood B, Self S, Williams C, Gorny MK, Zolla-Pazner S.** 2010. Anti-V3 monoclonal antibodies display broad neutralizing activities against multiple HIV-1 subtypes. PloS one **5:**e10254.

201. **Zolla-Pazner S, Kong XP, Jiang X, Cardozo T, Nadas A, Cohen S, Totrov M, Seaman MS, Wang S, Lu S.** 2011. Cross-clade HIV-1 neutralizing antibodies induced with V3-scaffold protein immunogens following priming with gp120 DNA. Journal of virology **85:**9887-9898.

202. **Choi BK, Bobrowicz P, Davidson RC, Hamilton SR, Kung DH, Li H, Miele RG, Nett JH, Wildt S, Gerngross TU.** 2003. Use of combinatorial genetic libraries to humanize N-linked glycosylation in the yeast Pichia pastoris. Proc Natl Acad Sci U S A **100:**5022-5027.

203. **Hamilton SR, Davidson RC, Sethuraman N, Nett JH, Jiang Y, Rios S, Bobrowicz P, Stadheim TA, Li H, Choi BK, Hopkins D, Wischnewski H, Roser J, Mitchell T, Strawbridge RR, Hoopes J, Wildt S, Gerngross TU.** 2006. Humanization of yeast to produce complex terminally sialylated glycoproteins. Science **313:**1441-1443.

204. **Li Y, O'Dell S, Walker LM, Wu X, Guenaga J, Feng Y, Schmidt SD, McKee K, Louder MK, Ledgerwood JE, Graham BS, Haynes BF, Burton DR, Wyatt**

RT, Mascola JR. 2011. Mechanism of neutralization by the broadly neutralizing HIV-1 monoclonal antibody VRC01. Journal of virology **85:**8954-8967.

205. **Morelli AB, Becher D, Koernig S, Silva A, Drane D, Maraskovsky E.** 2012. ISCOMATRIX: a novel adjuvant for use in prophylactic and therapeutic vaccines against infectious diseases. Journal of medical microbiology **61:**935-943.

206. **Duewell P, Kisser U, Heckelsmiller K, Hoves S, Stoitzner P, Koernig S, Morelli AB, Clausen BE, Dauer M, Eigler A, Anz D, Bourquin C, Maraskovsky E, Endres S, Schnurr M.** 2011. ISCOMATRIX adjuvant combines immune activation with antigen delivery to dendritic cells in vivo leading to effective cross-priming of CD8+ T cells. Journal of immunology **187:**55-63.

207. **Agrawal-Gamse C, Luallen RJ, Liu B, Fu H, Lee FH, Geng Y, Doms RW.** 2011. Yeast-elicited cross-reactive antibodies to HIV Env glycans efficiently neutralize virions expressing exclusively high-mannose N-linked glycans. Journal of virology **85:**470-480.

208. **Luallen RJ, Lin J, Fu H, Cai KK, Agrawal C, Mboudjeka I, Lee FH, Montefiori D, Smith DF, Doms RW, Geng Y.** 2008. An engineered Saccharomyces cerevisiae strain binds the broadly neutralizing human immunodeficiency virus type 1 antibody 2G12 and elicits mannose-specific gp120-binding antibodies. Journal of virology **82:**6447-6457.

209. **Doores KJ, Burton DR.** 2010. Variable loop glycan dependency of the broad and potent HIV-1-neutralizing antibodies PG9 and PG16. Journal of virology **84:**10510-10521.

210. **Bonomelli C, Doores KJ, Dunlop DC, Thaney V, Dwek RA, Burton DR, Crispin M, Scanlan CN.** 2011. The glycan shield of HIV is predominantly oligomannose independently of production system or viral clade. PloS one **6:**e23521.

211. **Abdel-Motal U, Wang S, Lu S, Wigglesworth K, Galili U.** 2006. Increased immunogenicity of human immunodeficiency virus gp120 engineered to express Galalpha1-3Galbeta1-4GlcNAc-R epitopes. Journal of virology **80:**6943-6951.

212. **Abdel-Motal UM, Wang S, Awad A, Lu S, Wigglesworth K, Galili U.** 2010. Increased immunogenicity of HIV-1 p24 and gp120 following immunization with gp120/p24 fusion protein vaccine expressing alpha-gal epitopes. Vaccine **28:**1758-1765.

213. **Vaine M, Duenas-Decamp M, Peters P, Liu Q, Arthos J, Wang S, Clapham P, Lu S.** 2011. Two closely related Env antigens from the same patient elicited different spectra of neutralizing antibodies against heterologous HIV-1 isolates. Journal of virology **85:**4927-4936.

214. **Astronomo RD, Burton DR.** 2010. Carbohydrate vaccines: developing sweet solutions to sticky situations? Nature reviews. Drug discovery **9:**308-324.

215. **Doores KJ, Fulton Z, Hong V, Patel MK, Scanlan CN, Wormald MR, Finn MG, Burton DR, Wilson IA, Davis BG.** 2010. A nonself sugar mimic of the HIV glycan shield shows enhanced antigenicity. Proceedings of the National Academy of Sciences of the United States of America **107:**17107-17112.

216. **Patel V, Jalah R, Kulkarni V, Valentin A, Rosati M, Alicea C, von Gegerfelt A, Huang W, Guan Y, Keele BF, Bess JW, Jr., Piatak M, Jr., Lifson JD,**

Williams WT, Shen X, Tomaras GD, Amara RR, Robinson HL, Johnson W, Broderick KE, Sardesai NY, Venzon DJ, Hirsch VM, Felber BK, Pavlakis GN. 2013. DNA and virus particle vaccination protects against acquisition and confers control of viremia upon heterologous simian immunodeficiency virus challenge. Proceedings of the National Academy of Sciences of the United States of America **110:**2975-2980.

217. **Li J, Valentin A, Kulkarni V, Rosati M, Beach RK, Alicea C, Hannaman D, Reed SG, Felber BK, Pavlakis GN.** 2013. HIV/SIV DNA vaccine combined with protein in a co-immunization protocol elicits highest humoral responses to envelope in mice and macaques. Vaccine **31:**3747-3755.

218. **Jalah R, Kulkarni V, Patel V, Rosati M, Alicea C, Bear J, Yu L, Guan Y, Shen X, Tomaras GD, LaBranche C, Montefiori DC, Prattipati R, Pinter A, Bess J, Jr., Lifson JD, Reed SG, Sardesai NY, Venzon DJ, Valentin A, Pavlakis GN, Felber BK.** 2014. DNA and protein co-immunization improves the magnitude and longevity of humoral immune responses in macaques. PloS one **9:**e91550.

219. **Zhao J, Lai L, Amara RR, Montefiori DC, Villinger F, Chennareddi L, Wyatt LS, Moss B, Robinson HL.** 2009. Preclinical studies of human immunodeficiency virus/AIDS vaccines: inverse correlation between avidity of anti-Env antibodies and peak postchallenge viremia. Journal of virology **83:**4102-4111.

220. **Xiao P, Zhao J, Patterson LJ, Brocca-Cofano E, Venzon D, Kozlowski PA, Hidajat R, Demberg T, Robert-Guroff M.** 2010. Multiple vaccine-elicited nonneutralizing antienvelope antibody activities contribute to protective efficacy by reducing both acute and chronic viremia following simian/human immunodeficiency virus SHIV89.6P challenge in rhesus macaques. Journal of virology **84:**7161-7173.

221. **Kayman SC, Wu Z, Revesz K, Chen H, Kopelman R, Pinter A.** 1994. Presentation of native epitopes in the V1/V2 and V3 regions of human immunodeficiency virus type 1 gp120 by fusion glycoproteins containing isolated gp120 domains. J Virol **68:**400-410.

222. **Karasavvas N, Billings E, Rao M, Williams C, Zolla-Pazner S, Bailer RT, Koup RA, Madnote S, Arworn D, Shen X, Tomaras GD, Currier JR, Jiang M, Magaret C, Andrews C, Gottardo R, Gilbert P, Cardozo TJ, Rerks-Ngarm S, Nitayaphan S, Pitisuttithum P, Kaewkungwal J, Paris R, Greene K, Gao H, Gurunathan S, Tartaglia J, Sinangil F, Korber BT, Montefiori DC, Mascola JR, Robb ML, Haynes BF, Ngauy V, Michael NL, Kim JH, de Souza MS, Collaboration MT.** 2012. The Thai Phase III HIV Type 1 Vaccine trial (RV144) regimen induces antibodies that target conserved regions within the V2 loop of gp120. AIDS research and human retroviruses **28:**1444-1457.

223. **Fazekas de St G, Webster RG.** 1966. Disquisitions on Original Antigenic Sin. II. Proof in lower creatures. The Journal of experimental medicine **124:**347-361.

224. **Wherry EJ, McElhaugh MJ, Eisenlohr LC.** 2002. Generation of CD8(+) T cell memory in response to low, high, and excessive levels of epitope. Journal of immunology **168:**4455-4461.

225. **Park SO, Han YW, Aleyas AG, George JA, Yoon HA, Lee JH, Kang HY, Kang SH, Eo SK.** 2008. Low-dose antigen-experienced CD4+ T cells display reduced clonal expansion but facilitate an effective memory pool in response to secondary exposure. Immunology **123:**426-437.

226. **Chanh TC, Dreesman GR, Kanda P, Linette GP, Sparrow JT, Ho DD, Kennedy RC.** 1986. Induction of anti-HIV neutralizing antibodies by synthetic peptides. The EMBO journal **5:**3065-3071.

227. **Kutzler MA, Weiner DB.** 2008. DNA vaccines: ready for prime time? Nature reviews. Genetics **9:**776-788.

228. **Lu S, Wyatt R, Richmond JF, Mustafa F, Wang S, Weng J, Montefiori DC, Sodroski J, Robinson HL.** 1998. Immunogenicity of DNA vaccines expressing human immunodeficiency virus type 1 envelope glycoprotein with and without deletions in the V1/2 and V3 regions. AIDS Res Hum Retroviruses **14:**151-155.

229. **Peters PJ, Bhattacharya J, Hibbitts S, Dittmar MT, Simmons G, Bell J, Simmonds P, Clapham PR.** 2004. Biological analysis of human immunodeficiency virus type 1 R5 envelopes amplified from brain and lymph node tissues of AIDS patients with neuropathology reveals two distinct tropism phenotypes and identifies envelopes in the brain that confer an enhanced tropism and fusigenicity for macrophages. J Virol **78:**6915-6926.

230. **Hu SL, Klaniecki J, Dykers T, Sridhar P, Travis BM.** 1991. Neutralizing antibodies against HIV-1 BRU and SF2 isolates generated in mice immunized with recombinant vaccinia virus expressing HIV-1 (BRU) envelope glycoproteins and boosted with homologous gp160. AIDS research and human retroviruses **7:**615-620.

231. **Huson DH, Richter DC, Rausch C, Dezulian T, Franz M, Rupp R.** 2007. Dendroscope: An interactive viewer for large phylogenetic trees. BMC Bioinformatics **8:**460.

232. **Lefranc MP, Giudicelli V, Ginestoux C, Jabado-Michaloud J, Folch G, Bellahcene F, Wu Y, Gemrot E, Brochet X, Lane J, Regnier L, Ehrenmann F, Lefranc G, Duroux P.** 2009. IMGT, the international ImMunoGeneTics information system. Nucleic Acids Res **37:**D1006-1012.

233. **Montefiori DC.** 2004. Evaluating neutralizing antibodies against HIV, SIV and SHIV in luciferase reporter gene assays, p. 1-15. *In* Coligan JE, Kruisbeek AM, Margullies DH, Shevach EM, Strober W (ed.), Current Protocols in Immunology, vol. 12. John Wiley, Hoboken.

234. **Burke V, Williams C, Sukumaran M, Kim S, Li H, Wang X-H, Gorny MK, Zolla-Pazner S, Kong X-P.** 2009. Structural Basis of the Cross-Reactivity of Genetically Related Human Anti-HIV-1 mAbs: Implications for Design of V3-Based Immunogens. Structure **17:**1538-1546.

235. **Otwinowski Z, Minor W.** 1997. Processing of X-ray Diffraction Data Collected in Oscillation Mode, p. 307-326. *In* Carter CW, Sweet R (ed.), Macromolecular Crystallography, part A, vol. 276. Academic Press, New York.

236. **Emsley P, Cowtan K.** 2004. Coot: model-building tools for molecular graphics. Acta crystallographica. Section D, Biological crystallography **60:**2126-2132.

237. **Adams PD, Grosse-Kunstleve RW, Hung LW, Ioerger TR, McCoy AJ, Moriarty NW, Read RJ, Sacchettini JC, Sauter NK, Terwilliger TC.** 2002.

PHENIX: building new software for automated crystallographic structure determination. Acta crystallographica. Section D, Biological crystallography **58:**1948-1954.

238.   **Abagyan RA, Totrov M, Kuznetsov D.** 1994. ICM - A new method for protein modeling and design: Applications to docking and structure prediction from the distorted native conformation. J Comput Chem **15:**488-506.

239.   **DeLano WL.** 2002. The PyMOL User's Manual. DeLano Scientific, Palo Alto.

240.   **Tomaras GD, Binley JM, Gray ES, Crooks ET, Osawa K, Moore PL, Tumba N, Tong T, Shen X, Yates NL, Decker J, Wibmer CK, Gao F, Alam SM, Easterbrook P, Abdool Karim S, Kamanga G, Crump JA, Cohen M, Shaw GM, Mascola JR, Haynes BF, Montefiori DC, Morris L.** 2011. Polyclonal B cell responses to conserved neutralization epitopes in a subset of HIV-1-infected individuals. Journal of virology **85:**11502-11519.

241.   **Suschak JJ, Wang S, Fitzgerald KA, Lu S.** 2015. Identification of aim2 as a sensor for DNA vaccines. Journal of immunology **194:**630-636.

242.   **Ivanoff LA, Dubay JW, Morris JF, Roberts SJ, Gutshall L, Sternberg EJ, Hunter E, Matthews TJ, Petteway SR, Jr.** 1992. V3 loop region of the HIV-1 gp120 envelope protein is essential for virus infectivity. Virology **187:**423-432.

243.   **White-Scharf ME, Potts BJ, Smith LM, Sokolowski KA, Rusche JR, Silver S.** 1993. Broadly neutralizing monoclonal antibodies to the V3 region of HIV-1 can be elicited by peptide immunization. Virology **192:**197-206.

244.   **Scheid JF, Mouquet H, Feldhahn N, Seaman MS, Velinzon K, Pietzsch J, Ott RG, Anthony RM, Zebroski H, Hurley A, Phogat A, Chakrabarti B, Li Y, Connors M, Pereyra F, Walker BD, Wardemann H, Ho D, Wyatt RT, Mascola JR, Ravetch JV, Nussenzweig MC.** 2009. Broad diversity of neutralizing antibodies isolated from memory B cells in HIV-infected individuals. Nature **458:**636-640.

245.   **Laman JD, Schellekens MM, Lewis GK, Moore JP, Matthews TJ, Langedijk JP, Meloen RH, Boersma WJ, Claassen E.** 1993. A hidden region in the third variable domain of HIV-1 IIIB gp120 identified by a monoclonal antibody. AIDS research and human retroviruses **9:**605-612.

246.   **Rini JM, Stanfield RL, Stura EA, Salinas PA, Profy AT, Wilson IA.** 1993. Crystal structure of a human immunodeficiency virus type 1 neutralizing antibody, 50.1, in complex with its V3 loop peptide antigen. Proceedings of the National Academy of Sciences of the United States of America **90:**6325-6329.

247.   **Stanfield R, Cabezas E, Satterthwait A, Stura E, Profy A, Wilson I.** 1999. Dual conformations for the HIV-1 gp120 V3 loop in complexes with different neutralizing fabs. Structure **7:**131-142.

248.   **Burke V, Williams C, Sukumaran M, Kim SS, Li H, Wang XH, Gorny MK, Zolla-Pazner S, Kong XP.** 2009. Structural basis of the cross-reactivity of genetically related human anti-HIV-1 mAbs: implications for design of V3-based immunogens. Structure **17:**1538-1546.

249.   **Gorny MK, Sampson J, Li H, Jiang X, Totrov M, Wang XH, Williams C, O'Neal T, Volsky B, Li L, Cardozo T, Nyambi P, Zolla-Pazner S, Kong XP.** 2011. Human anti-V3 HIV-1 monoclonal antibodies encoded by the VH5-51/VL lambda genes define a conserved antigenic structure. PloS one **6:**e27780.

250. **Abhinandan KR, Martin AC.** 2008. Analysis and improvements to Kabat and structurally correct numbering of antibody variable domains. Molecular immunology **45:**3832-3839.
251. **Ratner L, Fisher A, Jagodzinski LL, Liou RS, Mitsuya H, Gallo RC, Wong-Staal F.** 1987. Complete nucleotide sequences of functional clones of the virus associated with the acquired immunodeficiency syndrome, HTLV-III/LAV. Haematology and blood transfusion **31:**404-406.
252. **Spurrier B, Sampson JM, Totrov M, Li H, O'Neal T, Williams C, Robinson J, Gorny MK, Zolla-Pazner S, Kong XP.** 2011. Structural analysis of human and macaque mAbs 2909 and 2.5B: implications for the configuration of the quaternary neutralizing epitope of HIV-1 gp120. Structure **19:**691-699.
253. **LaRosa GJ, Weinhold K, Profy AT, Langlois AJ, Dreesman GR, Boswell RN, Shadduck P, Bolognesi DP, Matthews TJ, Emini EA, et al.** 1991. Conserved sequence and structural elements in the HIV-1 principal neutralizing determinant: further clarifications. Science **253:**1146.
254. **Vranken WF, Fant F, Budesinsky M, Borremans FA.** 2001. Conformational model for the consensus V3 loop of the envelope protein gp120 of HIV-1 in a 20% trifluoroethanol/water solution. European journal of biochemistry / FEBS **268:**2620-2628.
255. **Gorny MK, Wang XH, Williams C, Volsky B, Revesz K, Witover B, Burda S, Urbanski M, Nyambi P, Krachmarov C, Pinter A, Zolla-Pazner S, Nadas A.** 2009. Preferential use of the VH5-51 gene segment by the human immune response to code for antibodies against the V3 domain of HIV-1. Molecular immunology **46:**917-926.
256. **Tugarinov V, Zvi A, Levy R, Hayek Y, Matsushita S, Anglister J.** 2000. NMR structure of an anti-gp120 antibody complex with a V3 peptide reveals a surface important for co-receptor binding. Structure **8:**385-395.
257. **Rosen O, Chill J, Sharon M, Kessler N, Mester B, Zolla-Pazner S, Anglister J.** 2005. Induced fit in HIV-neutralizing antibody complexes: evidence for alternative conformations of the gp120 V3 loop and the molecular basis for broad neutralization. Biochemistry **44:**7250-7258.
258. **Rosen O, Sharon M, Quadt-Akabayov SR, Anglister J.** 2006. Molecular switch for alternative conformations of the HIV-1 V3 region: implications for phenotype conversion. Proceedings of the National Academy of Sciences of the United States of America **103:**13950-13955.
259. **Stanfield RL, Gorny MK, Zolla-Pazner S, Wilson IA.** 2006. Crystal structures of human immunodeficiency virus type 1 (HIV-1) neutralizing antibody 2219 in complex with three different V3 peptides reveal a new binding mode for HIV-1 cross-reactivity. Journal of virology **80:**6093-6105.